AD NUMBER: AD0376942
CLASSIFICATION CHANGES
TO: Unclassified
FROM: Confidential
AUTHORITY
10 Dec 1978, Group 4, DoDD 5200.10

GENERAL DECLASSIFICATION SCHEDULE

IN ACCORDANCE WITH
DOD 5200.1-R & EXECUTIVE ORDER 11652

THIS DOCUMENT IS:

CLASSIFIED BY_____

Subject to General Declassification Schedule of Executive Order 11652-Automatically Downgraded at 2 Years Intervals- DECLASSIFIED ON DECEMBER 31, ____.

BY

Defense Documentation Center
Defense Supply Agency
Cameron Station
Alexandria, Virginia 22314

SECURITY MARKING

The classified or limited status of this report applies to each page, unless otherwise marked.
Separate page printouts MUST be marked accordingly.

THIS DOCUMENT CONTAINS INFORMATION AFFECTING THE NATIONAL DEFENSE OF THE UNITED STATES WITHIN THE MEANING OF THE ESPIONAGE LAWS, TITLE 18, U.S.C., SECTIONS 793 AND 794. THE TRANSMISSION OR THE REVELATION OF ITS CONTENTS IN ANY MANNER TO AN UNAUTHORIZED PERSON IS PROHIBITED BY LAW.

NOTICE: When government or other drawings, specifications or other data are used for any purpose other than in connection with a definitely related government procurement operation, the U. S. Government thereby incurs no responsibility, nor any obligation whatsoever; and the fact that the Government may have formulated, furnished, or in any way supplied the said drawings, specifications, or other data is not to be regarded by implication or otherwise as in any manner licensing the holder or any other person or corporation, or conveying any rights or permission to manufacture, use or sell any patented invention that may in any way be related thereto.

CONFIDENTIAL

BOEING

SEATTLE, WASHINGTON

CONFIDENTIAL

Form 1473

CONFIDENTIAL

THE BOEING COMPANY

REV LTR

CODE IDENT. NO. 81205

NUMBER (14) D2-36139-1 / B

TITLE: (6) Aerodynamics of Conical Bodies (U) (8)

FOR LIMITATIONS IMPOSED ON THE USE OF THE INFORMATION CONTAINED IN THIS DOCUMENT AND ON THE DISTRIBUTION OF THIS DOCUMENT, SEE LIMITATIONS SHEET.

MODEL Research CONTRACT

ISSUE NO. ISSUED TO:

PREPARED BY D. W. Eastman

SUPERVISED BY B. E. Wetzel

APPROVED BY J. A. Brousseau 12/20/65

APPROVED BY M N Hilleke 12/21/65

GROUP 4
DOWNGRADED AT 3 YEAR INTERVALS; DECLASSIFIED AFTER 12 YEARS.
DOD DIR 5200.10

(10) Donald W. Eastman

(11) 12 Oct 66

(12) 187 p.

(059 600)

CONFIDENTIAL

SHEET 1

LIMITATIONS

This document is controlled by Flight Technology

All revisions to this document shall be approved by the above noted organization prior to release.

DDC AVAILABILITY NOTICE

☐ Qualified requesters may obtain copies of this document from DDC.

☐ Foreign announcement and dissemination of this report by DDC is not authorized.

☒ U. S. Government agencies may obtain copies of this document directly from DDC. Other qualified DDC users shall request through The Boeing Company, Seattle, Wn.

☐ U. S. military agencies may obtain copies of this document directly from DDC. Other users shall request through The Boeing Company, Seattle, Wn.

☐ All distribution of this document is controlled. Qualified DDC users shall request through The Boeing Company, Seattle, Wn.

PROPRIETARY NOTES

NUMBER D2-36139-1
REV LTR A

THE BOEING COMPANY

ACTIVE SHEET RECORD

SHEET NUMBER	REV LTR	ADDED SHEETS				SHEET NUMBER	REV LTR	ADDED SHEETS			
		SHEET NUMBER	REV LTR	SHEET NUMBER	REV LTR			SHEET NUMBER	REV LTR	SHEET NUMBER	REV LTR
1						46					
2						47					
3	A					48					
4	A					49					
5	A					50					
6	4					51					
7						52	A				
8						53	A	53 a	A		
9						54	A				
10						55	A				
11						56					
12						57					
13						58					
14						59					
15						60					
16	A					61					
17	A					62					
18	A					63					
19						64					
20						65					
21						66					
22						67					
23						68					
24						69					
25						70					
26						71					
27						72					
28						73					
29						74					
30						75					
31						76					
32	A					77					
33	A	33 a	A			78					
34	A					79					
35						80					
36						81					
37						82					
38						83					
39						84					
40						85					
41						86					
42						87					
43						88	A				
44						89	A				
45						90					

U3 4802 1436 ORIG. 4/65

ACTIVE SHEET RECORD

SHEET NUMBER	REV LTR	ADDED SHEETS				SHEET NUMBER	REV LTR	ADDED SHEETS			
		SHEET NUMBER	REV LTR	SHEET NUMBER	REV LTR			SHEET NUMBER	REV LTR	SHEET NUMBER	REV LTR
91						136					
92						137					
93						138					
94						139					
95						140	A				
96						141					
97						142					
98						143					
99						144					
100						145					
101						146					
102						147	A				
103						148					
104	A					149					
105	A					150					
106						151					
107						152					
108						153					
109						154					
110						155	A				
111						156					
112						157					
113						158					
114						159					
115	A					160					
116						161					
117						162					
118						163					
119						164	A	164 a	A		
120	A					165	A				
121						166	A				
122						167	A				
123						168	A				
124	A					169	A				
125						170					
126						171					
127						172					
128						173	A				
129						174	A				
130						175					
131						176					
132						177	A	177 a	A		
133	A					178	A	178 a	A		
134						179					
135						180					

THE BOEING COMPANY

ACTIVE SHEET RECORD

SHEET NUMBER	REV LTR	ADDED SHEETS				SHEET NUMBER	REV LTR	ADDED SHEETS			
		SHEET NUMBER	REV LTR	SHEET NUMBER	REV LTR			SHEET NUMBER	REV LTR	SHEET NUMBER	REV LTR
181	A										
182											
183											
184											
185											
186											
187											

REVISIONS

LTR	DESCRIPTION	DATE	APPROVAL
A	Page 16 - Updated summary by adding several references. 17 - " 18 - " 32 - " 33 - " 33 a - " 34 - " 52 - " 53 - " 53 a - " 54 - " 55 - " 88 - " 89 - " 104 - " 105 - " 115 - " 120 - " 124 - " 133 - " 140 - " 147 - On Ref. 9, changed Defense Documentation Center number from AD-336285 to AD-365790. 155 - Added Refs. 74 through 82. 164 - Added Refs. 176 through 181. 164 a - Added Refs. 182 through 187. 165 - Changed Ref. 210 from RAD-SR-64-307 to RAD-SR-65-259. 166 - Added Ref. 216. 167 - On Refs. 304 and 306, changed classification from secret to confidential. 168 - On Ref. 407, changed classification from secret to confidential. 169 - Added Ref. 414. 173 - On Ref. 536, changed Central Library report number from T7-4613-59-X to ASTIC-009521. 174 - On Ref. 539, added Central Library report number A64-14-1963 Vol 3. 177 - Added Refs. 574 through 576. 177 a - Added Refs. 577 through 586. 178 - Added Refs. 607 thgouh 610. 178 a - Added Refs. 611 through 613. 181 - Added Refs. 724 through 726.	10-12-66	B.E. Wetzel

ABSTRACT

A compilation and evaluation of theoretical and experimental aerodynamic data are presented for conical shapes at Mach numbers from 0 to 25. Emphasis is placed on slender cones such as might be used for ballistic missile reentry. Plots for obtaining estimates of static and dynamic aerodynamic characteristics are included.

Several hundred references are listed by originating company or publishing source. Contents of the references are summarized by test condition and model geometry.

KEY WORDS

Ablation Effects
Aerodynamic Characteristics
Aerodynamic Controls
Axial Force
Base Drag
Base Geometry
Base Pressure
Blowing Effects
Boundary Layer Transition
Center of Pressure
Cones
Drag
Dynamic Damping
Lift
Low Density
Normal Force
Nose Bluntness
Pitching Moment
Pressure Coefficient
Skin Friction
Stability
Viscous Effects
Wave Drag

TABLE OF CONTENTS

LIST OF SYMBOLS

c.g.	center of gravity
c.p.	center of pressure, see Section 3.0
$C_{o\infty}$	see equation 10.1
C_A	axial force coefficient, see Section 4.0
C_D	drag coefficient, see Section 1.0
C_L	lift coefficient, see Section 1.0
C_N	normal force coefficient, see Section 2.0
C_m	pitching moment coefficient, see Section 3.0
C_P	pressure coefficient, see Section 6.0
C_{m_q}, C_{N_q}	stability derivatives due to angular velocity, see Section 5.0
$C_{m_{\dot{\alpha}}}$, $C_{N_{\dot{\alpha}}}$	stability derivatives due to vertical acceleration, see Section 5.0
$C_{F_{cone}}$	average skin friction coefficient for cone
d	diameter, feet
h	altitude, feet
l	cone length, feet
M	Mach number
$\dot{m}$	mass flow, lb-sec/ft
q	dynamic pressure, psf
q	angular velocity, rad/sec
r	cone radius, feet
R_{e_c}	boundary layer edge Reynolds number/ft

Re_∞	free stream Reynolds number/ft
S	reference area, ft^2
T	temperature
V	velocity, fps
x	axial distance along cone, ft
y	radial distance from cone axis, ft
Z	compressibility
θ	angle of oscillation, degree
α	angle of attack, degree
γ	isentropic exponent
δ	cone half-angle, degree
ξ	moment reference length, ft
ρ	density, $slugs/ft^3$
φ	peripheral angle measured from most windward streamline, degree
μ	viscosity, $lb\text{-}sec/ft^2$

SUBSCRIPTS

b	cone base
c	cone surface
l	based on cone axial length
N	of nose cap
0	moment measured about cone nose
∞	free stream
r	recovery

USE FOR TYPEWRITTEN MATERIAL ONLY

1.0 INTRODUCTION

A compilation and evaluation of theoretical and experimental aerodynamic data are presented for conical shapes at Mach numbers from approximately 0 to 25. Plots which can be used to provide accurate estimates of aerodynamic characteristics are included.

The subjects included are:

Static Force and Moment Coefficients

Dynamic Force and Moment Coefficients

Pressure Coefficients

Boundary Layer Transition

Aerodynamic Controls

Low Density Effects

Ablation and Blowing Effects

Emphasis has been placed on slender cones such as might be used for ballistic missile re-entry.

A comprehensive literature search was conducted and several hundred references are listed by originating company or publishing source. References include documents, technical reports, journals, conference papers, etc. Many excellent and relatively unknown references, which are not available through the Boeing library, have been included and are available from Donald W. Eastman.

Contents of the references are summarized by test conditions and model geometry, since many of the titles are not definitive. Desired information can be located quickly with this handy summary.

It is recommended that Reference 537 be obtained by aerodynamicists using the present document, as it reprints cone data directly from many references listed in this document. However, Reference 537 includes only unclassified material and does not evaluate any data or present theoretical methods.

The aerodynamic data in this document are generally referred to the body axis coordinate system, not the wind axis coordinate system.

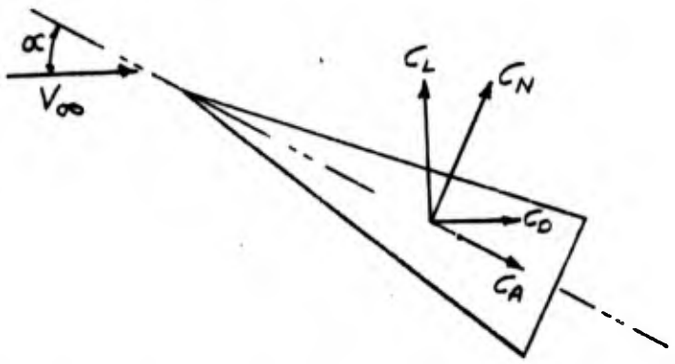

The relationships between these coordinate systems are:

Body to Wind

$$C_L = C_N \cos\alpha - C_A \sin\alpha$$

$$C_D = C_N \sin\alpha + C_A \cos\alpha$$

Wind to Body

$$C_N = C_L \cos\alpha + C_D \sin\alpha$$

$$C_A = -C_L \sin\alpha + C_D \cos\alpha$$

2.0 NORMAL FORCE

The normal force coefficient on a cone is defined by

$$C_N = \frac{(\text{force normal to cone axis})}{(\text{dynamic pressure})\ (\text{reference area})} \qquad 2.1$$

The reference area is usually taken as the base area, though occasionally it is based on the planform area. The latter is indicated when required.

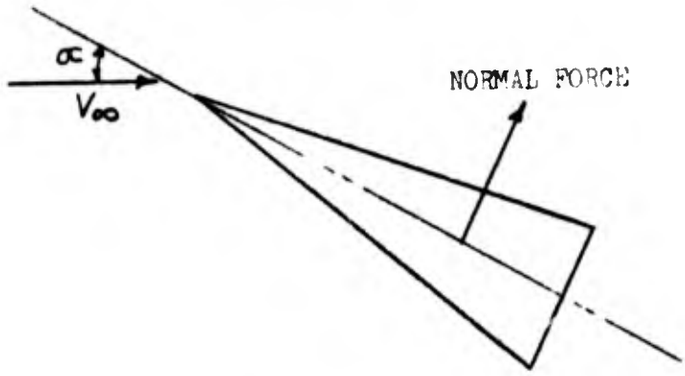

References which contain normal force coefficient data are summarized on Pages 16 through 18.

Subsonic and Transonic Speeds

Although no adequate theory exists for predicting the normal force coefficient at subsonic and transonic speeds, sufficient experimental data are available for estimating C_N and C_{N_α}, the derivative of C_N with respect to α at $\alpha = 0$.

Figures 2.1 through 2.3 show correlations of experimental data for sharp cones for $\alpha \leq 20°$. Very little data are available for $\alpha > 20°$. The effect on C_N of blunting the nose is shown in Figures 2.4 and 2.5. Large bluntness causes a substantial increase in the transonic C_{N_α}.

Figure 2.6 shows that rounding the base of a sharp 12.5° cone decreases C_N

at subsonic speeds. This suggests that base flow effects, and hence the method of mounting models in a subsonic wind tunnel, may significantly influence the aerodynamic forces and moments. (The effects on the static and dynamic stability are shown in Figures 3.4 and 5.1).

Supersonic Speeds

Although very accurate theoretical predictions of normal forces for cones in unseparated supersonic flows can be made, calculations for cones at angle of attack can be tedious. They are, moreover, generally unnecessary because of the large amount of experimental data available.

Sharp cone data are presented in Figures 2.1 through 2.3. Figure 2.1 includes a comparison of the experimental C_{N_α} with the values predicted by Small Angle of Attack theory[140] at supersonic speeds. Because of the excellent agreement, results of the theory are shown for a much wider range of cone angles in Figure 2.7.

The effect on C_{N_α} of blunting the nose is shown in Figures 2.4 and 2.5. Large reductions in C_{N_α} occur at high supersonic Mach numbers, which are much greater for slender cones than the reductions predicted by "simple" Newtonian theory ($C_p = 2 \sin^2 \delta$).

The addition of a rounded base to a sharp cone should have little effect on either the pressure distributions on the inclined surfaces or the normal force coefficients at supersonic speeds, since the propagation of base disturbances is limited to the subsonic portion of the boundary layer. This is shown by the test data for a 12.5° cone in Figure 2.6.

Hypersonic Speeds

Newtonian theory[117] accurately predicts C_N for sharp cones at most angles of attack. Figure 2.8 shows the excellent comparison of experimental data and Newtonian theory*. Newtonian theory overpredicts C_N for $\alpha > 60°$; however, sufficient experimental data are available at these angles so that accurate estimates of C_N can be made. Figure 2.9 shows plots of C_N vs α calculated using Newtonian theory, where the local pressure is

$$C_p = 2 \sin^2 \delta$$

The results of calculations by the Small Angle of Attack theory[140], plotted in Figure 2.7, can be used to obtain $(C_{N_\alpha})_{\alpha=0}$ for sharp cones at hypersonic speeds.

As was noted earlier (Figures 2.4 and 2.5), C_{N_α} at $\alpha = 0$ cannot be adequately predicted for blunted cones by Newtonian theory. Modified Shock Expansion theory[517] does, however, give good agreement with experiment, as shown in Figure 2.10. The development of a computer program at Boeing using this theory is anticipated. Newtonian theory does, however, provide good predictions of C_N at angle of attack as shown in Figure 2.11.

An excellent discussion of cone bluntness effects is presented in Reference 130.

Rounding the base is expected to have no effect on normal force at hypersonic speeds, at small angles of attack.

*Computer programs available; see Section 12.0.

EXPERIMENTAL NORMAL FORCE DATA

REF.	MACH NUMBER	δ DEGREES	r_N/r_b	α_{MAX}
114.	.1	33.2	0	12
801.	.1	15 AND 30	0 - .5	20
574.	.2	5 - 45	0	180
558.	.22 - 2.9	14	0	22
129.	.25 - 2.2	12.5	0 AND .6	18
157.	.25 - 2.2	12.5	.6	20
201.	.4 - 20	NONCONICAL SHAPES	-	15
204.	.4 - 20	NONCONICAL SHAPES	-	20
206.	.4 - 20	NONCONICAL SHAPES	-	20
562.	.47 - 1.93	10 - 50	0 - .8	6
525.	.5 - 4	9	.25	0
538.	.5 - 4.06	20 - 40	0 - .6	12
546.	.5 - 4.9	10 - 50	0 - .62	0
176.	.5 - 5	10 - 50	0 - .62	0
180.	.5 - 1.1	0	5.7	28
817.	.5 - 7	8	0 AND .11	28
36.	.6 - 1.4	9	.04	16
127.	.6 - 3.2	10.7	.23	0
505.	.6 - 7.5	7	.22	0
136.	.65 - 2.2	20	0 AND .4	21
148.	.7 - 1.3	11.6	.38	8
181.	.7 - 2	10 - 40	0	4
306.	.8 - 9.9	10	.2	11
530.	1 - 4	10	0	0
211.	1 - 25	SUMMARY OF ALL LORV VEHICLE FLIGHT TESTS		
777.	1.36 - 4	10	0	0
163.	1.4 AND 2	3.55	0	26
561.	1.5 AND 2	10 AND 15	0	2
186.	1.5 - 4.6	5.7	0	28
526.	1.56 - 4.24	3.48 - 14.1	0	20
776.	1.56 - 4.24	3.48 - 14.1	0	20
508.	1.6 - 3.9	7.1	.22	11
576.	1.6 - 9	10 - 60	0 - 1	5
531.	1.7 - 3.3	9.5	0	0
524.	1.75 - 5	DOUBLE CONE	0	13
167.	2	10 AND 15	.26 AND .32	90
112.	2 AND 3	7.75	0	20
75.	2 - 6	NONCONICAL SHAPES	-	20
55.	2 - 8	8.7	0	25
13	2 - 10	9	.017 - .207	18

EXPERIMENTAL NORMAL FORCE DATA

REF.	MACH NUMBER	δ DEGREES	r_N/r_b	α_{MAX}
30.	2 - 10	9	.05	15
61.	2 - 10	9	NONSPHERICAL	16
16.	2 - 10	NONCONICAL SHAPES	-	18
29.	2 - 10	11	0	18
171.	2.4 - 3.9	3.2	.5	25
165.	2.4 - 3.9	3.2	.5	90
102.	2.75 - 5	4.1 - 9.4	0	25
168.	2.94 - 4.78	15	0	90
177.	3 - 6.3	4.1 AND 5.72	0	0
138.	3 - 8	15	VARIOUS SHAPES	0
305.	3 - 22	8	0	-
520.	3.8 - 5.8	9	0	108
77.	4	9	0	15
705.	4	7	0	180
303.	4 - 20	8	0	20
815.	5 AND 6.1	8	.144	25
513.	5 - 8	8	0	12
45.	6 - 10	15	.333	15
302.	6 - 19	9	0	16
816.	6.1	10	0	30
506.	6.5 - 14	SLENDER CONE	-	30
202.	6.5 - 17	8 - 16	.03 - .15	16
169.	6.7	22.3	.27	27
128.	6.77	9	0 - .66	180
101.	6.8	20	0	20
609.	6.8 - 4.7	9	0 - .3	30
117.	6.8 AND 9.6	10 - 40	0 AND .2	72
80.	6.8 - 14.7	9	0 - .3	30
126.	6.8 - 18	5 - 20	0	90
161.	6.8 AND 21.2	9	.33 AND .66	180
132.	6.8 - 25	5 - 50	0	30
124.	6.83	5 - 45	0	130
182.	6.9	5	0 - .2	30
162.	7	10 - 20	0 - .44	25
507.	7.3 AND 9	9	.03 - .3	15
503.	8	6.33	0	15
401.	8	9	0 - .36	15
569.	8	9	0	25
54.	8	20	0 AND .4	46
407.	8 AND 10	9	0 - .36	15

EXPERIMENTAL NORMAL FORCE DATA

REF.	MACH NUMBER	δ DEGREES	r_N/r_b	α_{MAX}
37.	8 - 21.7	.3 - 12.5	0 - .5	40
702.	8 - 22	6.3 - 20	0 - .5	30
571.	8.07	6.3	0	15
586.	8.3	20	0	30
203.	9 - 15	5.7 AND 8.3	VARIOUS SHAPES	20
33.	9 - 21	9 AND 10	0 - .3	25
410.	9 - 24	VARIOUS SHAPES	-	-
170.	9.6	10 - 40	.26	60
130.	9.7 - 19	10	0 - .76	45
54.	9.8	10	.9	180
54.	9.8	50	0	180
40.	10	6	VARIOUS SHAPES	26
20.	10	6.3	VARIOUS SHAPES	15
62.	10	8	.04	11
59.	10	9	0	13
79.	10	9	0 - .3	24
402.	10	9	0 - .36	15
24.	10	9	0	20
28.	10	11	0	15
406.	10 - 20	OGIVE	0 - .12	15
715.	10 - 21	8 - 10	0 AND .035	25
539.	10 AND 21.2	7.5 - 10	0 AND .04	10
603.	11	9	.05	0
604.	11 - 16	8	.035	20
10.	13 - 21	6.5 AND 9	.03 AND .3	45
12.	14 - 22	7.1 AND 9	.03 - .3	40
523.	15 AND 18	10	.5 - .9	10
210.	16 - 25	9	0	7
38.	17 - 20	11	0	16
76.	18	9	.1	20
209.	18 - 24	8	0	10
154.	18 AND 24.5	30 - 40	.22	180
42.	19	6	VARIOUS SHAPES	20
15.	19	9	0	15
43.	19	9	.045	20
18.	19	11	0	15
509.	20	7.1	.225	30
179.	20.3	5 - 90	0	110
134.	20.5 AND 24	5 - 20	0	20
131.	24.5	26 AND 45	0 - 1	20

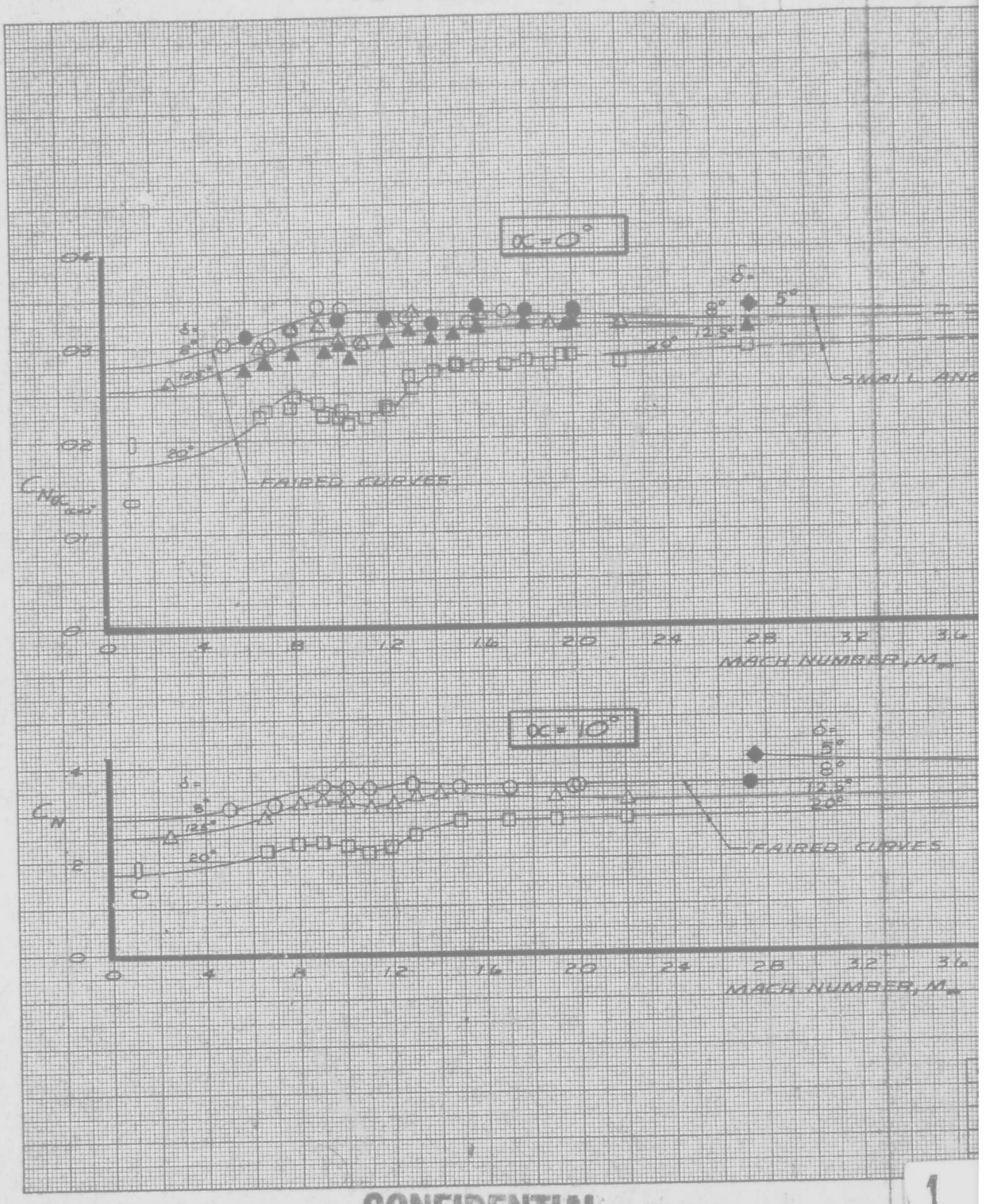
α = 0°
δ =
5°
8°
12.5°
20°
FAIRED CURVES
SMALL ANG
$C_{N_{\alpha_{\alpha=0}}}$
0.4
0.3
0.2
0.1
0
0
.4
.8
1.2
1.6
2.0
2.4
2.8
3.2
3.6
MACH NUMBER, M_∞
α = 10°
δ =
5°
8°
12.5°
20°
FAIRED CURVES
C_N
4
2
0
0
.4
.8
1.2
1.6
2.0
2.4
2.8
3.2
3.6
MACH NUMBER, M_∞

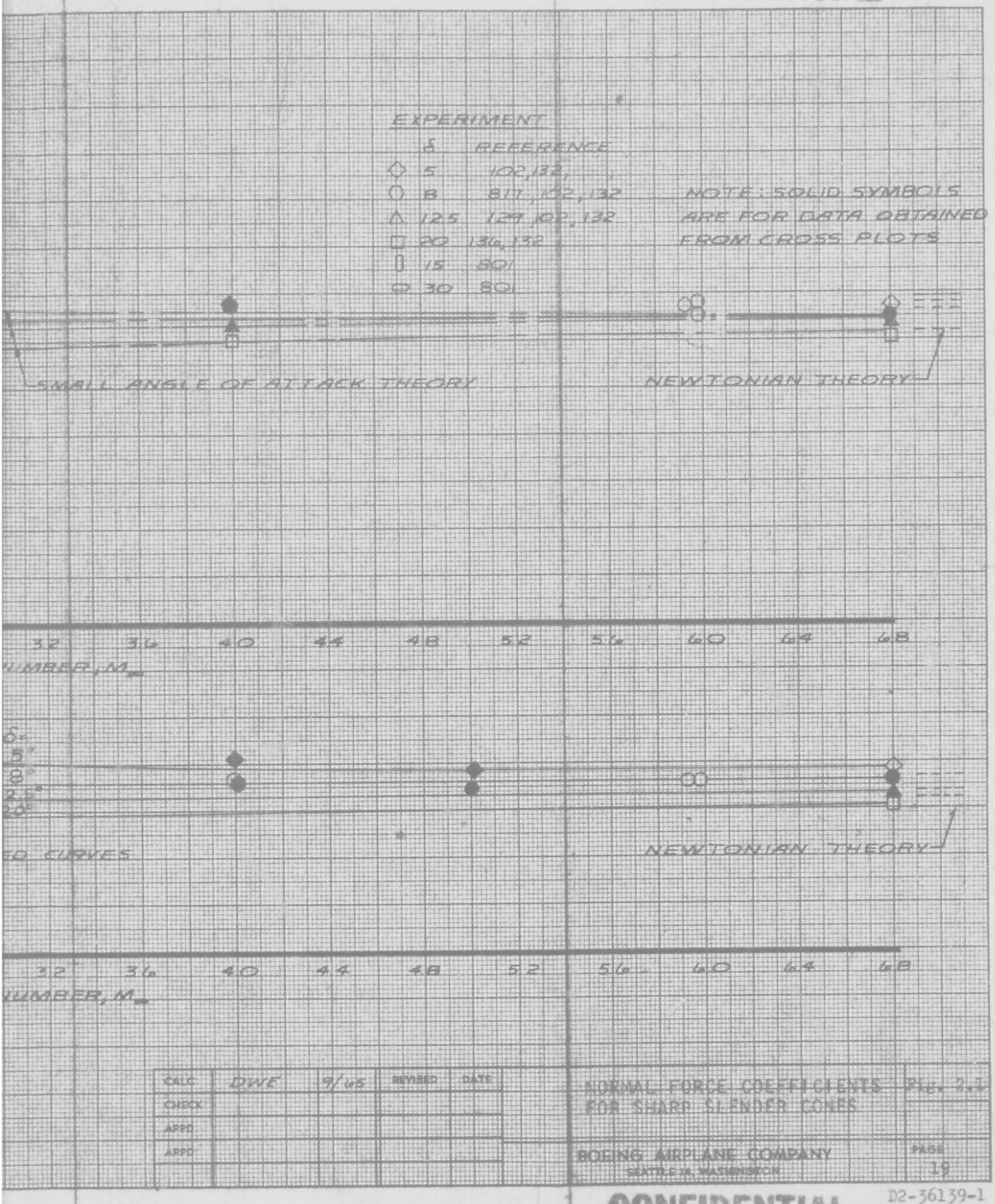

CALC	DWE	9/65	REVISED	DATE
CHECK				
APPD				
APPD				

NORMAL FORCE COEFFICIENTS FOR SHARP SLENDER CONES

BOEING AIRPLANE COMPANY
SEATTLE 24, WASHINGTON

PAGE 19

D2-36139-1

ALBANENE 1951 TRACING PAPER 61288

BAC 1053-R-4

2

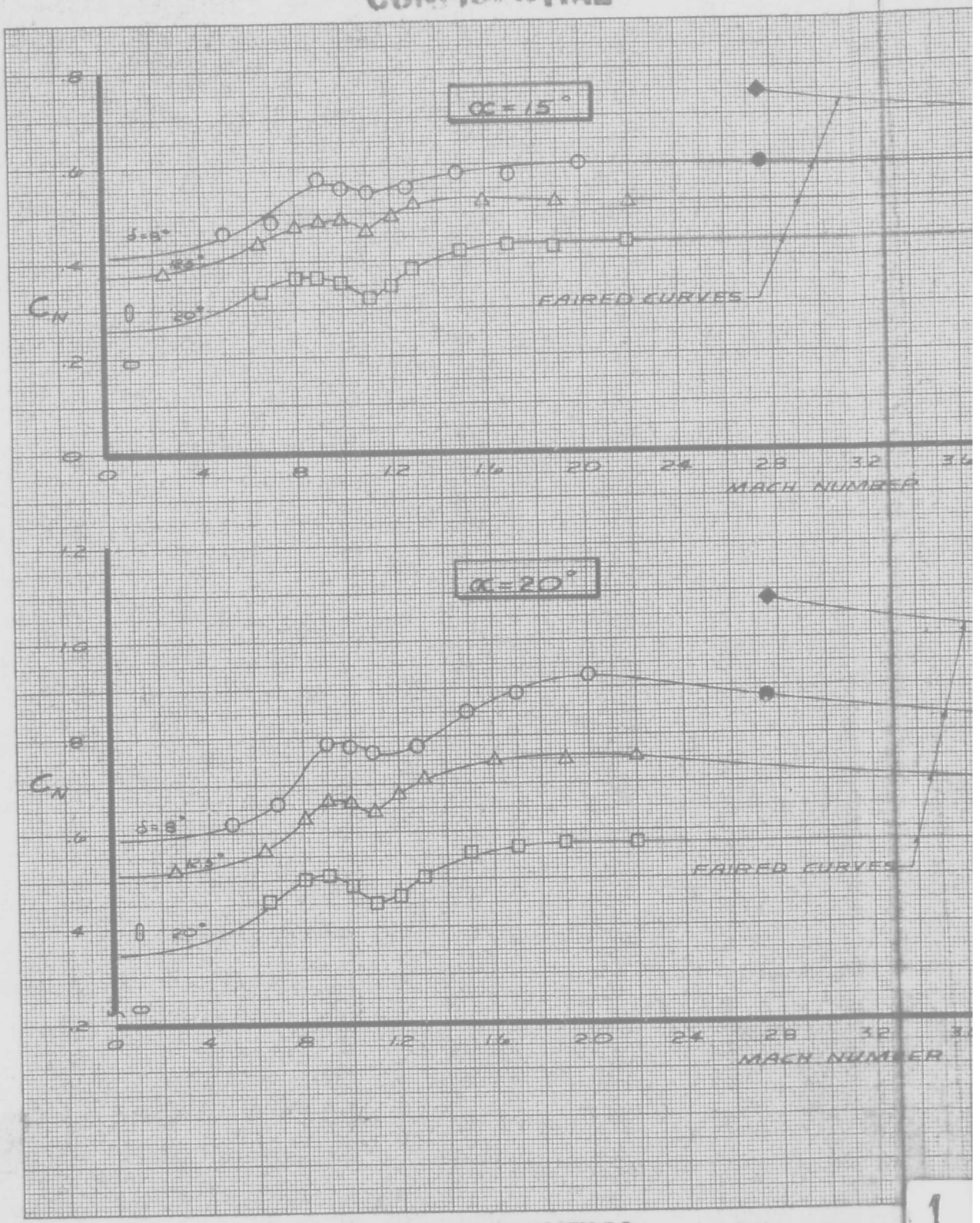
α = 15°
δ = 8°
δ = 5°
δ = 0°
C_N
FAIRED CURVES
MACH NUMBER
α = 20°
δ = 8°
δ = 5°
δ = 0°
C_N
FAIRED CURVES
MACH NUMBER

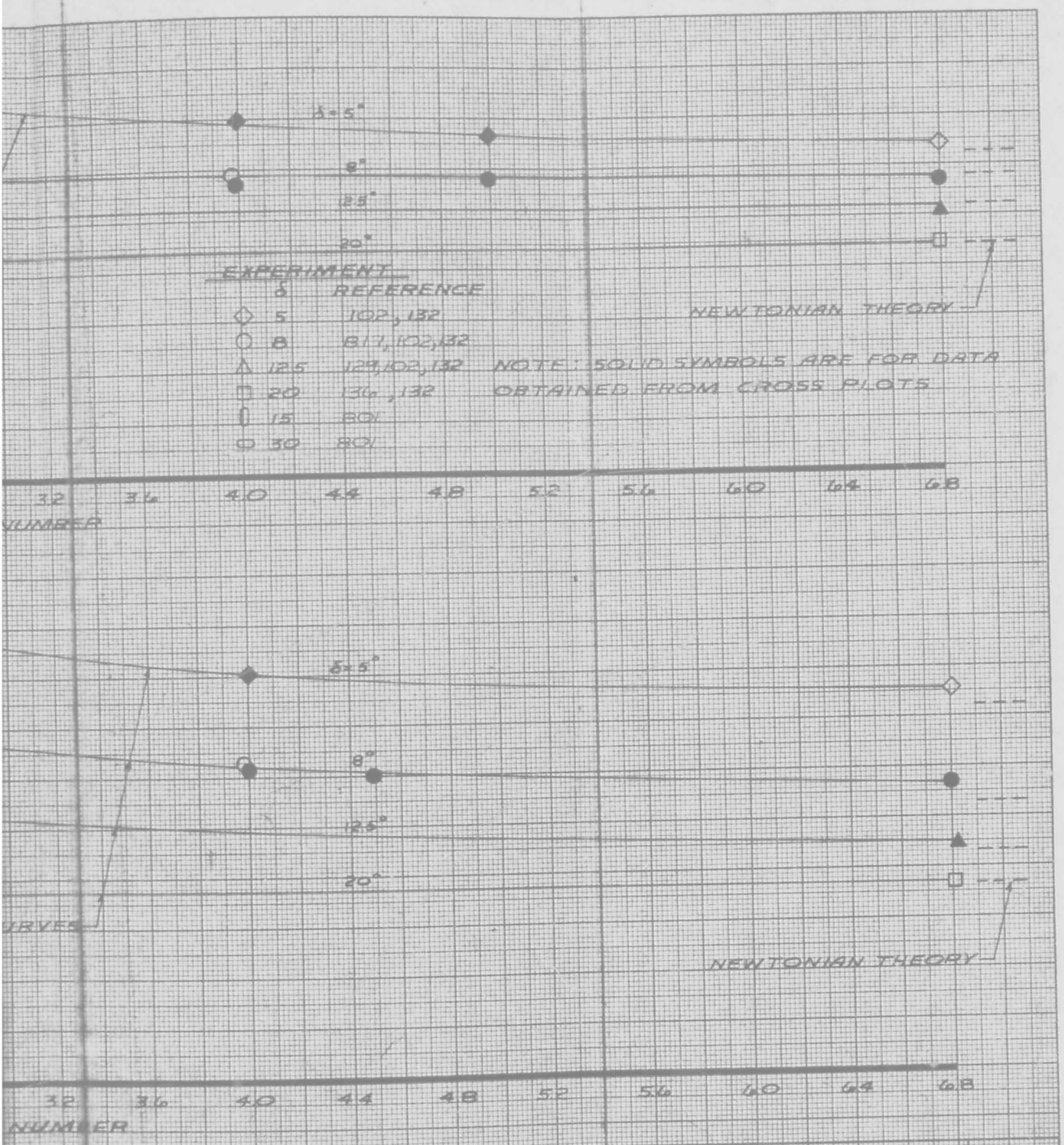

CALC	DWE	9/6/5	REVISED	DATE
CHECK				
APPD				
APPD				

NORMAL FORCE COEFFICIENTS FIG. 8-2
FOR SHARP SLENDER CONES

BOEING AIRPLANE COMPANY
SEATTLE 24, WASHINGTON

PAGE 20

D2-36139-1

BAC 1053-R-4

ALBANENE 1961 61265

2

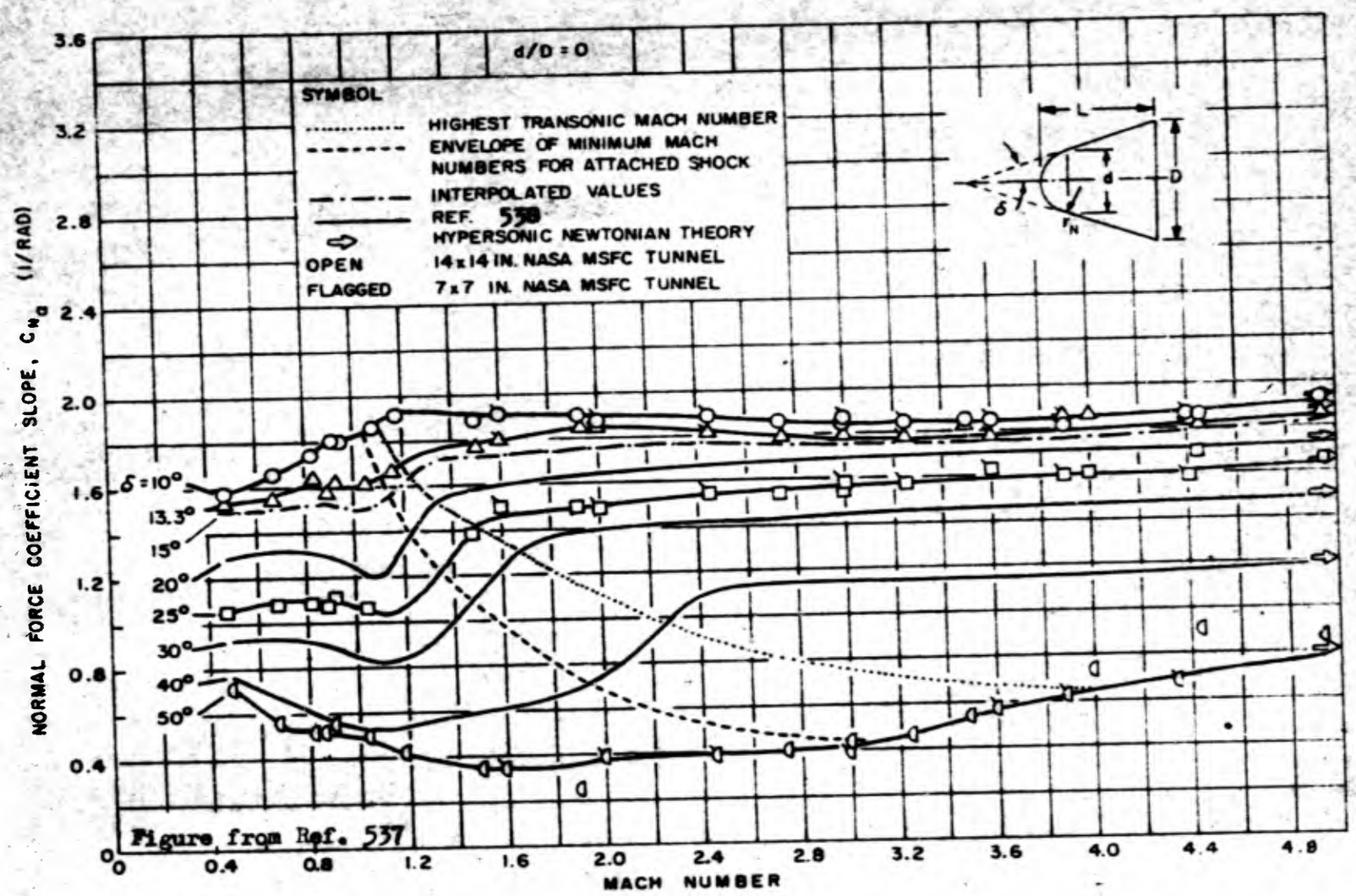

Figure 2.3 Variation of Normal Force Coefficient Slope with Mach Number for Sharp Cones

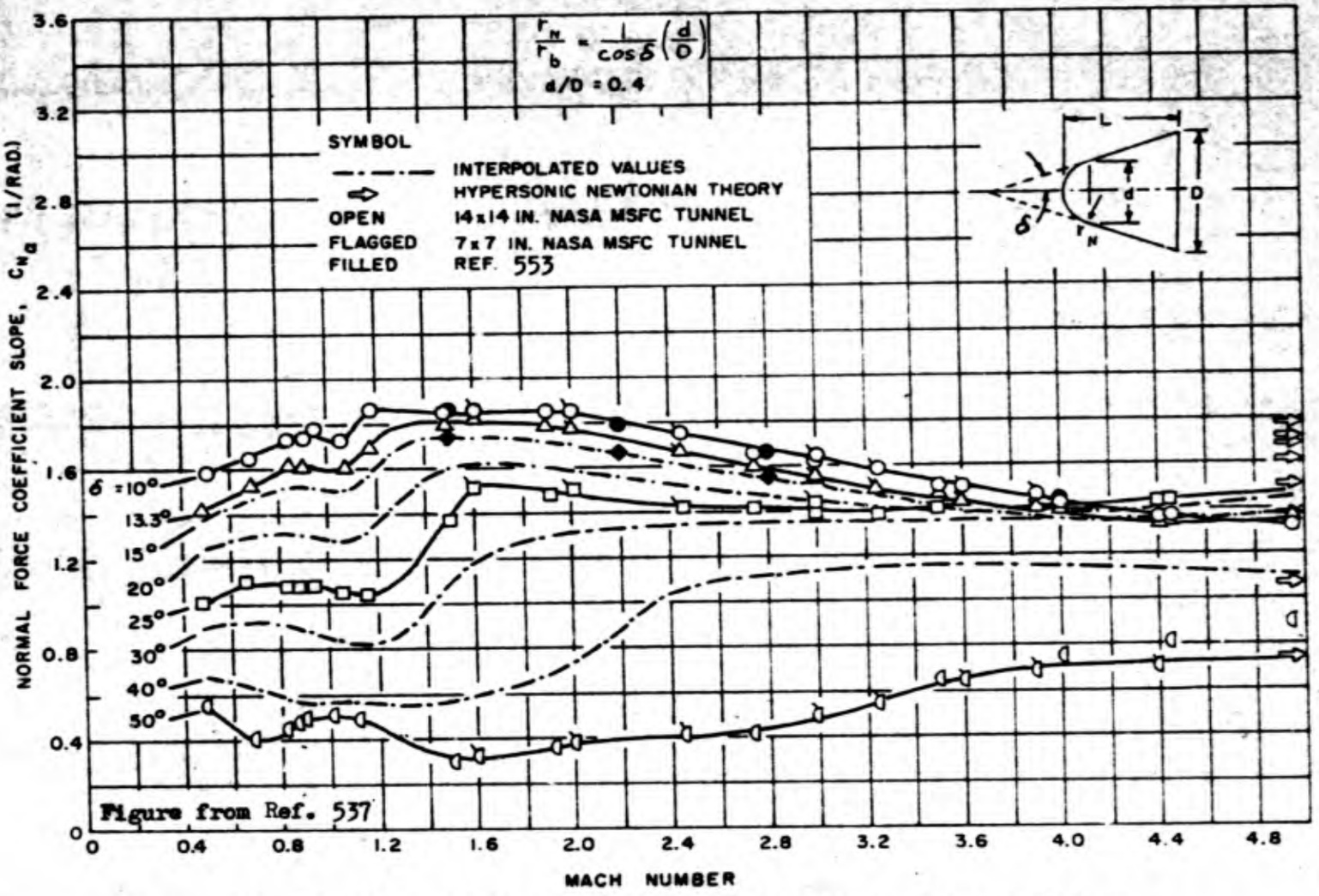

Figure 2.4 Variation of Normal Force Coefficient Slope with Mach Number for Blunt Cones with d/D = 0.4

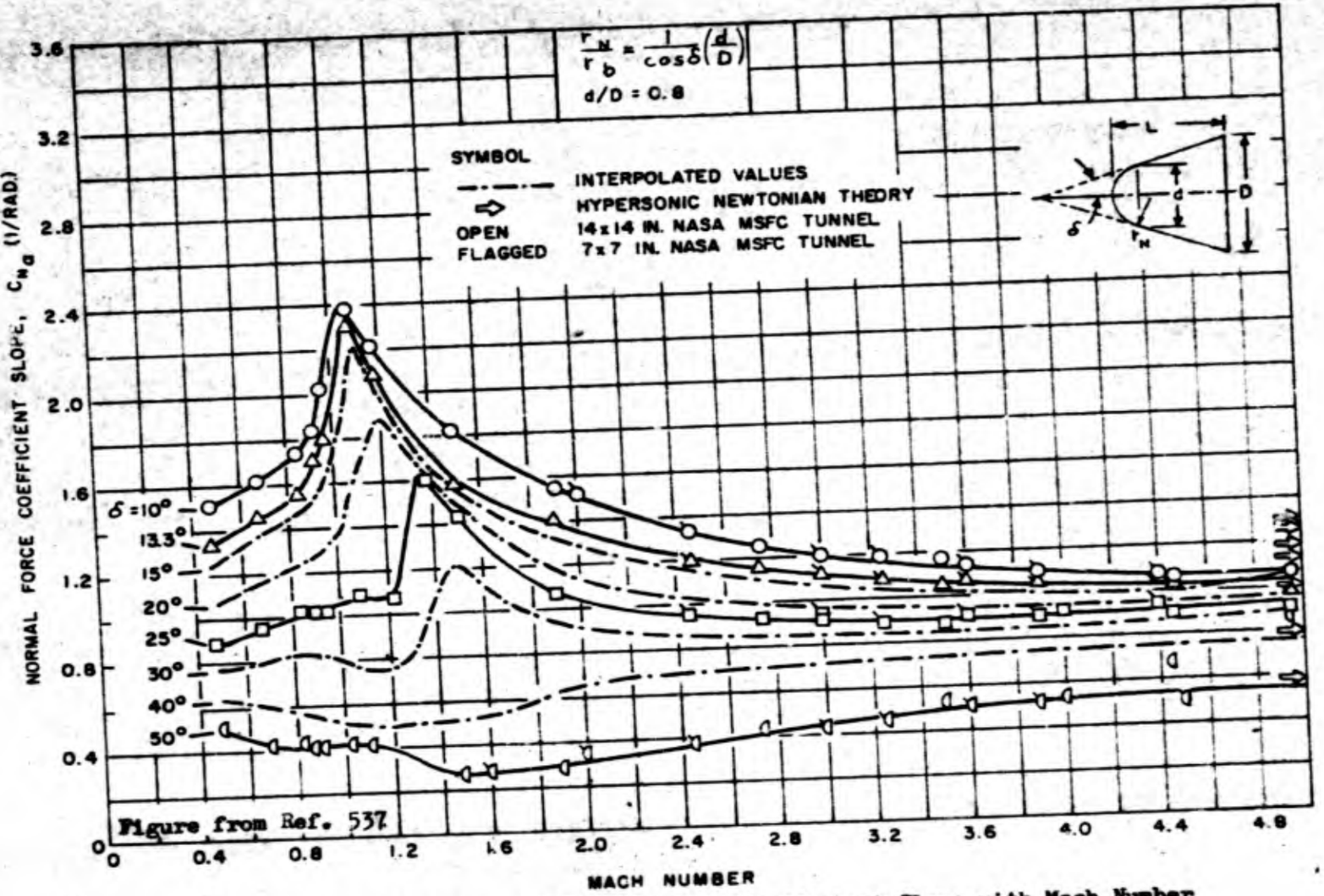

Figure 2.5 Variation of Normal Force Coefficient Slope with Mach Number for Blunt Cones with d/D = 0.8

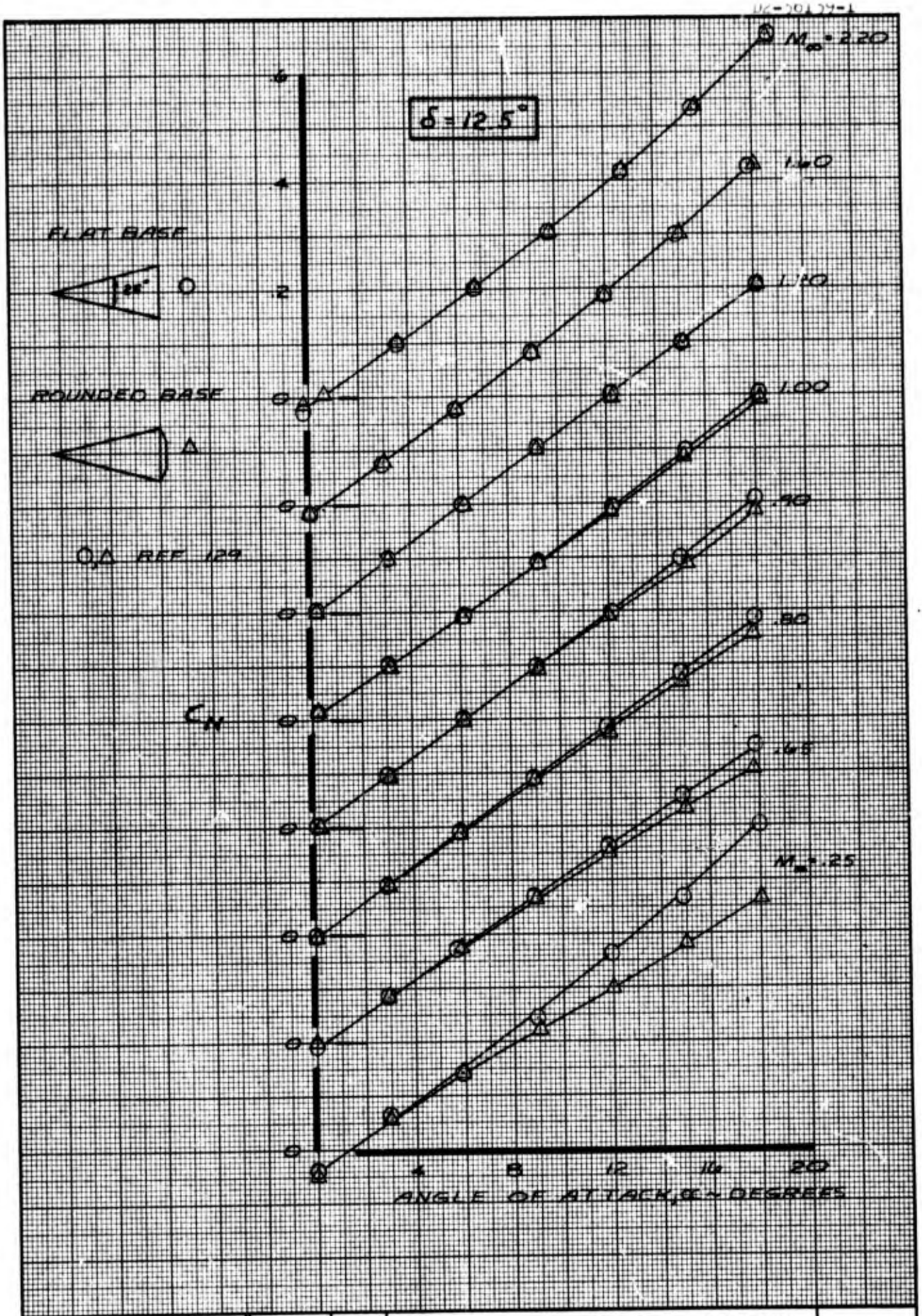

CALC	DWE	9/65	REVISED	DATE	THE EFFECT OF ROUNDING THE BASE ON CONE NORMAL FORCE COEFFICIENT
CHECK					
APR					
APR					THE BOEING COMPANY

Fig. 2.6

PAGE 24

US 4013 8000

K•E ALBANENE® TRACING PAPER 71898

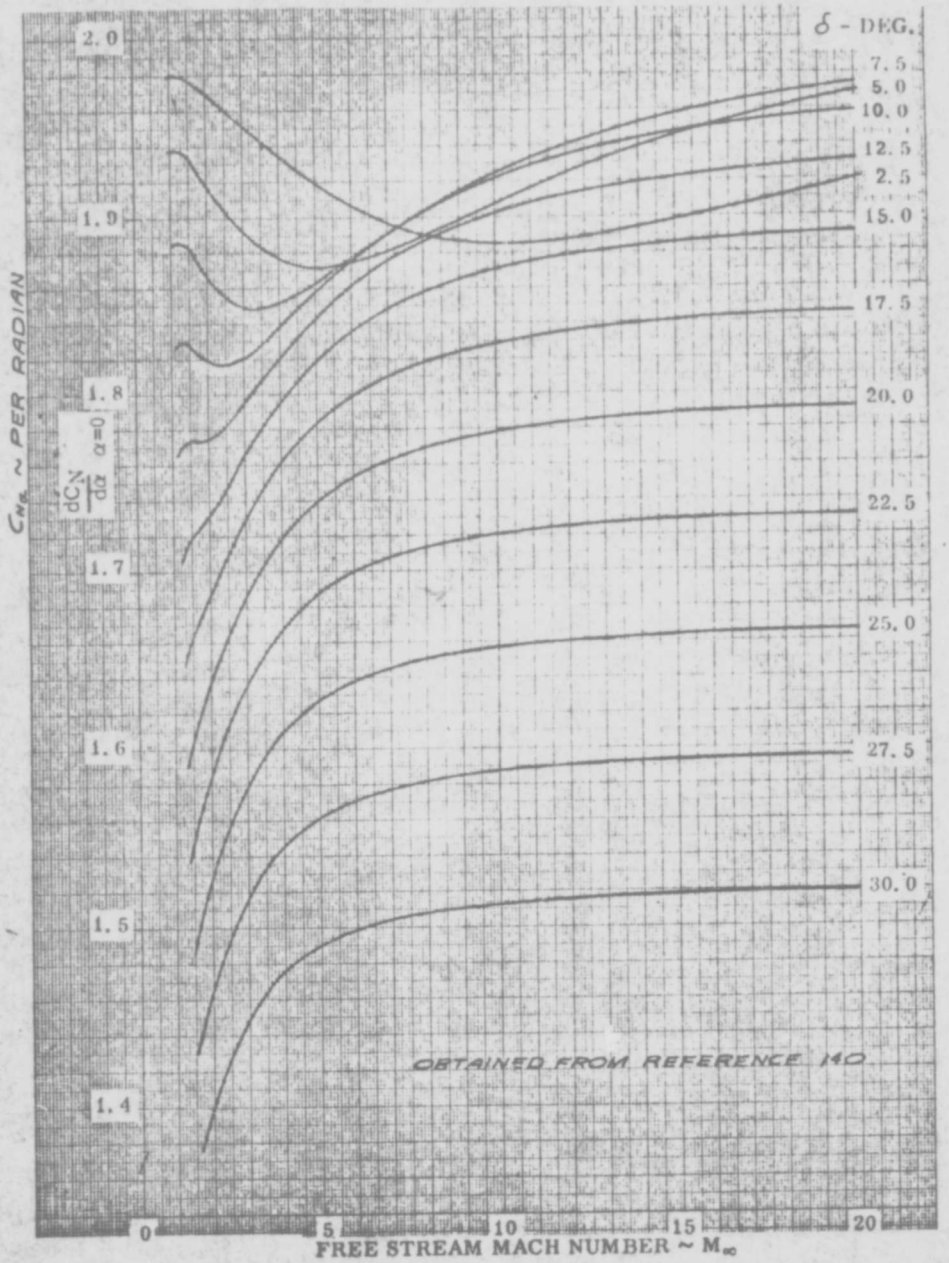

FIGURE 2.7 Slope of the normal-force-coefficient curve with change in free-stream Mach number for $\delta = 7.5$ to 30.

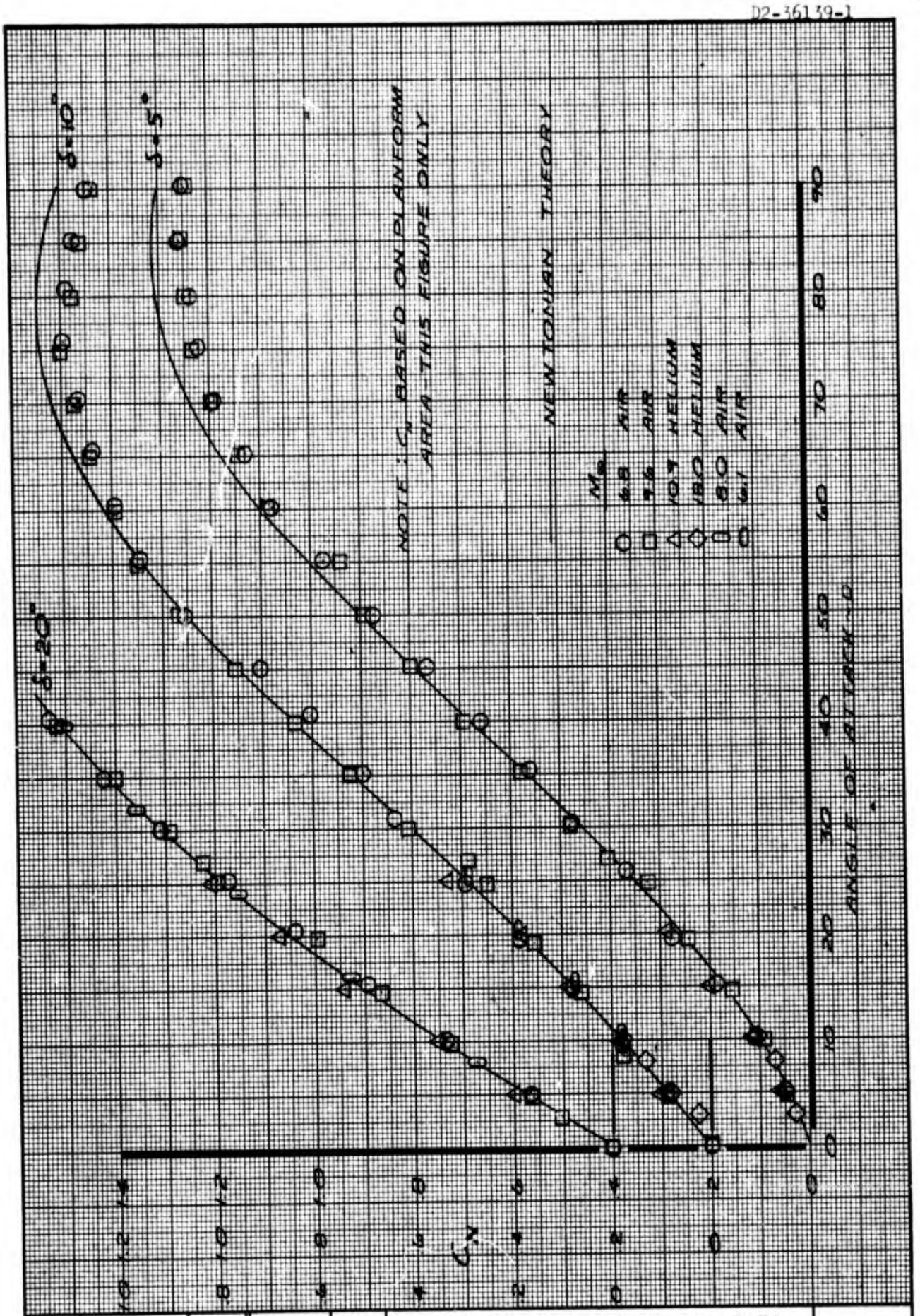

CALC	DWE	8/65	REVISED	DATE	COMPARISON OF EXPERIMENTAL DATA AND NEWTONIAN THEORY FOR SHARP CONES AT HYPERSONIC SPEEDS	Fig. 2.8
CHECK						
APR						
APR					THE BOEING COMPANY	PAGE 26

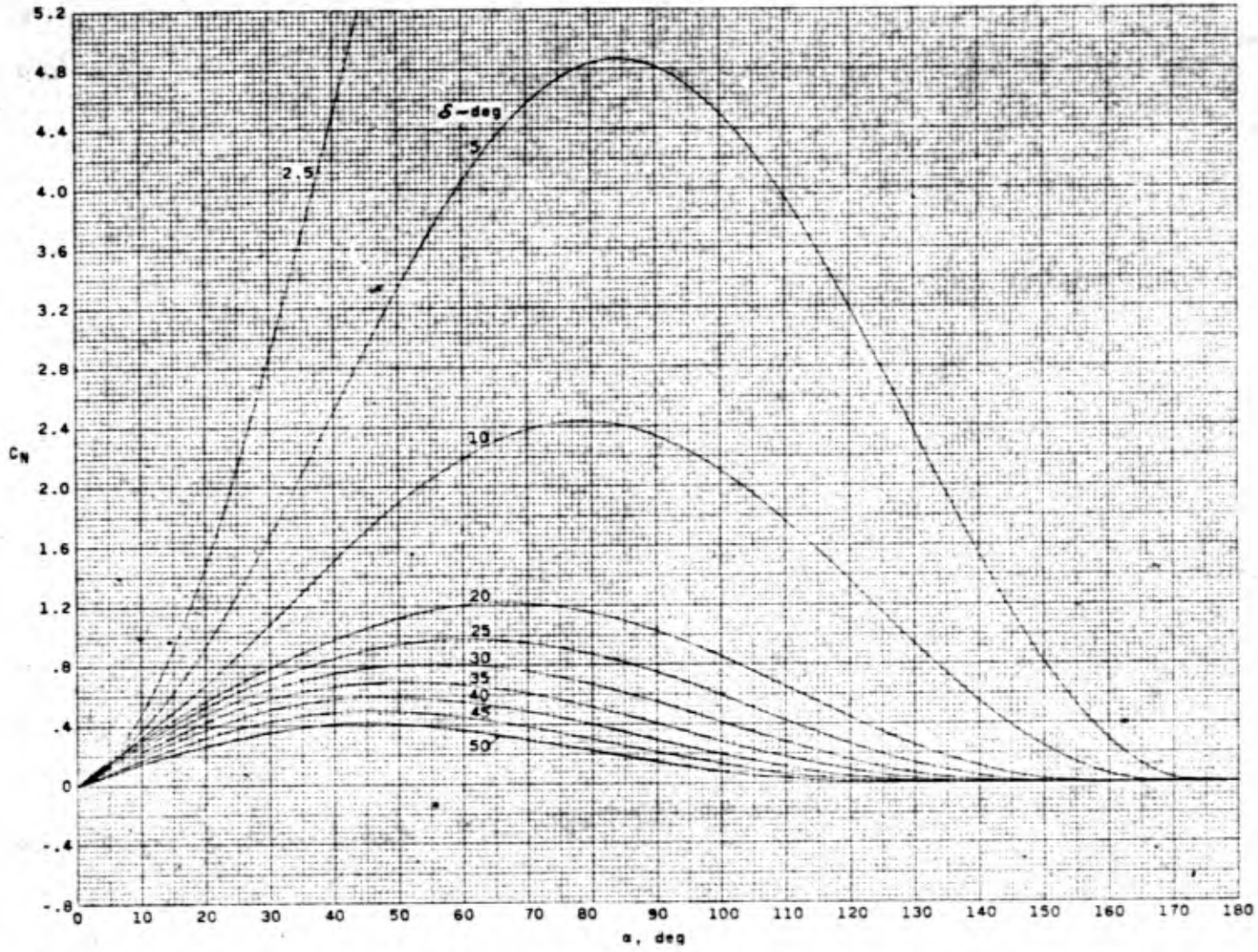

Figure 2.9 Normal-force coefficients of various cones in Newtonian flow; $C_{p,max} = 2.0$. Coefficients referenced to base area.

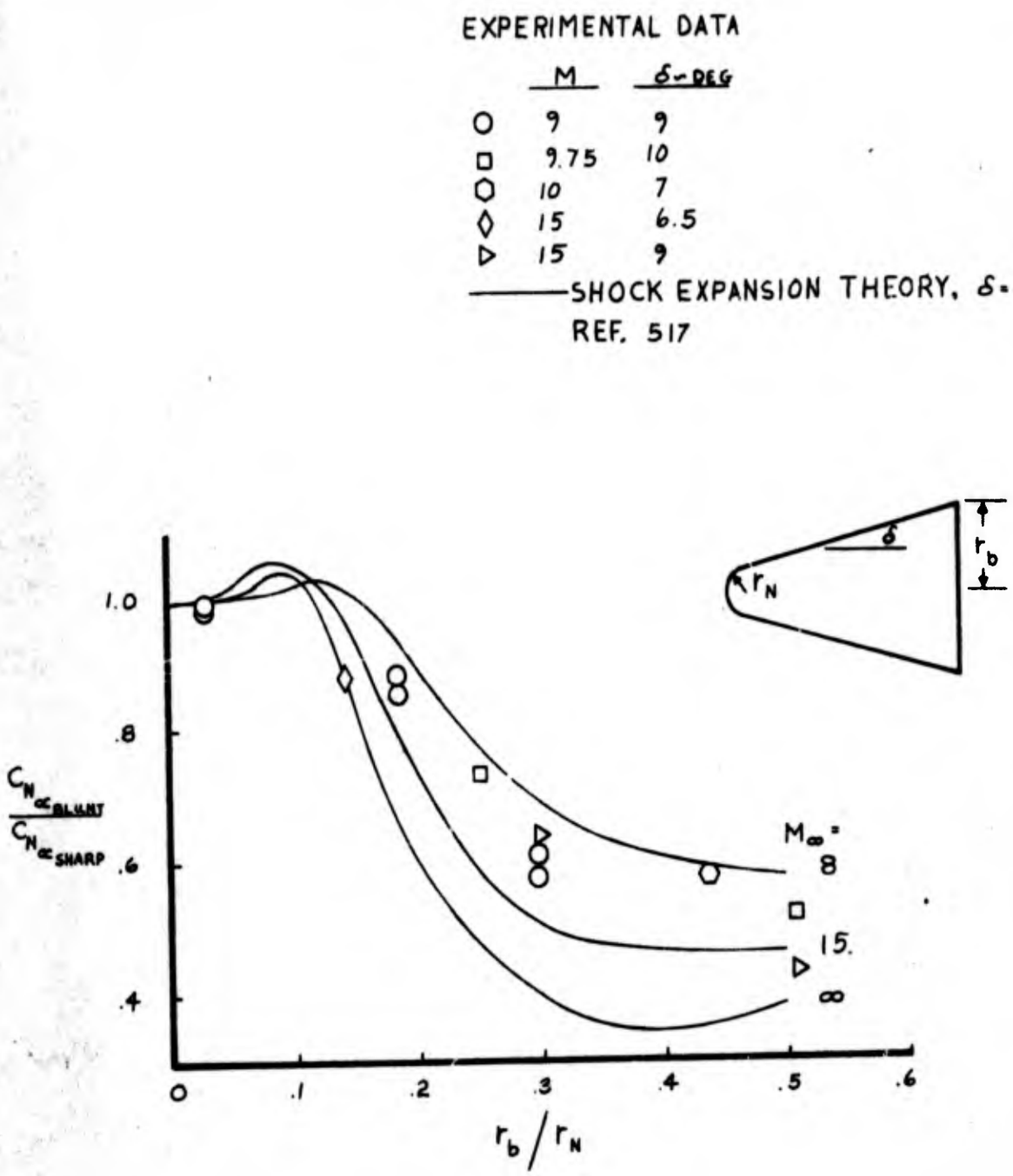

FIG. 2-10 EFFECT OF CONE NOSE BLUNTNESS ON C_{N_α} AT HYPERSONIC SPEEDS

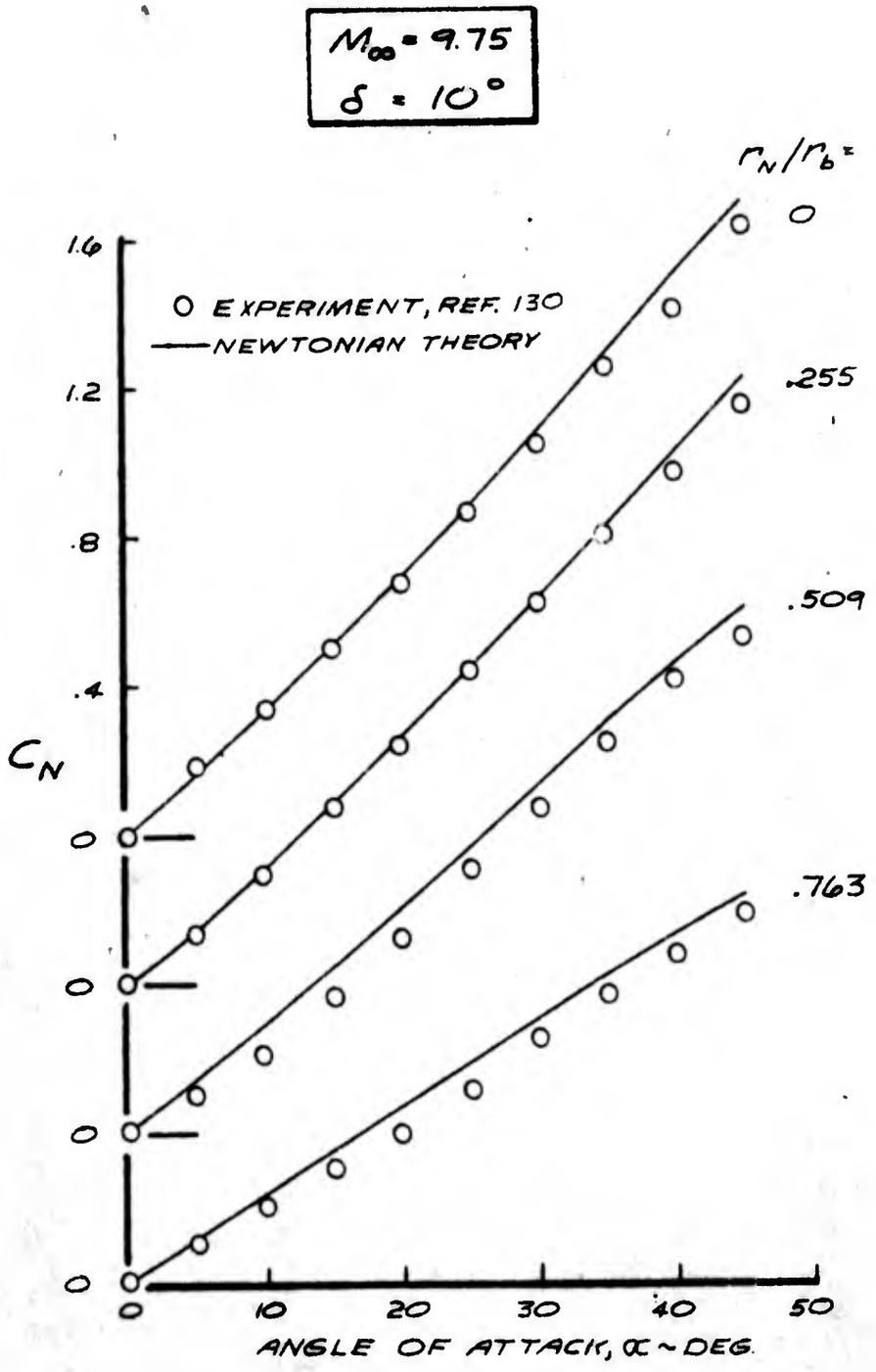

FIG. 2.11 COMPARISON OF EXPERIMENTAL DATA AND NEWTONIAN THEORY NORMAL FORCE COEFFICIENTS FOR CONES OF VARIOUS NOSE BLUNTNESS

3.0 PITCHING MOMENT AND CENTER OF PRESSURE

The pitching moment on a cone is defined by

$$C_M = \frac{C_N \quad X_{cp}}{\text{reference length}} \qquad 3.1$$

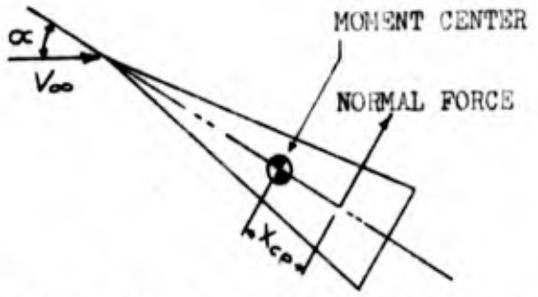

where X_{cp} is the distance from a given moment center to the center of pressure, cp. Since a clockwise moment is considered positive, X_{cp} is negative when measured aft of the moment center. The reference length is usually the cone length or base diameter.

References which contain pitching moment and center of pressure data are summarized on Pages 32 through 34.

Subsonic and Transonic Speeds

No adequate theory exists for calculating the normal force coefficient or the center of pressure at these speeds, but good estimates of X_{cp} can be made from experimental data. Figure 3.1 shows the variation of center of pressure with Mach number for sharp cones with several cone half-angles. The variation of X_{cp} with angle of attack is generally small; however, when accurate results are required data from the references listed on Page 30 should be used.

For blunt cones, the center of pressure can be estimated using Figures 3.1 through 3.3.

Figure 3.4 shows that rounding the base of a 12.5° cone changes the pitching moment characteristics at subsonic speeds significantly. These results suggest that base flow effects, and hence the method of mounting the model in a subsonic

wind tunnel may influence the aerodynamic forces and moments significantly. (The effects of rounding the base on C_N and $(C_{m_q} + C_{m_{\dot{\alpha}}})$ are shown in Figures 2.6 and 5.1.)

Supersonic and Hypersonic Speeds

For sharp cones both conical flow and Newtonian theories predict that the pressure is constant along a given ray passing through the cone apex and therefore, it can be shown geometrically that

$$\frac{X_{cp}}{\ell} = -\frac{2}{3\cos^2\delta} \qquad X_{cp} \text{ measured from apex} \qquad 3.2$$

For supersonic flow, the bow shock wave must be attached to the cone for this equation to be valid. Excluding this restriction, X_{cp} is independent of Mach number and is constant with angle of attack for $\alpha \leq 90^\circ$ for a flat based cone. Experimental results substantiate equation 3.2. Figures 3.5 and 3.6 show comparisons of theory and experimental data for cones at angles of attack to 60 degrees.

Figures 3.1 through 3.3 can be used to estimate the center of pressure location for blunt cones at supersonic speeds. At hypersonic speeds, Newtonian theory[117] can be used to calculate the center of pressure location. Figure 3.7 shows the Newtonian center of pressure for blunt cones at zero angle of attack, which is in excellent agreement with the experimental data of Figures 3.1 through 3.3. An excellent discussion of cone bluntness effects is presented in Reference 130.

As noted in Section 2.0, rounding the bases is not expected to alter the pressure distributions on the inclined surfaces and, consequently, will not alter the center of pressure location when referred to the apex, for small angles of attack.

EXPERIMENTAL CENTER OF PRESSURE AND PITCHING MOMENT DATA

REF.	MACH NUMBER	δ DEGREES	r_N / r_b	α_{MAX}
114.	.1	33.2	0	12
574.	.2	5 - 45	0	180
558.	.22 - 2.9	14	0	22
129.	.25 - 2.2	12.5	0 AND .5	18
157.	.25 - 2.2	12.5	.6	20
201.	.4 - 20	NONCONICAL SHAPES	-	15
204.	.4 - 20	NONCONICAL SHAPES	-	20
206.	.4 - 20	NONCONICAL SHAPES	-	20
562.	.47 - 1.93	10 - 50	0 - .8	6
180.	.5 - 1.1	0	5.7	28
529.	.5 - 4	9	.25	0
538.	.5 - 4.06	20 - 40	0 - .6	12
546.	.5 - 4.9	10 - 50	0 - .62	0
176.	.5 - 5	10 - 50	0 - .62	0
817.	.5 - 7	8	0 AND .11	28
69.	.5 - 21	10	.019	0
36.	.6 - 1.4	9	.04	16
4.	.6 - 1.5	7	0 - .022	6
405.	.6 - 2	7 - 10	0 - .8	0
127.	.6 - 3.2	10.7	.23	0
505.	.6 - 7.5	7	.22	0
136.	.65 - 2.2	20	0 AND .4	21
148.	.7 - 1.3	11.6	.38	8
131.	.7 - 2	10 - 40	0	4
306.	.8 - 9.9	10	.2	11
530.	1 - 4	10	0	0
211.	1 - 25	SUMMARY OF ALL LORV VEHICLE FLIGHT TESTS		
777.	1.36 - 4	10	0	0
163.	1.4 AND 2	3.55	0	20
186.	1.5 - 4.6	5.7	0	28
608.	1.5 - 10	10	0 - .85	22
526.	1.56 - 4.24	3.48 - 14.1	0	20
776.	1.56 - 4.24	3.48 - 14.1	0	20
508.	1.6 - 3.9	7.1	.22	11
576.	1.6 - 9	10 - 60	0 - 1	5
531.	1.7 - 3.3	9.5	0	0
524.	1.75 - 5	DOUBLE CONE	0	13
167.	2	10 AND 15	.26 AND .32	90
112.	2 AND 3	7.75	0	0
35.	2 - 10	9	.047	0

EXPERIMENTAL CENTER OF PRESSURE AND PITCHING MOMENT DATA

REF.	MACH NUMBER	δ DEGREES	r_N / r_b	α_{MAX}
75.	2 - 6	NONCONICAL SHAPES	-	20
30.	2 - 10	9	.05	15
61.	2 - 10	9	NONSPHERICAL	16
13	2 - 10	9	.017 - .207	18
70.	2 - 6	10 AND 15	0 AND .2	25
601.	2 - 5.6	10	0 - .5	30
55.	2 - 8	6.7	0	25
29.	2 - 10	11	0	18
16.	2 - 10	NONCONICAL SHAPES	-	18
171.	2.4 - 3.9	3.2	.5	25
165.	2.4 - 3.9	3.2	.5	90
31.	2.5 - 4	10	0	0
102.	2.75 - 5	4.1 - 9.4	0	25
504.	2.87	6.35	0	50
168.	2.94 - 4.78	15	0	90
177.	3 - 6.3	4.1 AND 5.72	0	0
64.	3 - 12	15	.113	10
305.	3 - 22	8	0	-
557.	3.1 - 5.5	8	.155	10
520.	3.8 - 5.8	9	0	108
705.	4	9	0	180
303.	4 - 20	8	0	20
513.	5 - 8	6	0	12
68.	5 - 10	10	.015	2
521.	6	9 AND 45	0	30
578.	6	15	.11	10
302.	6 - 19	8	0	16
816.	6.1	10	0	30
506.	6.5 - 14	SLENDER CONE	-	30
202.	6.5 - 17	8 - 16	.03 - .15	16
169.	6.7	22.3	.27	27
128.	6.77	9	0 - .66	180
101.	6.8	20	0	20
609.	6.8 - 4.7	9	0 - .3	30
117.	6.8 AND 9.6	10 - 40	0 AND .2	72
-80.	6.8 - 14.7	9	0 - .3	30
161.	6.8 AND 21.2	9	.33 AND .66	180
132.	6.8 - 25	5 - 50	0	30
174.	6.86	10.7	.23	5
182.	6.9	5	0 - .2	30

EXPERIMENTAL CENTER OF PRESSURE AND PITCHING MOMENT DATA

REF.	MACH NUMBER	δ DEGREES	r_N / r_b	α_{MAX}
162.	7	10 - 20	0 - .44	25
723.	7 - 10	6 - 15	0 - .2	0
527.	7.3 AND 9	9	.03 - .3	15
503.	8	6.33	0	15
401.	8	9	0 - .36	15
569.	8	9	0	25
54.	8	20	0 AND .4	46
407.	8 AND 10	9	0 - .36	15
37.	8 - 21.7	.3 - 12.5	0 - .5	40
702.	8 - 22	6.3 - 20	0 - .5	30
572.	8.04	9	0	25
571.	8.07	6.3	0	15
586.	8.3	20	0	30
203.	9 - 15	5.7 AND 8.3	VARIOUS SHAPES	20
33.	9 - 21	9 AND 10	0 - .3	25
410.	9 - 24	VARIOUS SHAPES	-	-
170.	9.6	10 - 40	.26	60
130.	9.7 - 19	10	0 - .76	45
54.	9.8	50	0	180
54.	9.8	10	.9	180
40.	10	6	VARIOUS SHAPES	26
20.	10	6.3	VARIOUS SHAPES	15
9.	10	8	0	12
78.	10	8	0 - .15	9
62.	10	8	.04	11
57.	10	8	.04	12
212.	10	8	.04	14
24.	10	9	0	20
79.	10	9	0 - .3	24
402.	10	9	0 - .36	15
59.	10	9	0	13
81.	10	9	.04	25
19.	10	10	0 - .3	10
28.	10	11	0	15
406.	10 - 20	OGIVE	0 - .12	15
715.	10 - 21	8 - 10	0 AND .035	25
539.	10.5 - 21	7.5 AND 10	0 AND .04	10
603.	11	9	.05	0
604.	11 - 16	8	.035	20
178.	11.5 - 34	30	0 AND .2	30

EXPERIMENTAL CENTER OF PRESSURE AND PITCHING MOMENT DATA

REF.	MACH NUMBER	δ DEGREES	r_N / r_b	α_{MAX}
10.	13 - 21	6.5 AND 9	.03 AND .3	45
66.	14	5.6	0 - .3	10
12.	14 - 22	7.1 AND 9	.03 - .3	40
523.	15 AND 18	10	.5 - .9	10
210.	16 - 25	9	0	7
65.	17	9	0	10
38.	17 - 20	11	0	16
76.	18	9	.1	20
209.	18 - 24	8	0	10
42.	19	5	VARIOUS SHAPES	20
15.	19	9	0	15
43.	19	9	.045	20
16.	19	11	0	15
584.	20	SUMMARY REPORT		
509.	20	7.1	.225	30
179.	20.3	5 - 90	0	110
134.	20.5 AND 24	5 - 20	0	20
131.	24.5	20 AND 45	0 - 1	20

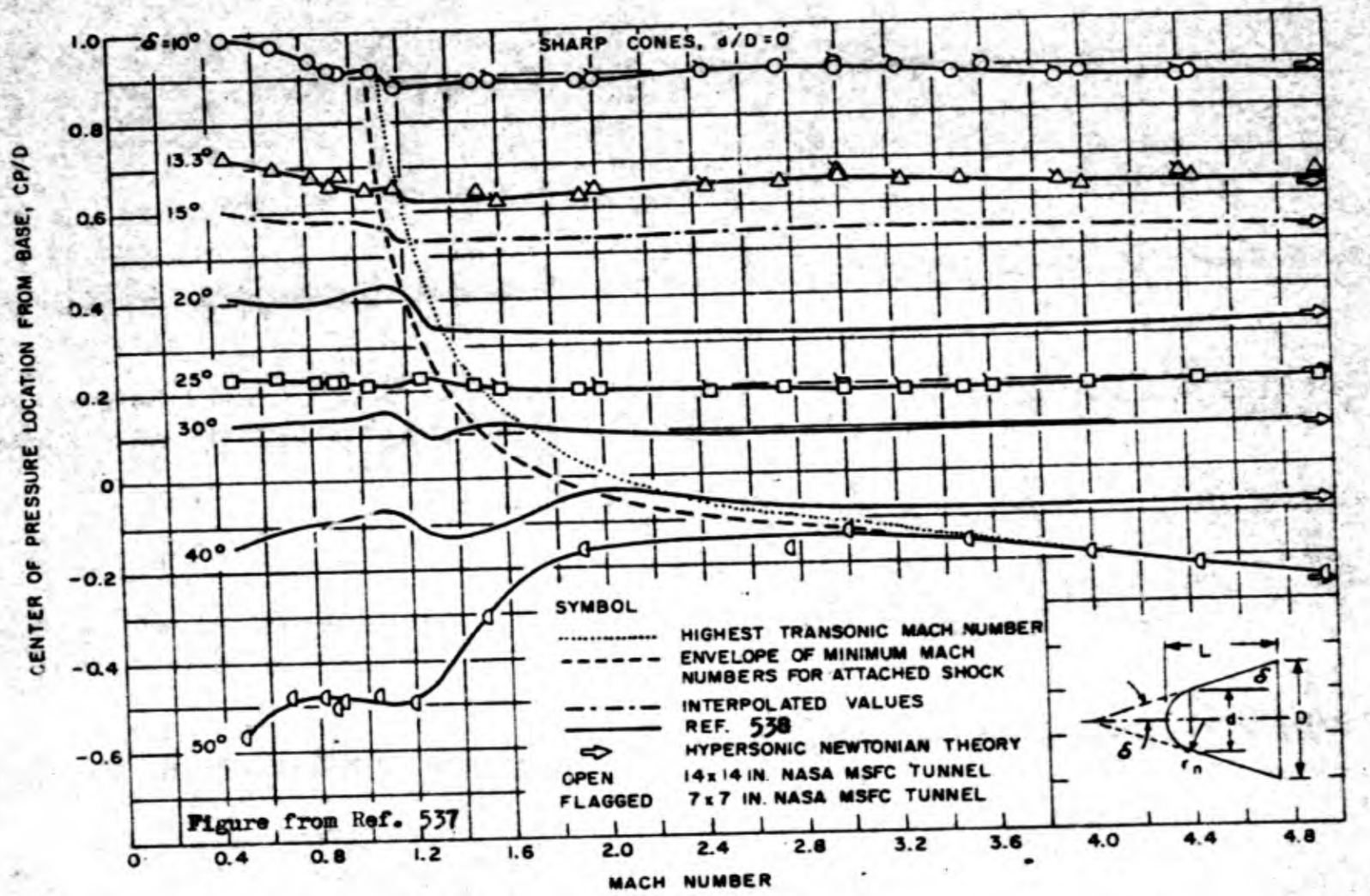

Figure 3.1 Variation of Center-of-Pressure with Mach Number for Various Sharp Nose Cones

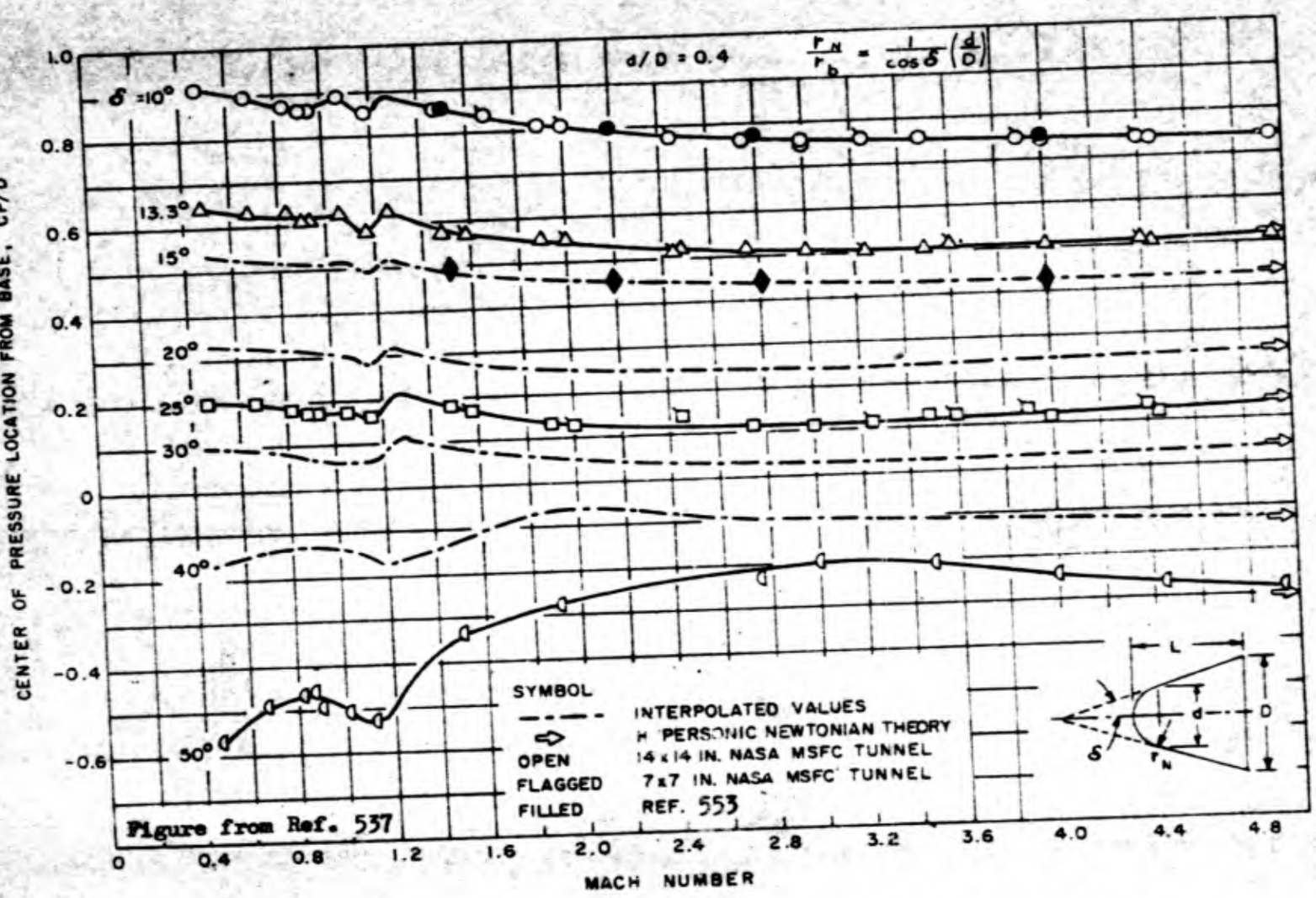

Figure 3.2 Variation of Center of Pressure with Mach Number for Blunt Cones with d/D = 0.4

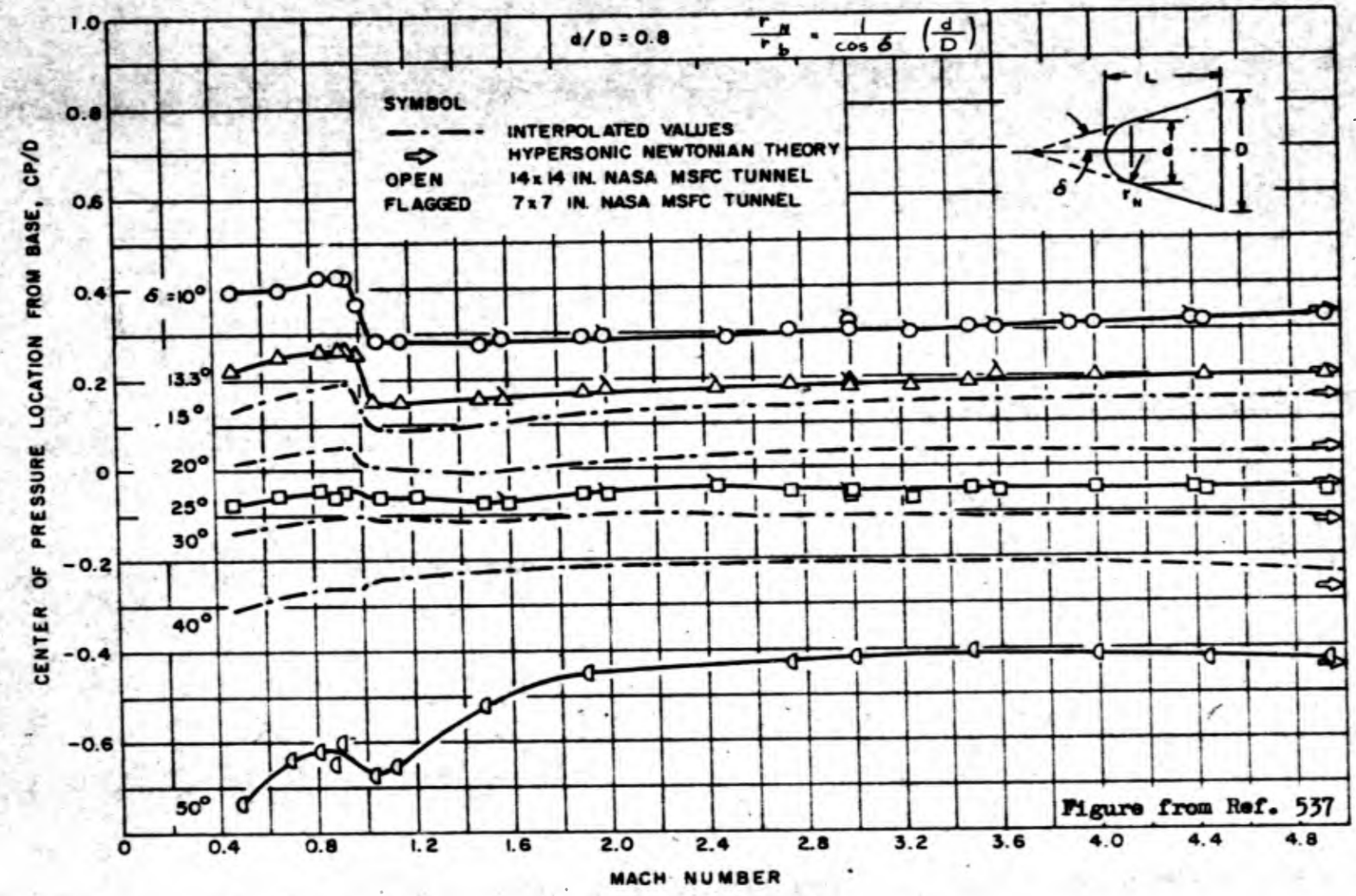

Figure 3.3 Variation of Center of Pressure with Mach Number for Blunt Cones with d/D = 0.8

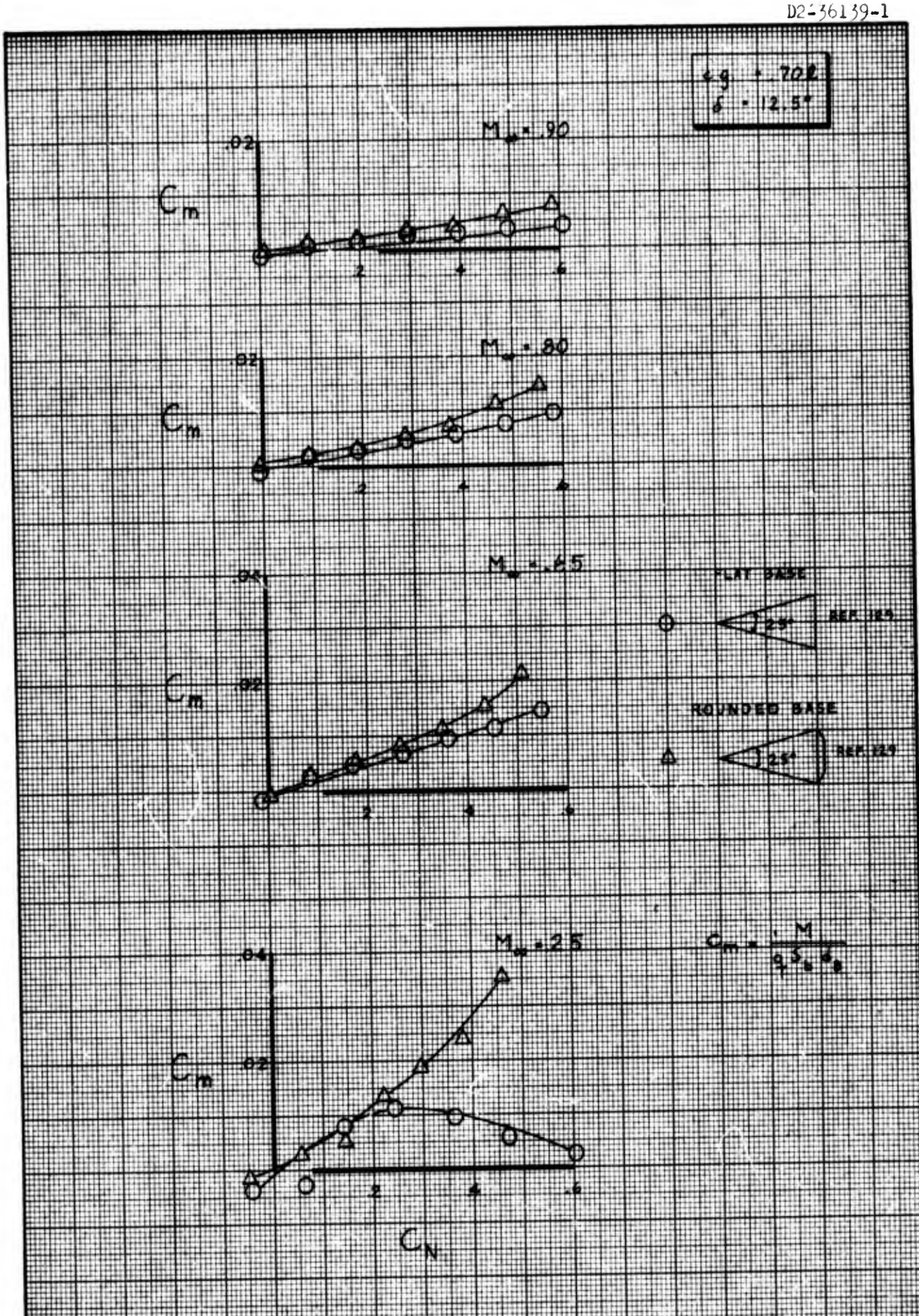

CALC	DWE	8/65	REVISED	DATE	THE EFFECT OF ROUNDING THE BASE ON CONE PITCHING MOMENT CHARACTERISTICS
CHECK					
APR					
APR					THE BOEING COMPANY

Fig. 3.4

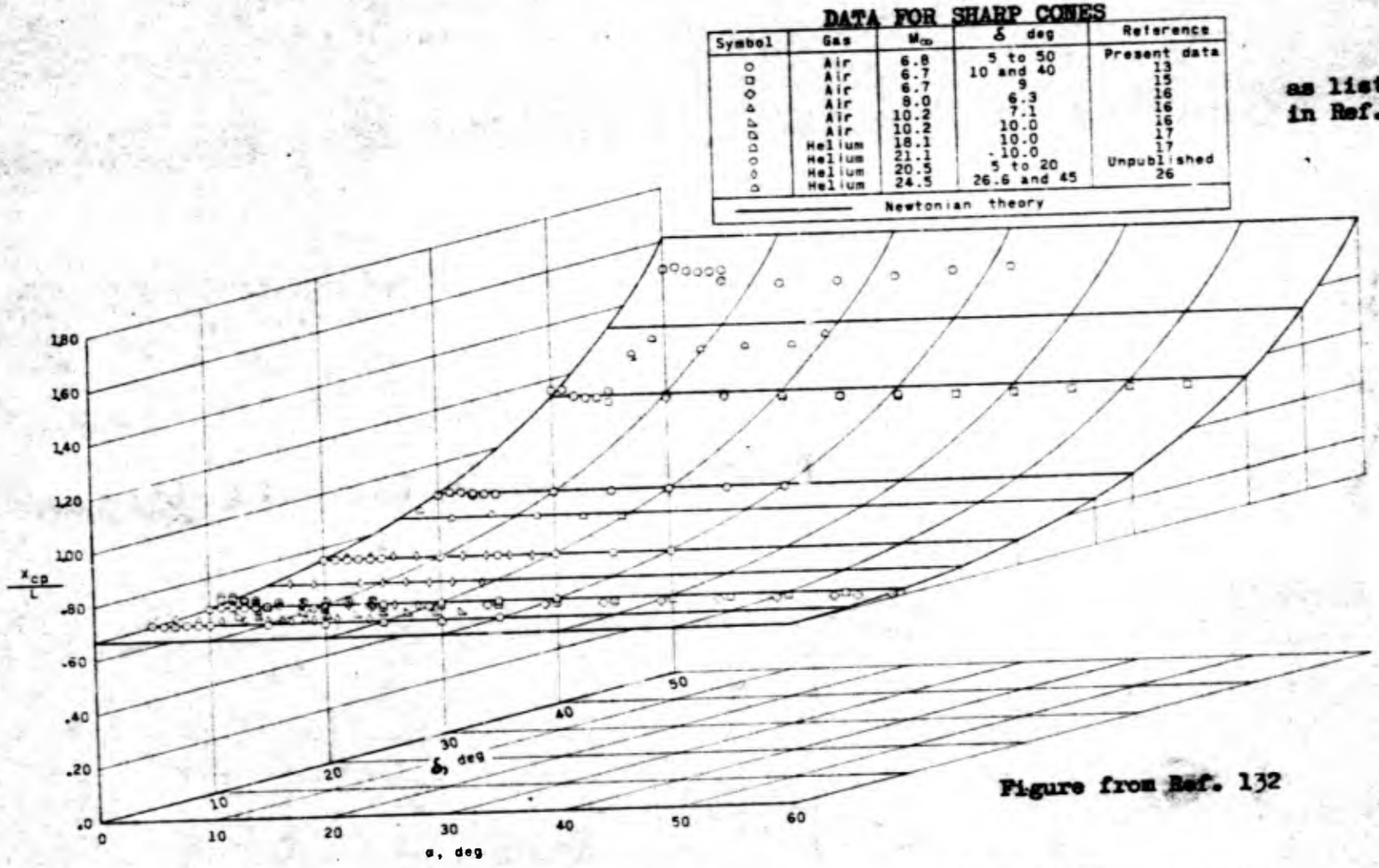

Figure 3.5 Variation of the location of center of pressure with angle of attack and semivertex angle for various hypersonic Mach numbers.

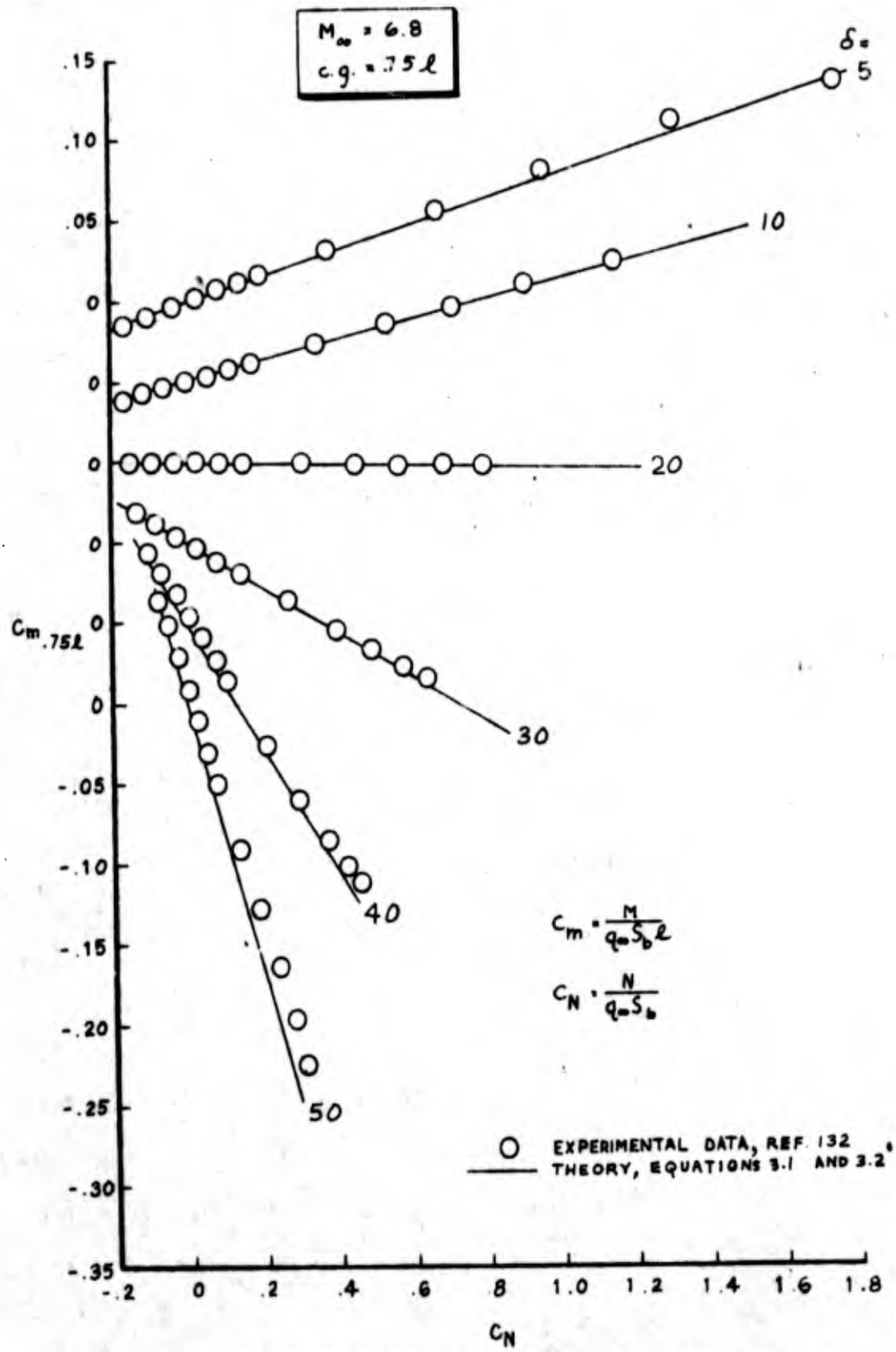

FIG. 3.6 COMPARISON OF THEORETICAL AND EXPERIMENTAL CENTER OF PRESSURE LOCATIONS FOR SHARP CONES

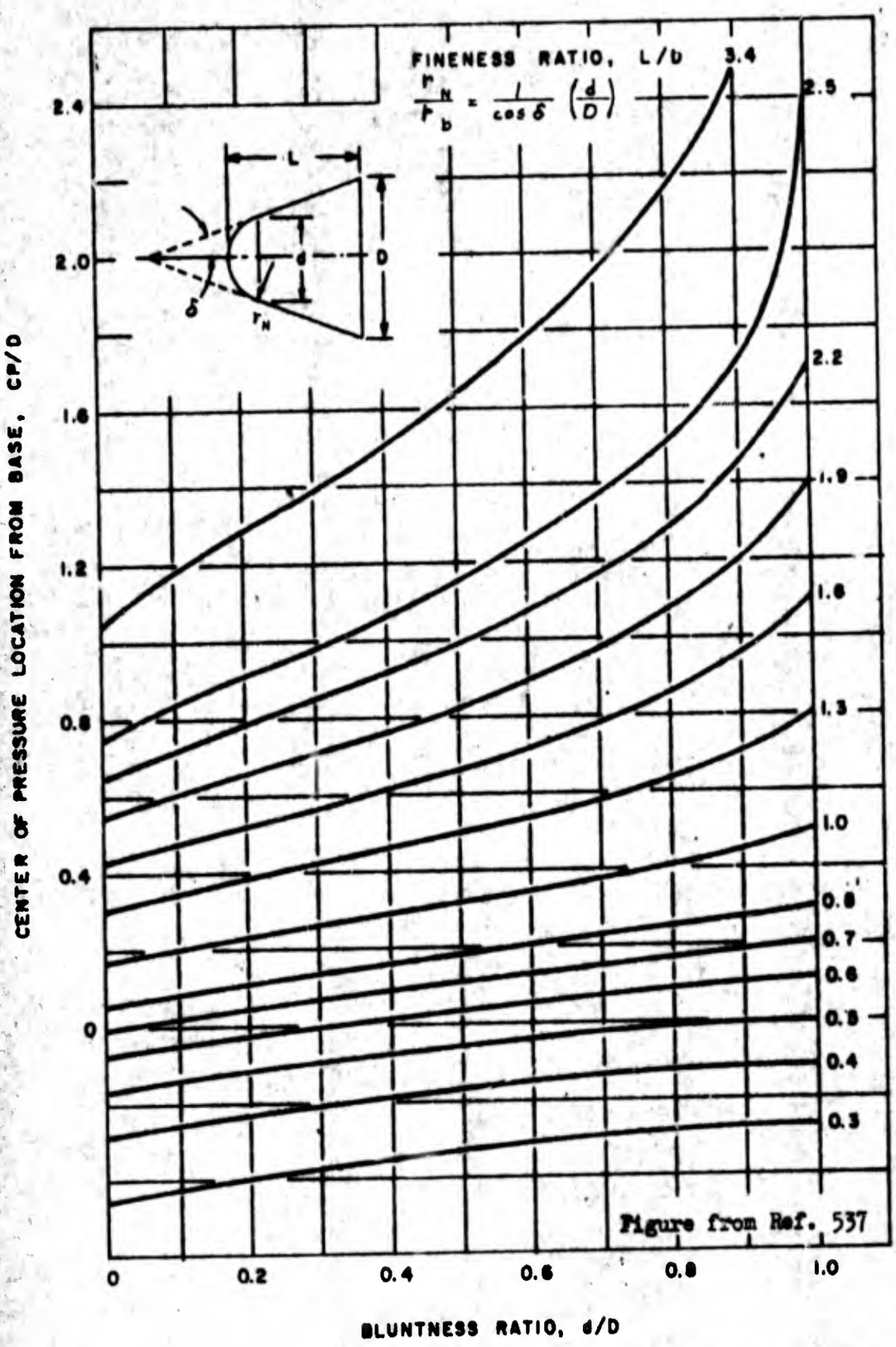

Figure 3.7 Hypersonic Newtonian Centers-of-Pressure for Cones of Varying Geometry. $\alpha \approx 0$

4.0 AXIAL FORCE

The axial force coefficient on a cone is defined by

$$C_A = \frac{(\text{force along cone axis})}{(\text{dynamic pressure})(\text{reference area})}$$

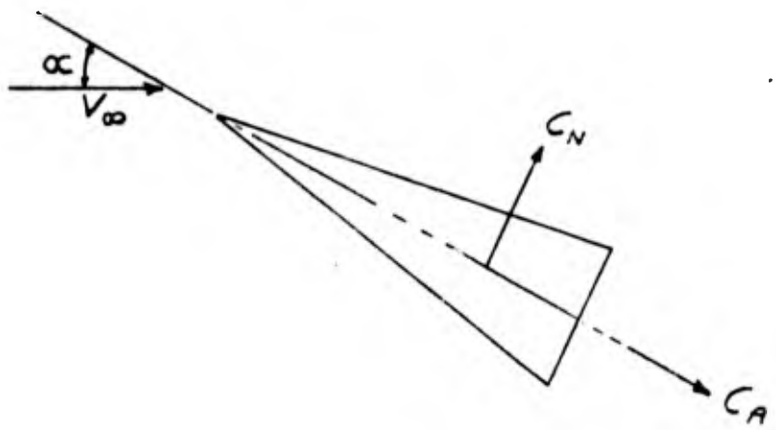

The reference area is usually taken as the cone base area, though occasionally it is based on the planform area.

References which contain axial force coefficient data are summarized on Pages 52 through 55.

For simplicity of calculation, the axial force coefficient is usually assumed to be the sum of the following increments:

1) Forebody axial pressure force coefficient (commonly called wave drag at supersonic and hypersonic speeds)
2) Base pressure axial force coefficient
3) Skin friction axial force coefficient.

At zero angle of attack the axial force and drag force vectors coincide (see Page 12). Therefore, many of the curves included here are labeled "drag

coefficient" instead of axial force coefficient. The terms are interchangeable only at zero angle of attack.

Forebody Axial Pressure Force

a. Subsonic and Transonic Speeds

No theory has been established at these speeds, however, the experimental data shown in Figure 4.1 can be used to accurately estimate forebody axial pressure coefficients for sharp unyawed cones. The data in this figure do not include base pressure axial force but include skin friction axial force which is small and can be considered negligible for cones with half-angles greater than 10 degrees. Experimental data indicate that forebody axial pressure force is essentially constant with angle of attack at $\alpha \leq 20°$; for $\alpha > 20°$ little experimental data are available.

For blunt cones, Figures 4.1 through 4.3 can be used to determine the effect of bluntness on forebody axial pressure forces. For blunt cones the force can be assumed constant for $\alpha \leq 20°$.

b. Supersonic and Hypersonic Speeds

The theoretical forebody axial pressure force coefficient (referenced to cone base area) for a sharp unyawed cone is equal to the pressure coefficient on the cone surface. This coefficient, as well as the skin friction coefficients and the complete shock layer flow field, is calculated by the unyawed cone computer programs* discussed in Section 12. Either a perfect gas or real air may be used. Solutions for a wide range of cone

* See Figures 4.17 and 4.18 for sample outputs.

angles and freestream conditions are published in Reference 139 for perfect air ($\gamma = 1.4$), and in References 515 and 566 for equilibrium real air.

The theoretical forebody axial pressure force coefficients for unyawed cones in perfect air are shown in Figures 4.4 and 4.5. Figure 4.6, as well as other calculations,[566] shows that real air effects have little influence on the forebody axial pressure force and therefore, Figures 4.4 and 4.5 can be used at most freestream conditions.

Unfortunately, the hypersonic zero angle of attack forebody axial pressure force coefficient is too often calculated using Newtonian theory

$$C_{A_{\substack{\text{FOREBODY}\\\text{PRESSURE}}}} = 2 \sin^2 \delta \qquad 4.1$$

Figure 4.6 shows this equation underestimates $C_{A_{FP}}$ for very slender cones and for cones at low hypersonic Mach numbers.

The variation of forebody axial pressure force coefficient with angle of attack at supersonic speeds can be determined using the existing experimental data summarized on Page 54 . These data include skin friction and base pressure forces; however, when it is assumed that skin friction and base pressure are constant with angle of attack, the forebody axial pressure force component can be obtained by

$$C_{A_{\substack{\text{FOREBODY}\\\text{PRESSURE}}}} = C_{A_{TOTAL}} - \left(C_{A_{\substack{\text{BASE}\\\text{DRAG}}}} + C_{A_{FRICTION}}\right)_{\alpha=0} \qquad 4.2$$

At hypersonic speeds the variation of the forebody axial pressure force coefficient with angle of attack can be obtained from Figures 4.7 and 4.8. Figure 4.7 was obtained by fairing the results from Newtonian theory[117] into the "exact" zero angle of attack results[139] evaluated at $M_\infty = 20$.

The Inverse Method Blunt Body and Method of Characteristics Body Computer Programs were used to calculate the forebody axial pressure force coefficient for blunt slender cones at zero angle of attack. The forebody axial pressure force coefficient for the corresponding sharp cones were then subtracted from these coefficients to give the incremental change in forebody axial pressure force coefficient due to nose bluntness, i.e.

$$\left(\Delta C_{A_{FP}}\right)_{BLUNTNESS} = \left(C_{A_{FP}}\right)_{\substack{BLUNT \\ CONE}} - \left(C_{A_{FP}}\right)_{\substack{SHARP \\ CONE}}$$

Figures 4.9a-c show the variation of this increment with nose bluntness ratio for cones of 5°, 9°, and 13° half-angle. Also shown are Newtonian results obtained from Figure 4.10.

The experimental results in Figures 4.9a-c were obtained by subtracting the <u>total</u> axial force for a sharp cone from the <u>total</u> axial force for a corresponding blunt cone. Therefore, the effects of bluntness on skin friction and base pressure are included in the experimental results. ase pressure is small and is probably not significantly changed by nose bluntness. A preliminary study indicates that blunting the nose will reduce skin friction. Therefore, the experimental data in Figures 4.9a-c should fall below the theoretical results. Such is the case.

Figures 4.9a-c show that the axial force on a slender cone may be reduced by some blunting. The reason for this is discussed in Section 6.0.

Base Pressure and Base Axial Force

References which contain experimental base pressure data are summarized on Page 55.

Of all static aerodynamic data, the base axial force (or drag) coefficient is probably the most difficult to determine, both theoreticall and experimentally. Experimental results depend on cone geometry, Mach number, Reynolds number and the method of mounting the cone in the experimental facility. The base pressure is usually assumed to be constant over the base and is related to the base drag by

$$C_{A_{BASE}} = -C_{P_{BASE}} S_{BASE} \qquad 4.3$$

Figure 4.11 shows wind tunnel data which indicate that the base pressure coefficient is:

1) nearly constant with angle of attack
2) nearly independent of cone half angle
3) larger for a cone than for a cone-cylinder

Figure 4.12 indicates that blunting the nose or rounding the base has little effect on the base pressure.

Figures 4.13 shows the large effect of free stream Reynolds number and wind tunnel mounting method on the base pressure coefficient. Transition of the base flow from laminar to turbulent flow was assumed to occur at the point where the base pressure coefficient was a minimum. This location was verified by schlieren photographs. The base pressure appears to be nearly independent of Reynolds number for turbulent flow. This is in agreement with results predicted by the Boeing Turbulent Base Flow theory[808]. The ratio of sting

to model diameter appears to have opposite effects on laminar and turbulent base pressures. Increasing sting diameter decreases the laminar base pressure, while increasing the turbulent base pressure.

Figure 4.14 shows existing wind tunnel test data for cones. Also shown is the Boeing Turbulent Base Flow theory[808] for supersonic flow which compares well with experimental data. This figure is intended to give an approximate estimate of wind tunnel base pressure, since it does not show the effects of cone geometry, Reynolds number or model mounting.

Base drag on bodies in free flight appears to be significantly different from base drag measured in wind tunnel tests. Figure 4.15 shows the total cone axial forces measured in a ballistic range test and a free flight test. Note that at subsonic speeds the total drag for these bodies is <u>less</u> than the wind tunnel base drag from Figure 4.14. Two possible explanations for this discrepancy are:

1) The pressure distribution over the cone forebody gives a net thrust, thus reducing drag. This is observed in Reference 129, where measured subsonic total drag is slightly less than base drag. However, this difference is small compared to that shown in Figure 4.15.
2) Wind tunnel mounting effects may significantly increase the base pressure over the free flight value.

Until additional experimental results are obtained it is recommended that for subsonic speeds wind tunnel drag data be corrected using Figure 4.14 and free flight data be estimated using Figure 4.15.

Skin Friction Axial Force

Many theories have been proposed for calculating laminar and turbulent skin friction coefficients. These theories are referenced in the Boeing Skin Friction Handbook[821]. The Reference Temperature and Reference Enthalpy methods for calculating laminar and turbulent boundary layers have gained wide acceptance because of their simplicity and accuracy. Boeing has developed more sophisticated techniques for calculating laminar[820 and 821] and turbulent[822] boundary layers. However, the results differ little from those calculated using the Reference Temperature and Enthalpy methods.

a. Subsonic and Transonic Flow

For subsonic and transonic flow assume that the boundary layer edge conditions are equal to free steam conditions.

$$Re_{c_\ell} \approx Re_{\infty_\ell} \qquad T_c \approx T_\infty$$

$$q_c \approx q_\infty \qquad \rho_c \approx \rho_\infty$$

The skin friction can then be calculated using Equations 4.4, 4.10 and 4.11. The viscosity can be obtained from Figure 4.16.

b. Supersonic and Hypersonic Flow

The Unyawed Cone computer programs discussed in Section 12 compute the laminar and turbulent average skin friction coefficients for cones in supersonic and hypersonic flows. For perfect air the reference temperature method is used, and for real air the reference enthalpy method is used. A summary of these methods follows.

The reference temperature and enthalpy are

$$T^* = .22\,T_r + .28\,T_c + .5\,T_w \qquad 4.4$$

$$h^* = .22\,h_r + .28\,h_c + .5\,h_w \qquad 4.5$$

where the recovery conditions are

$$T_r = T_\infty + \frac{r V_\infty^2}{12{,}000} \qquad 4.6$$

$$h_r = h_\infty + \frac{r V_\infty^2}{50{,}000} \qquad 4.7$$

A recovery factor, r, of .85 is used for laminar flow and a factor of .90 is used for turbulent flow.

For laminar flow

$$C_{F_{CONE}} \sqrt{Re_{c_\ell}} = 1.53 \sqrt{\cos\delta} \sqrt{\frac{\rho^* \mu^*}{\rho_c \mu_c}} \qquad 4.8$$

For turbulent flow

$$C_{F_{CONE}} = \frac{.481\,(\rho^*/\rho_c)}{\left[\log_{10}\left(Re_{c_\ell}\, \rho^* \mu_c / (\rho_c \mu^* \cos\delta)\right)\right]^{2.6}} \qquad 4.9$$

It is preferable to base the skin friction on free stream dynamic pressure and cone base area. For laminar flow

$$C_{A_{FRICTION}} = \left(\frac{q_c}{q_\infty}\right) \frac{1.53}{\sin\delta} \sqrt{\frac{\cos\delta}{Re_{c_\ell}}} \sqrt{\frac{\rho^* \mu^*}{\rho_c \mu_c}} \qquad 4.10$$

For turbulent flow

$$C_{A_{FRICTION}} = \left(\frac{q_c}{q_\infty}\right) \frac{1}{\sin\delta} \frac{.481\,(\rho^*/\rho_c)}{\left[\log_{10}\left(Re_{c_\ell}\, \rho^* \mu_c / (\rho_c \mu^* \cos\delta)\right)\right]^{2.6}} \qquad 4.11$$

The Perfect Air Unyawed Cone computer program also calculates the incremental drag due to viscous interaction effects on cones in low density

hypersonic flow. The method of calculation and results are completely discussed in Reference 824.

The approximate effect of nose bluntness on skin friction is also calculated by the Unyawed Cone computer programs. The following assumptions are made.

1. The boundary layer edge pressure is the same as for a sharp cone with the same half angle. Figure 6.7 shows this assumption to be quite valid downstream of the blunt nose.
2. The boundary layer edge entropy is assumed to be equal to the entropy of the streamline which passes through the normal shock at the blunt nose. This assumption neglects the fact that the high entropy flow from the blunt nose is absorbed into the boundary layer as it moves downstream. This assumption gives the maximum change in skin friction due to nose bluntness. Actually the change in skin friction will be somewhat less.

The other boundary layer edge conditions are calculated as a function of sharp cone pressure and normal shock entropy. The skin friction is then calculated using Equations 4.4 through 4.11. Calculated results show that nose bluntness reduces skin friction drag.

Sample output from the Real Air Unyawed Cone computer program is shown in Figure 4.18. The required input for this program are free stream pressure, temperature and velocity; cone half-angle and length; and wall temperature.

Sample output from the Perfect Air Unyawed Cone computer program is shown in Figure 4.17. The required input for this program are gas constant, isentropic exponent, free stream Mach number, pressure and temperature; cone half-angle length; and wall temperature.

Figure 4.19 shows the excellent comparison of experimental and theoretical drag, calculated using the Perfect Air Unyawed Cone program, for slender nearly sharp cones. The experimental results were obtained in low Reynolds number flow where the boundary layer is laminar and viscous interaction effects are significant.

Figure 4.20 shows the excellent comparison of experimental and calculated drag for sharp and blunt cones in low Reynolds number flow. Note that by slightly blunting the cone (r_N/r_b = .03) the drag coefficient is reduced. The incremental pressure drag due to bluntness for the highly blunted cone (r_N/r_b = .30) was obtained from Figure 4.9b.

Figure 4.21 shows the comparison of flight test and calculated drag coefficient for the slender cone LORV reentry vehicle. The LORV data is classified SECRET and therefore, the scales have been left off the axes in Figure 4.21. Theoretical results were calculated using the Real Air Unyawed Cone computer program. Boundary layer transition was estimated using Figure 7.3. Transition was assumed to end when the boundary layer at one-tenth of the cone length became turbulent. Figure 4.21 shows that at high altitudes, where laminar flow occurs, the drag coefficient is overestimated. However, at these altitudes the total drag force is small and the flight test measurements may have been inaccurate. Note that as altitude decreases the laminar prediction compares better with flight test data. At low altitudes, where turbulent flow occurs, theoretical and test data compare very well.

EXPERIMENTAL AXIAL FORCE DATA

REF.	MACH NUMBER	δ DEGREES	r_N / r_b	α_{MAX}
801.	.1	15 AND 30	0 - .5	20
114.	.1	33.2	0	12
574.	.2	5 - 45	0	180
507.	.2 - 3.5	10	0 - 1	0
129.	.25 - 2.2	12.5	0 AND .6	18
157.	.25 - 2.2	12.5	.6	20
201.	.4 - 20	NONCONICAL SHAPES	-	15
204.	.4 - 20	NONCONICAL SHAPES	-	20
206.	.4 - 20	NONCONICAL SHAPES	-	20
562.	.47 - 1.93	10 - 50	0 - .8	6
180.	.5 - 1.1	0	5.7	28
525.	.5 - 4	9	.25	0
538.	.5 - 4.06	20 - 40	0 - .5	12
546.	.5 - 4.9	10 - 50	0 - .62	0
176.	.5 - 5	10 - 50	0 - .62	0
817.	.5 - 7	8	0 AND .11	28
543.	.6 - 1.4	5 - 25	0	0
36.	.6 - 1.4	9	.04	16
4.	.6 - 1.5	7	0 - .022	6
127.	.6 - 3.2	10.7	.23	0
529.	.6 - 5	45	0	0
505.	.6 - 7.5	7	.22	0
136.	.65 - 2.2	20	0 AND .4	21
148.	.7 - 1.3	11.6	.38	8
181.	.7 - 2	10 - 40	0	4
306.	.8 - 9.9	10	.2	11
211.	1 - 25	SUMMARY OF ALL LORV VEHICLE FLIGHT TESTS		
155.	1.2 - 7.5	5.2 - 9.5	0 - .5	0
113.	1.24 - 7.4	5 - 10	0 - 1	0
163.	1.4 AND 2	3.55	0	26
561.	1.5 AND 2	10 AND 15	0	2
186.	1.5 - 4.6	5.7	0	28
608.	1.5 - 10	10	0 - .85	22
526.	1.56 - 4.24	3.48 - 14.1	0	20
153.	1.6 - 2.4	15	0	0
508.	1.6 - 3.9	7.1	.22	11
576.	1.6 - 9	10 - 60	0 - 1	5
524.	1.75 - 5	DOUBLE CONE	0	13
167.	2	10 AND 15	.26 AND .32	90
112.	2 AND 3	7.75	0	0

EXPERIMENTAL AXIAL FORCE DATA

REF.	MACH NUMBER	δ DEGREES	r_N / r_b	α_{MAX}
541.	2 - 4	15	0	0
601.	2 - 5.6	10	0	30
75.	2 - 6	NONCONICAL SHAPES	-	20
70.	2 - 6	10 AND 15	0 AND .2	25
13	2 - 10	9	.017 - .207	18
30.	2 - 10	9	.05	15
61.	2 - 10	9	NONSPHERICAL	16
29.	2 - 10	11	0	18
16.	2 - 10	NONCONICAL SHAPES	-	18
6.	2 - 11	SPHERE	-	-
704.	2 - 11	SPHERE	-	-
171.	2.4 - 3.9	3.2	.5	25
102.	2.75 - 5	4.1 - 9.4	0	25
168.	2.94 - 4.78	15	0	90
177.	3 - 6.3	4.1 AND 5.72	0	0
602.	3 - 15	10 - 18	0 - .05	0
305.	3 - 22	8	0	-
557.	3.1 - 5.5	8	.155	10
67.	3.5 - 4.8	9	0	0
580.	3.5 - 9.2	9	0 AND .28	0
520.	3.8 - 5.8	9	0	180
710.	3.9 AND 5.6	5	0	0
303.	4 - 20	8	0	20
705.	4	9	0	180
45.	6 - 10	15	.333	15
32.	6 AND 10	7.5	0	0
577.	6 - 14	6.3	.03	0
302.	6 - 19	8	0	16
816.	6.1	10	0	30
506.	6.5 - 14	SLENDER CONE	-	30
202.	6.5 - 17	8 - 16	.03 - .15	16
169.	6.7	22.3	.27	27
128.	6.77	9	0 - .66	180
101.	6.8	20	0	20
609.	6.8 - 4.7	9	0 - .3	30
117.	6.8 AND 9.6	10 - 40	0 AND .2	72
80.	6.8 - 14.7	9	0 - .3	30
161.	6.8 AND 21.2	9	.33 AND .66	180
132.	6.8 - 25	5 - 50	0	30
182.	6.9	5	0 - .2	30

EXPERIMENTAL AXIAL FORCE DATA

REF.	MACH NUMBER	δ DEGREES	r_N / r_b	α_{MAX}
162.	7	10 - 20	0 - .44	25
723.	7 - 10	6 - 15	0 - .2	0
527.	7.3 AND 9	9	.03 - .3	15
564.	7.2 - 21.5	FLAT PLATE	-	20
17.	7.5 - 12	10	.9	170
503.	8	6.33	0	15
401.	8	9	0 - .36	15
569.	8	9	0	25
54.	8	20	0 AND .4	46
407.	8 AND 10	9	0 - .36	15
406.	8 - 20	OGIVE	0 - .12	15
571.	8.07	6.3	0	15
586.	8.3	20	0	30
203.	9 - 15	5.7 AND 8.3	VARIOUS SHAPES	20
58.	9 AND 18	9	.3	
33.	9 - 21	9 AND 10	0 - .3	25
8.	9 - 22	6.34 - 13.35	0 - .38	0
712.	9 - 22	6 - 13.5	0 - .38	0
410.	9 - 24	VARIOUS SHAPES	-	-
585.	9.1 - 16	10	0	0
170.	9.6	10 - 40	.26	60
130.	9.7 - 19	10	0 - .76	45
54.	9.8	10	.9	180
54.	9.8	50	0	180
40.	10	6	VARIOUS SHAPES	26
20.	10	6.3	VARIOUS SHAPES	15
24.	10	9	0	20
402.	10	9	0 - .36	15
28.	10	11	0	15
715.	10 - 21	8 - 10	0 AND .035	25
539.	10 AND 21.2	7.5 10	0 AND .04	10
539.	10.5 - 21	7.5 AND 10	0 AND .04	10
603.	11	9	.05	0
604.	11 - 16	8	.035	20
178.	11.5 - 34	30	0 AND .2	30
10.	13 - 21	6.5 AND 9	.03 AND .3	45
12.	14 - 22	7.1 AND 9	.03 - .3	40
523.	15 AND 18	10	.5 - .9	10
210.	16 - 25	9	0	7
38.	17 - 20	11	0	16

EXPERIMENTAL AXIAL FORCE DATA

REF.	MACH NUMBER	δ DEGREES	r_N / r_b	α_{MAX}
76.	18	9	.1	20
209.	18 - 24	8	0	10
154.	18 AND 24.5	30 - 40	.22	180
42.	19	6	VARIOUS SHAPES	20
15.	19	9	0	15
43.	19	9	.045	20
18.	19	11	0	15
582.	20	SUMMARY REPORT		
583.	20	SUMMARY REPORT		
509.	20	7.1	.225	30
721.	20	9 AND 13.5	.03 - .38	0
179.	20.3	5 - 90	0	110
134.	20.5 AND 24	5 - 20	0	20
131.	24.5	26 AND 45	0 - 1	20

EXPERIMENTAL BASE PRESSURE DATA

REF.	MACH NUMBER	δ DEGREES	r_N / r_b	α_{MAX}
518.	0 - 5	VARIOUS SHAPES	-	-
801.	.1	15 AND 30	0 - .5	20
129.	.25 - 2.2	12.5	0 AND .6	18
157.	.25 - 2.2	12.5	.6	20
547.	.3 - 1.3	15	0	0
204.	.4 - 20	NONCONICAL SHAPES	-	20
206.	.4 - 20	NONCONICAL SHAPES	-	20
180.	.5 - 1.1	0	5.7	28
36.	.6 - 1.4	9	.04	16
4.	.6 - 1.5	7	0 - .222	6
108.	1 - 3	5 - 15	-	-
724	1 - 10	5 - 12.5	0 - .6	0
211.	1 - 25	SUMMARY OF ALL LORV VEHICLE FLIGHT TESTS		
163.	1.4 AND 2	3.55	0	26
502.	1.5 - 4	10	0	0
186.	1.5 - 4.6	5.7	0	28
153.	1.6 - 2.4	15	0	0
34.	2 - 5.1	9	0 AND .29	0
579.	2 - 20	8 - 30	0 .5	0
544.	2.35 - 4.75	10	0 AND .5	0
31.	2.5 - 4	10	0	0
107.	2.73 - 5	VARIOUS SHAPES	-	0
305.	3 - 22	8	0	0
103.	3.12	5 - 20	0	9
580.	3.5 - 9.2	9	0 AND .28	0
725.	3.5 - 9.2	9	0 AND .28	0
580.	3.5 - 9.2	9	0 AND .28	0
513.	5 - 8	6	0	12
68.	5 - 10	10	.015	2
302.	6 - 19	8	0	16
723.	7 - 10	6 - 15	0 - .2	0
571.	8.07	6.3	0	15
33.	9 - 21	9 AND 10	0 - .3	25
210.	16 - 25	9	0	7
209.	18 - 24	8	0	10

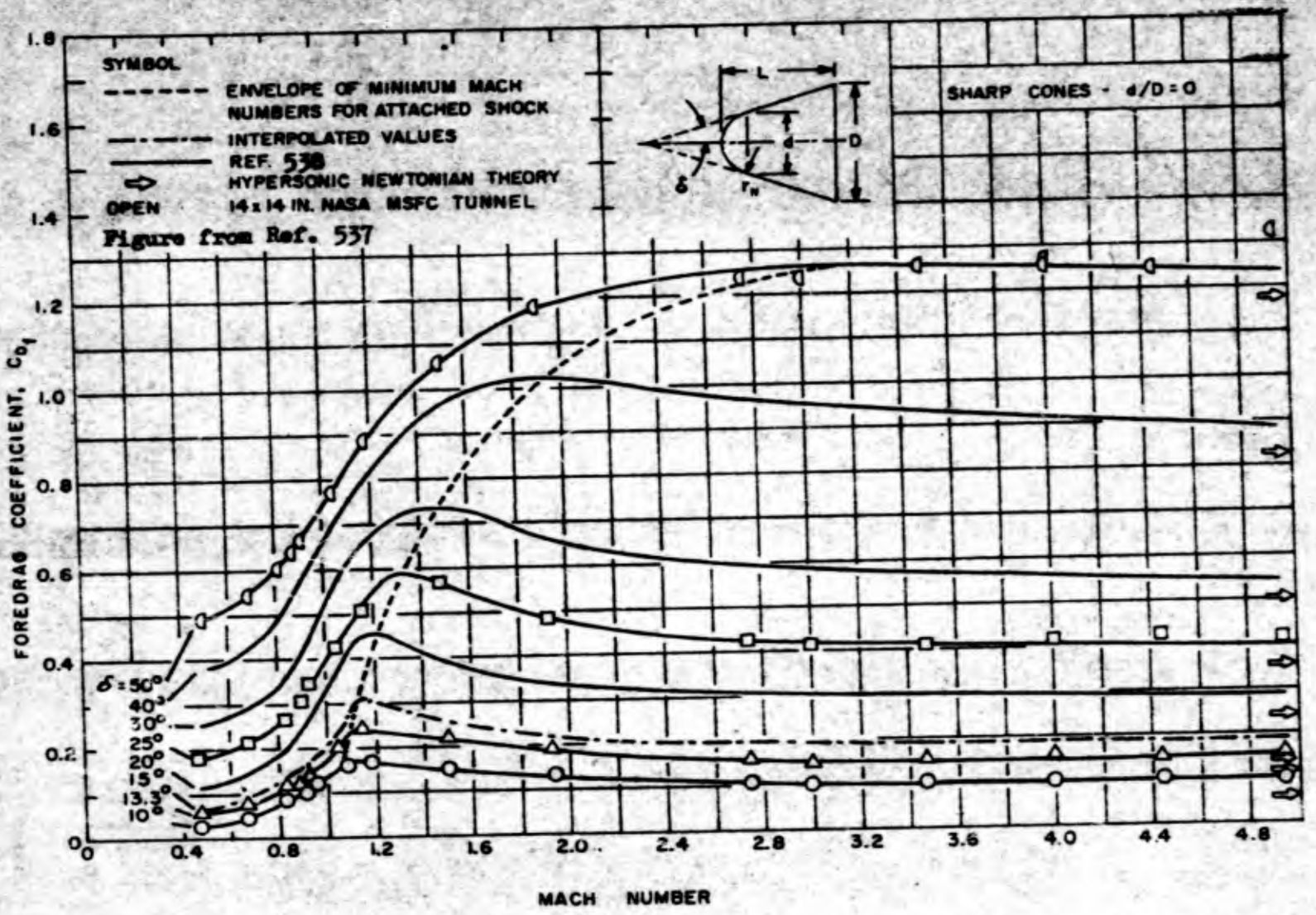

Figure 4.1 Variation of Foredrag Coefficient with Mach Number for Various Sharp Nose Cones

$$\frac{r_N}{r_b} = \frac{1}{\cos\delta}\left(\frac{d}{D}\right)$$

Figure from Ref. 537

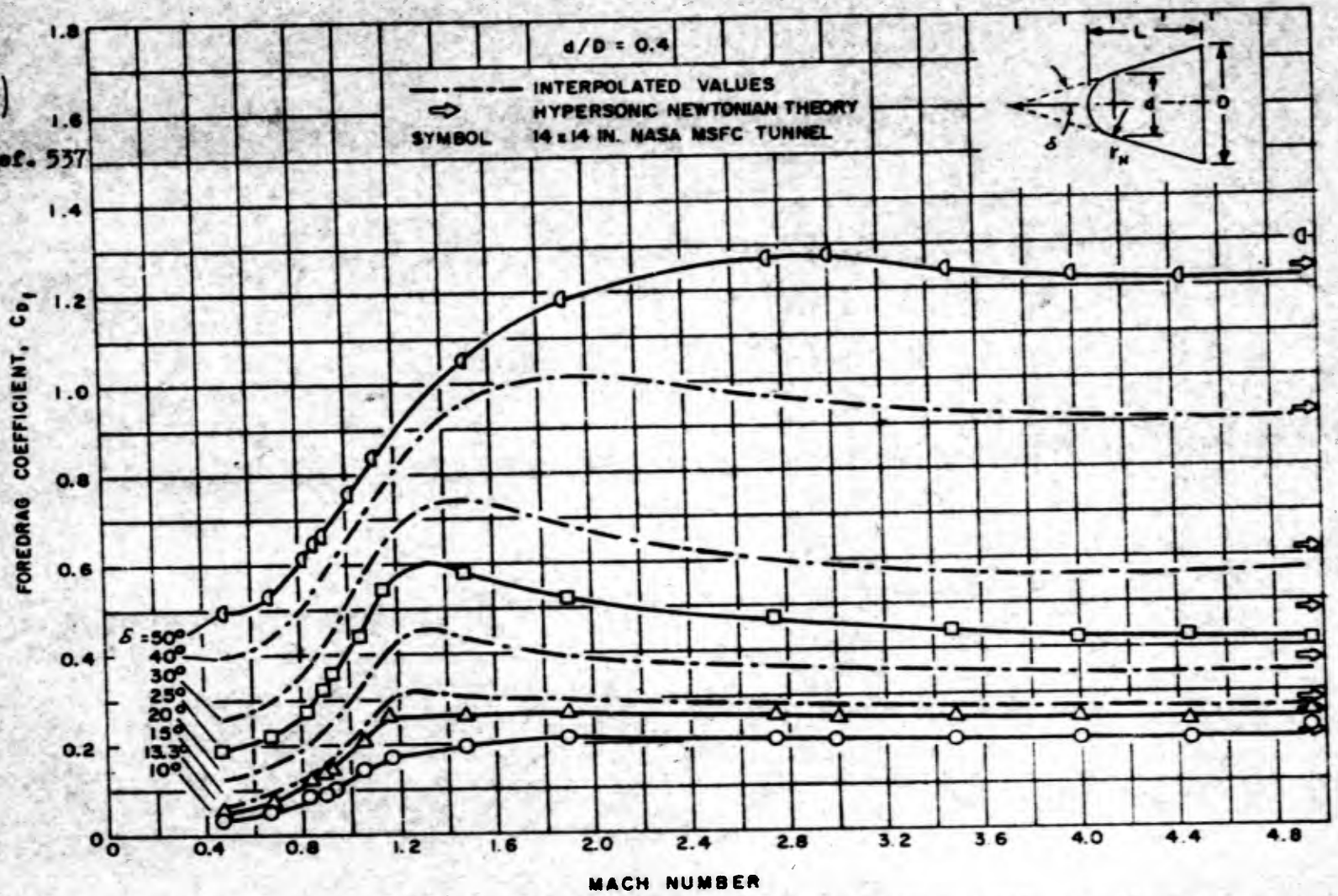

Figure 4.2 Variation of Foredrag Coefficient with Mach Number for Various Blunt Nose Cones, d/D = 0.4

Figure from Ref. 537

$$\frac{r_N}{r_b} = \frac{1}{\cos\delta}\left(\frac{d}{D}\right)$$

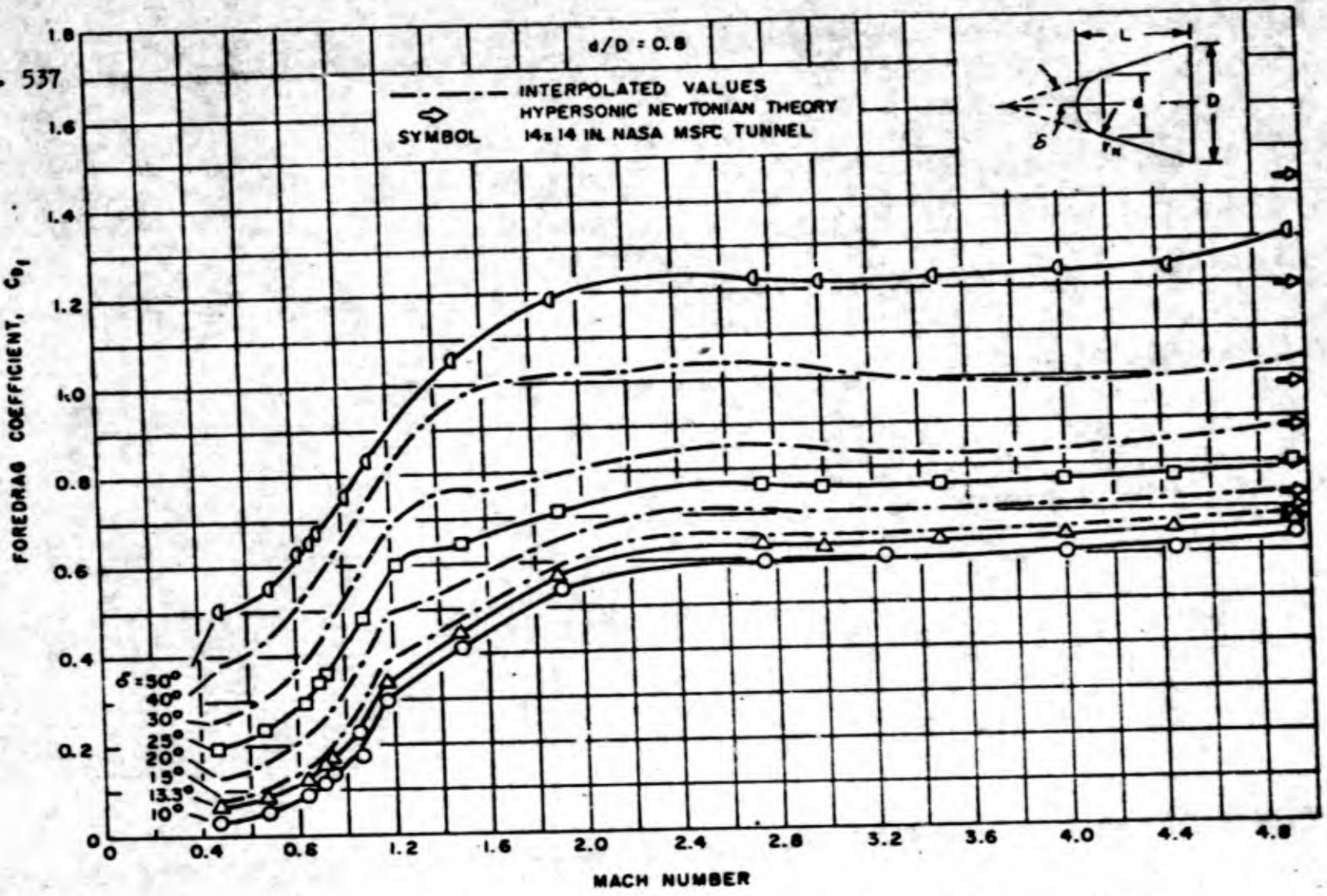

Figure 4.3 Variation of Foredrag Coefficient with Mach Number for Various Blunt Nose Cones with d/D = 0.8

Figure from Ref. 133

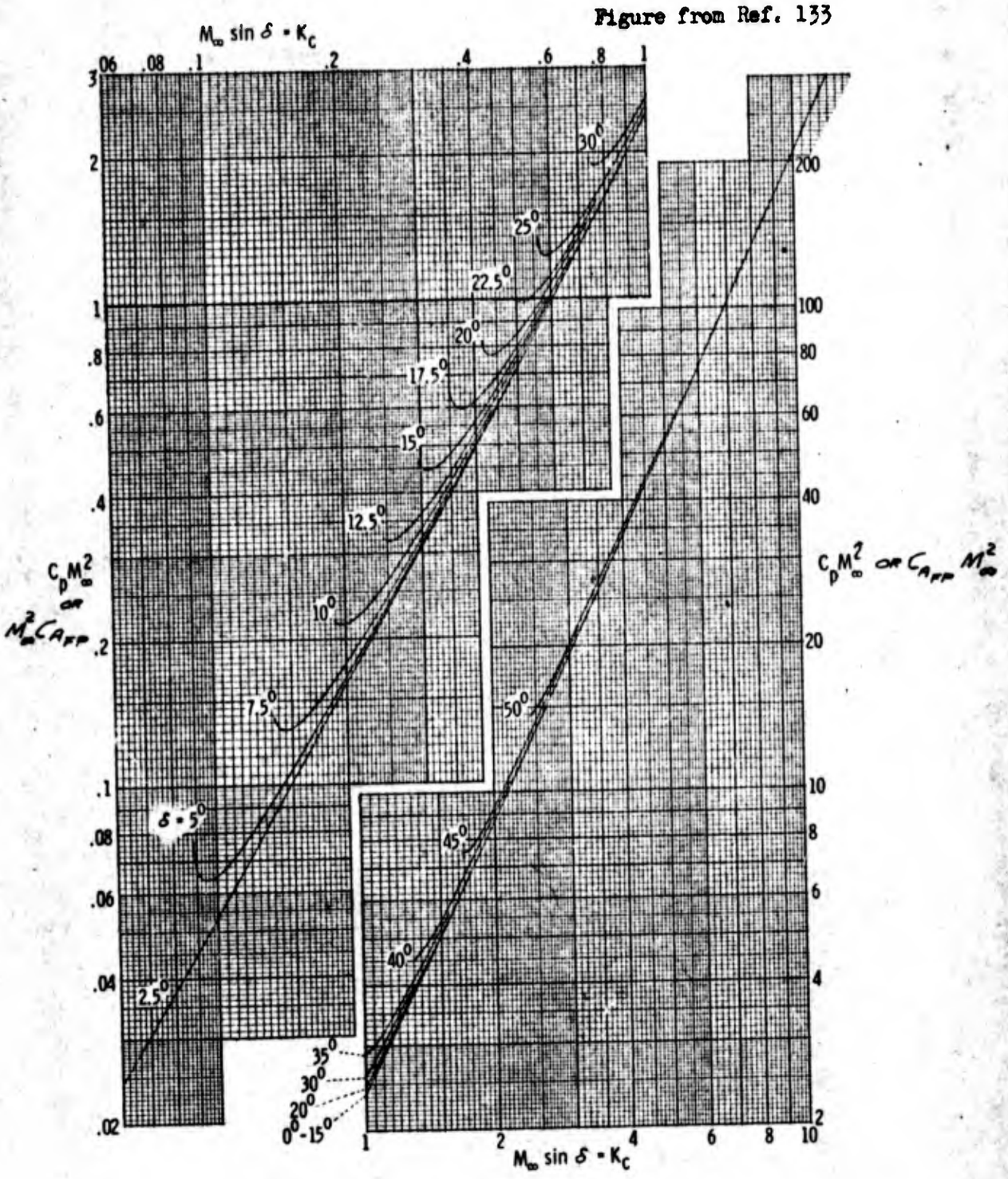

Values of K_c from 0.06 to 12

Figure 4.4 Cone-surface-pressure coefficient in similarity form, applicable to $\gamma = 7/5$ and 1.405

Figure from Ref. 133

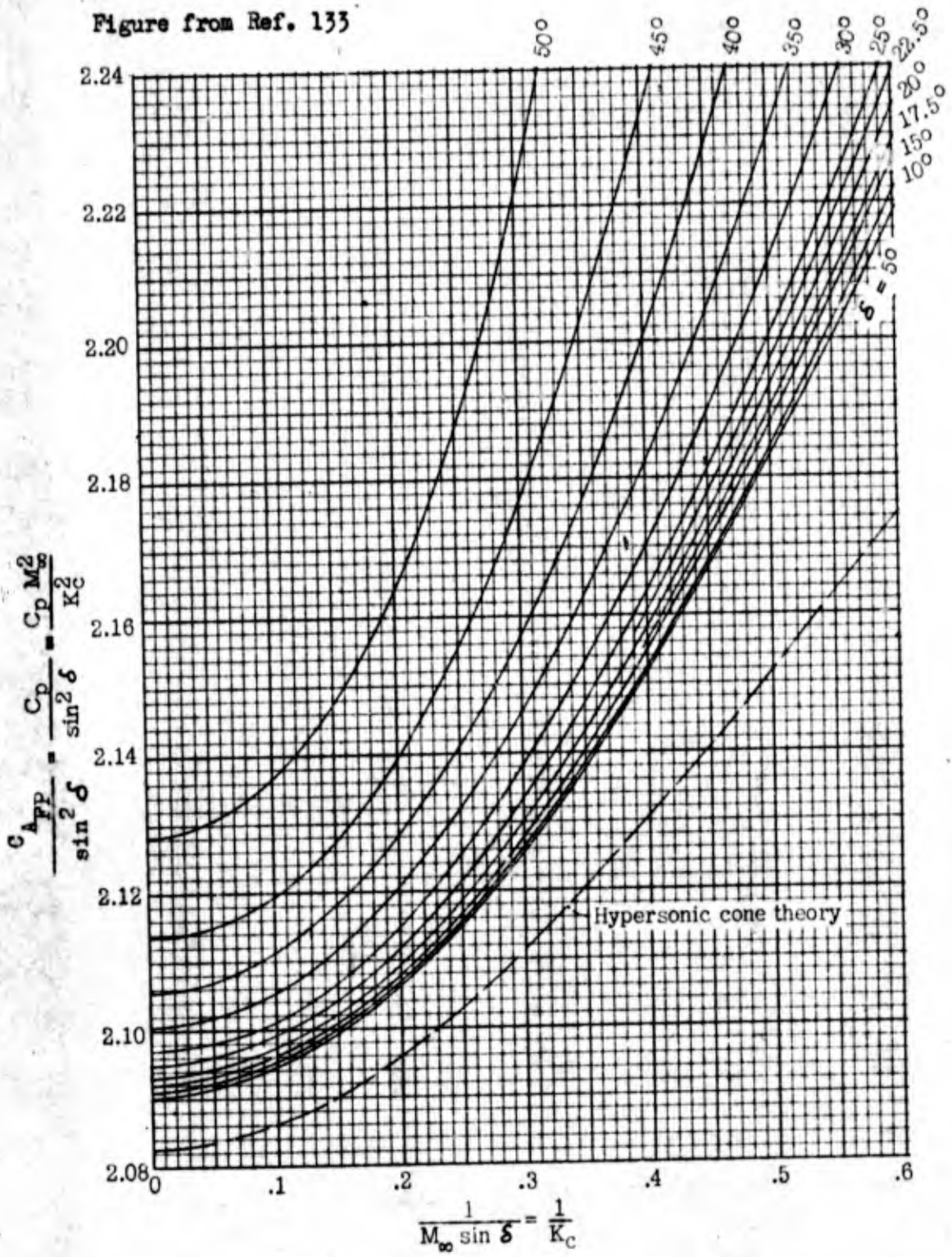

Values of K_c from 1.7 to ∞

Figure 4.5 Cone-surface-pressure coefficient in similarity form, applicable to $\gamma = 7/5$ and 1.405

$\alpha = 0°$
$\delta = 8.17°$

h^* 1000 FT.	M_∞	C_p or $C_{A_{WAVE}}$		
		REAL AIR	PERFECT AIR	NEWTONIAN
180	20.98	.0433	.0430	.0404
120	22.09	.0432		
80	22.80	.0432		
40	20.66	.0433		
20	14.86	.0442	.0436	

* TYPICAL RV TRAJECTORY

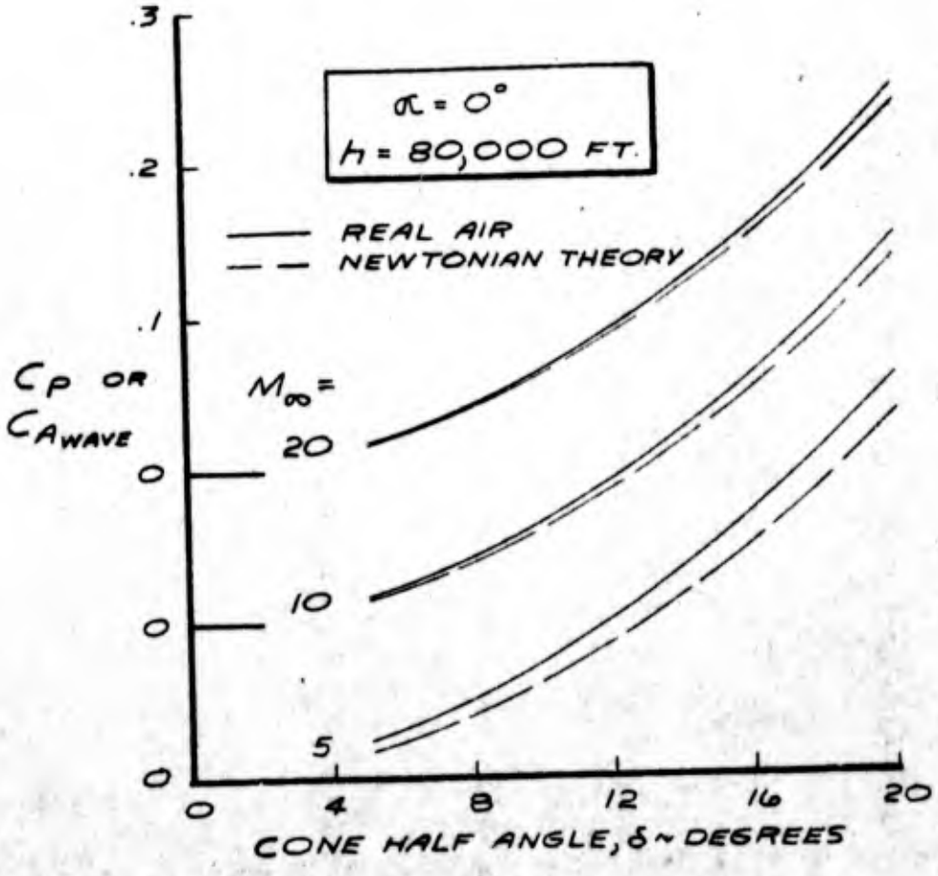

FIG. 4.6 COMPARISON OF METHODS FOR CALCULATING SHARP CONE PRESSURE COEFFICIENTS

USE FOR TYPEWRITTEN MATERIAL ONLY

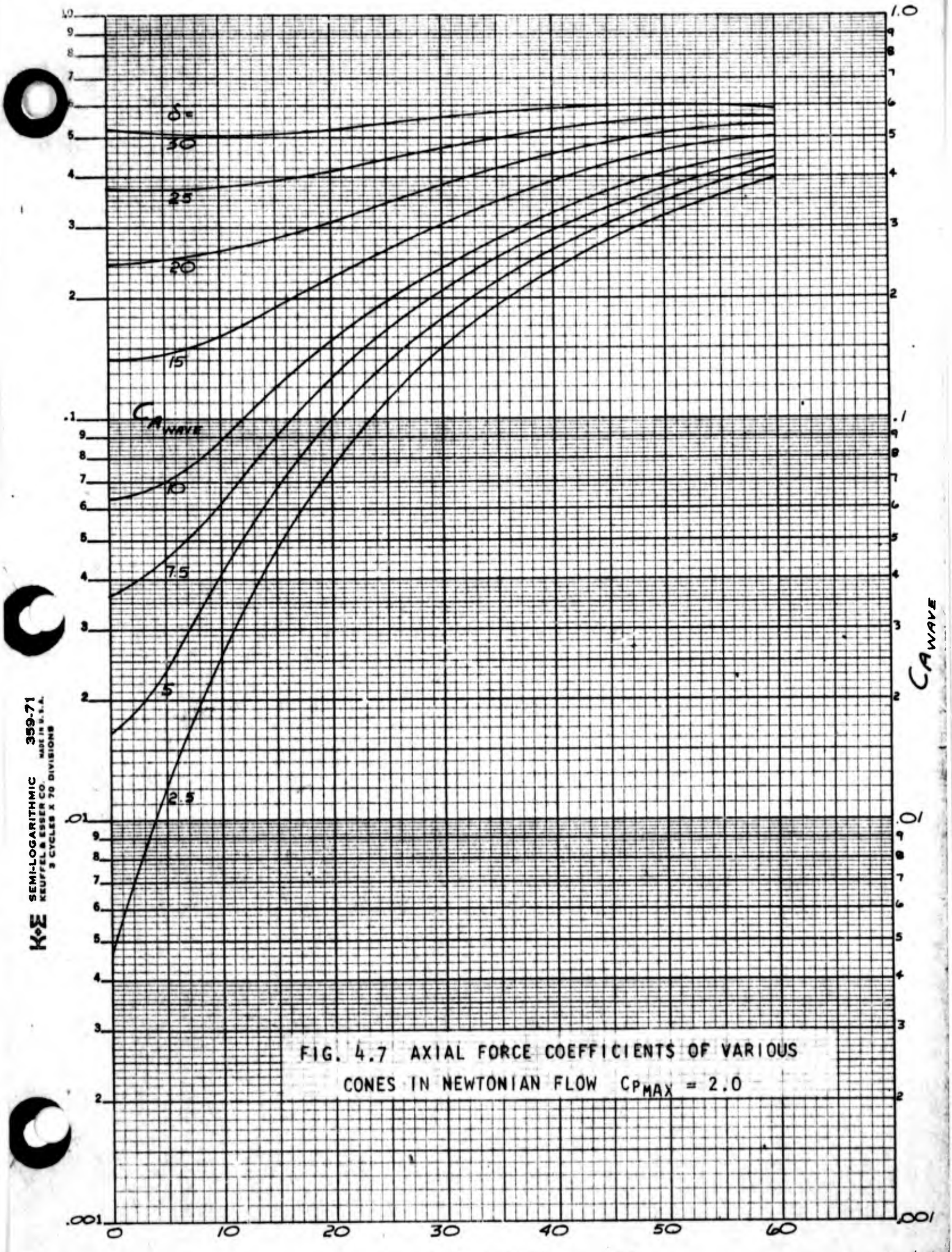

FIG. 4.7 AXIAL FORCE COEFFICIENTS OF VARIOUS CONES IN NEWTONIAN FLOW $C_{P_{MAX}} = 2.0$

Figure from Ref. 132

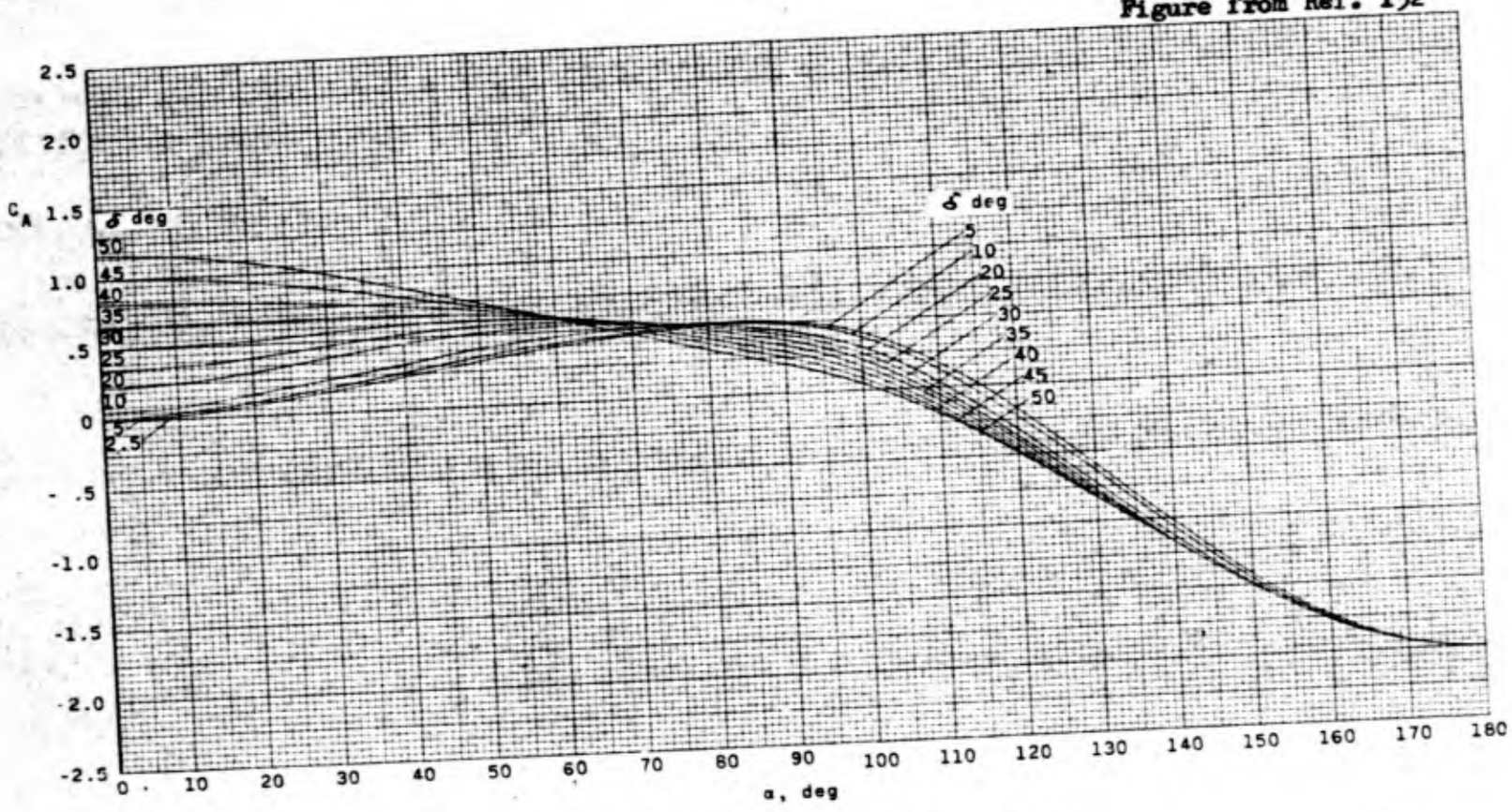

Figure 4.8 Axial-force coefficients of various cones in Newtonian flow; $C_{p,max.} = 2.0$.

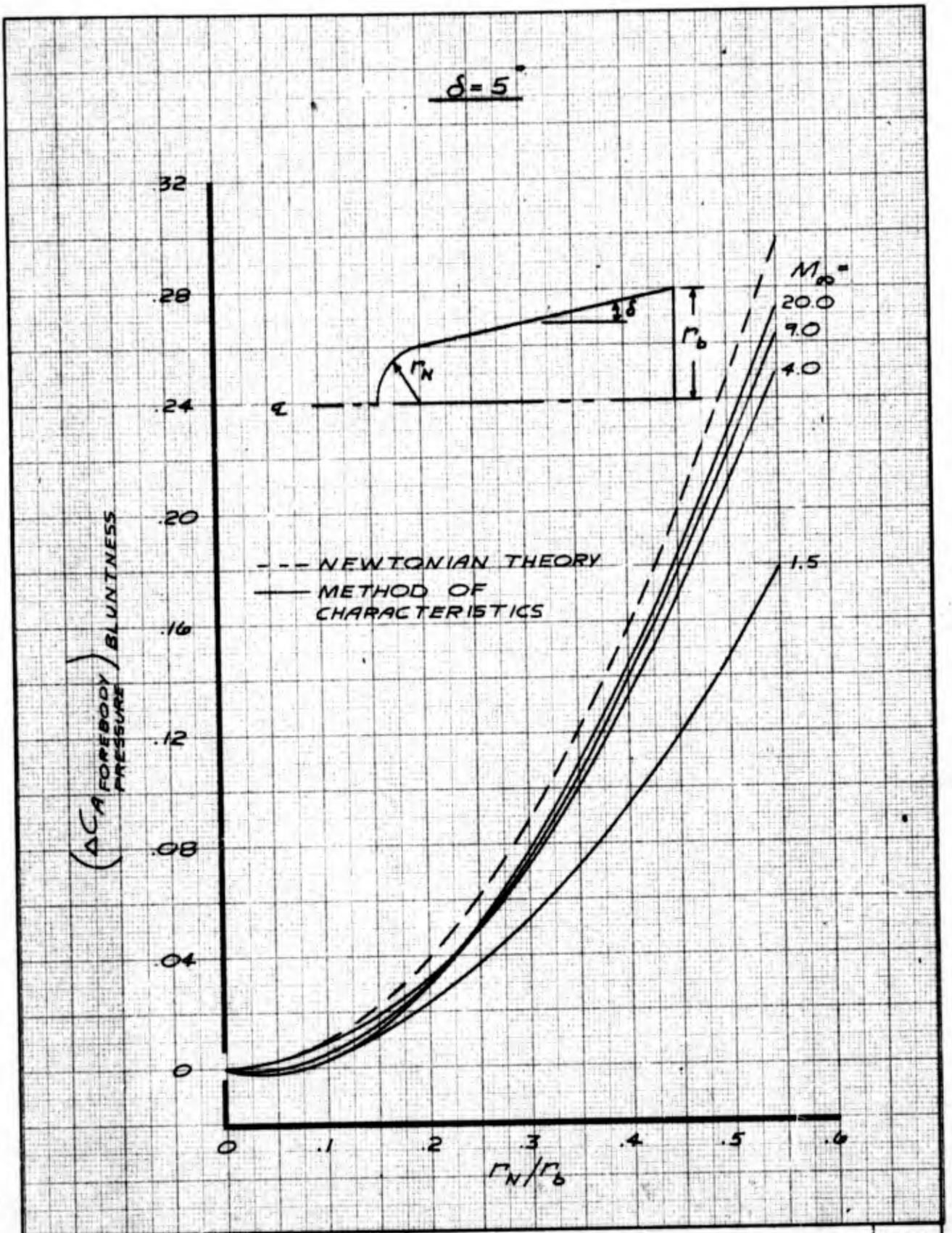

	INITIALS	DATE	REV BY INITIALS	DATE	TITLE	MODEL
CALC	DWE	10/65			EFFECT OF NOSE BLUNTNESS ON THE FOREBODY AXIAL PRESSURE FORCE COEFFICIENT	Fig. 4.9a
CHECK						
APPD.						
APPD.						

U3 4013 8000 REV. 12-64

REV LTR

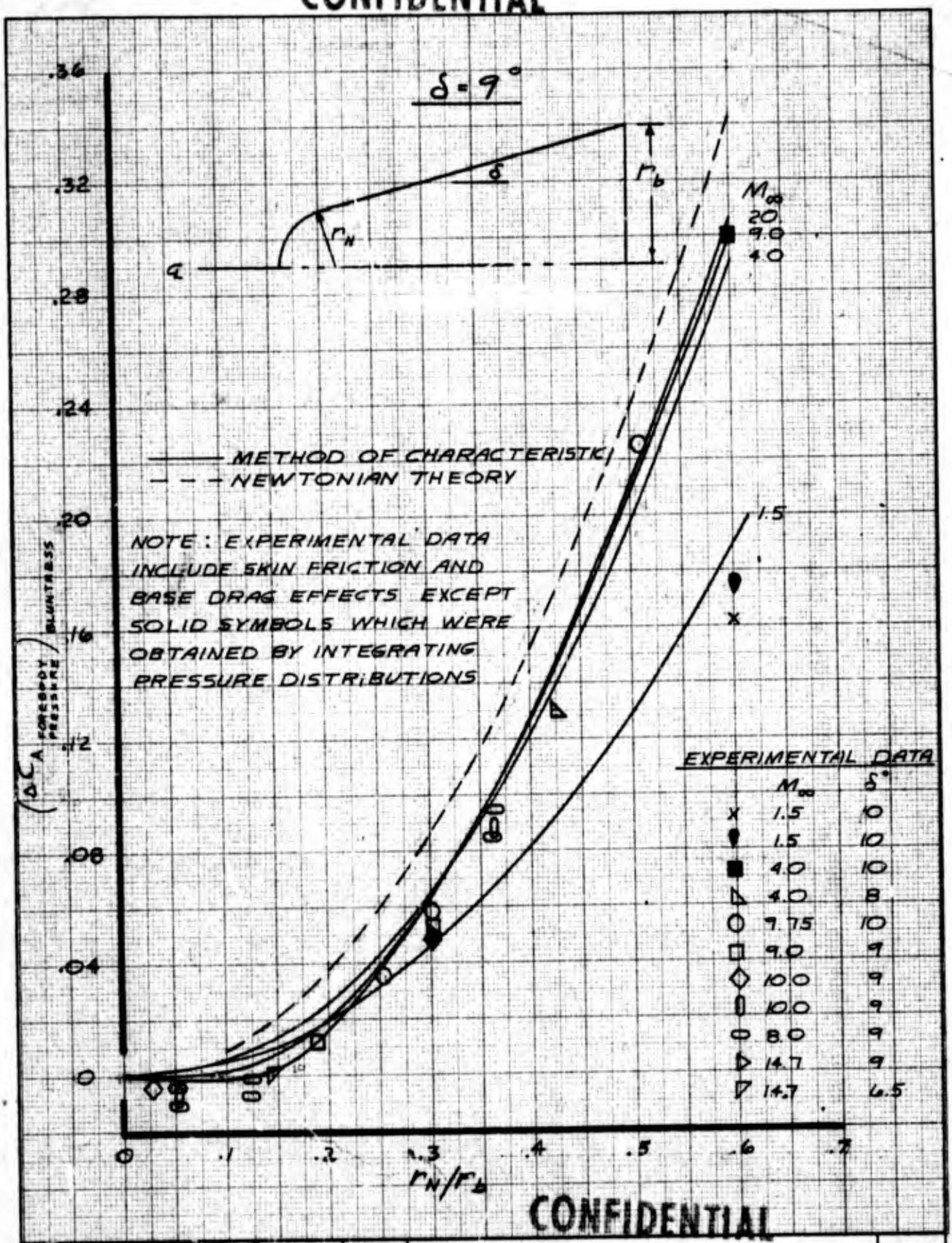

	INITIALS	DATE	REV BY INITIALS	DATE	TITLE	MODEL
CALC	DWE	10/65			EFFECT OF NOSE BLUNTNESS ON THE FOREBODY AXIAL PRESSURE FORCE COEFFICIENT	Fig. 4.9b
CHECK						
APPD.						
APPD.						

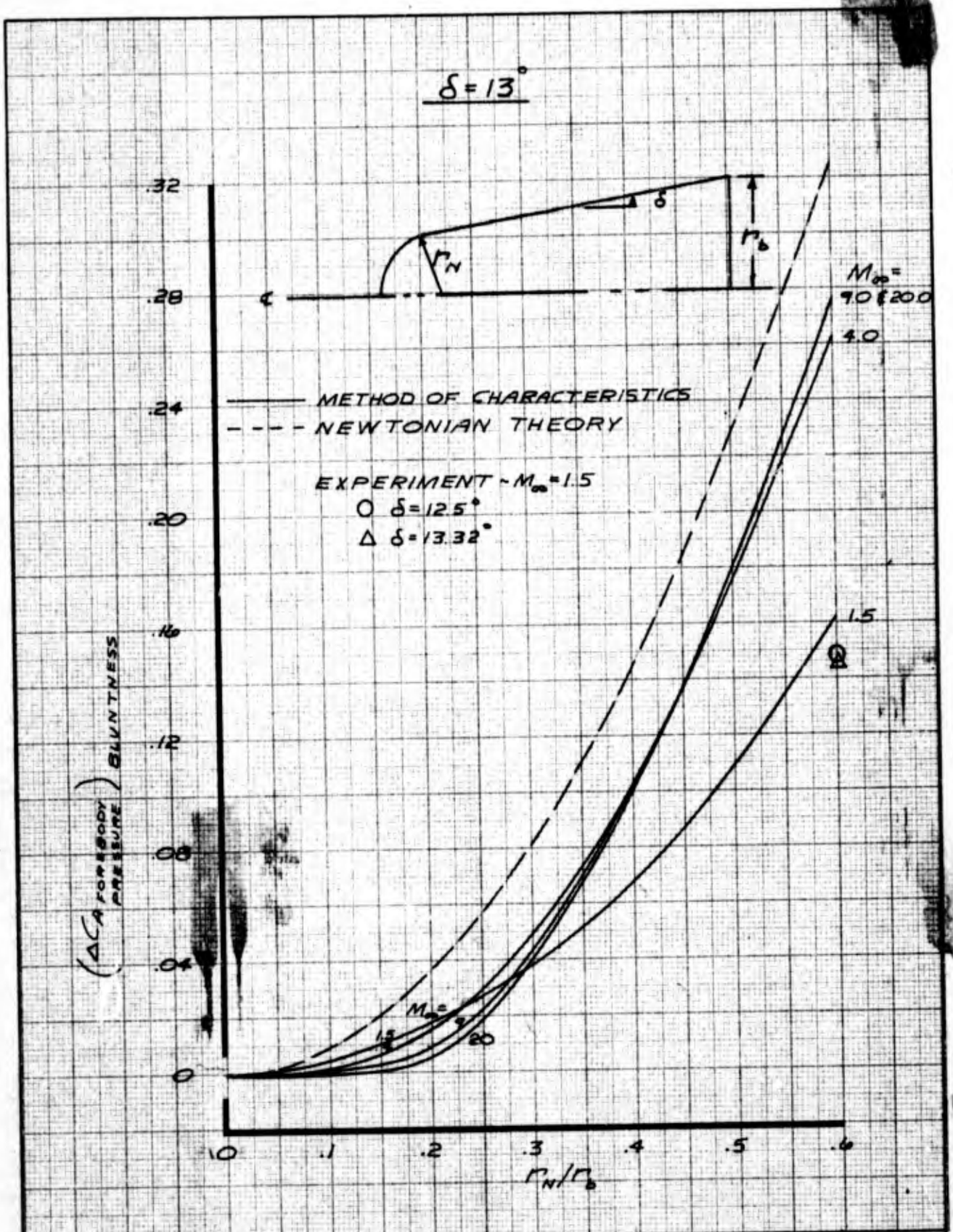

	INITIALS	DATE	REV BY INITIALS	DATE	TITLE	MODEL
CALC	DWE	10/65			EFFECT OF NOSE BLUNTNESS ON THE FOREBODY AXIAL PRESSURE FORCE COEFFICIENT	Fig. 4.9c
CHECK						
APPD.						
APPD.						

U3 4013 8000 REV. 12-64

REV LTR_____

BOEING NO D2-36139-1

SH. 66

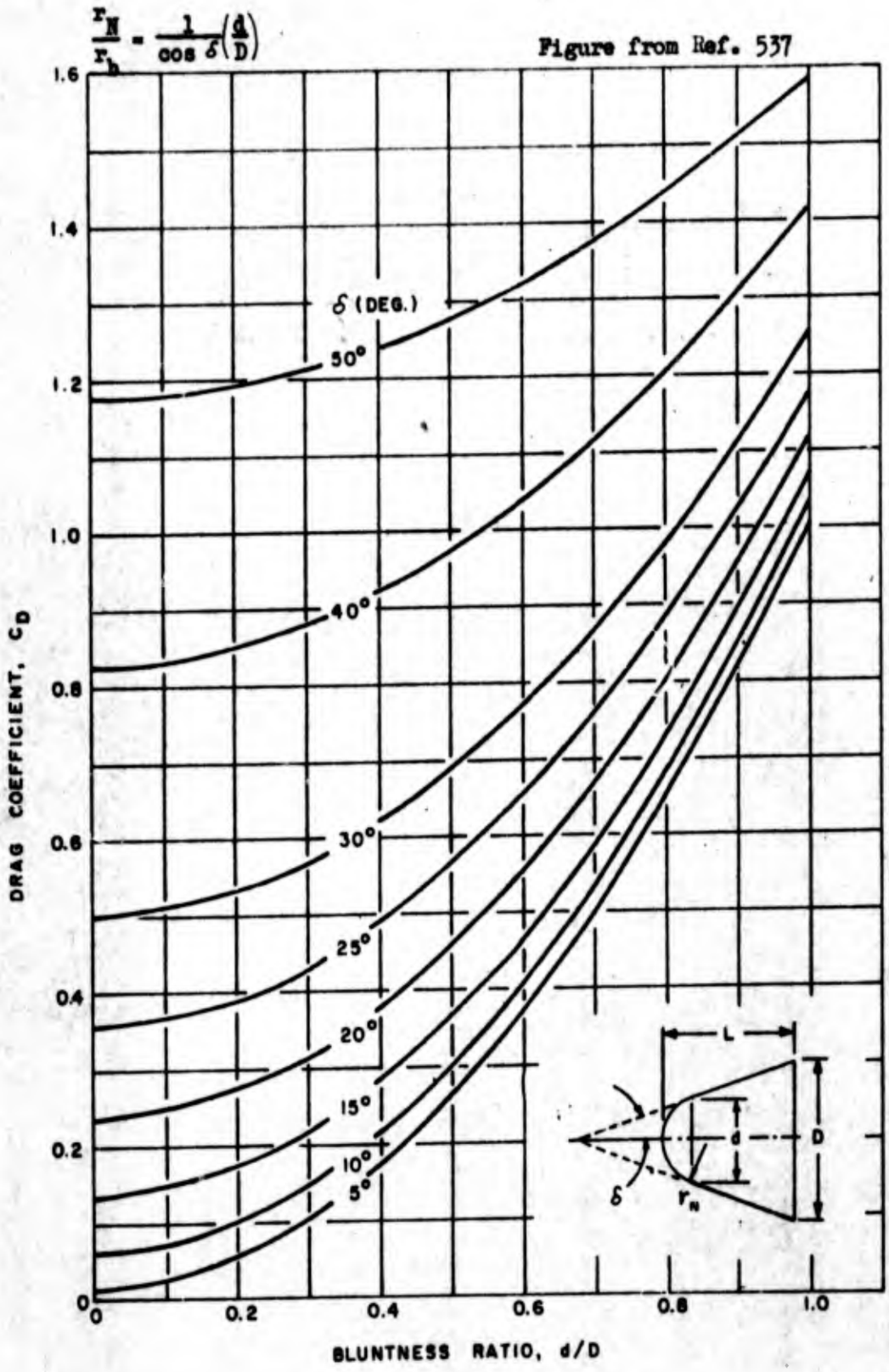

Figure 4.10 Hypersonic Newtonian Wave Drag for Cones of Varying Geometry.

FIG. 4.11 VARIOUS EFFECTS ON WIND TUNNEL BASE PRESSURE COEFFICIENT

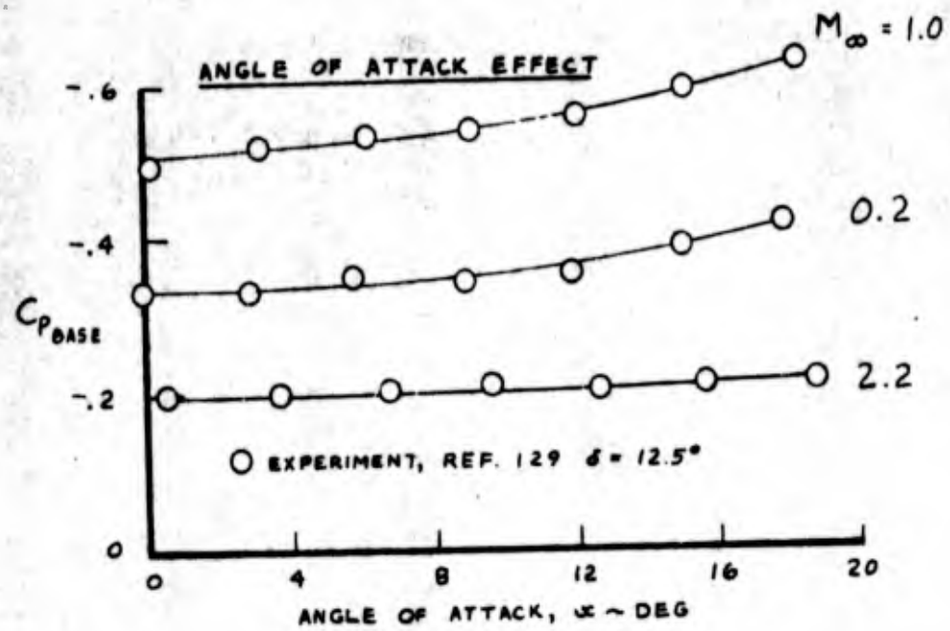

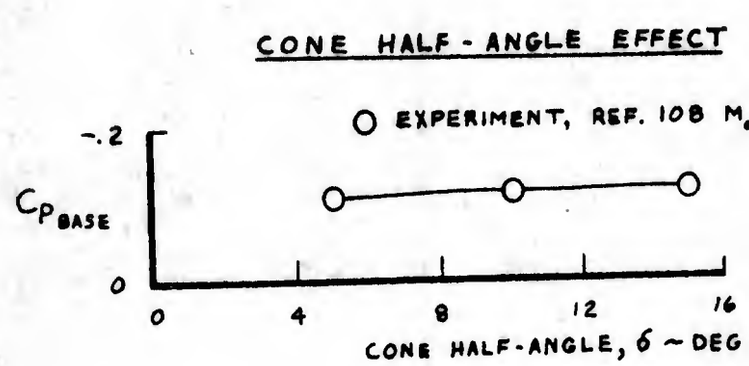

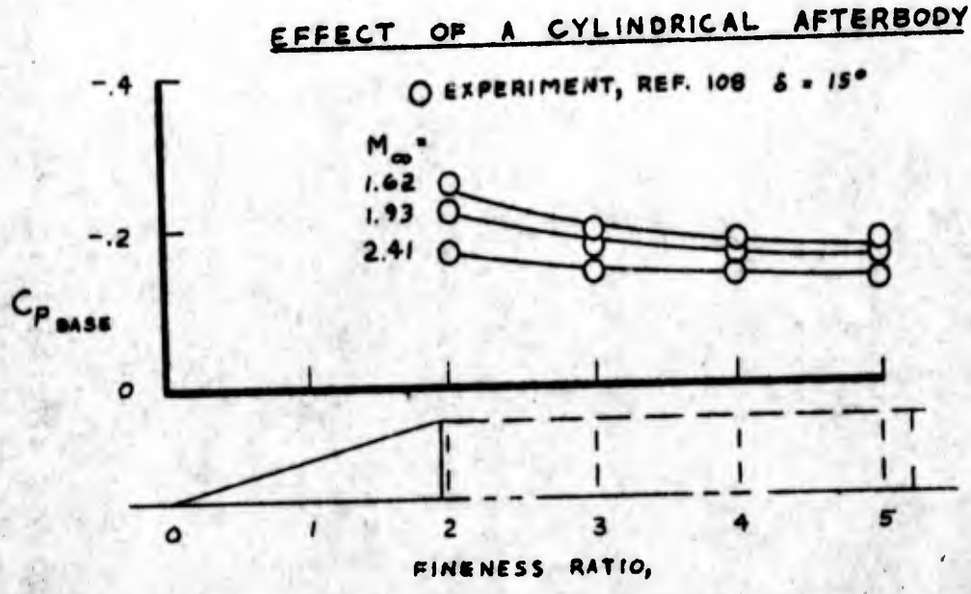

USE FOR TYPEWRITTEN MATERIAL ONLY

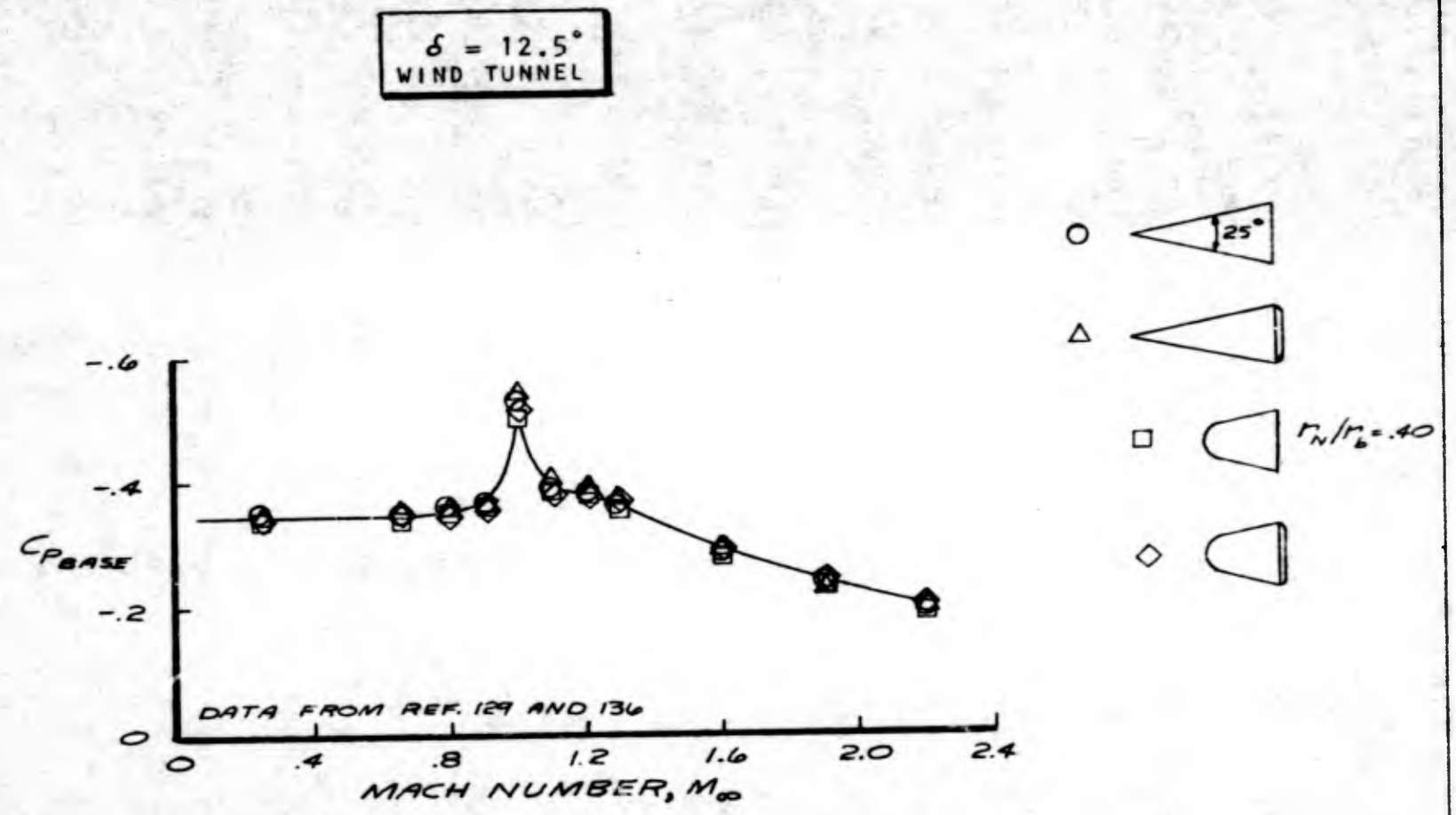

FIG. 4.12 THE EFFECT OF CONE BLUNTING AND ROUNDING THE BASE ON WIND TUNNEL BASE PRESSURE

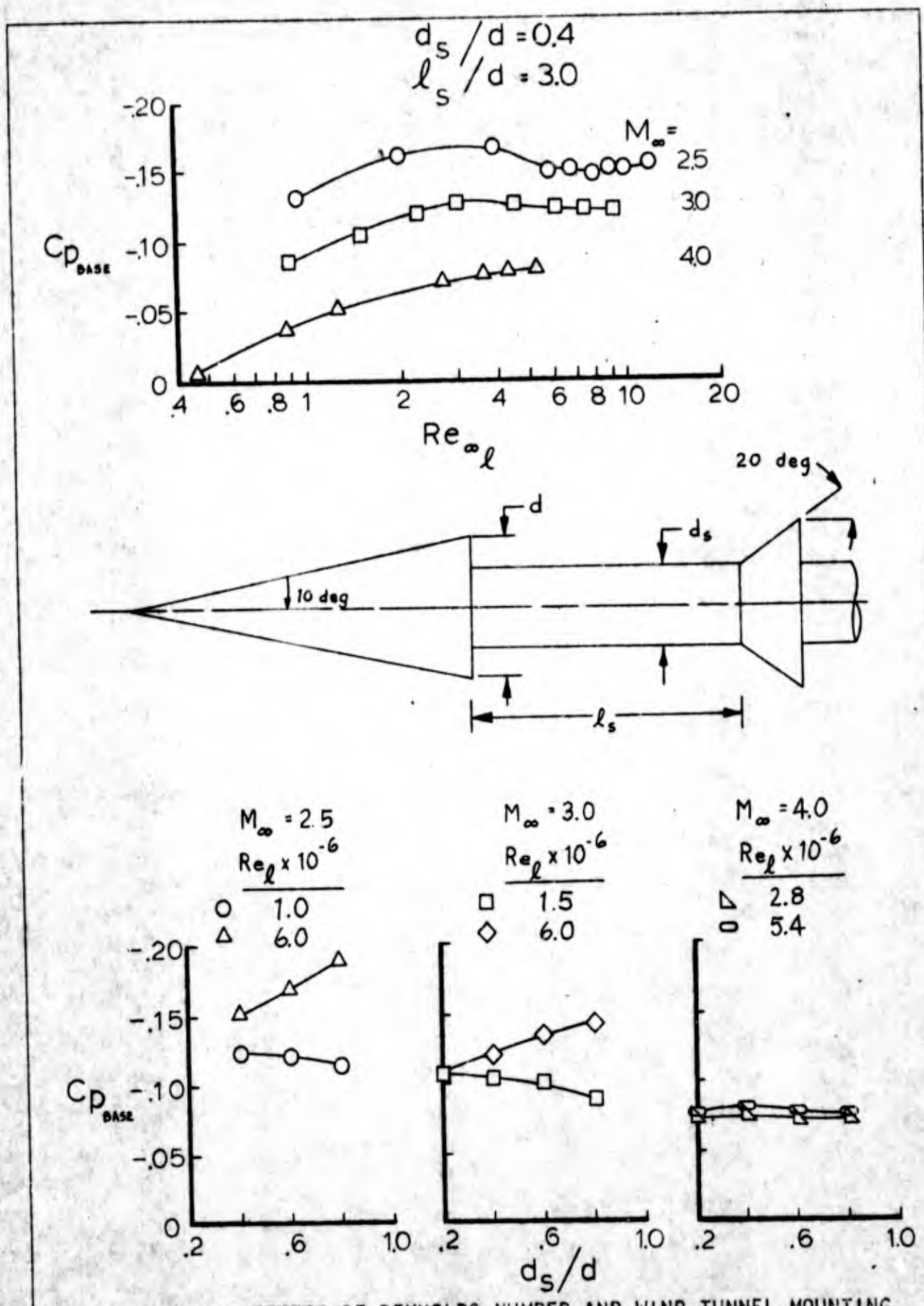

FIG. 4.13 EFFECT OF REYNOLDS NUMBER AND WIND TUNNEL MOUNTING ON BASE PRESSURE

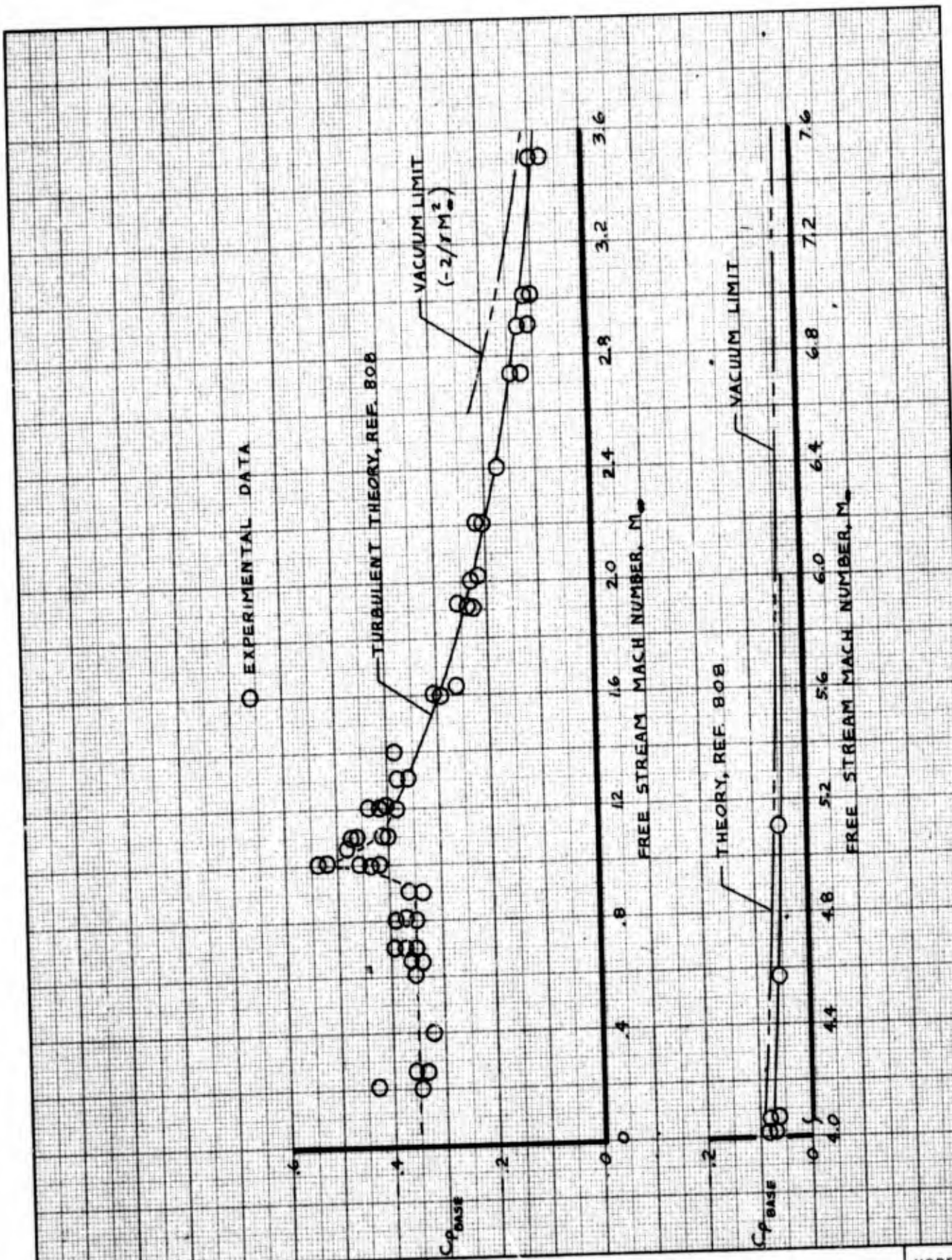

	INITIALS	DATE	REV BY INITIALS	DATE	TITLE	MODEL
CALC	DWE	8/65			CORRELATION OF AVAILABLE WIND TUNNEL BASE PRESSURE DATA FOR CONES	Fig. 4-14
CHECK						
APPD						
APPD						

U3 4013 8000 REV. 12-64

REV LTR_____

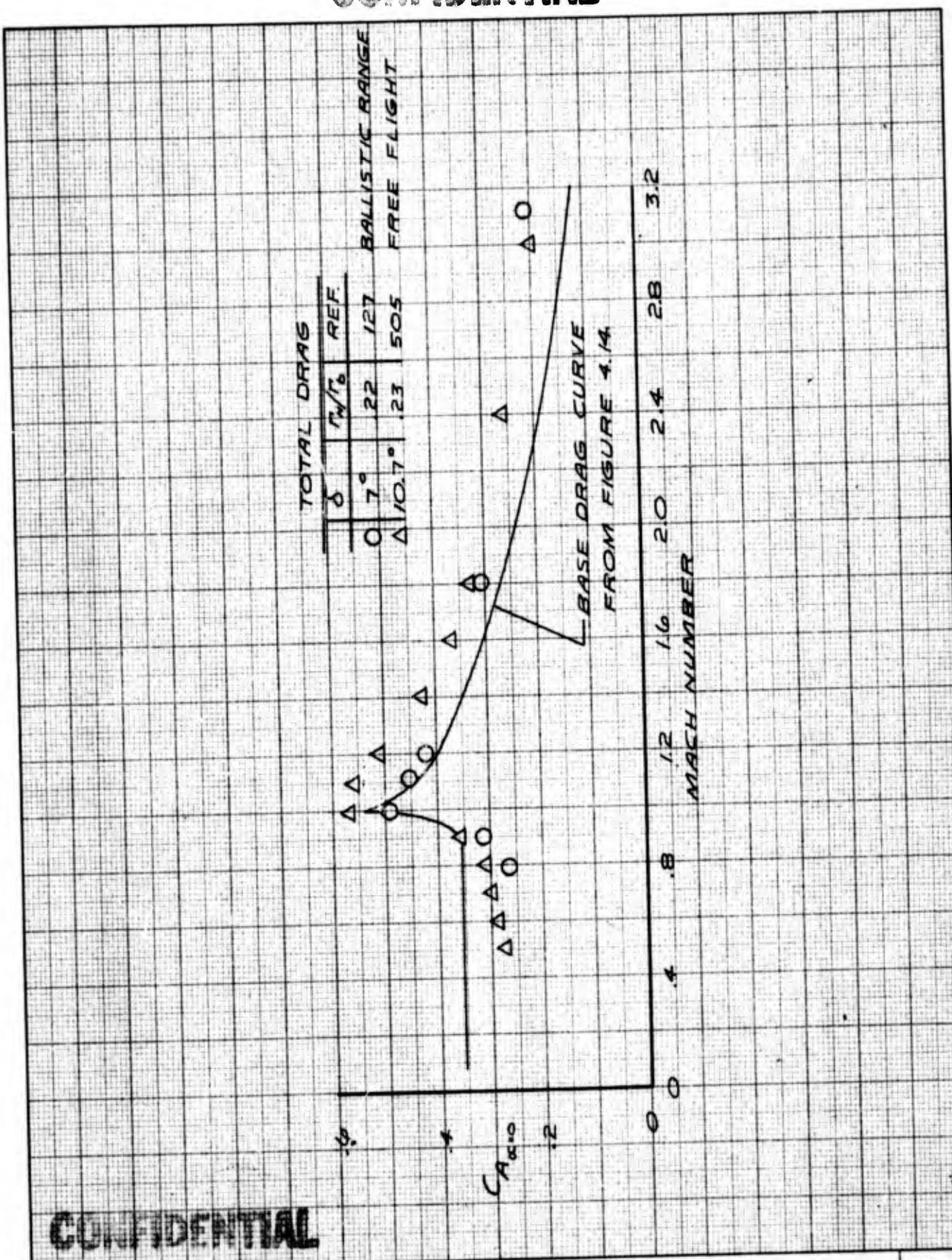

CONFIDENTIAL

	INITIALS	DATE	REV BY INITIALS	DATE	TITLE	MODEL
CALC	DWE	8/65			COMPARISON OF FREE FLIGHT TOTAL DRAG WITH WIND TUNNEL BASE DRAG FOR CONES	Fig. 4-15
CHECK						
APPD.						
APPD						

U3 4013 8000 REV. 12-64

REV LTR_____

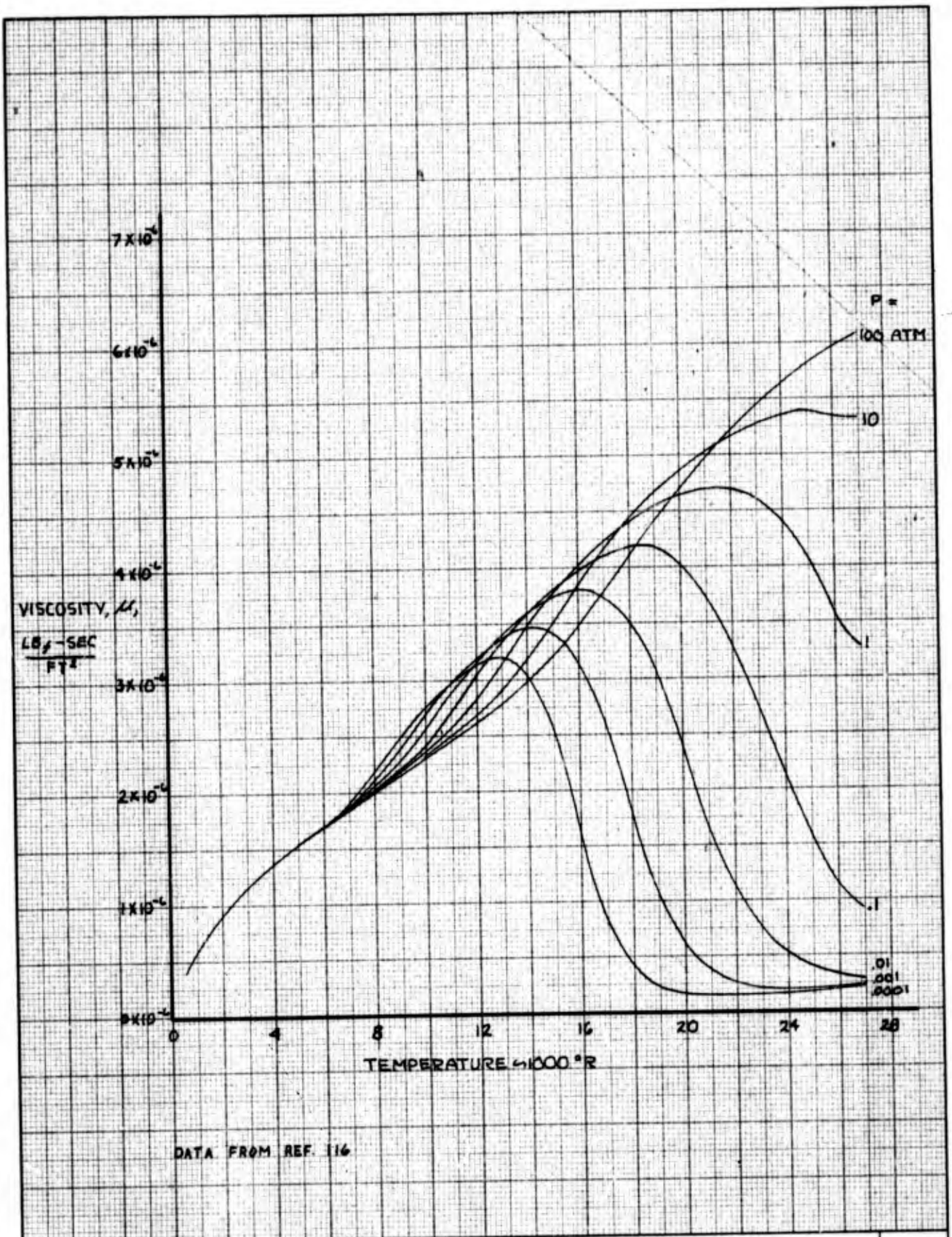

	INITIALS	DATE	REV BY INITIALS	DATE	TITLE	MODEL
CALC	DWE	9/65			VISCOSITY OF AIR VS TEMPERATURE	Fig. 4-16
CHECK						
APPD.						
APPD.						

U3 4013 8000 REV. 12-64

REV LTR_____

FLOW FIELD ABOUT A SHARP NOSED CONE AT ZERO ANGLE OF ATTACK

GAS CONSTANT= 1716.000 .SQ.FT./SQ.SEC.-DEGREES RANKINE
CONE SEMIANGLE= 8.000000 DEGREES
GAMMA= 1.400000

} Input Conditions

FREE STREAM CONDITIONS
MACH NUMBER= 9.040000
PRESSURE= 4.280000 LB./SQ.FT.
TEMPERATURE= 83.00000 DEGREES RANKINE

} Input Conditions

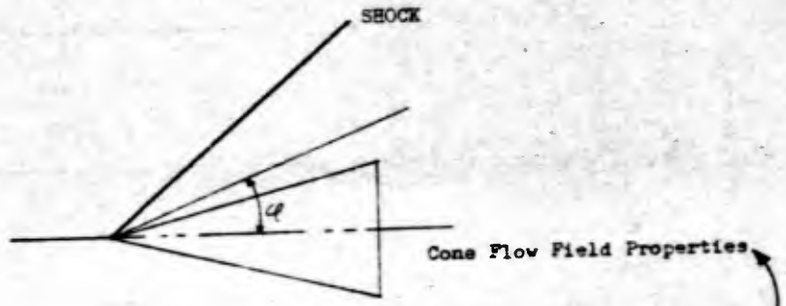

Cone Flow Field Properties

I	M	RHO	P	T	V	THETA	PHI	
1	7.016991	.780444-04	17.77293	132.7090	3962.085	8.999806	8.999806	BODY
2	7.030738	.773540-04	17.55322	132.2382	3962.798	8.197646	9.873229	
3	7.071849	.753320-04	16.91422	130.8445	3964.910	7.463642	10.74646	
4	7.145011	.718856-04	15.84091	128.4164	3968.586	6.706688	11.61969	SHOCK

SHOCK ANGLE= 11.61969 DEGREES
BODY MACH NUMBER= 7.016991
BODY PRESSURE COEFFICIENT= .551097-01
WAVE DRAG COEFFICIENT= .551097-01
BASE DRAG COEFFICIENT = .1573285B-01

LAMINAR CF = (LAM TERM)/SQRTF(L) See Equation 4.10
TURBULENT CF = TUR NUM/LOG10(TUR-DEN*L))**2.6) See Equation 4.11

DISPLACEMENT INDUCED PRESSURE DRAG = CD4
DISPLACEMENT INDUCED FRICTION DRAG = CD5
TRANSVERSE CURVATURE INDUCED FRICTION DRAG = CD6

} Viscous Interaction Effects

ALL DRAG COEFFICIENTS ARE REFERENCED TO CONE BASE AREA Note:

SHARP NOSE CONE SKIN FRICTION

REYNOLDS NUMBER/FOOT= .296925+07 on edge of cone, can be used to determine transition. See Section 7.0
WALL TEMPERATURE = 1100.00000 DEGREES RANKINE
LAMINAR TERM = .12639761-01 TURBULENT NUMERATOR = 1.1666173o TURBULENT DENOMINATOR = 86638.3980

D2-36139-1
Figure 4-17a
74

LENGTH	TUR CF	BASIC LAM CF	CD4	CD5	CD6	TOTAL LAM CD
1.05499998	.18132468-01	.12305879-01	.19877823-02	.37572049-03	.34647781-03	.85858383-01

BLUNT NOSE CONE SKIN FRICTION

BLUNT NOSE CONE EDGE CONDITIONS

Note: Includes Wave and Base Drag

P = 17.772935o T = 570.965780 V = 3230.13550

REYNOLDS NUMBER/FOOT= .145600+06 on edge of cone, can be used to determine transition. See Section 7.0

WALL TEMPERATURE = 1100.00000 DEGREES RANKINE

LAMINAR TERM = .90861110-02 TURBULENT NUMERATOR = .67352856o TURBULENT DENOMINATOR = 55772.9900

LENGTH	TUR CF	BASIC LAM CF	CD4	CD5	CD6	TOTAL LAM CD
1.05499998	.11595377-01	.88460992-02	.57511729-03	.73264592-04	.29982889-03	.80636834-01

FLOW FIELD ABOUT A SHARP NOSED CONE AT ZERO ANGLE OF ATTACK IN A REAL GAS

CONE SEMIANGLE= .800000+01 DEGREES **Input Condition**

FREE STREAM CONDITIONS

MACH NUMBER= .227073+02
PRESSURE= .232720+02 LB./SQ.FT.
TEMPERATURE= .408570+03 DEGREES RANKINE
VELOCITY= .225000+05 FT./SEC.
ALTITUDE= .100000+06 FT.

} **Input Conditions**

DENSITY= .331804-04 SLUGS/CU.FT.
SPEED OF SOUND= .990869+03 FT./SEC.

DIMENSIONS

MACH NUMBER (M)---DIMENSIONLESS
DENSITY (RHO)---SLUGS/CU.FT.
PRESSURE (P)---ATMOSPHERES
TEMPERATURE (T)---DEGREES RANKINE
TEMPERATURE (TK)---DEGREES KELVIN
VELOCITY (V)---FT./SEC.
FLOW ANGLE (THETA)---DEGREES
CONICAL ANGLE (PHI)---DEGREES
ENTROPY (S/R)---DIMENSIONLESS
ENTHALPY (H)---BTU/LB.
COMPRESSIBILITY (Z)---DIMENSIONLESS
SPEED OF SOUND (A)---FT./SEC.

D2-36139-1
Figure 4-18a
76

I	M	RHO	P	TK	V	PHI	
1	.123242+02	.154507-03	.175017-00	.775693+03	.222270+05	.799990+01	BODY
2	.123295+02	.154122-03	.174426-00	.775003+03	.222272+05	.821229+01	
3	.123429+02	.153163-03	.172954-00	.773276+03	.222280+05	.842458+01	
4	.123642+02	.151654-03	.170644-00	.770543+03	.222293+05	.863688+01	
5	.123938+02	.149586-03	.167493-00	.766768+03	.222311+05	.884917+01	
6	.124331+02	.146907-03	.163433-00	.761822+03	.222336+05	.906146+01	SHOCK

I	S/R	H	Z	A	T	THETA	
1	.290363+02	.342844+03	.100000+01	.180353+04	.139625+04	.799990+01	BODY
2	.290363+02	.342520+03	.100000+01	.180277+04	.139501+04	.779352+01	
3	.290363+02	.341709+03	.100000+01	.180098+04	.139190+04	.759397+01	
4	.290363+02	.340427+03	.100000+01	.179788+04	.138695+04	.739758+01	
5	.290363+02	.338657+03	.100000+01	.179372+04	.138018+04	.720061+01	
6	.290363+02	.336341+03	.100000+01	.178827+04	.137128+04	.699850+01	SHOCK

SHOCK ANGLE= .906146+01 DEGREES

BODY MACH NUMBER= .123242+02

BODY PRESSURE COEFFICIENT= .413232-01 ←

WAVE DRAG COEFFICIENT= .413232-01 ←

LAMINAR CF = (LAM TERM)/SQRTF(L) See Equation 4.10

TURBULENT CF = TUR NUM/(LOG10(TUR DEN*L))**2.6 See Equation 4.11

ALL DRAG COEFFICIENTS ARE REFERENCED TO CONE BASE AREA Note!

SHARP NOSE CONE

REYNOLDS NUMBER/FOOT= .462410+07 on edge of cone, can be used to determine transition. See Section 7.0

WALL TEMPERATURE = 1800.00000 DEGREES RANKINE

LAMINAR TERM = .16456999-01 TURBULENT NUMERATOR = 3.46956830 TURBULENT DENOMINATOR = 45719.890

LENGTH	LAM CF	TUR CF
10.0000000	.52041600-02	.25074060-01

BLUNT NOSE CONE

BLUNT NOSE CONE EDGE CONDITIONS

P = .175017280 T = 9848.51510 H = 5996.71220 S = 43.8526890

RHO = .16760157-04 Z = 1.30695845 A = 4998.81160 V = 14531.2165

REYNOLDS NUMBER/FOOT= .106479+06 on edge of cone, can be used to determine transition. See Section 7.0

WALL TEMPERATURE = 1800.00000 DEGREES RANKINE

LAMINAR TERM = .76322805-02 TURBULENT NUMERATOR = .948463080 TURBULENT DENOMINATOR = 157131.470

LENGTH	LAM CF	TUR CF
10.0000000	.24135390-02	.82695681-02

D2-36139-1
Figure 4-18c
78

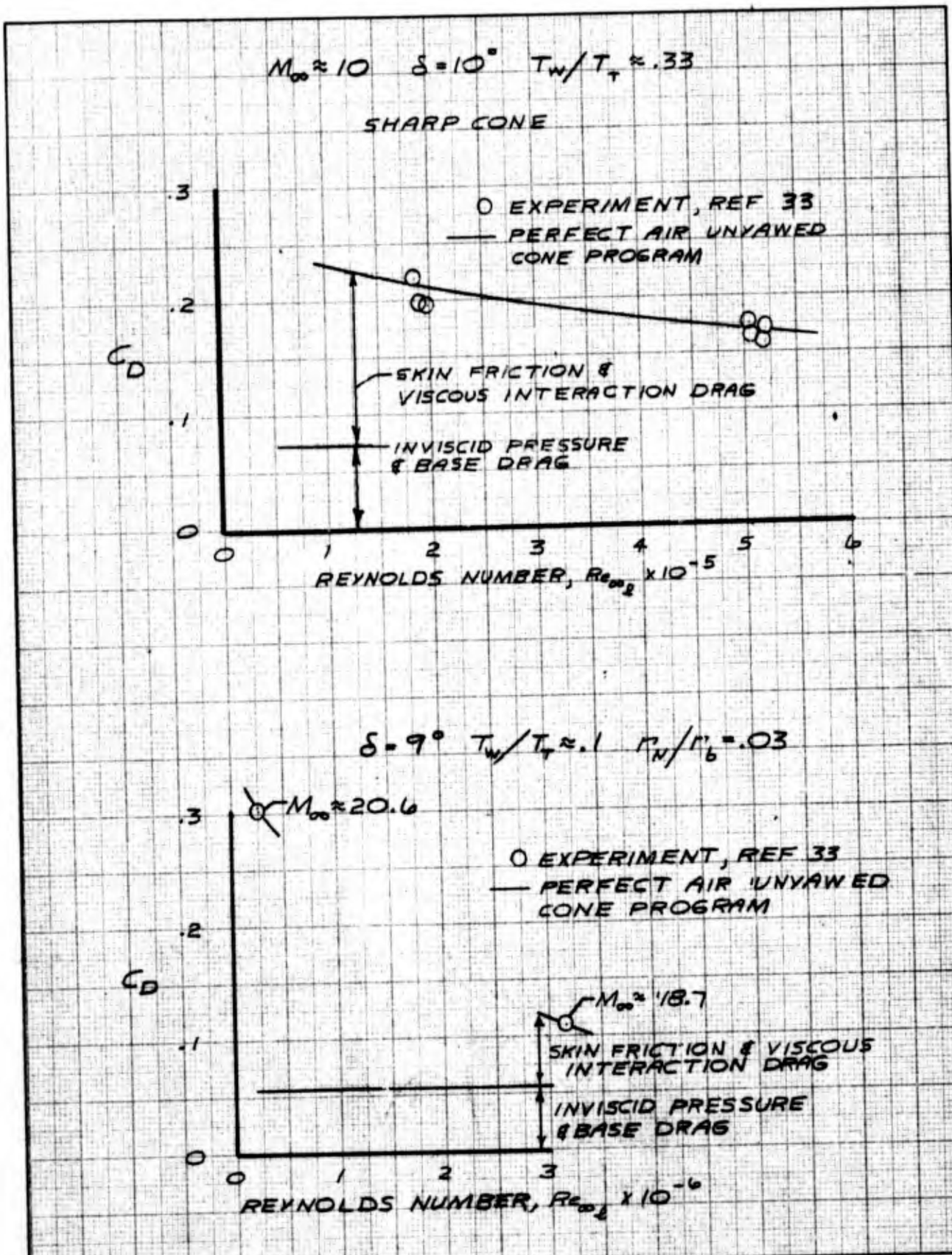

	INITIALS	DATE	REV BY INITIALS	DATE	TITLE	MODEL
CALC	OWE	11/65			COMPARISON OF CALCULATED AND EXPERIMENTAL DRAG ON SLENDER CONES IN LAMINAR FLOW	Fig. 4-19
CHECK						
APPD.						
APPD.						

U3 4013 8000 REV. 12-64

REV LTR_____

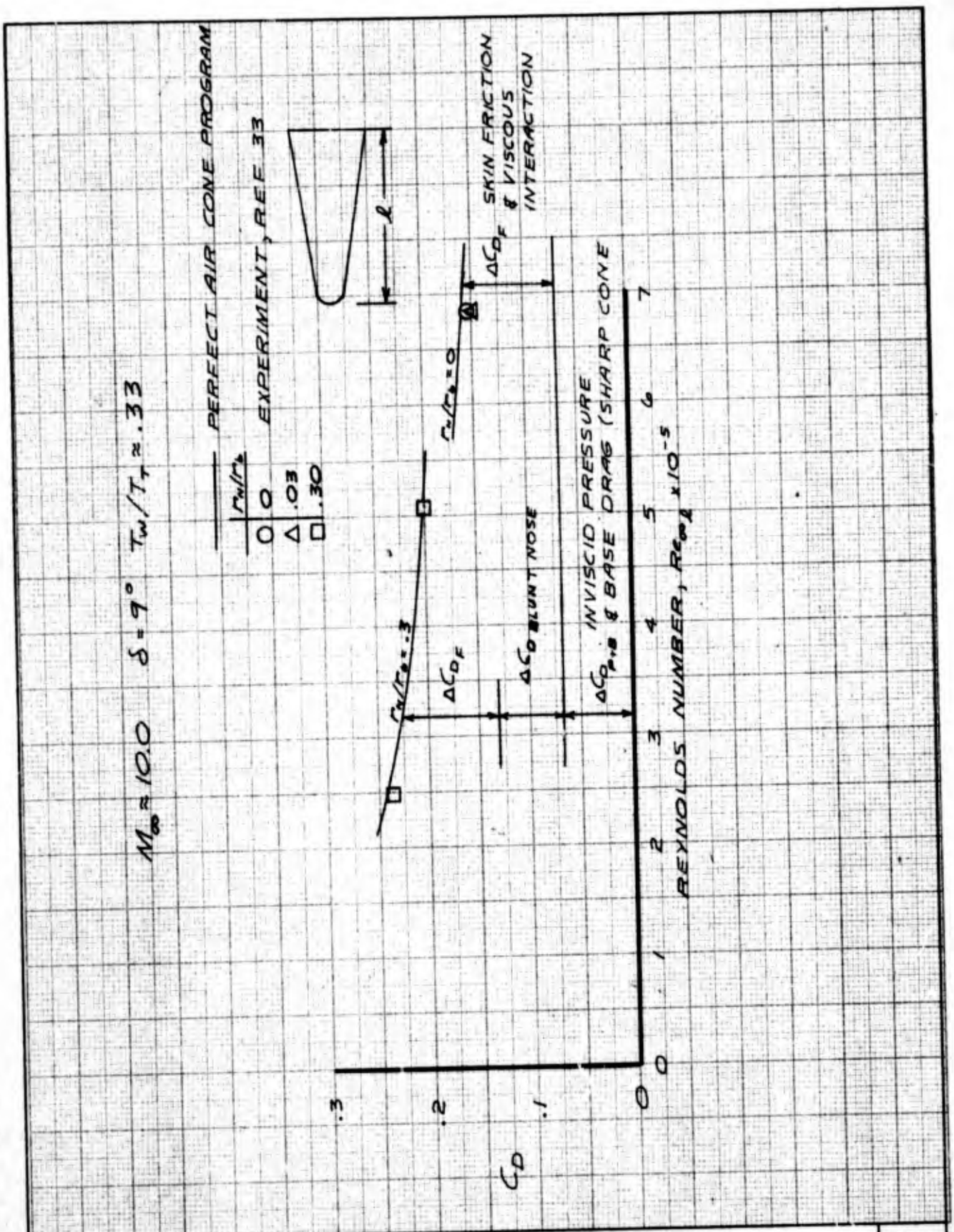

	INITIALS	DATE	REV BY INITIALS	DATE	TITLE	MODEL
CALC	DWE	11/65			COMPARISON OF CALCULATED AND EXPERIMENTAL DRAG ON SLENDER CONES IN LAMINAR FLOW	Fig. 4.20
CHECK						
APPD.						
APPD.						

U3 4013 8000 REV. 12-64

REV LTR_____

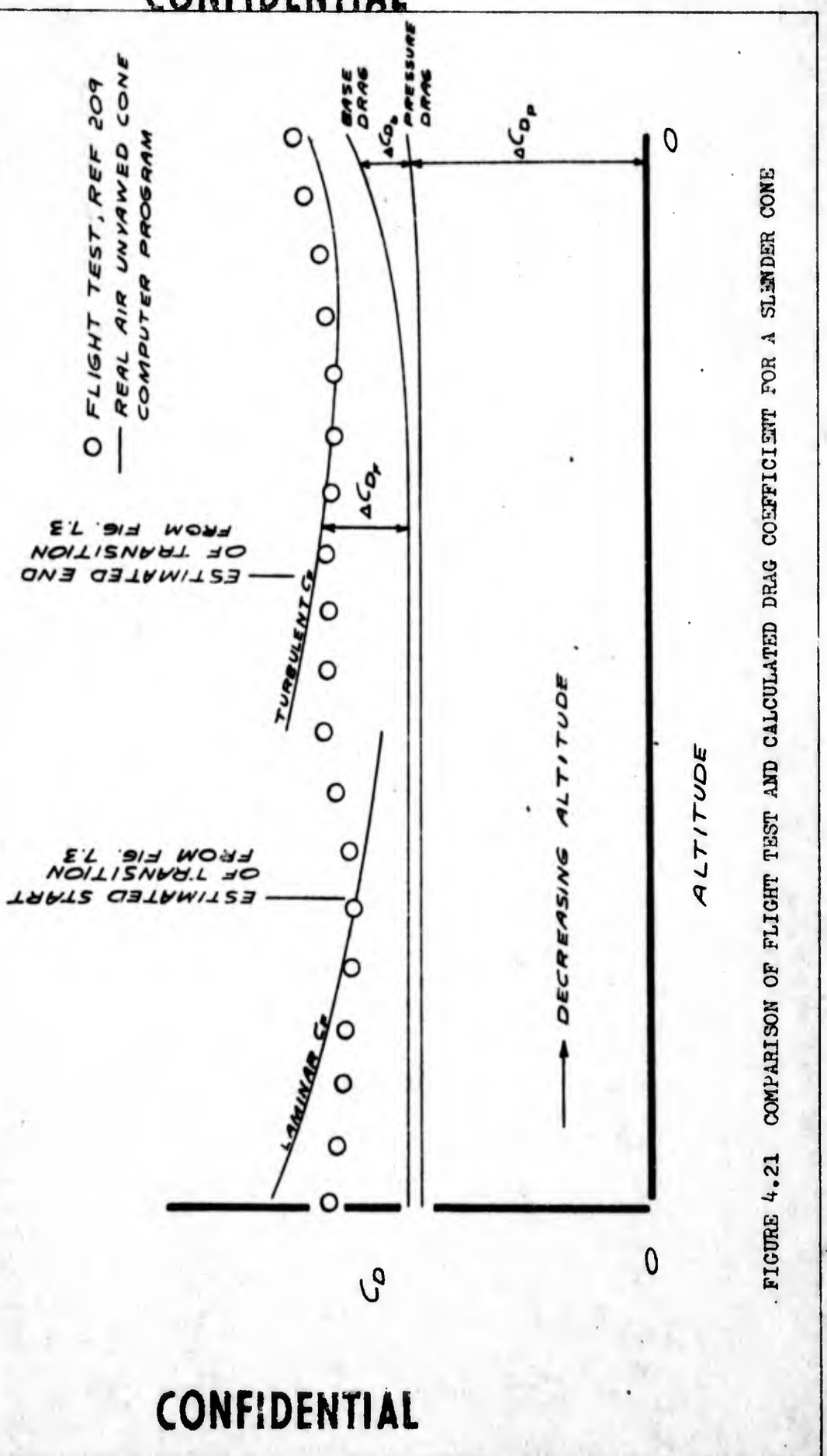

FIGURE 4.21 COMPARISON OF FLIGHT TEST AND CALCULATED DRAG COEFFICIENT FOR A SLENDER CONE

5.0 DYNAMIC DAMPING IN PITCH

References which contain dynamic damping data are summarized on Pages 88 and 89.

The determination, both theoretically and experimentally, of dynamic force and moment coefficients is much more difficult than the determination of static coefficients.

Several types of nomenclature are currently in use, necessitating considerable care when working with dynamic coefficients. The damping-in-pitch normal force coefficients is usually defined

$$C_{N_q} + C_{N_{\dot{\alpha}}} = \frac{\partial C_N}{\partial\left(\frac{qd}{V}\right)_{q\to 0}} + \frac{\partial C_N}{\partial\left(\frac{\dot{\alpha}d}{V}\right)_{\dot{\alpha}\to 0}} \qquad 5.1$$

$$\text{or} \quad = \frac{\partial C_N}{\partial\left(\frac{qd}{2V}\right)_{q\to 0}} + \frac{\partial C_N}{\partial\left(\frac{\dot{\alpha}d}{2V}\right)_{\dot{\alpha}\to 0}} \qquad 5.2$$

$$\text{or} \quad = \frac{\partial C_N}{\partial\left(\frac{ql}{V}\right)_{q\to 0}} + \frac{\partial C_N}{\partial\left(\frac{\dot{\alpha}l}{V}\right)_{\dot{\alpha}\to 0}} \qquad 5.3$$

$$\text{or} \quad = \frac{\partial C_N}{\partial\left(\frac{ql}{2V}\right)_{q\to 0}} + \frac{\partial C_N}{\partial\left(\frac{\dot{\alpha}l}{2V}\right)_{\dot{\alpha}\to 0}} \qquad 5.4$$

Note that either the cone base diameter or cone length can be used in the reduced frequency term. The term may or may not include a factor of 2.

The damping-in-pitch moment coefficient is usually defined

$$C_{m_q} + C_{m_{\dot{\alpha}}} = \frac{\partial C_m}{\partial\left(\frac{qd}{V}\right)_{q\to 0}} + \frac{\partial C_m}{\partial\left(\frac{\dot{\alpha}d}{V}\right)_{\dot{\alpha}\to 0}} \qquad 5.5$$

$$\text{or} \quad = \frac{\partial C_m}{\partial\left(\frac{qd}{2V}\right)_{q\to 0}} + \frac{\partial C_m}{\partial\left(\frac{\dot{\alpha}d}{2V}\right)_{\dot{\alpha}\to 0}} \qquad 5.6$$

$$\text{or} \quad = \frac{\partial C_m}{\partial\left(\frac{ql}{V}\right)_{q\to 0}} + \frac{\partial C_m}{\partial\left(\frac{\dot{\alpha}l}{V}\right)_{\dot{\alpha}\to 0}} \qquad 5.7$$

$$\text{or} \quad = \frac{\partial C_m}{\partial\left(\frac{ql}{2V}\right)_{q\to 0}} + \frac{\partial C_m}{\partial\left(\frac{\dot{\alpha}l}{2V}\right)_{\dot{\alpha}\to 0}} \qquad 5.8$$

C_m, the pitching moment coefficient, can be referenced to either the cone base diameter or cone length.

The following moment transfer equations can be used to transfer the dynamic coefficients from the cone apex to a new moment center. The moment transfer equations depend upon which of the preceding definitions is used. x is the distance from the apex to the new moment center, positive measured aft. ℓ is the moment reference length, generally the cone base diameter or the cone length.

For C_{N_q}

$$C_{N_q} = C_{N_{q_o}} - \frac{X}{S} C_{N_\alpha} \qquad \text{when} \qquad C_{N_q} = \frac{\partial C_N}{\partial\left(\frac{qS}{V}\right)} \qquad 5.9$$

or

$$C_{N_q} = C_{N_{q_o}} - \frac{2X}{S} C_{N_\alpha} \qquad \text{when} \qquad C_{N_q} = \frac{\partial C_N}{\partial\left(\frac{qS}{2V}\right)} \qquad 5.10$$

For C_{m_q}

$$C_{m_q} = C_{m_{q_o}} + \frac{X}{S} C_{N_{q_o}} - \frac{X}{S} C_{m_{\alpha_o}} - \left(\frac{X}{S}\right)^2 C_{N_\alpha} \qquad \text{when} \qquad C_{m_q} = \frac{\partial C_m}{\partial\left(\frac{qS}{V}\right)} \qquad 5.11$$

or

$$C_{m_q} = C_{m_{q_o}} + \frac{X}{S} C_{N_{q_o}} - 2\frac{X}{S} C_{m_{\alpha_o}} - 2\left(\frac{X}{S}\right)^2 C_{N_\alpha} \qquad \text{when} \qquad C_{m_q} = \frac{\partial C_m}{\partial\left(\frac{qS}{2V}\right)} \qquad 5.12$$

For $C_{m_{\dot\alpha}}$

$$C_{m_{\dot\alpha}} = C_{m_{\dot\alpha}} + \frac{X}{S} C_{N_{\dot\alpha}} \qquad \text{for either definition} \qquad 5.13$$

Note that C_{N_α} and $C_{N_{\dot\alpha}}$ are independent of moment center location.

Subsonic and Transonic Speeds

No theory exists and little experimental data are available. It is difficult to correlate existing experimental data, since the data are obtained for a wide range of moment center locations. Existing experimental data are summarized on Page 88.

Figure 5.1 shows that slightly rounding the base has a large effect on the dynamic damping of slender cones. However, it is difficult to ascertain if this difference is due directly to rounding the base or if it is due to a change in sting interference effects resulting from rounding the base.

Nose bluntness reduces the dynamic damping as shown in Figure 5.2.

References 129 and 136 show that the variation of damping coefficient is irregular with angle of attack.

Supersonic Speeds

For supersonic speeds Combined First and Second Order Linearized theory[109] can be used to estimate dynamic damping*. (Appendix 13 shows two misprints which occurred in Reference 109). This theory is restricted to slender bodies at small angles of attack. Figure 5.3 shows plots of C_{N_q} and $C_{N_{\dot{\alpha}}}$ calculated using Linearized theory. The dynamic moment coefficients, measured at the cone apex and based on cone length can be calculated by

$$C_{m_{q_0}} = \frac{-.75}{\cos^2\delta} C_{N_{q_0}} \qquad 5.14$$

$$C_{m_{\dot{\alpha}}} = \frac{-.75}{\cos^2\delta} C_{N_{\dot{\alpha}}} \qquad 5.15$$

*BLITZ program available, See Section 12.0.

These data can be transformed to other moment centers using equations 5.10, 5.12 and 5.13.

Figures 5.1, 5.2 and 5.5 show comparisons of theory and experiment at supersonic speeds. Comparison is good, considering the assumptions made in linearized theory and the difficulty in measuring experimental data.

Experimental data shows the damping to be nearly constant at small angle of attack.

No theory is available for predicting the effect of nose bluntness at supersonic speeds. Experimental data in Figure 5.2 show that bluntness reduces dynamic damping.

Hypersonic Speeds

In the past, Newtonian theory[109] was used to estimate hypersonic dynamic damping. The recently developed Hypersonic Shock Expansion theory[517] has been found to give a better comparison with experimental data*. This theory is limited to small angles of attack and to $M_\infty \sin\delta \geq 1.4$. Figure 5.4 shows plots of $C_{N_{q_o}}$ and $C_{m_{q_o}}$ calculated using this theory. At hypersonic speeds, $C_{N_{\dot{\alpha}}}$ and $C_{m_{\dot{\alpha}}}$ are small and are assumed to be equal to zero. Figures 5.5 and 5.6 show comparisons of experimental data with Shock Expansion theory, as well as Newtonian theory.

Both experiment and theory show that the damping coefficient is nearly constant with angle of attack as shown in Figure 5.6.

*BLITZ programs available, See Section 12.0.

Experimental data show that blunting a cone reduces the dynamic damping as shown in Figure 5.7. Unfortunately no adequate theory is currently available for predicting the effect of blunting. Newtonian theory gives a poor prediction. A modified version of Shock Expansion theory has been developed. However, some of the results from this theory presented in Reference 517 are inconsistent with each other and show a poor comparison with experimental data. This method needs further evaluation.

All theoretical methods for calculating dynamic damping assume that the reduced frequency is small (i.e., $\frac{\omega l}{V} \to 0$) and that viscous effects are small. Figure 5.8 shows the effect of Reynolds number and the reduced frequency on the dynamic damping for a slender cone.

EXPERIMENTAL DYNAMIC DAMPING DATA

REF.	MACH NUMBER	δ DEGREES	r_N / r_b	α_{MAX}
114.	.1	33.2	0	12
129.	.25 - 2.2	12.5	0 AND .6	18
157.	.25 - 2.2	12.5	.6	20
2.	.5 - 1.5	15	.175	0
525.	.5 - 4	9	.25	0
69.	.5 - 21	10	.019	0
135.	.6 .95	7.5 AND 13.3	0 AND .38	0
172.	.6 - 1.35	11.6	.384	10
36.	.6 - 1.4	9	.04	16
4.	.6 - 1.5	7	0 - .022	6
127.	.6 - 3.2	10.7	.23	0
505.	.6 7.5	7	.22	0
136.	.65 - 2.2	20	0 AND .4	21
306.	.8 - 9.9	10	.2	11
211.	1 - 25	SUMMARY OF ALL LORV VEHICLE FLIGHT TESTS		
608.	1.5 - 10	10	0 - .85	22
508.	1.6 - 3.9	7.1	.22	11
531.	1.7 - 3.3	9.5	0	0
601.	2 - 5.6	10	0	30
70.	2 - 6	10 AND 15	0 AND .2	25
35.	2 - 10	9	.047	0
63.	2 - 10	9	NONSPHERICAL	10
31.	2.5 - 4	10	0	0
71.	3 - 8	10	0 AND .3	0
64.	3 - 12	15	.113	10
305.	3 - 22	8	0	-
67.	3.5 - 4.6	9	0	0
303.	4 - 20	8	0	20
517.	4.8	20	0 AND .3	5
68.	5 - 10	10	.015	2
521.	6	9 AND 45	0	30
578.	6	15	.11	10
506.	6.5 - 14	SLENDER CONE	-	30
202.	6.5 - 17	8 - 16	.03 - .15	16
174.	6.86	10.7	.23	5
569.	8	9	0	25
3.	8	20	0 AND .4	14
407.	8 AND 10	9	0 - .36	15
403.	8 - 21	7.1 AND 10	0 AND .222	0
540.	8 AND 25	SLENDER CONE	-	-

EXPERIMENTAL DYNAMIC DAMPING DATA

REF.	MACH NUMBER	δ DEGREES	r_N / r_b	α_{MAX}
203.	9 - 15	5.7 AND 8.3	VARIOUS SHAPES	20
8.	9 - 22	6.34 - 13.35	0 - .38	0
208.	10	8	0	6
9.	10	8	0	12
78.	10	8	0 - .15	9
57.	10	8	.04	12
212.	10	8	.04	14
72.	10	9	.04	10
81.	10	9	.04	25
19.	10	10	0 - .3	10
22.	10	11	0	15
39.	10	6	VARIOUS SHAPES	9
23.	10	6.3	VARIOUS SHAPES	0
304.	10 - 20	8	0	12
603.	11	9	.05	0
709.	14	3.5	0	0
66.	14	5.6	0 - .3	10
751.	14	5.6	.166	0
555.	14	10	.15	23
753.	14	CONE	.04 AND .14	28
651.	14	SLENDER CONE	-	35
210.	16 - 25	9	0	7
654	17	9	0	10
511.	17	9	.076 AND .3	0
209.	18 - 24	8	0	10
52.	20	10	.02	0
584.	20	SUMMARY REPORT		

$$C_{m_q} + C_{m_{\dot{\alpha}}} = \frac{\partial C_m}{\partial\left(\frac{qd}{V_\infty}\right)_{q\to 0}} + \frac{\partial C_m}{\partial\left(\frac{qd}{V_\infty}\right)_{\dot{\alpha}\to 0}}$$

$$C_m = \frac{M}{q_\infty S d}$$

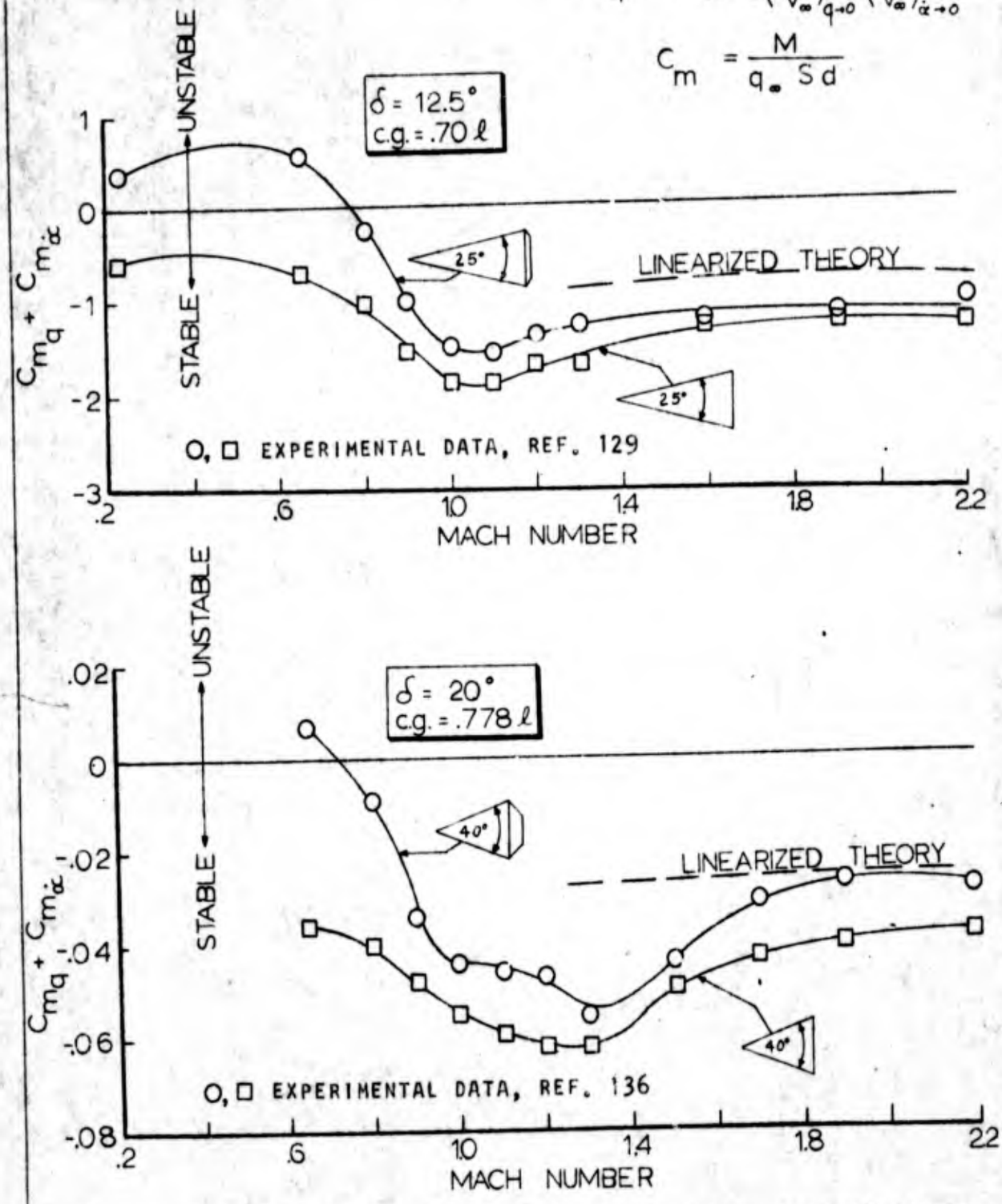

FIG. 5.1 THE EFFECTS OF ROUNDING CONE BASE ON DYNAMIC DAMPING

$$C_{m_q} + C_{m_{\dot{\alpha}}} = \frac{\partial C_m}{\partial\left(\frac{qd}{V_\infty}\right)_{q\to 0}} + \frac{\partial C_m}{\partial\left(\frac{qd}{V_\infty}\right)_{\dot{\alpha}\to 0}}$$

$$C_m = \frac{M}{q_\infty S d}$$

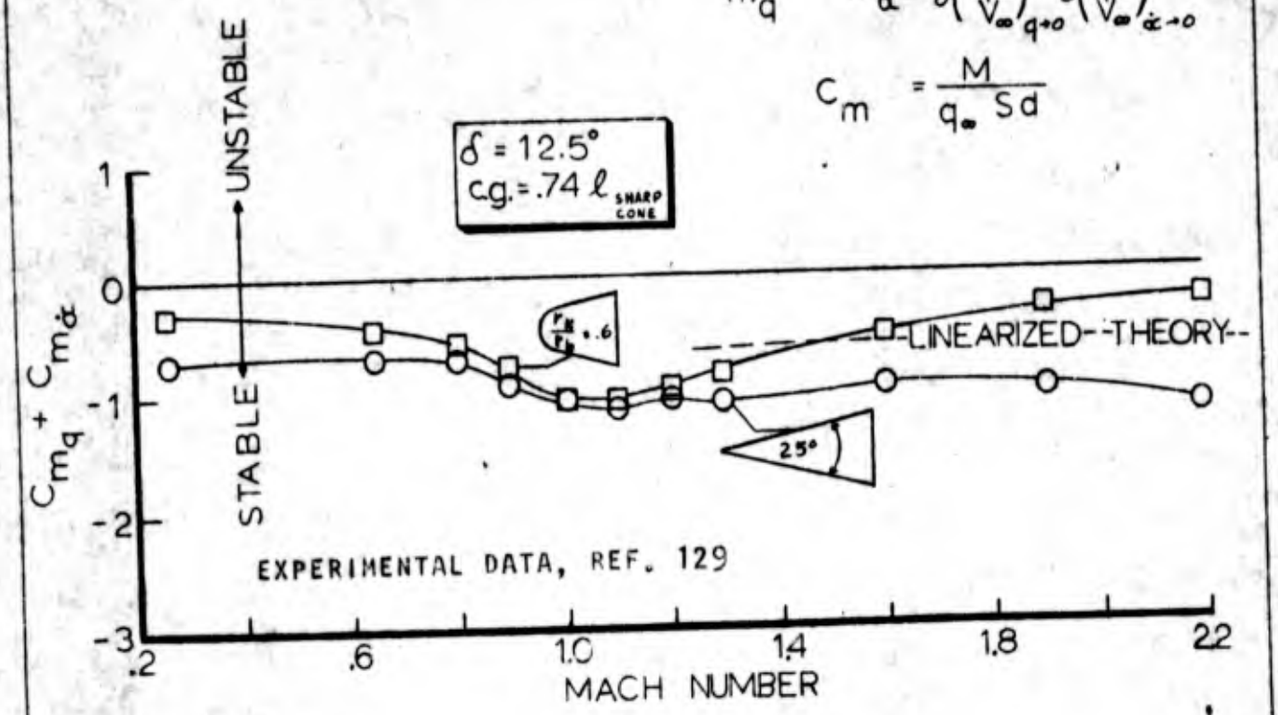

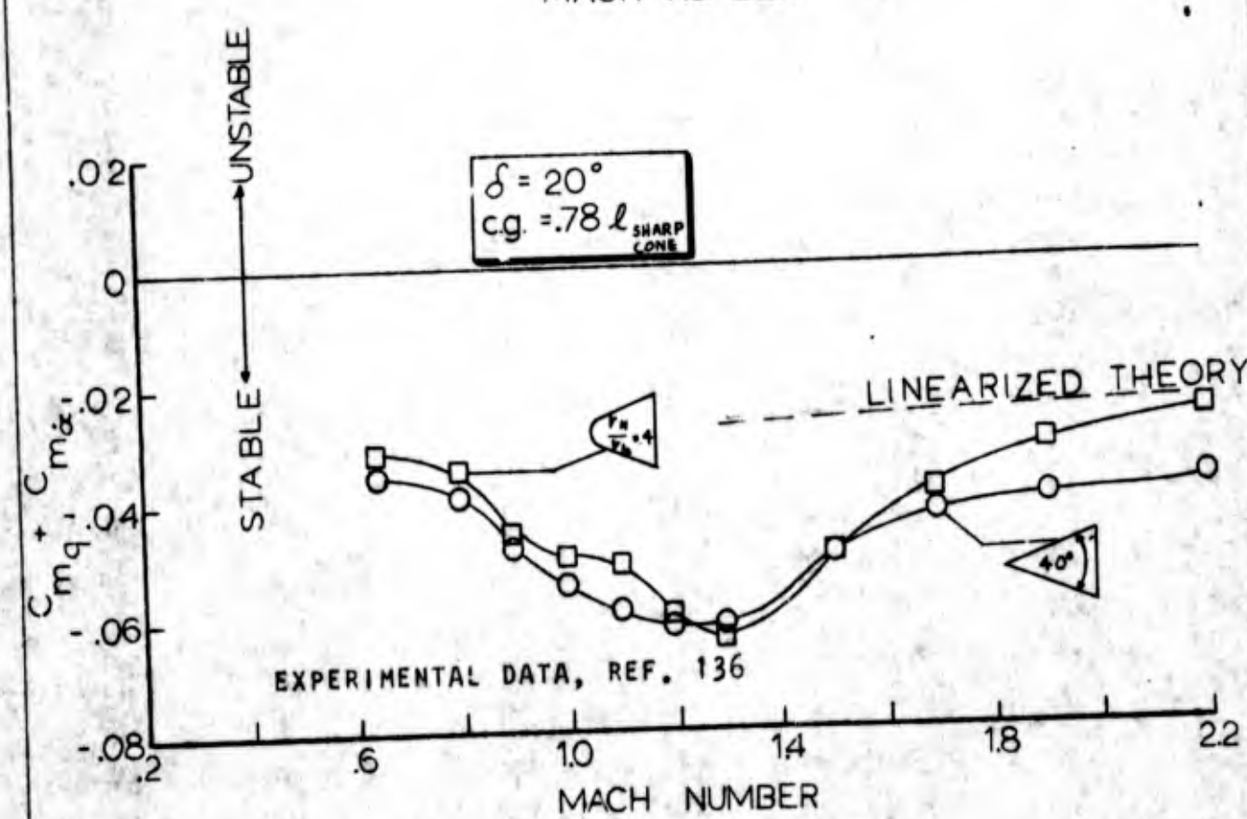

FIG. 5.2 THE EFFECTS OF NOSE BLUNTNESS ON DYNAMIC DAMPING

$$C_N = \frac{N}{q_\infty S_{BASE}}$$

$$C_{N_{q_0}} = \frac{\partial C_N}{\partial\left(\frac{q\ell}{2V}\right)_{q\to 0}}$$

$$C_{m_{q_b}} = \frac{-.75}{\cos^2\delta} C_{N_{q_0}}$$

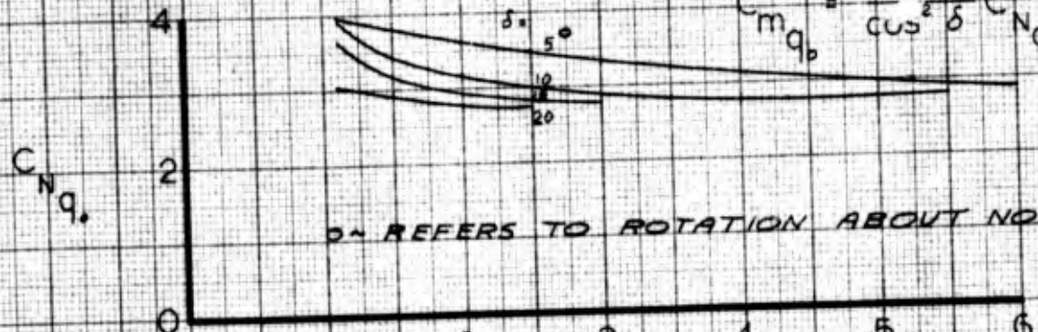

b~ REFERS TO ROTATION ABOUT NOSE

$$C_{N_{\dot\alpha}} = \frac{\partial C_N}{\partial\left(\frac{\dot\alpha\ell}{2V}\right)_{\dot\alpha\to 0}}$$

$$C_{m_{\dot\alpha_0}} = \frac{-.75}{\cos^2\delta} C_{N_{\dot\alpha}}$$

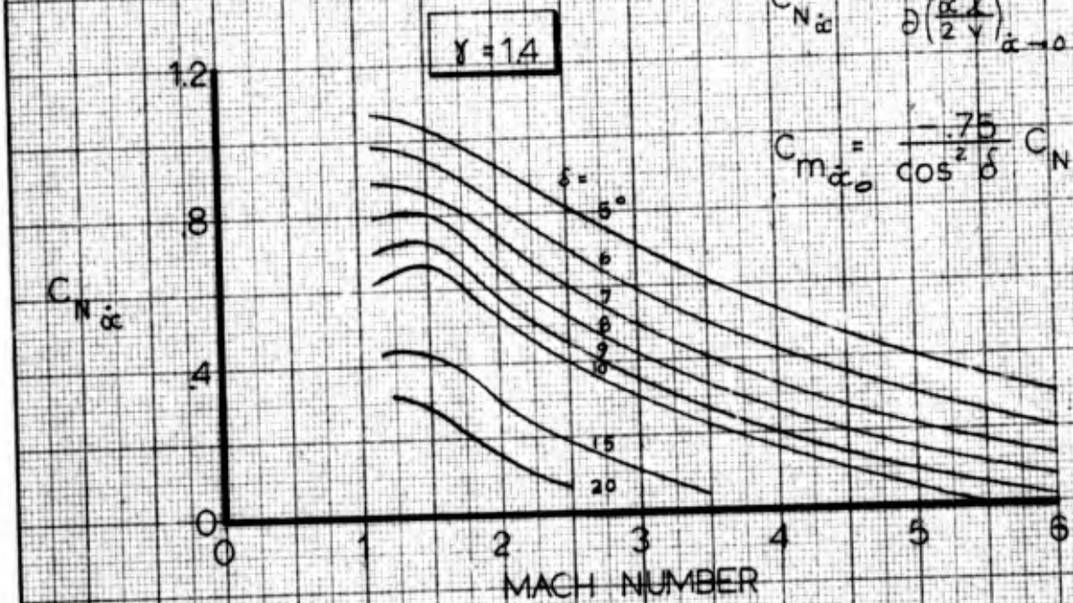

THEORY FROM REF. 109

	INITIALS	DATE	REV BY INITIALS	DATE	TITLE	MODEL
CALC	DWE	8/65			DYNAMIC DAMPING FOR SHARP CONES CALCULATED USING LINEARIZED THEORY	Fig. 5.3
CHECK						
APPD.						
APPD.						

U3 4013 8000 REV. 12-64

REV LTR

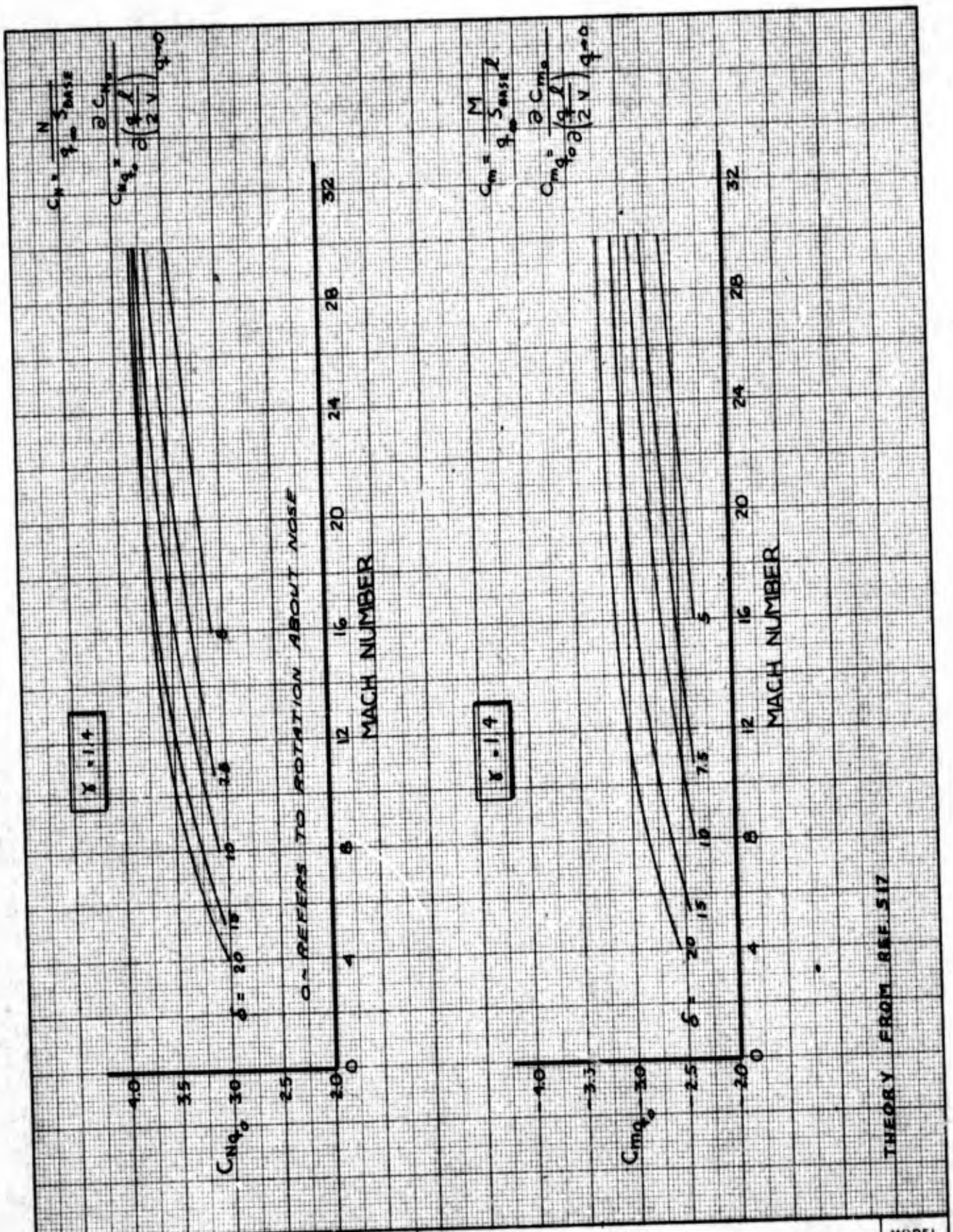

	INITIALS	DATE	REV BY INITIALS	DATE	TITLE	MODEL
CALC	OWE	8/65			DYNAMIC DAMPING FOR SHARP CONES CALCULATED USING SHOCK EXPANSION THEORY	Fig. 5.4
CHECK						
APPD.						
APPD.						

U3 4013 8000 REV. 12-64

REV LTR

BOEING NO D2-36139-1

SH 93

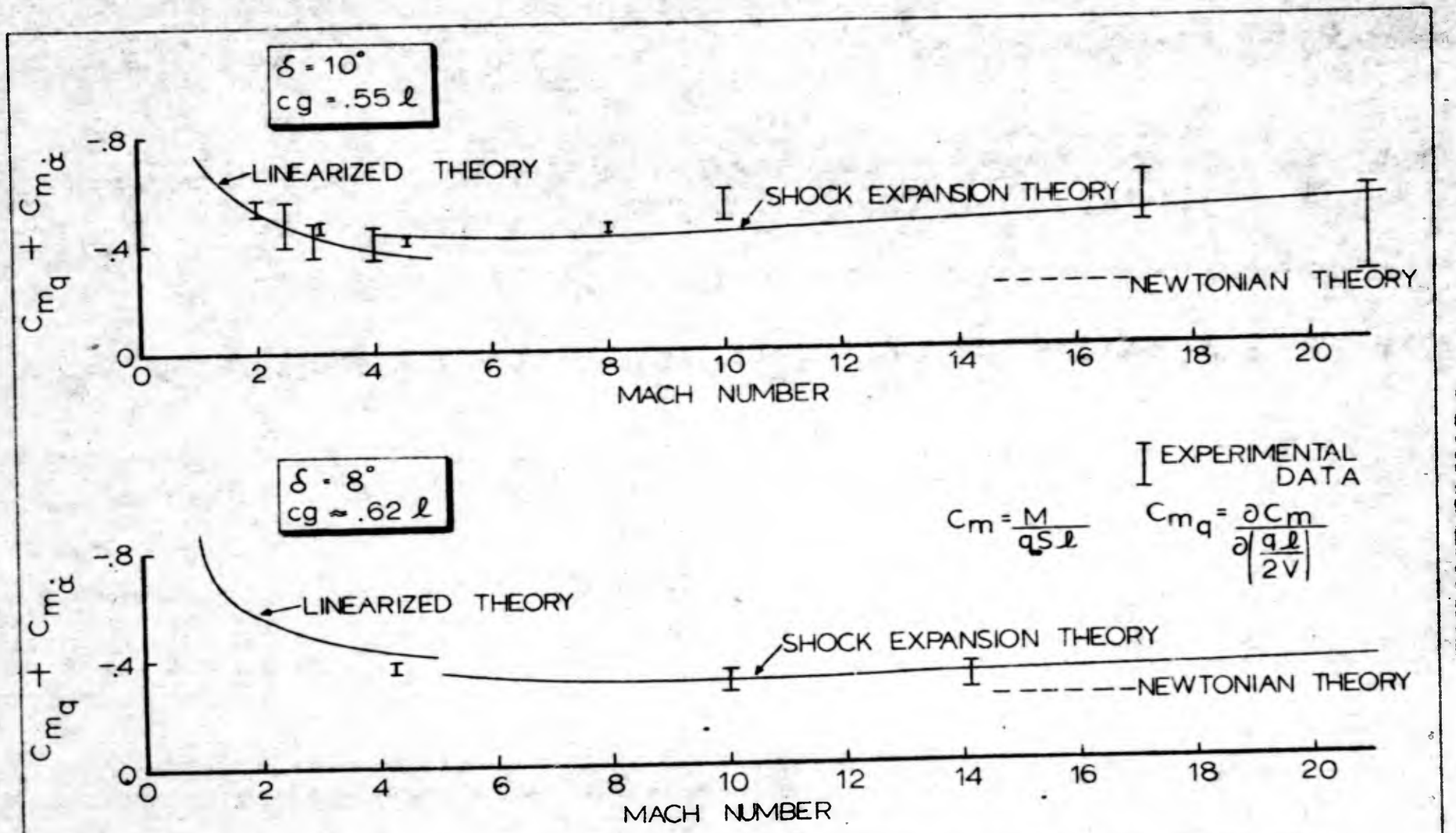

FIG. 5.5 COMPARISONS OF THEORETICAL AND EXPERIMENTAL DYNAMIC DAMPING FOR SHARP CONES

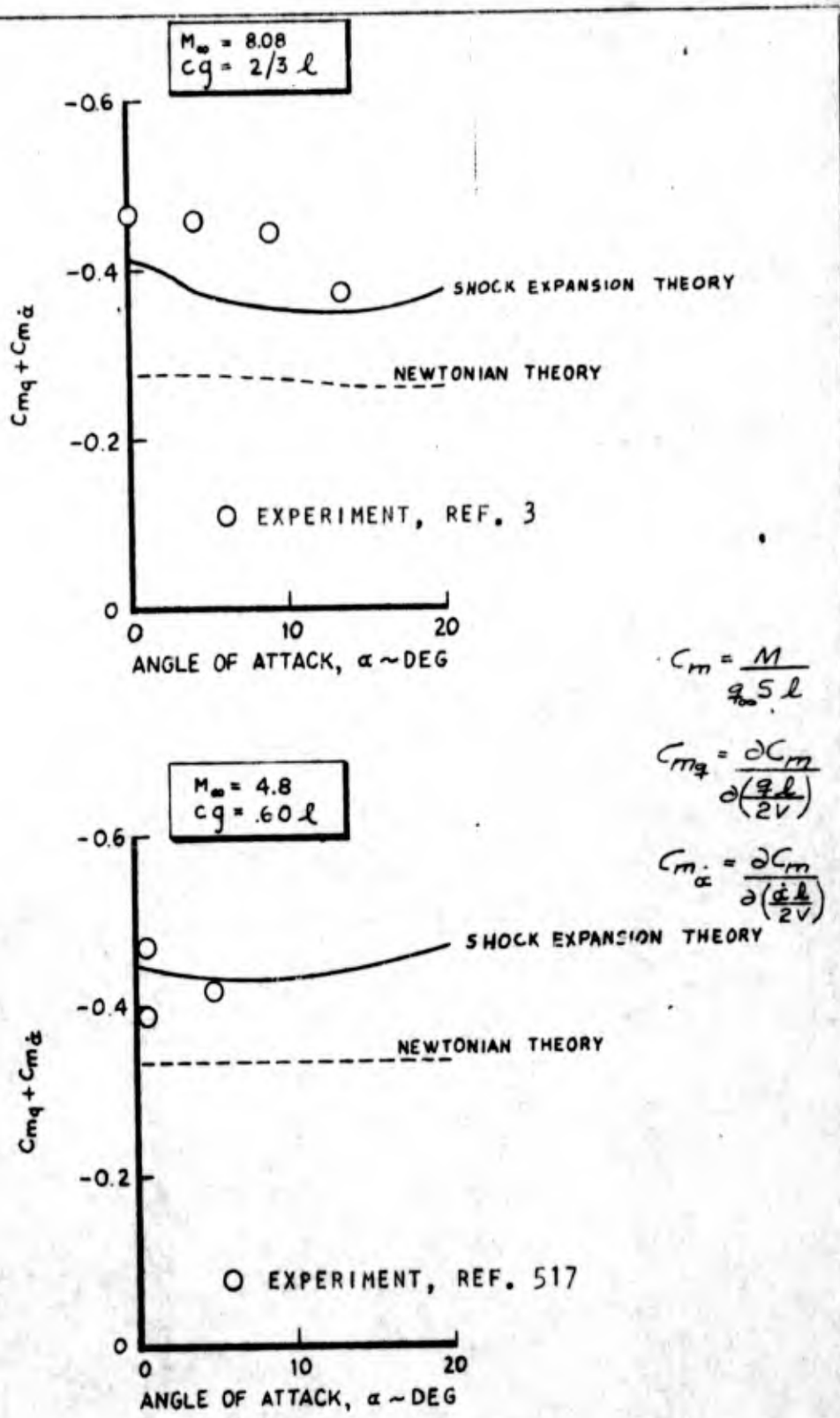

FIG. 5.6 COMPARISONS OF THEORETICAL AND EXPERIMENTAL DYNAMIC DAMPING FOR HYPERSONIC SHARP CONES AT ANGLES OF ATTACK $\delta = 20°$

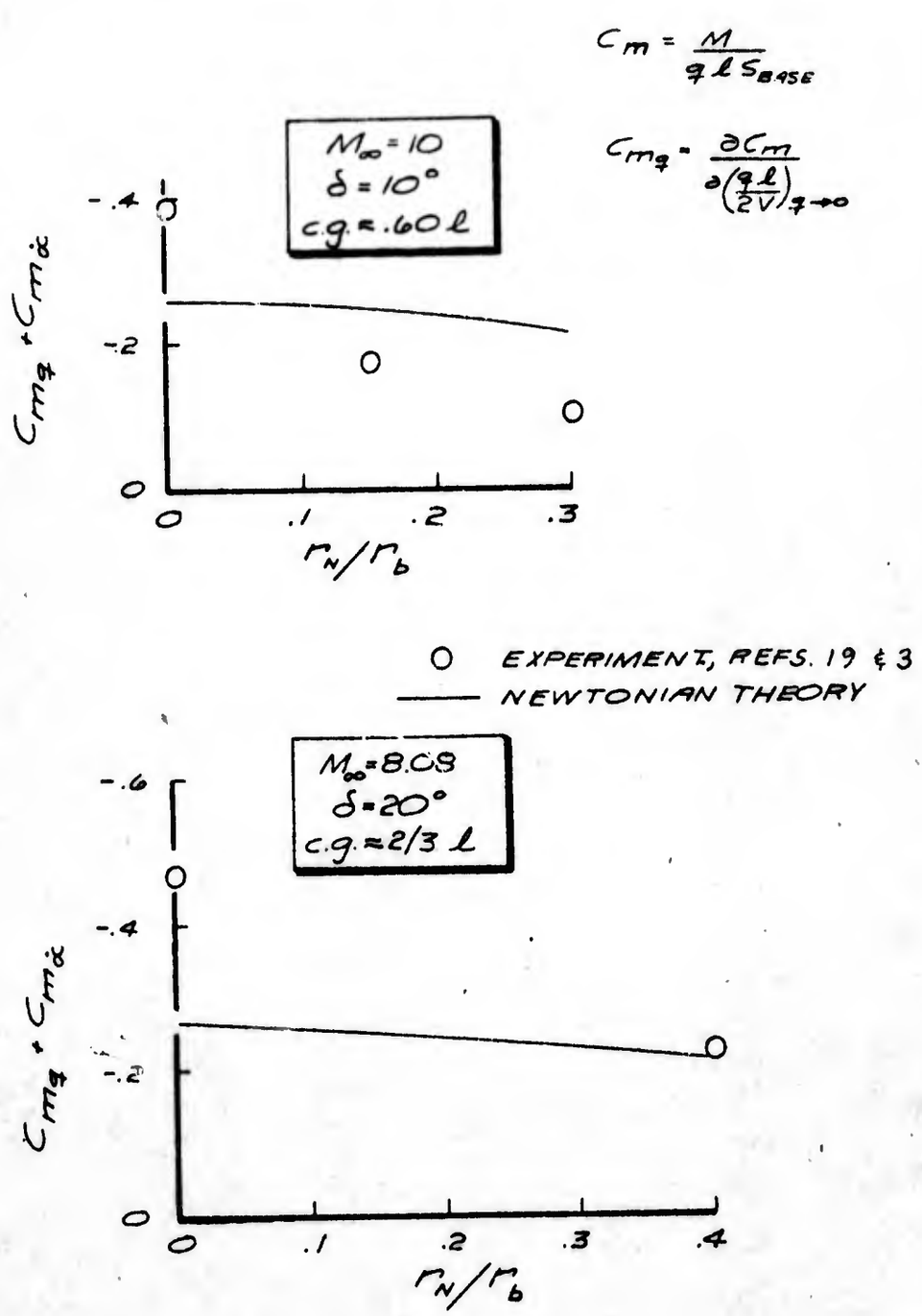

FIG. 5.7 THE EFFECTS OF NOSE BLUNTNESS ON CONE DYNAMIC DAMPING

Figure From Ref. 304

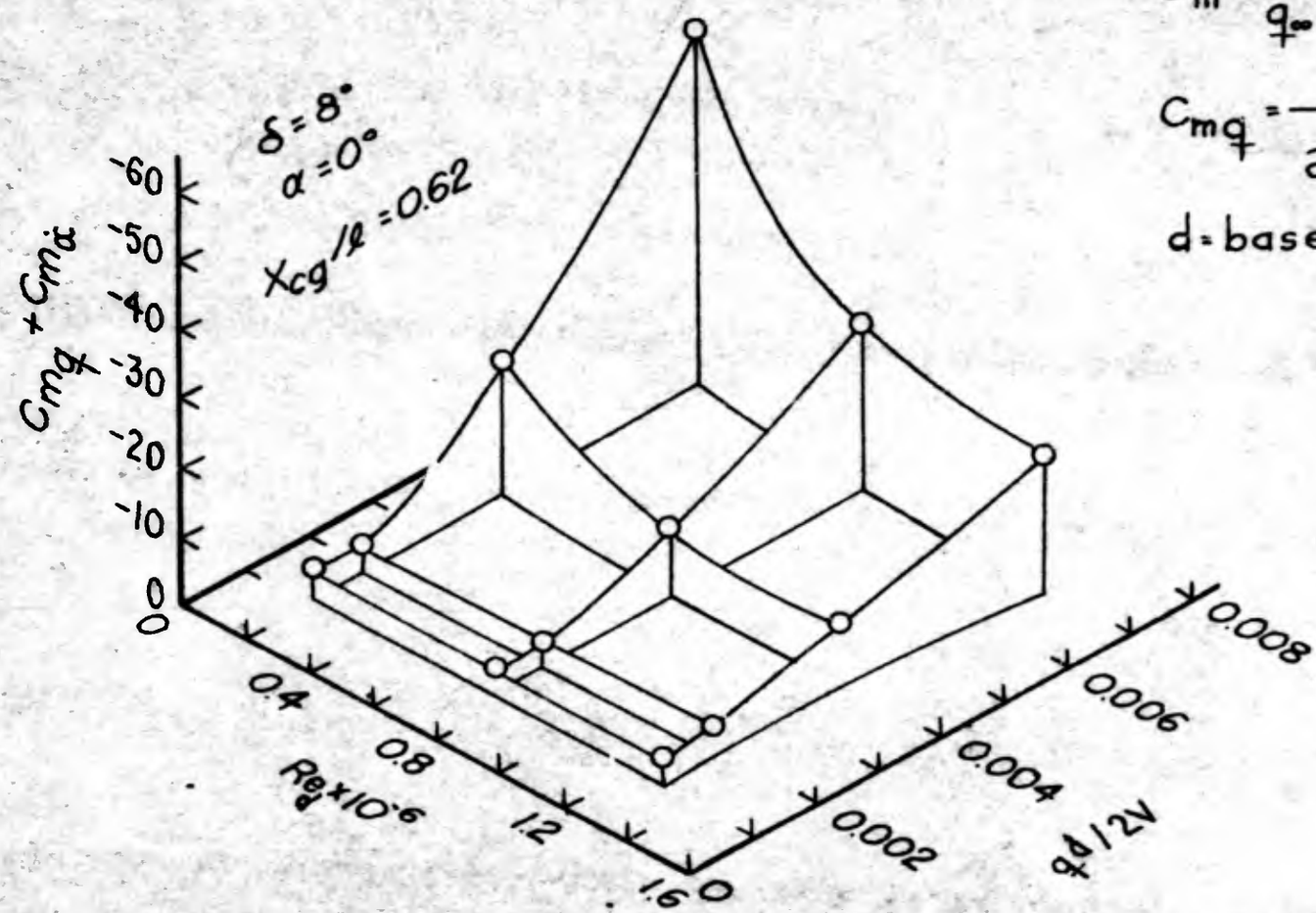

FIG. 5.8 THE EFFECTS OF REYNOLDS NUMBER AND REDUCED FREQUENCY ON THE DYNAMIC DAMPING OF A SHARP CONE

6.0 PRESSURE COEFFICIENT

References which contain pressure coefficient data are found on Pages 104 and 105.

The pressure coefficient is defined

$$C_p = \frac{P_c - P_\infty}{\rho_\infty V_\infty^2/2}$$ all conditions

$$C_p = \frac{2}{\gamma M_\infty^2}\left(\frac{P_c}{P_\infty} - 1\right)$$ perfect gas

$$C_p = 1 - \left(\frac{V_c}{V_\infty}\right)^2$$ incompressible flow

Subsonic Speeds

A theoretical method, known as the Neumann program, has been developed by the Douglas Aircraft Company [507] to calculate the incompressible subsonic pressure distribution on a sharp or blunt cone-cylinder. Unfortunately, this program is not available at Boeing at the present time.

It has been found that existing experimental data for unyawed cones could be successfully correlated by plotting $C_p/(\delta)^{1.35}$ versus x/l as shown in Figure 6.1. Most of the data are for cone-cylinders. Removing the trailing cylinder increases the pressure coefficient near the base of the cone.

Reference 115 states that the influence of Mach number at subsonic speeds on a slender cone can be calculated by

$$C_p = -8\delta_{RAD}^2 \ln_e \sqrt{1-M_\infty^2} + C_{p_{incompressible}} \qquad 6.1$$

Figure 6.2 shows the excellent comparison of this equation with experimental data.

A modification of Slender Body theory is proposed for calculating angle of attack effects. The original theory predicts that the change in pressure coefficient due to angle of attack is

$$\Delta C_p = 4\alpha \tan\delta \cos\varphi + \alpha^2(1-4\sin^2\varphi)$$

However, when integrated around the body these pressures give

$$C_{N\alpha_{\alpha=0}} = .035/\,deg$$

which does not agree with the values of normal force coefficient slope plotted in Figures 2.1 and 2.3. Therefore, to give a better prediction of incremental pressure due to angle of attack and to assure that the integrated pressures give the correct normal force curve slope let

$$\Delta C_p = \frac{C_{N\alpha_{\alpha=0}}}{.035}\left[4\alpha \tan\delta \cos\varphi + \alpha^2(1-4\sin^2\varphi)\right] \qquad 6.2$$

$C_{N_{\alpha}}$ is obtained from Figure 2.1, or Figure 2.3 divided by 57.3. This theory can also be used at transonic and supersonic speeds. Figure 6.3 shows the good comparison of equation 6.2 with experimental data.

The effect of nose bluntness on pressure can be obtained from the references summarized on Pages 104 and 105.

Transonic Speeds

For $M_\infty \approx 1.0$, Reference 115 shows that the pressure distribution on the cone portion of a cone-cylinder can be calculated over the front one-third of the cone by

$$C_p = \frac{2(M_\infty^2 - 1)}{M_\infty^2(\gamma+1)} - 8\delta^2 \ln_e\left(\frac{2\delta x}{l}\right) + 4\delta^2 \ln_e\left\{\left[\frac{4}{1.78 M_\infty^2 \delta^2(\gamma+1)}\right] + \left[\frac{x}{l}\left(1-\frac{x}{l}\right)\right]\right\} + 2\delta^2\left[\frac{1-3\frac{x}{l}}{1-\frac{x}{l}}\right] - 4\delta^2 \qquad 6.3$$

and over the rear two-thirds of the cone by

$$C_p = \frac{2(M_\infty^2 - 1)}{M_\infty^2(\gamma+1)} - 8\delta^2 \ln_e\left(\frac{2\delta x}{l}\right) + 4\delta^2 \ln_e\left\{4\delta^2 + \frac{\left[1-\left(\frac{x}{l}\right)^2\right]}{1.78 M_\infty^2 \delta^2(\gamma+1)}\right\} - 4\delta^2 \qquad 6.4$$

Figure 6.4 shows a comparison of these equations with experimental data. It is assumed that removing the cylindrical afterbody has little effect on the cone

pressure distribution.

The effect of angle of attack on pressure can be calculated using the modified slender body theory of equation 6.2.

The effect of nose bluntness on pressure can be obtained from references listed on Pages 104 and 105.

Supersonic and Hypersonic Speeds

The zero angle of attack pressure coefficient on a cone is calculated by the Unyawed Cone computer programs discussed in Section 12.0. Sample output from these programs are shown in Figure 4.17 for a cone in real air, and in Figure 4.18 for a cone in perfect air. Solutions for a wide range of cone angles and free stream conditions are published in References 139 and 152 for perfect air ($\gamma = 1.4$), and in References 515 and 566 for equilibrium real air.

The pressure coefficient for unyawed cones in perfect air are shown in Figures 4.4 and 4.5. Figure 4.6 as well as other calculated results[566] shows that real air effects have little influence on the pressure coefficient and therefore, Figures 4.4 and 4.5 can be used at most free stream conditions.

Unfortunately, the hypersonic zero angle of attack pressure coefficient is too often calculated using Newtonian theory

$$C_p = 2 \sin^2 \delta \qquad 6.5$$

Figure 4.6 shows this equation underestimates C_p for very slender cones and for cones at low hypersonic Mach numbers.

Four methods for calculating angle of attack effects at supersonic speeds are available.

1) For small angles of attack, $\alpha \ll \delta$, the 1st order method of Reference 140 can be used.

2) For moderate angles of attack, $\alpha \approx \delta$, modified Slender Body theory (Eq. 6.2) can be used to give approximate results.

3) For moderate angles of attack, $\alpha \approx \delta$, the 2nd order method of Reference 522 can be used.

4) For large angles of attack, the theory of Reference 123 can be used at higher supersonic Mach numbers.

None of these theories include the effect of flow separation which occurs on the leeward side of a yawed body. Figure 6.5 shows a comparison of the first three methods with experimental data.

At hypersonic speeds, Newtonian theory gives a good prediction of pressure coefficient at angles of attack not near zero.

$$C_p = 2\left(\sin\delta\cos\alpha + \cos\delta\sin\alpha\cos\varphi\right)^2 \qquad 6.6$$

Two minor improvements to this theory are discussed in References 123 and 807. Equation 6.6 is invalid for the "shadowed" region of the cone, i.e., when

$$\varphi > \cos^{-1}\left(\frac{-\tan\delta}{\tan\alpha}\right) \qquad 6.7$$

Figure 6.6 shows the excellent comparison of equation 6.6 and experimental data.

Blunting a cone at supersonic and hypersonic speeds will cause the pressure aft of the blunt nose to be lower than the corresponding pressure for a sharp cone as shown in Figure 6.7. The blunt cone pressure is lower because the flow "overexpands" as it passes around the nose. As the flow moves downstream, it starts to compress and eventually the pressure approaches the sharp cone value. This is why the pressure drag on a slightly blunted cone may be lower than the pressure drag for the corresponding sharp cone (see Section 4.0).

Theoretical results in Figure 6.7 were calculated using the Boeing Inverse Method Blunt Body and Method of Characteristics Body computer programs discussed in Section 12. These programs can be used to calculate the pressure distributions and pressure drag on unyawed blunt cones when $M_\infty > 1.5$. Reference 532 presents pressures calculated using similar methods for blunt cones with half-angles between 0 and 40 degrees and at Mach numbers between 3.0 and infinity ($\gamma = 1.4$).

For blunt cones at small and moderate angles of attack the Method of Characteristics Yawed Axisymmetric Body computer program discussed in Section 12 can be used to obtain the approximate pressure distribution. Figure 6.7 shows a comparison of pressures calculated by this program with experimental pressures on the most windward streamline of a cone at $\alpha = 10^\circ$. At large angles of attack, References 123 and 807 show that "overexpansion" effects become negligible and Newtonian theory[120] can be used to calculate the pressure distribution.

EXPERIMENTAL PRESSURE DATA

REF.	MACH NUMBER	δ DEGREES	r_N / r_b	α_{MAX}
801.	.1	15 AND 30	0 - .5	20
507.	.2 - 3.5	10	0 - 1	0
554.	.3 - 1.3	7.5	.143	15
184.	.3 - 1.3	7.5	.15	15
204.	.4 - 20.	NONCONICAL SHAPES	-	20
206.	.4 - 20	NONCONICAL SHAPES	-	20
105.	.55 - 1.4	20 - 30	0	0
164.	.6 - 1.2	14.5	.24	8
115.	.6 - 1.15	7	0	0
137.	.6 - 1.2	15.3 - 30	0 - .6	10
110.	.6 - 1.4	7	0	0
1.	.6 - 1.5	10	0	0
105.	.6 - 1.5	20 AND 25	0	0
181.	.7 - 2	10 - 40	0	4
173.	.9 - 4.1	50	0	0
211.	1 - 25	SUMMARY OF ALL LORV VEHICLE FLIGHT TESTS		
27.	1.5 - 10	5	.035	12
561.	1.5 AND 2	10 AND 15	0	2
153.	1.6 - 2.4	15	0	0
30.	2	9	.05	15
534.	2	15 AND 30	0	0
74.	2 - 6	9	0	15
75.	2 - 6	NONCONICAL SHAPES	-	20
556.	2 - 8	3.5 - 20	0 - .83	90
55.	2 - 8	8.7	0	25
16.	2 - 10	NONCONICAL SHAPES	-	18
108.	3 - 5	11.4 AND 18.9	-	-
557.	3.1 - 5.5	8	.155	10
103.	3.12	5 - 20	0	9
545.	3.23 AND 4.83	13.33	.39	18
775.	3.53	15 AND 20	0	25
106.	3.55	26.65	0	6
111.	3.7 - 5.7	3	0	0
707.	3.7 - 10.7	SPHERE	-	-
123.	3.86	5 + 15	0 - .42	100
710.	3.9 AND 5.6	5	0	0
77.	4	9	0	15
560.	4.07 - 7.6	10	FLAT NOSE	20
605.	4.5	10	0	0
121.	4.95	10	0	20

EXPERIMENTAL PRESSURE DATA

REF.	MACH NUMBER	δ DEGREES	r_N / r_b	α_{MAX}
815.	5 AND 6.1	8	.144	25
49.	5 AND 8	12.5	0	20
175.	5.25 - 10.6	15 AND 30	.167 AND .183	15
823.	5.8	10 - 40	.4 - 1	8
575.	5.8	15	0 - .6	0
151.	6	15	0 AND .14	90
550.	6	20	.27	15
187.	6	56 - 90	0	25
45.	6 - 10	15	.333	15
48.	6 - 19	9	.03 - .3	0
807.	6.1	10 - 30	0	90
803.	6.1	15	0 - 1	10
506.	6.5 - 14	SLENDER CONE	-	30
202.	6.5 - 17	8 - 16	.03 - .15	16
101.	6.8	20	0	20
516.	6.85 AND 8.6	12.5 - 22.5	0	30
519.	6.85 AND 8.6	14	0	30
522.	7.95	10	0	24
548.	7.95	10	0	24
11.	8 AND 10	9	0 - .36	0
21.	8 AND 20	15 - 19	.125 - .478	0
406.	8 - 20	OGIVE	0 - .12	15
572.	8.04	9	0	25
44.	8.08	15	.125	60
203.	9 - 15	5.7 AND 8.3	VARIOUS SHAPES	20
58.	9 AND 18	9	.3	0
410.	9 - 24	VARIOUS SHAPES	-	-
51.	10	6	0 - .25	0
79.	10	9	0 - .3	24
60.	10	11	.02	18
612.	10 - 15	15 AND 30	0 - .18	15
603.	11	9	.05	0
10.	13 - 21	6.5 AND 9	.03 AND .3	45
713.	14	10	0	0
12.	14 - 22	7.1 AND 9	.03 - .3	40
210.	16 - 25	9	0	7
76.	18	9	.1	20
209.	18 - 24	8	0	10
26.	19	11	0	15
159.	19	2 - 30	VARIOUS NOSE SHAPES	0

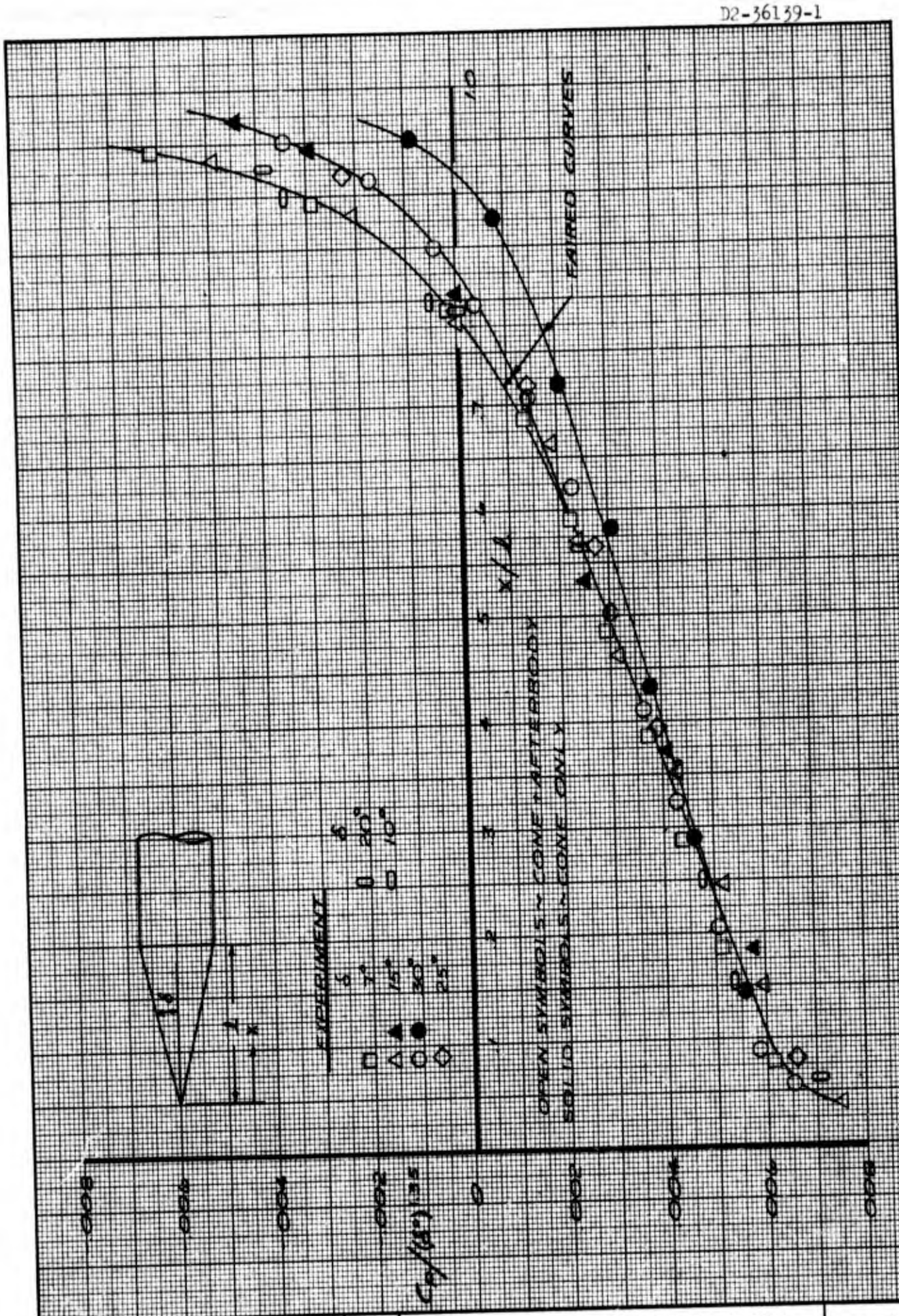

			REVISED	DATE	
CALC					CORRELATION OF PRESSURES ALONG CONES AT INCOMPRESSIBLE SUBSONIC SPEEDS
CHECK	DWE	7/65			
APR					
APR					THE BOEING COMPANY

Fig. 6.1

D2-36139-1

PAGE 106

US 4013 8000

K+E ALBANENE® TRACING PAPER 71896

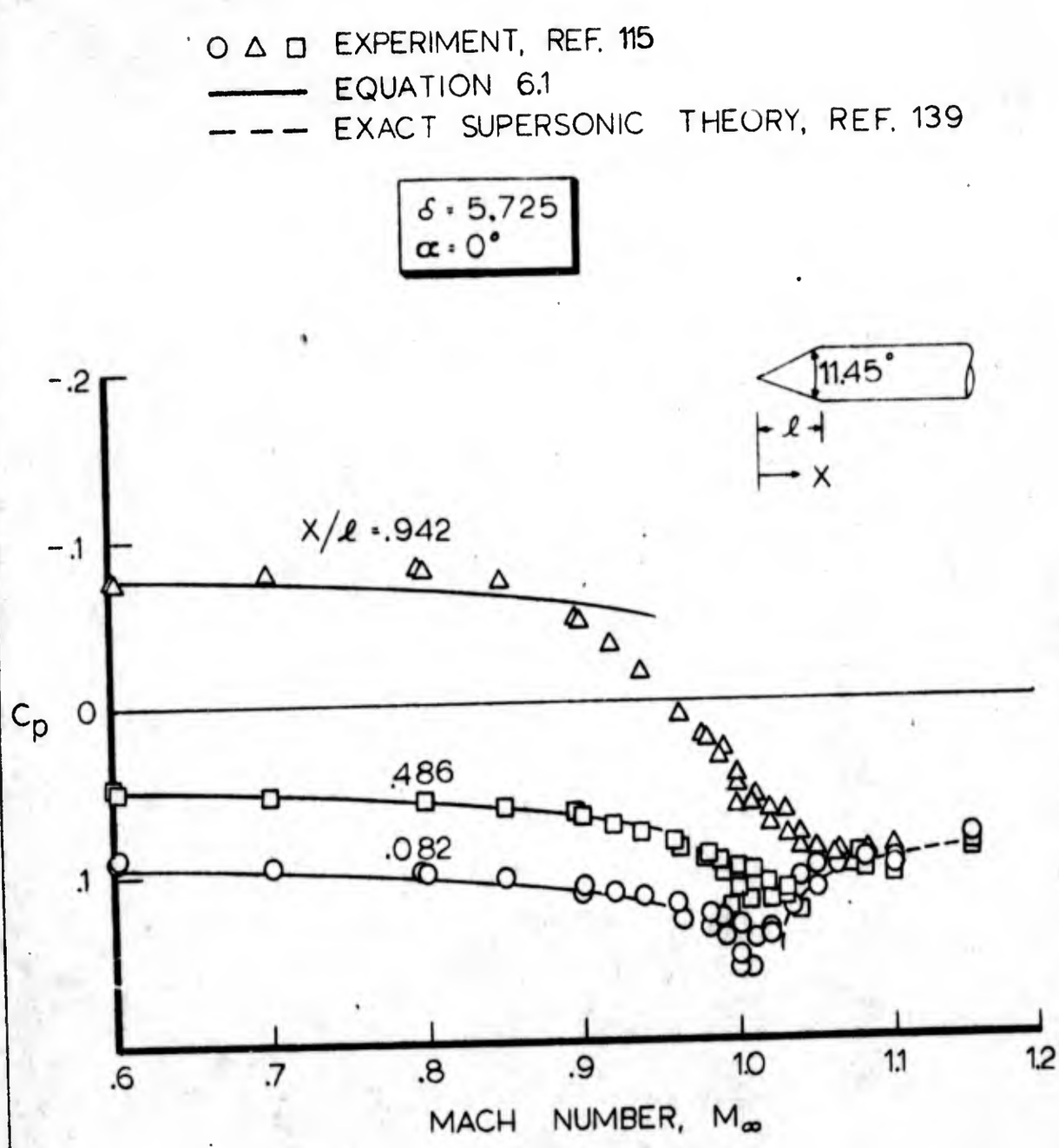

FIG. 6.2 COMPARISON OF EXPERIMENTAL AND THEORETICAL PRESSURES ON A SLENDER CONE AT TRANSONIC SPEEDS

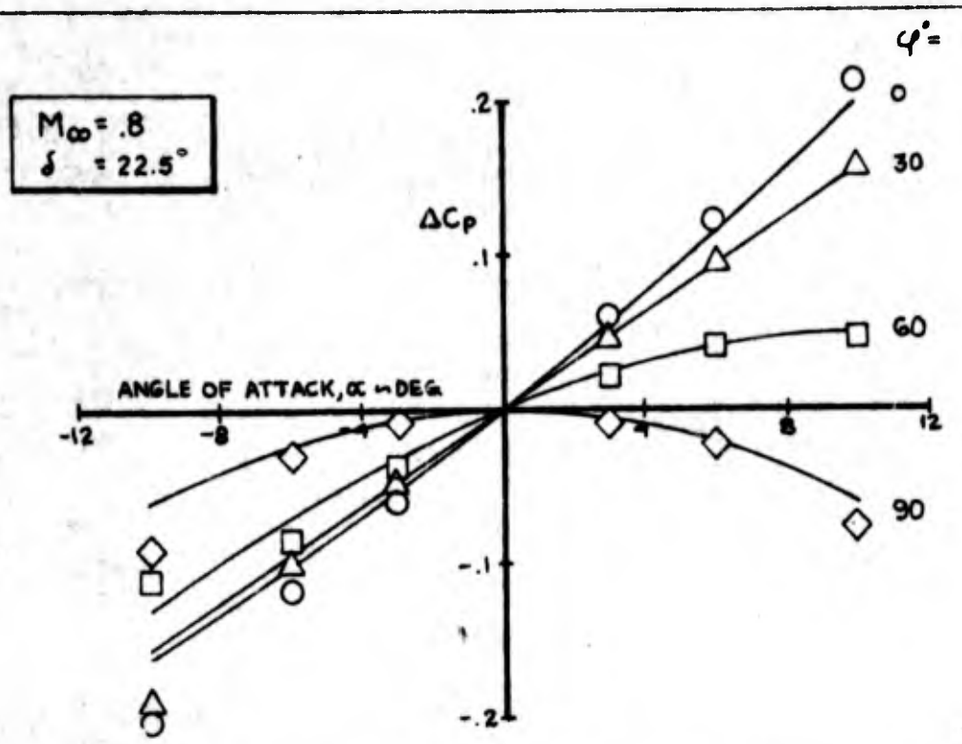

○△□◇ EXPERIMENT, REF. 137

——CORRECTED LINEARIZED THEORY

$$\Delta C_p = \frac{C_{N_\alpha}}{.033}\Big|_{\alpha=0} \left[4\alpha \tan\delta \cos\varphi + \alpha^2(1-4\sin^2\varphi)\right]$$

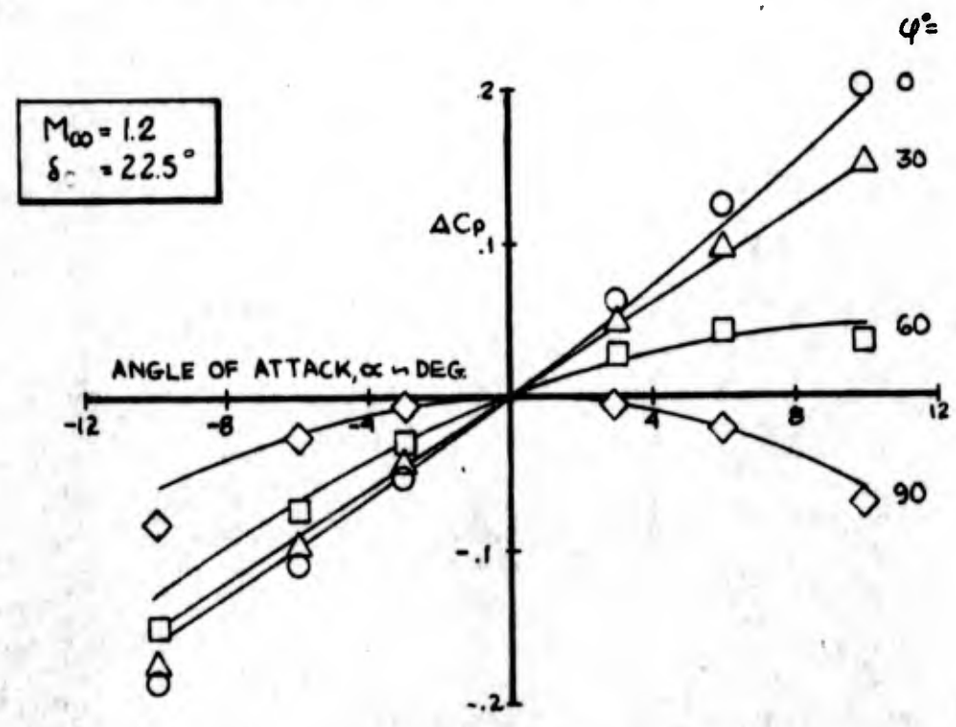

FIG. 6.3 COMPARISON OF EXPERIMENTAL AND THEORETICAL PRESSURES DUE TO ANGLE OF ATTACK ON A YAWED CONE AT TRANSONIC SPEEDS

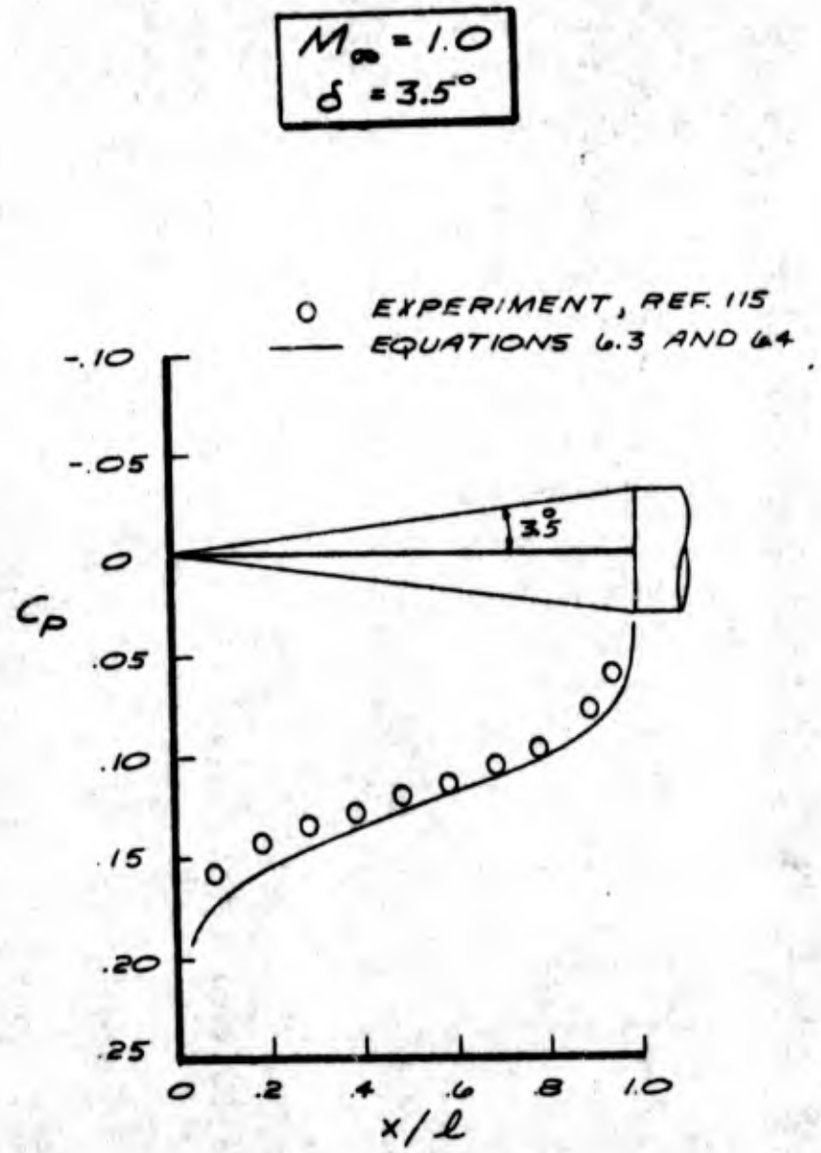

FIG. 6.4 COMPARISON OF EXPERIMENTAL AND THEORETICAL PRESSURES ON AN UNYAWED SLENDER CONE AT $M_\infty = 1.0$

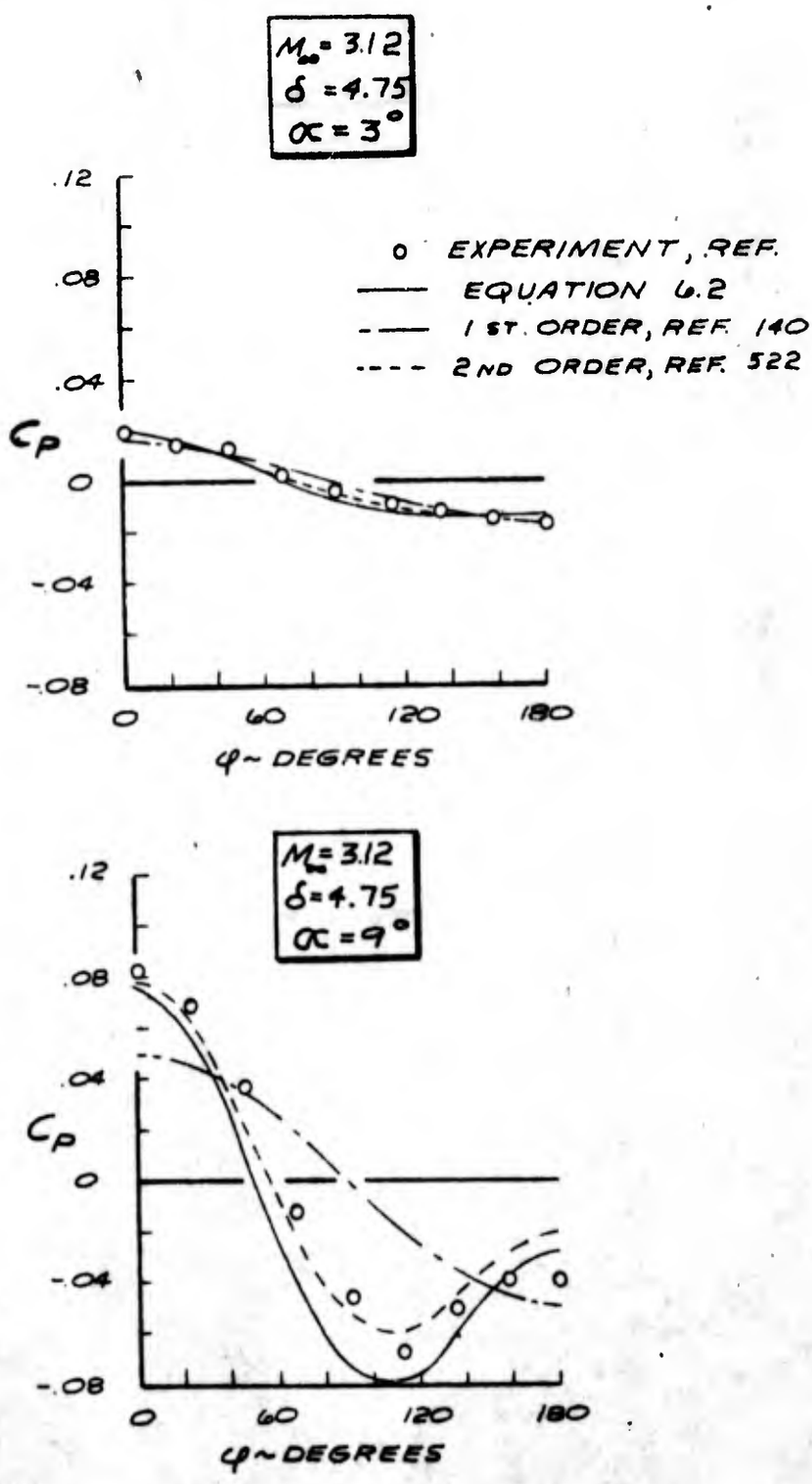

FIG. 6.5 COMPARISON OF EXPERIMENTAL AND THEORETICAL PRESSURES ON A YAWED SLENDER CONE AT A SUPERSONIC SPEED

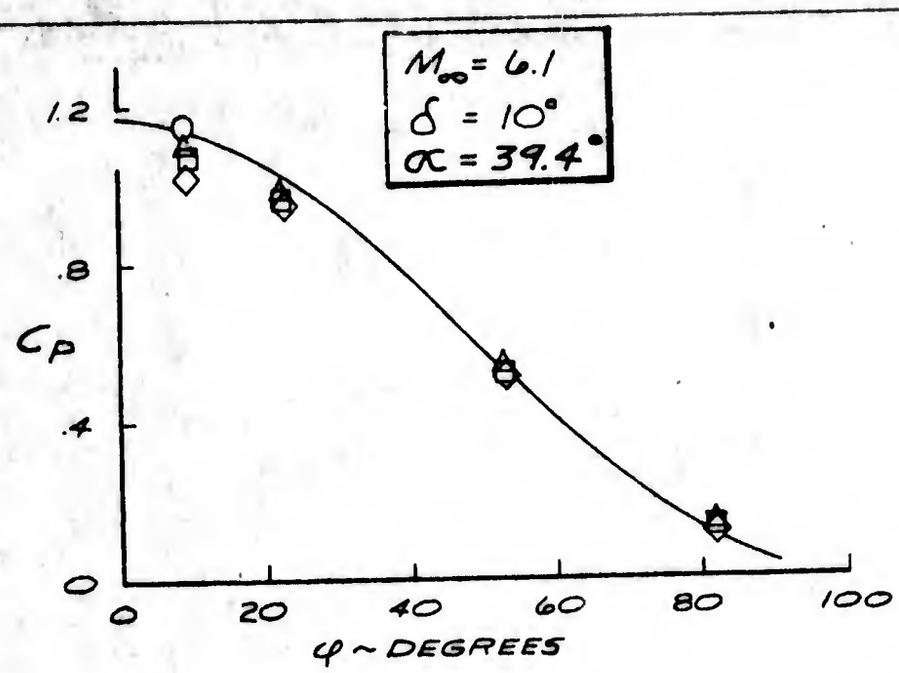

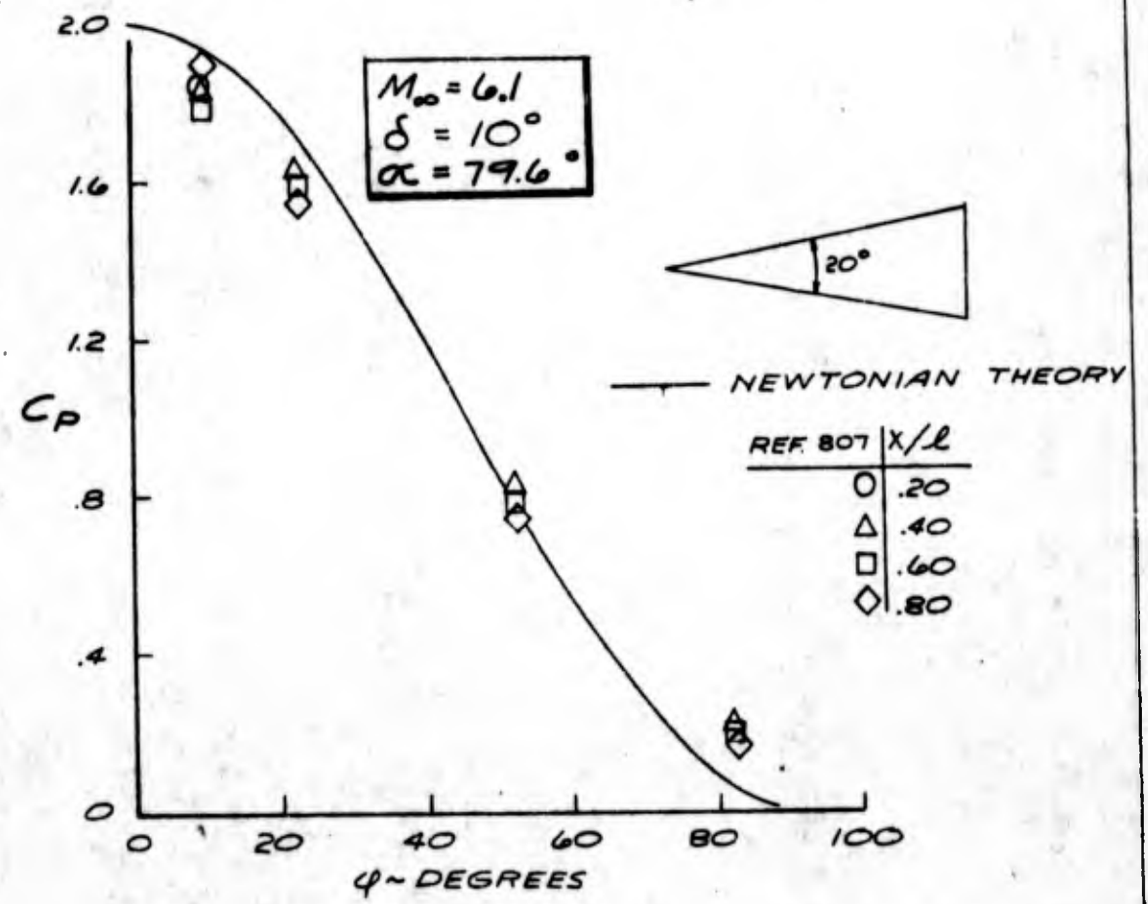

FIG. 6.6 COMPARISON OF EXPERIMENTAL AND THEORETICAL PRESSURES ON A HIGHLY YAWED CONE AT A HYPERSONIC SPEED

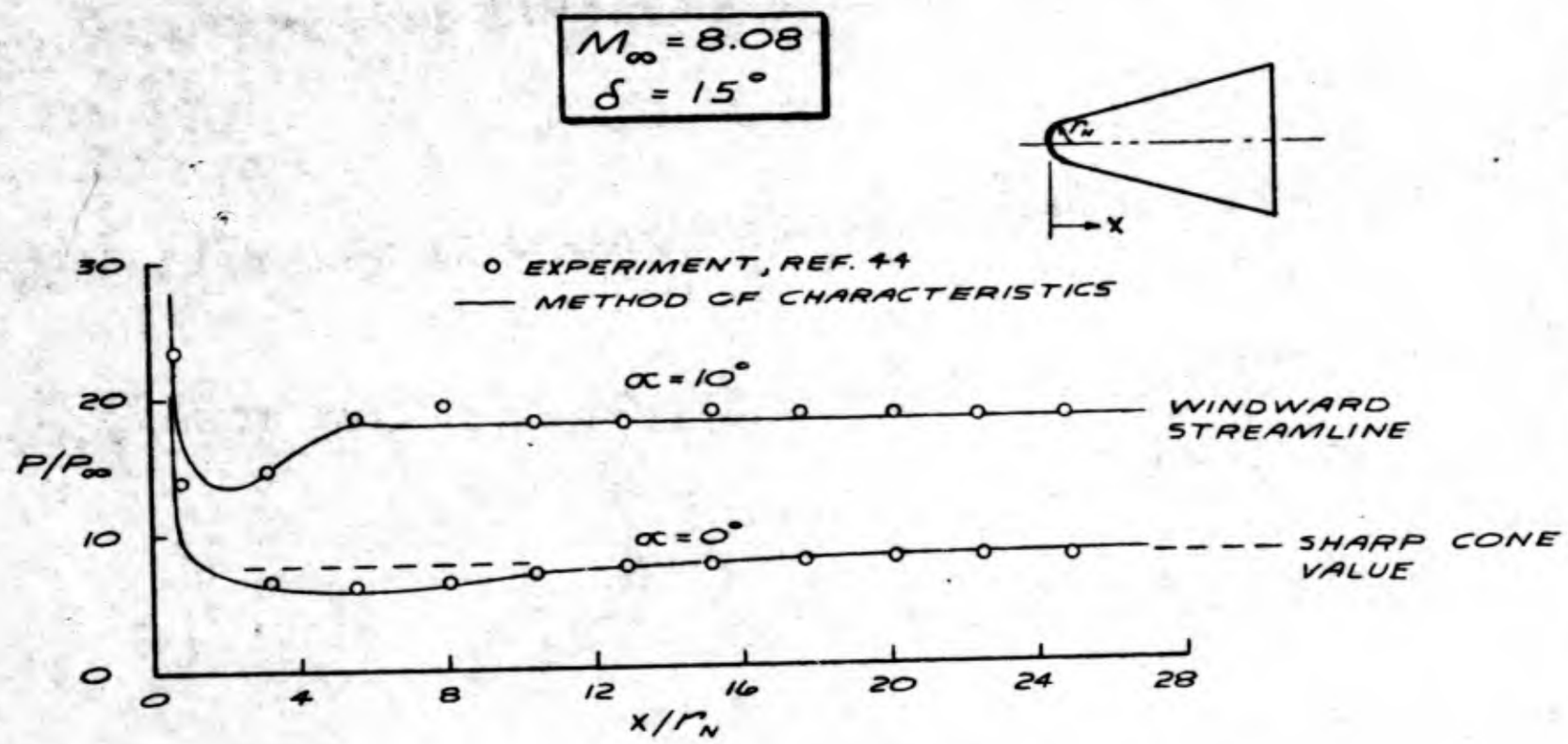

FIG. 6.7 THE EFFECT OF NOSE BLUNTNESS ON THE SURFACE PRESSURES FOR A CONE AT HYPERSONIC SPEEDS

7.0 BOUNDARY LAYER TRANSITION

References which contain transition experimental data are summarized on Page 115. A bibliography of transition data is presented in Reference 510.

Boundary layer transition is difficult to predict due to the number of factors influencing it. Reference 301 lists the following factors:

1) Reynolds number
2) Mach number
3) Surface roughness
4) Wall to edge total temperature or enthalpy ratio
5) Nose bluntness
6) Free stream turbulence
7) Pressure gradient
8) Injection at the surface
9) Vehicle dynamics
10) Configuration change due to ablation

Mach number and Reynolds number effects are generally conceded to be the most important.

Reference 536 (Secret) presents a summary of transition data obtained from flights of actual reentry vehicles.

Transition data is difficult to obtain in experimental facilities as they generally operate at Reynolds numbers lower than that required for transition.

Figures 7.1 and 7.2 show transition data obtained at $M_\infty = 10$ for a slender

cone with various nose radii. Figure 7.1 shows the variation of heat transfer on the cone with Reynolds number. Note that there are different Reynolds numbers associated with the beginning and end of transition. Figure 7.2 shows the variation of transition Reynolds numbers with wall temperature and nose bluntness. Figures 7.1 and 7.2 should be used cautiously as the results shown are for one cone tested at one Mach number and should not be overly extrapolated.

Figure 7.3 shows transition data for slender sharp nosed cones tested at various conditions. This figure can be used in conjunction with Reference 536 to give a good estimate of transition Reynolds number for conical reentry vehicles.

References 122 and 819 present additional transition data for cones at supersonic speeds.

The boundary layer edge Mach and Reynolds numbers are calculated by the Unyawed Cone computer programs discussed in Section 12. Sample output from these programs are shown in Figures 4.17 and 4.18.

EXPERIMENTAL BOUNDARY LAYER TRANSITION DATA

REF.	MACH NUMBER	δ DEGREES	r_N / r_b	α_{MAX}
		SUMMARY OF ALL LORV VEHICLE FLIGHT TESTS		
211.	1 - 25	VARIOUS SHAPES		0
122.	1.6 - 2.2	13.5 - 30	0	0
153.	1.6 - 2.4	15	0 - .05	0
602.	3 - 15	10 - 18	.015	2
68.	5 - 10	10		
551.	5 - 10	FLAT PLATE	-	-
606.	5 - 10	FLAT PLATE	-	-
213.	5 - 16	5 AND 10	.05 - .085	3
301.	5 - 20	8	0	0
214.	5.5	8	0	0
607.	5.5	8	0 - .5	10
577.	6 - 14	6.3	.03	0
56.	6 - 18	5 - 10	0 - .02	0
611.	7 - 21	30	0	0
536.	8 - 22	SLENDER CONES	-	-
411.	8.5 - 10.5	10	0 - .02	2
412.	8.5 - 16	10	0 - .12	2
585.	9.1 - 16	10	0	0
719.	10	5	0 - .06	0
409.	10 AND 12	5	0	0
610.	10	6	0 - .23	4
612.	10 - 15	15 AND 30	0 - .18	15
652.	11	10	0	0
709.	14	3.5	-	-
210.	16 - 25	9	0	7
209.	18 - 24	8	0	10
722.	19 - 22.2	2.87	0	0
414.	20	8	0	0

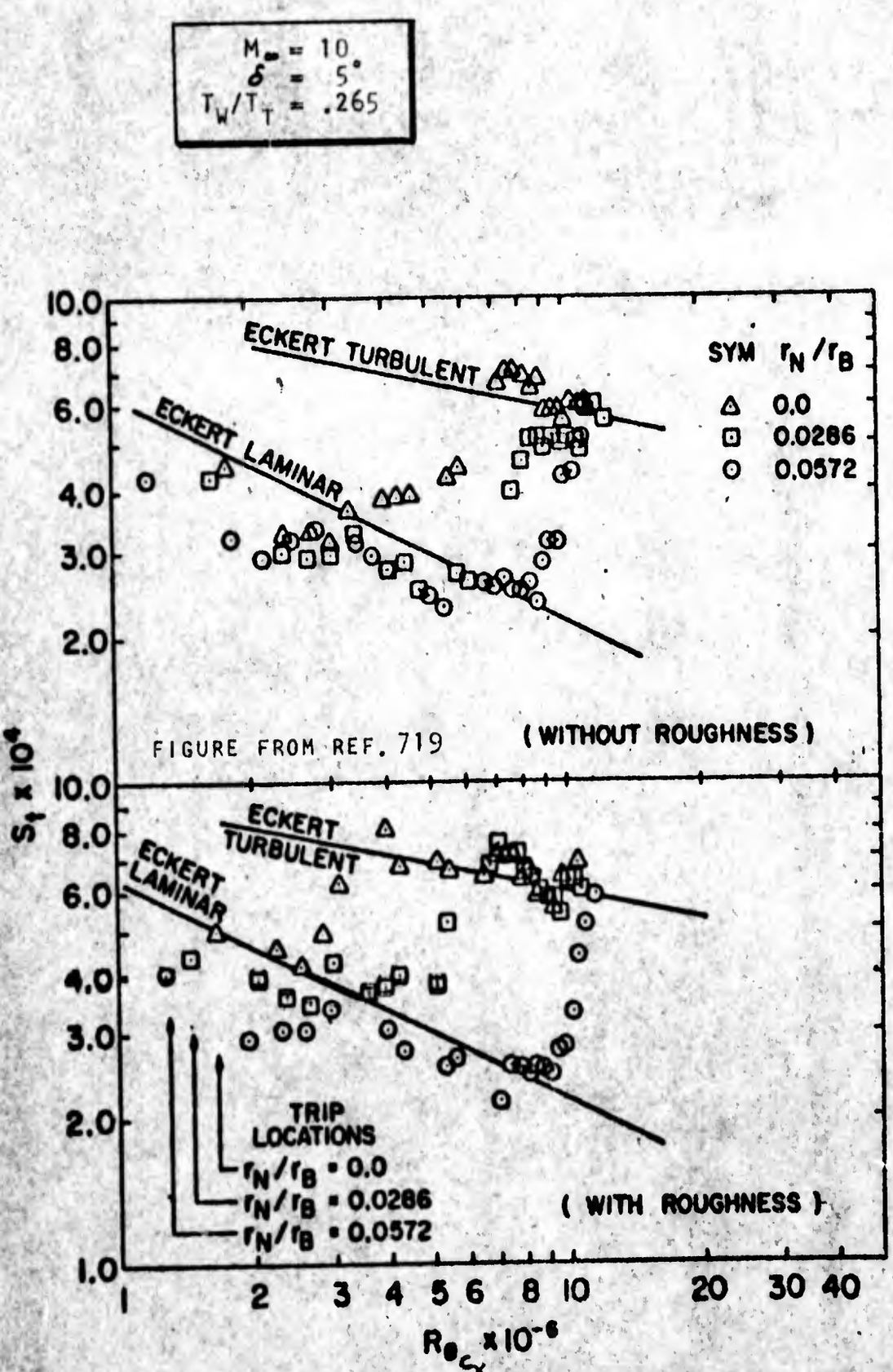

FIG. 7.1 HEAT-TRANSFER DISTRIBUTION ON A SLENDER CONE WITH AND WITHOUT NOSE BLUNTNESS AND SURFACE ROUGHNESS

$M_\infty = 10$
$\delta = 5°$

WITHOUT ROUGHNESS

FIGURE FROM REF. 719

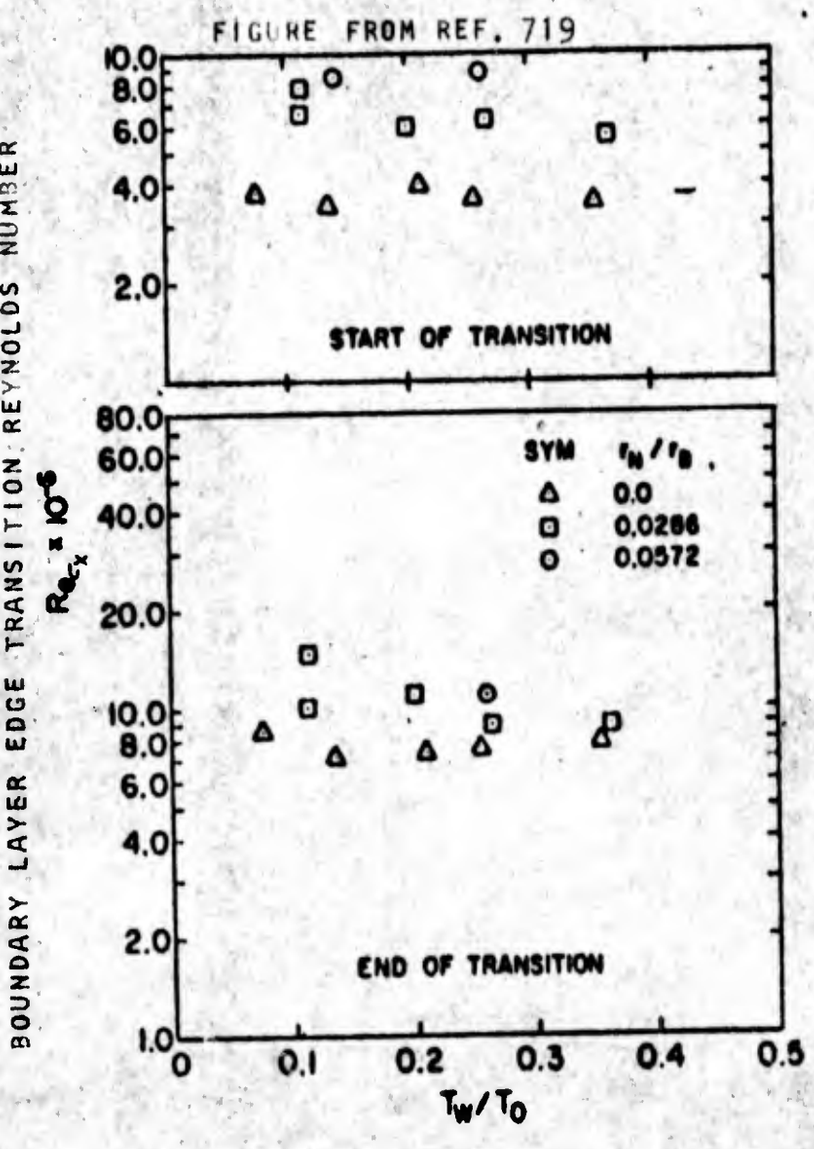

FIG. 7.2 TRANSITION REYNOLDS NUMBER VARIATION WITH WALL-TO-STAGNATION TEMPERATURE RATIO

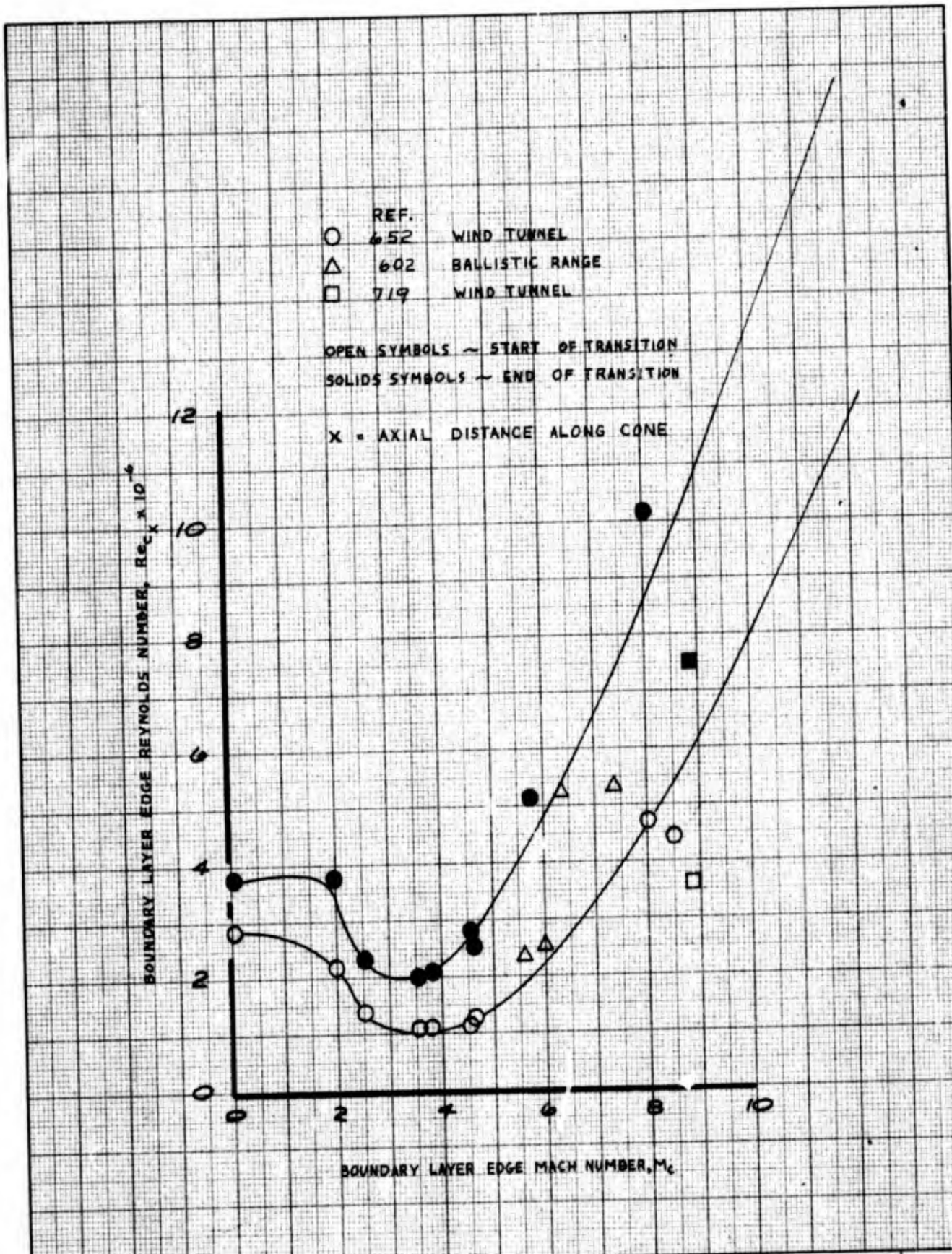

	INITIALS	DATE	REV BY INITIALS	DATE	TITLE	MODEL
CALC	DWE	10/65			BOUNDARY LAYER TRANSITION FOR SHARP SLENDER CONES	Fig. 7.3
CHECK						
APPD.						
APPD						

U3 4013 8000 REV. 12-64

REV LTR_____

BOEING NO D2-36139-1

SH 118

8.0 AERODYNAMIC CONTROLS

References which contain experimental aerodynamic control data are summarized on Page 120.

The next generation of reentry vehicles will likely have some type of aerodynamic controls. At the present time only limited experimental data are available so that additional testing is required.

Reference 816 presents results from a Boeing test conducted at $M_\infty = 6.1$ to evaluate methods of aerodynamic control. The effect of mass injection, a swivel nose, canard surfaces, fins and flaps on the static aerodynamic characteristics for a 10° half-angle cone were determined.

Control effectiveness data for the General Electric maneuverable R/V are found in references listed on Page 120. References 26 and 29 include hinge moment data. Reference 28 shows the effect of simulated ablation on the control effectiveness. References 26 and 11 contain pressure data.

One of the main problems associated with control effectiveness is to determine the amount of boundary layer separation ahead of the control surface. This problem is aggravated by ablation effects which have been shown[28] to increase separation and thus reduce control effectiveness.

EXPERIMENTAL AERODYNAMIC CONTROL DATA

REF.	MACH NUMBER	δ DEGREES	r_N / r_b	α_{MAX}
573.	0 - 3	NONCONICAL SHAPES	-	0
163.	1.4 AND 2	3.55	0	26
50.	1.5 - 8	CONE-CYLINDER-FLARE		-
55.	2 - 8	8.7	0	25
13.	2 - 10	9	.017 - .207	18
29.	2 - 10	11	0	18
613.	2 - 16	TWO DIMENSIONAL SURFACES		-
557.	3.1 - 5.5	8	.155	10
815.	5 AND 6.1	8	.144	25
512.	6	7.5	0	0
716.	6 AND 10	OGIVE	-	-
816.	6.1	10	0	30
169.	6.7	22.3	.27	27
182.	6.9	5	0 - .2	30
503.	8	6.33	0	15
401.	8	9	0 - .36	15
11.	8 AND 10	9	0 - .36	0
407.	8 AND 10	9	0 - .36	15
406.	8 - 20	OGIVE	0 - .12	15
572.	8.04	9	0	25
571.	8.07	6.3	0	15
24.	10	9	0	20
59.	10	9	0	13
79.	10	9	0 - .3	24
402.	10	9	0 - .36	15
28.	10	11	0	15
60.	10	11	.02	18
22.	10	11	.02	15
706.	16	TWO DIMENSIONAL SHAPES		-
38.	17 - 20	11	0	16
15.	19	9	0	15
18.	19	11	0	15
26.	19	11	0	15

9.0 ABLATION AND BLOWING EFFECTS

References which contain ablation and blowing effect data are summarized on Page 124.

Recent laboratory and flight tests have shown that ablation and blowing may considerably alter the aerodynamic coefficients. A discussion of this subject is hampered by lack of adequate theoretical methods of analysis and by the fact that most of the meager experimental data are classified SECRET.

It is very difficult to find ablation materials which are suitable for wind tunnel tests, and to measure the ablation rates of the few materials which are suitable for testing. Most experimenters have simulated ablation by using porous models and blowing a gas out the surface of the model. However, a question remains as to the validity of the results obtained from the simulation.

The following simulation parameter which relates the gas flow from the surface to the free stream mass flow has been suggested and is widely used.

$$\frac{\dot{m}_{surface}}{\rho_\infty V_\infty S_{cone\ base}}$$

However, experimental results indicate that this parameter, though useful, is too simple to correlate results from such a complicated flow phenomena.

Reference 539 presents experimental results for a slender sharp nosed porous cone. The entire model is porous and wall porosity is varied to simulate the axial distribution of the mass injection produced by ablation. The injection material and cone half-angle are not given in this report, however, the half-angle is thought to be approximately 8 degrees. Figure 9.1 shows the effect of blowing on the pressure distribution along the surface of the cone.

Figure 9.2 shows that blowing reduces $C_{N_{\alpha_{\alpha=0}}}$ by a large amount. However, Reference 539 shows that the normal force curve becomes increasingly nonlinear with increased blowing, so that Figure 9.2 is valid only at $\alpha = 0$. Figure 9.2 also shows the large variation of center of pressure with both Reynolds number and blowing rate.

Results from another comprehensive experimental program are presented in Reference 539. Figure 9.3 shows the variation of C_N and C_m with angle of attack for a slender porous cone tested in a helium tunnel with helium also being injected at the surface. Note the increasing nonlinearity of the curves with increasing injection rate. Figure 9.4 shows the variation of center of pressure and axial force with blowing rate for the same cone.

Reference 28, which is SECRET, also presents excellent experimental data on the effect of blowing on C_N and C_m.

Simulated ablation reduces the skin friction on a cone, but increases the wave drag due to the larger boundary layer displacement thickness (See Figure 9.1). Figure 9.4 shows that for small ablation rates the total axial force is reduced due to the lower skin friction drag. However for larger rates the total axial force increases due to the higher wave drag. Reference 32 (SECRET) also presents an excellent discussion of this problem. These references show that ablation can either increase or decrease the axial force, depending on the ablation rate.

Meager experimental results indicate that ablation has a large effect on the dynamic damping of a cone. Results from tests conducted on slender cones coated with different ablators are shown in Figure 9.5. Note that coating the entire vehicle, or even only the nose, can increase the dynamic damping by nearly an order of magnitude.

Ablation effects can also cause damping instability as is shown in Figure 9.6 The aft half of a slender cone was coated with an ablator. When released it damped slightly for the first few seconds; then as the ablation materials approached a full blowing rate, the motion began to diverge and continued to do so to the end of the run. This illustrates an approximate rule: ablation ahead of the c.g. causes increased dynamic damping; ablation aft of the c.g. causes decreased dynamic damping.

During re-entry if boundary layer transition occurs near the rear of a vehicle, the high heating rates and the associated high ablation rates there may cause dynamic instability. This has been observed during flight tests of conical re-entry vehicles.[408]

It has been hypothesized that an aerothermodynamic lag effect on an oscillating body may exist, due to time lag of the ablation rate, with respect to the heating rate. This effect may seriously alter the static and dynamic forces.

Extensive theoretical and experimental studies to determine the effects of ablation on aerodynamic characteristics are in progress throughout the aerospace industry.

EXPERIMENTAL ABLATION AND BLOWING EFFECTS DATA

REF.	MACH NUMBER	δ DEGREES	r_N / r_b	α_{MAX}
563.	.6 -	6.4	0	0
211.	1 - 25	SUMMARY OF ALL LURV VEHICLE FLIGHT TESTS		
74.	2 - 6	9	0	15
75.	2 - 6	NONCONICAL SHAPES	-	20
160.	3 - 5	6	0	2
64.	3 - 12	15	.113	10
305.	3 - 22	8	0	-
557.	3.1 - 5.5	8	.155	10
710.	3.9 AND 5.6	5	0	0
77.	4	9	0	15
605.	4.5	10	0	0
521.	6	9 AND 45	0	30
578.	6	15	.11	10
32.	6 AND 10	7.5	0	0
45.	6 - 10	15	.333	15
506.	6.5 - 14	SLENDER CONE	-	30
552.	7 AND 9.3	30	VARIOUS SHAPES	0
569.	8	9	0	25
407.	8 - 20	VARIOUS SHAPES	-	-
540.	8 AND 25	SLENDER CONES	-	-
572.	8.04	9	0	25
203.	9 - 15	5.7 AND 8.3	VARIOUS SHAPES	20
712.	9 - 22	6 - 13.5	0 - .38	0
208.	10	8	0	6
78.	10	8	0 - .15	9
62.	10	8	.04	11
57.	10	8	.04	12
212.	10	8	.04	14
79.	10	9	0 - .3	24
72.	10	9	.04	10
59.	10	9	0	13
28.	10	11	0	15
539.	10.5 - 21	7.5 AND 10	0 AND .04	10
603.	11	9	.05	0
555.	14	10	.15	23
651.	14	SLENDER CONE	-	35
753.	14	SLENDER CONE	.04 AND .14	28
210.	16 - 25	9	0	7
65.	17	9	0	10
511.	17	9	.076 AND .3	0
209.	18 - 24	8	0	10
584.	20	SUMMARY REPORT		

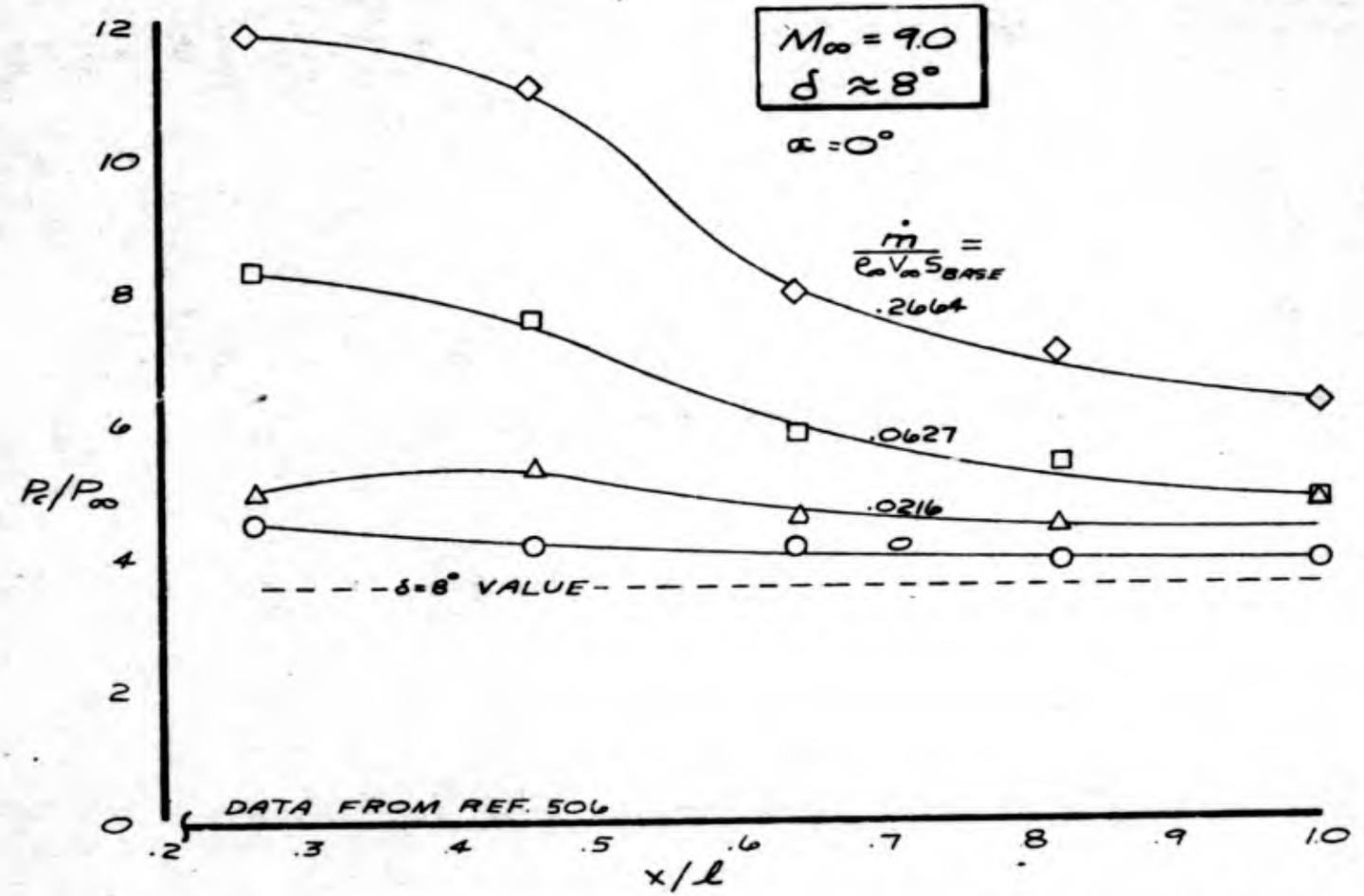

FIG. 9.1 THE EFFECT OF SURFACE BLOWING ON THE PRESSURE DISTRIBUTION ON A SLENDER POROUS CONE

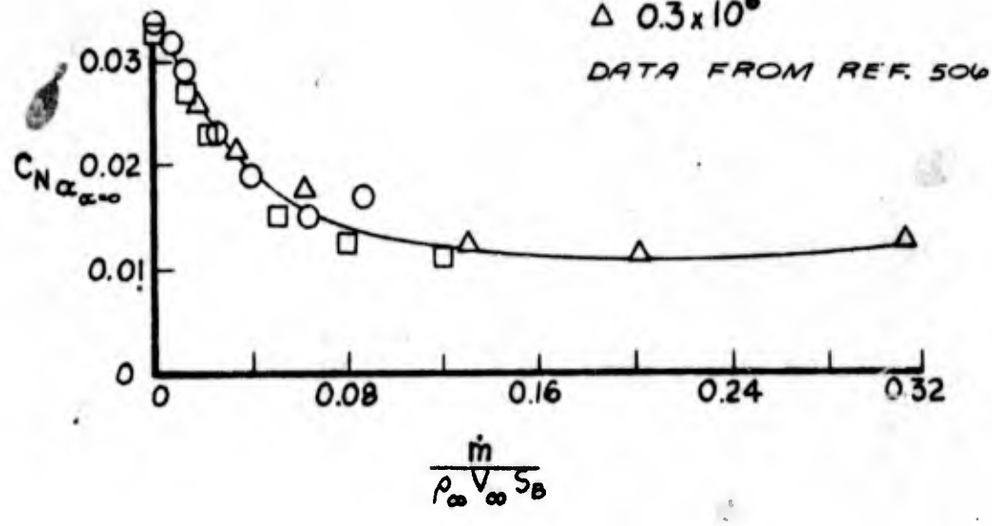

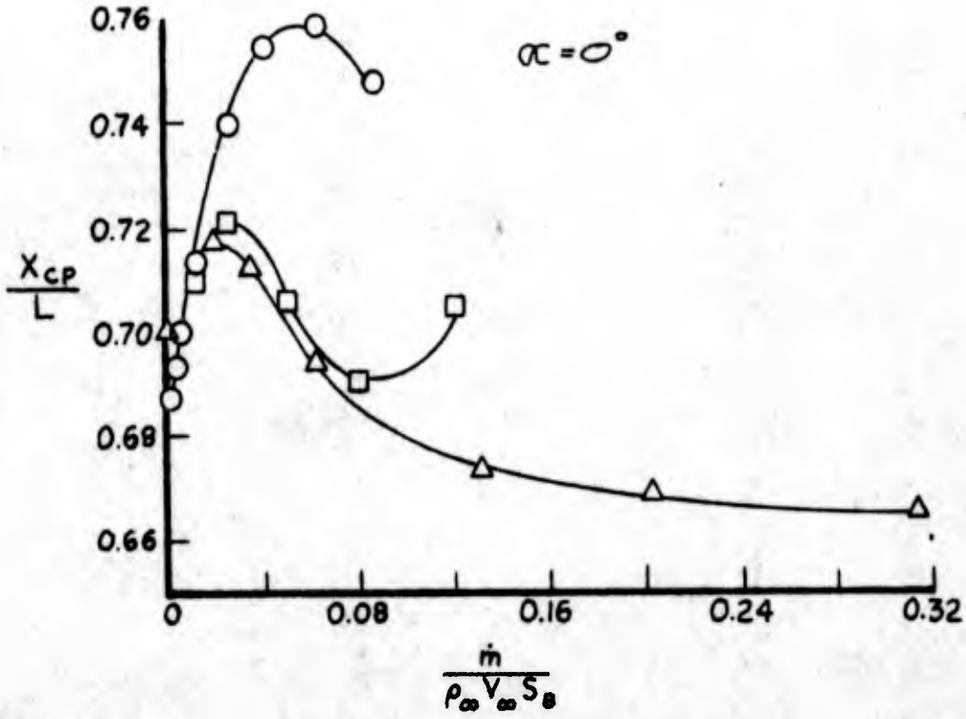

FIG. 9.2 THE EFFECT OF SURFACE BLOWING ON THE AERODYNAMIC CHARACTERISTICS OF A SLENDER POROUS CONE

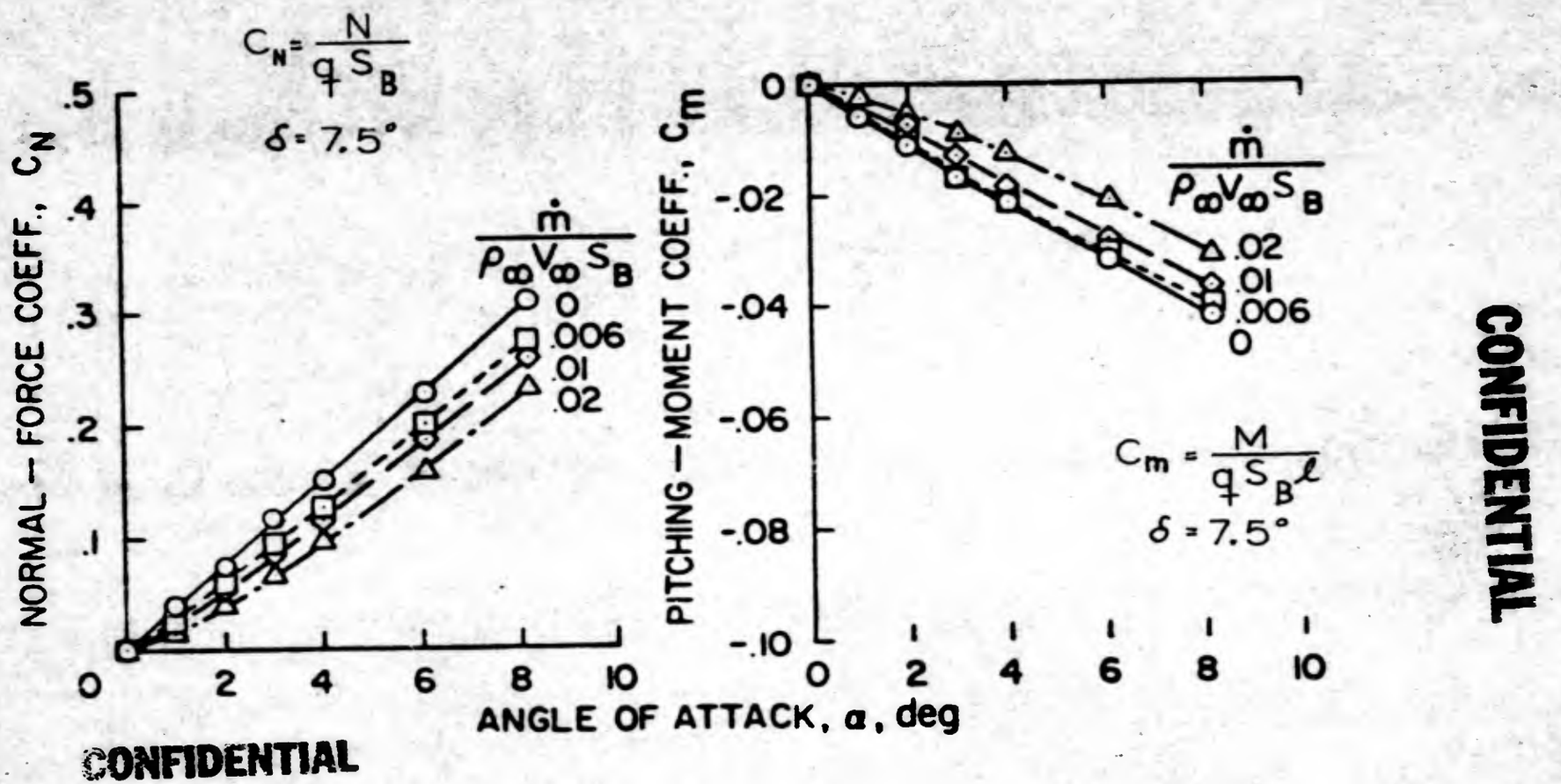

Fig. 9.3 Effect of Helium Ejection From the Porous Cone on Normal Forces and Pitching Moments at $M_\infty = 10.5$ in the 14-Inch Helium Tunnel

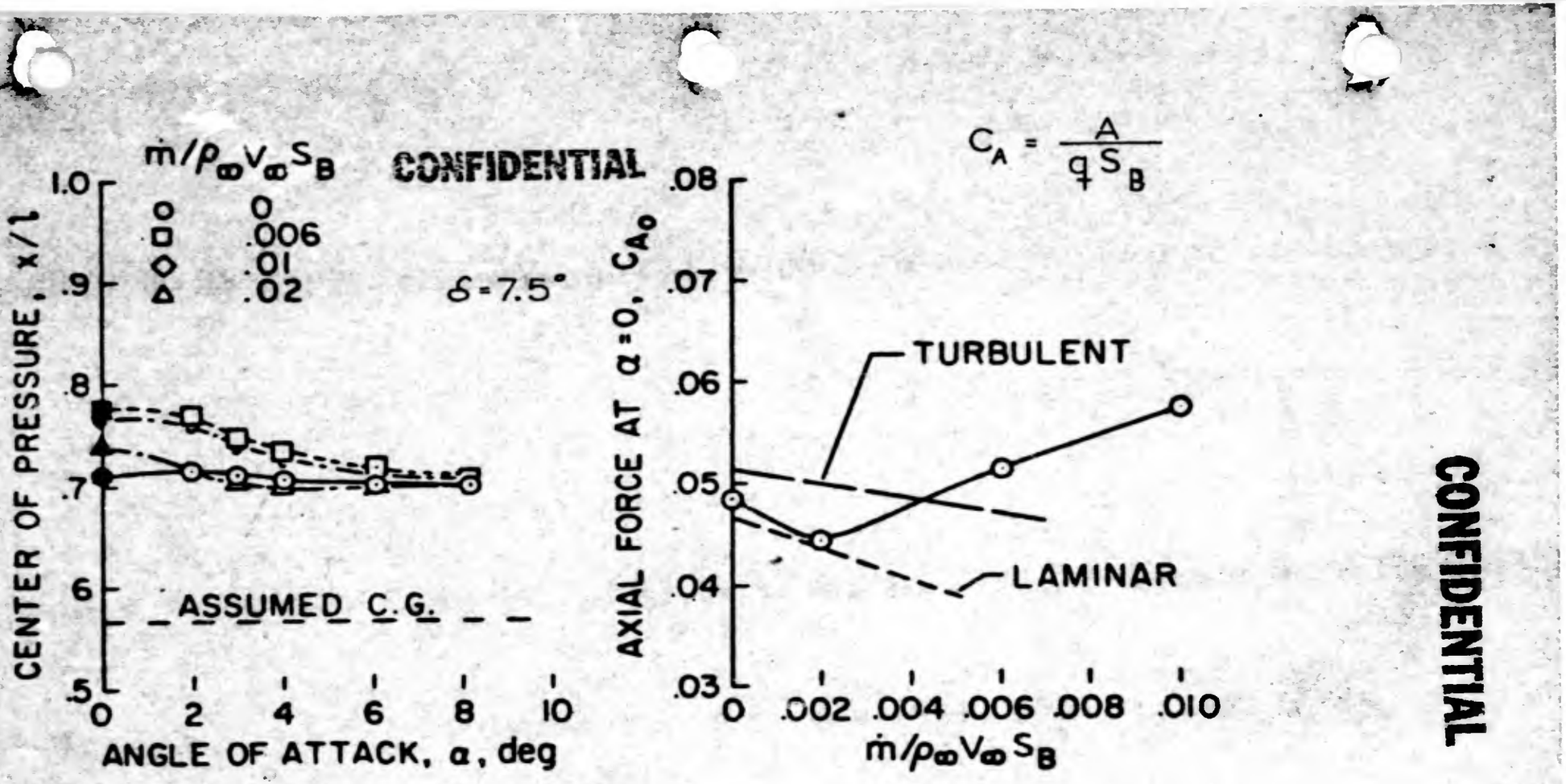

Fig. 9.4 Effect of Helium Ejection From the Porous Cone on Centers of Pressure and Axial Force at $M_\infty = 10.5$ in the 14-Inch Helium Tunnel

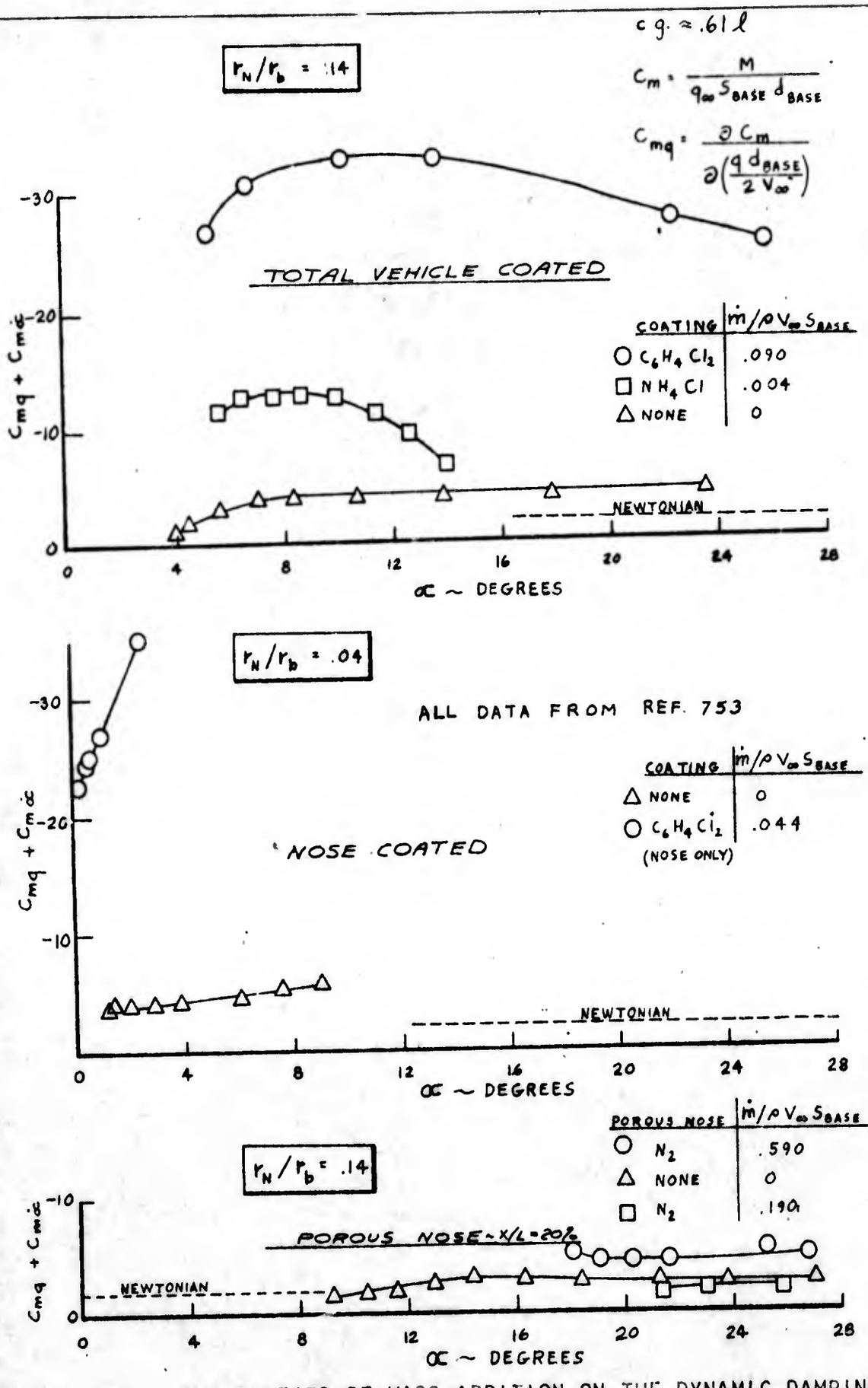

FIG. 9.5 THE EFFECTS OF MASS ADDITION ON THE DYNAMIC DAMPING OF SLENDER CONES

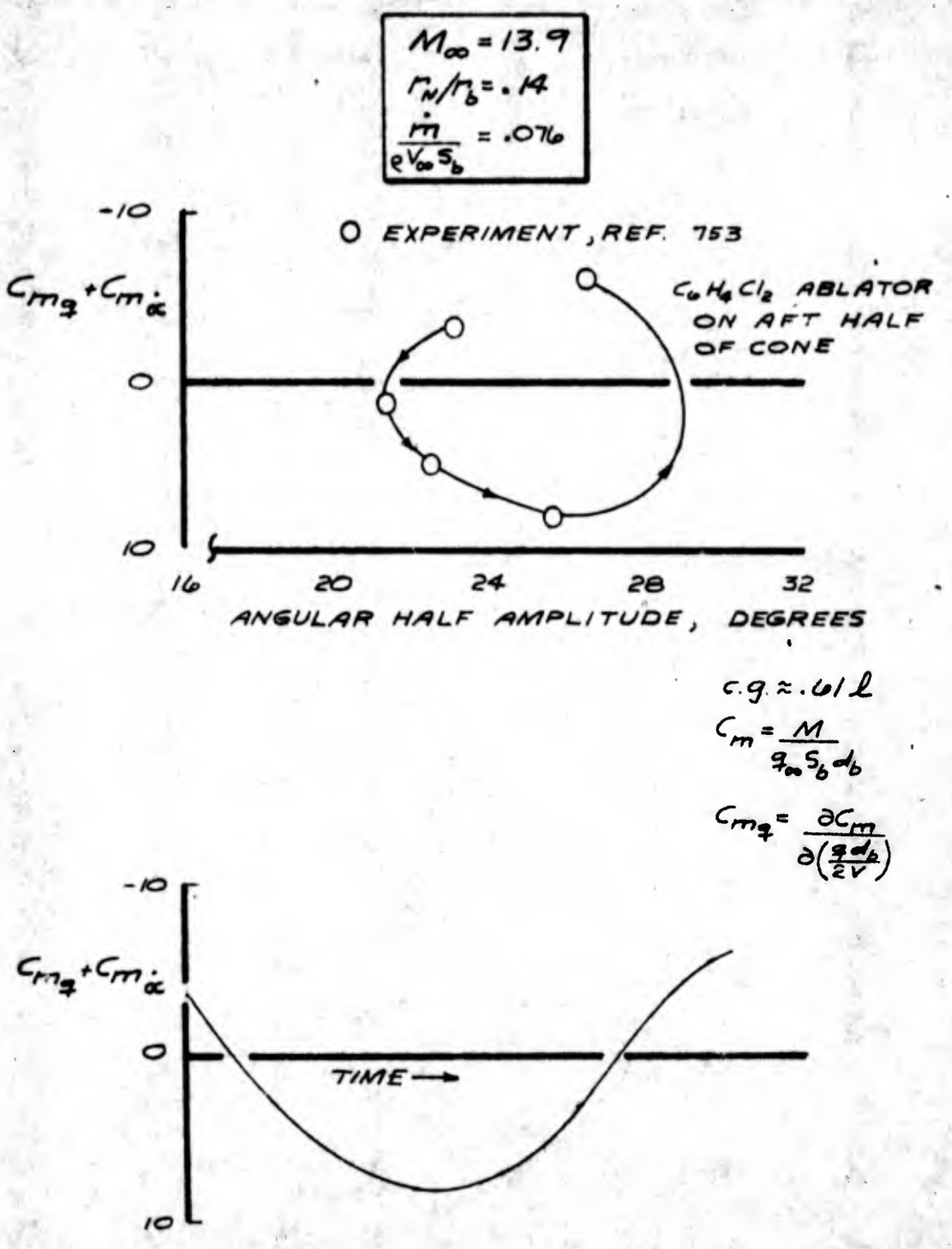

FIG. 9.6 EFFECT OF ABLATION ALONG THE AFT HALF OF A SLENDER CONE ON THE DYNAMIC DAMPING

10.0 LOW DENSITY AND VISCOUS EFFECTS

References which contain low density and viscous flow data are summarized on Page 133. Reference 824 presents a detailed discussion of this subject.

In this section only, the wind axis coordinate system (C_L, C_D) will be used. This is because C_L will be shown to be nearly independent of low density and/or viscous flow effects.

Low density and/or viscous flow effects may increase the drag on a slender cone by an order of magnitude. Data for these flows can be correlated by the following viscous parameter

$$\frac{M_\infty \sqrt{C_\infty}}{\sqrt{Re_{\infty_l}}} \qquad 10.1$$

where $C_\infty = (\mu_w T_\infty)/(\mu_\infty T_w)$. The viscosity, μ, can be obtained from Figure 4.16. Figure 10.1 shows a correlation of the viscous parameter with experimental data for several cones tested having cold walls. Note that the drag is nearly the same for all cones when $M_\infty \sqrt{C_\infty}/\sqrt{Re_{\infty_l}} > .12$. Also shown in Figure 10.1 are theoretical results calculated using Normal Shock theory[712]. This theory has been incorporated into the Unyawed Cone Computer Program (see Section 12.0).

Figure 10.2 shows that the ratio of wall temperature to total temperature has a large effect on the drag.

Figure 10.3 shows the variation of C_D with angle of attack for a 9° cone.

Figure 10.4 indicates that the lift on a slender cone is nearly independent of viscous effects. Therefore, Newtonian theory can be used to calculate C_L at all values of the viscous parameter.

Figure 10.5 shows that viscous effects appear to shift the center of pressure aft. If the cp location is to be determined accurately, experimental data must be corrected for viscous effects. Methods for making this correction are currently being developed.

EXPERIMENTAL LOW DENSITY AND VISCOUS EFFECTS DATA

REF.	MACH NUMBER	δ DEGREES	r_N / r_b	α_{MAX}
104.	ALL	2.5 - 30	0	90
211.	1 - 25	SUMMARY OF ALL LORV VEHICLE FLIGHT TESTS		
583.	20	SUMMARY REPORT		
534.	2	15 AND 30	0	0
6.	2 - 11	SPHERE	-	-
704.	2 - 11	SPHERE	-	-
557.	3.1 - 5.5	8	.155	10
111.	3.7 - 5.7	8	0	0
520.	3.8 - 5.8	9	0	108
710.	3.9 AND 5.6	5	0	0
303.	4 - 20	6	0	20
575.	5.8	15	0 - .6	0
302.	6 - 19	8	0	16
609.	6.8 - 4.7	9	0 - .3	30
80.	6.8 - 14.7	9	0 - .3	30
723.	7 - 10	6 - 15	0 - .2	0
527.	7.3 AND 9	9	0 - .3	15
17.	7.5 - 12	10	.9	170
702.	8 - 22	6.3 - 20	0 - .5	30
58.	9 AND 18	9	.3	0
33.	9 - 21	9 AND 10	0 - .3	25
8.	9 - 22	8.34 - 13.35	0 - .38	0
712.	9 - 22	6 - 13.5	0 - .38	0
410.	9 - 24	VARIOUS SHAPES	-	-
54.	9.8	50	0	180
54.	9.8	10	.9	180
604.	11 - 16	8	.035	20
709.	14	3.5	0	0
12.	14 - 22	7.1 AND 9	.03 - .3	40
210.	16 - 25	9	0	7
209.	18 - 24	8	0	10
721.	20	9 AND 13.5	.03 - .38	0
582.	20	SUMMARY REPORT		

FIGURE FROM REF. 712

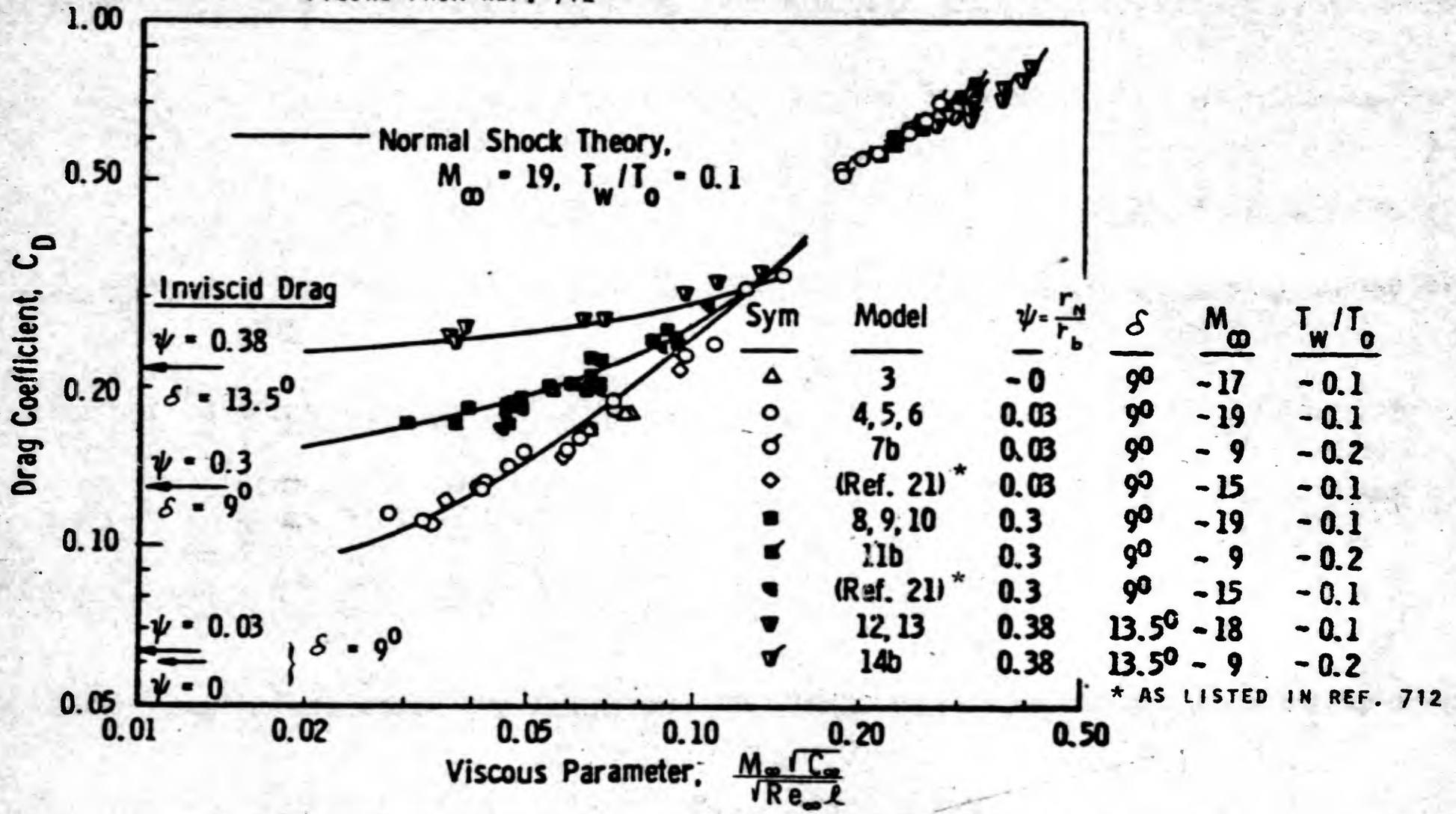

DR-36139-1
134

FIG. 10.1 COMPARISON OF HYPERSONIC, COLD WALL, VISCOUS DRAG OF SLENDER CONES

Symbol	Model	M_∞	T_w/T_0
○	8, 9, 10 *	~19	~0.1
◇	CAL (Ref. 21)	~15	~0.1
□	11a	~10	~0.75
▽	JPL (Ref. 22)*	~7-9	~0.75

* AS LISTED IN REF. 712

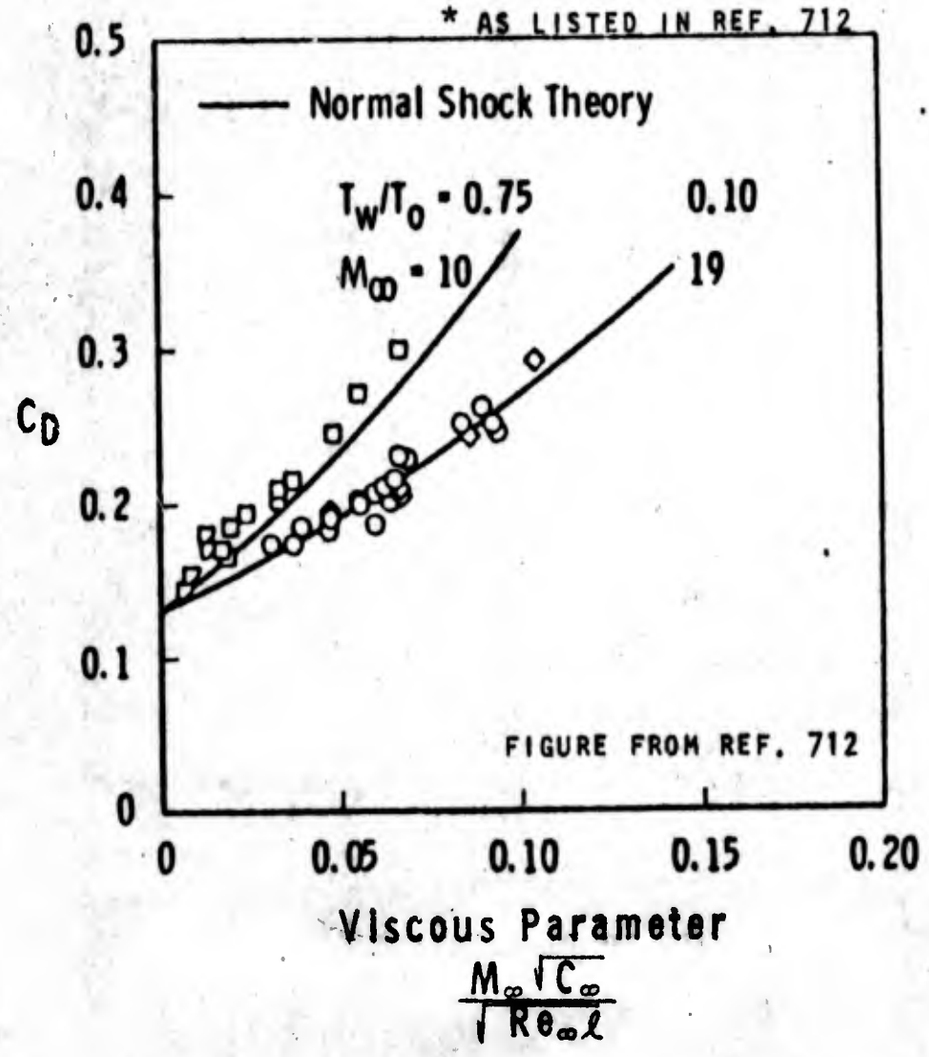

FIG. 10.2 THE EFFECT OF WALL TEMPERATURE ON THE VISCOUS DRAG, $r_N/r_b = .30$ $\delta = 9°$

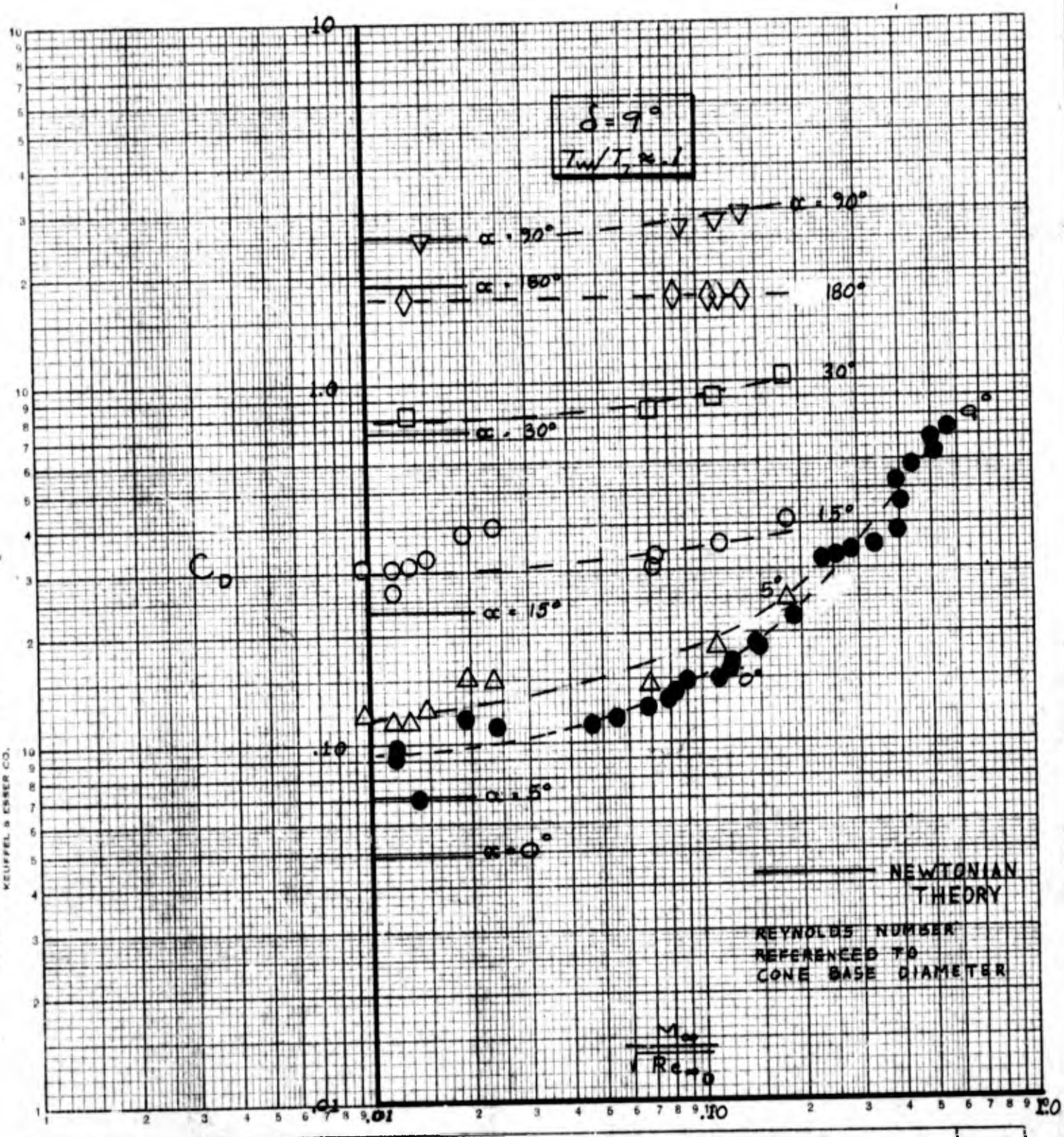

	INITIALS	DATE	REV. BY INITIALS	DATE	TITLE	MODEL
CALC	SSS	10/65			VARIATION OF DRAG WITH ANGLE OF ATTACK	Fig. 10.3
CHECK						
APPD						
APPD						

REV LTR _____

BOEING NO. D2-36139-1

SH 136

US 4044 2000 REV. 6-64

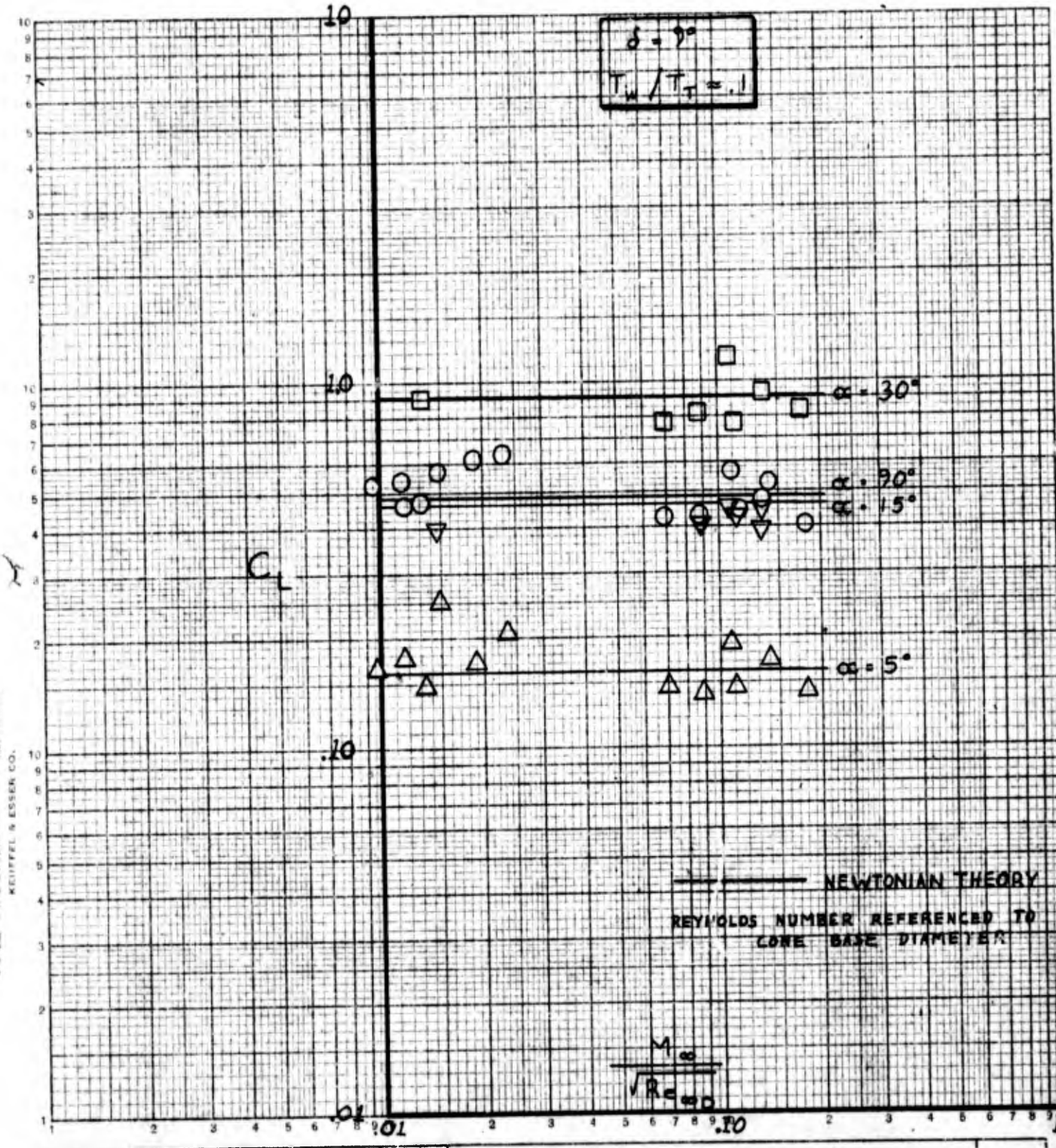

LOGARITHMIC 46 7403
KEUFFEL & ESSER CO.

	INITIALS	DATE	REV. BY INITIALS	DATE	TITLE	MODEL
CALC	SSS	10/65			VARIATION OF LIFT WITH ANGLE OF ATTACK	Fig. 10.4
CHECK						
APPD						
APPD						

REV LTR _____

BOEING NO. D2-36139-1

SH 137

U3 4044 2000 REV. 6-64

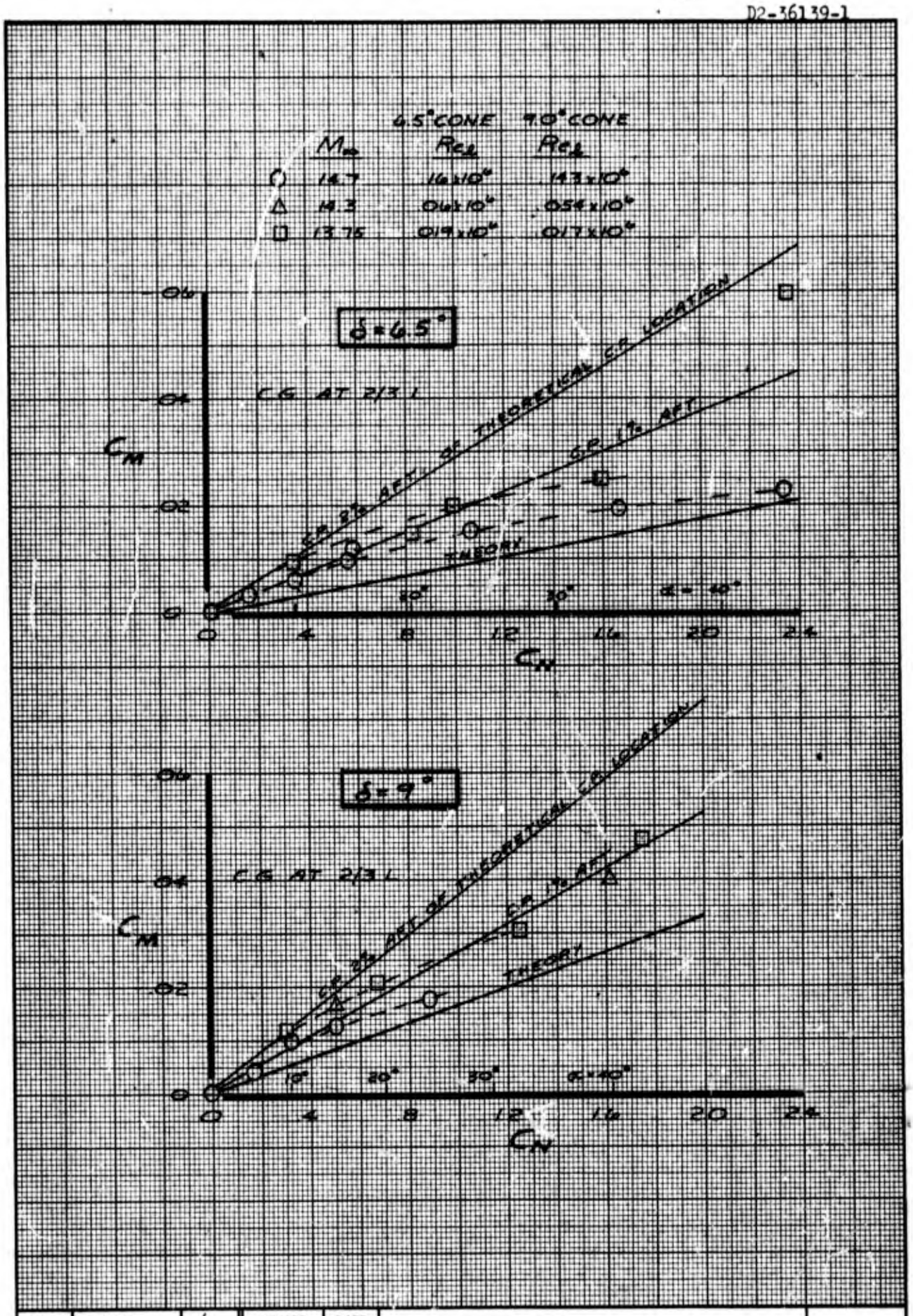

CALC	DWE	7/65	REVISED	DATE	HYPERSONIC VISCOUS EFFECTS ON THE STATIC STABILITY
CHECK					
APR					
APR					THE BOEING COMPANY

Fig. 10.5

11.0 BASE GEOMETRY EFFECTS

References which contain base geometry effects data are summarized on Page 140.

The base of a reentry vehicle is sometimes rounded to reduce the radar cross section.

This change of geometry will influence all the aerodynamic coefficients to some degree. Since the shape of the rounded base is arbitrary, it is difficult to correlate experimental data.

Figure 2.7, 3.4, 4.12, and 5.1 show some effects of rounding the bases of several different cones.

EXPERIMENTAL BASE GEOMETRY EFFECTS DATA

REF.	MACH NUMBER	δ DEGREES	r_N / r_b	α_{MAX}
129.	.25 - 2.2	12.5	0 AND .6	18
157.	.25 - 2.2	12.5	.6	20
201.	.4 - 20	NONCONICAL SHAPES	-	15
204.	.4 - 20	NONCONICAL SHAPES	-	20
206.	.4 - 20	NONCONICAL SHAPES	-	20
538.	.5 - 4.06	20 - 40	0 - .6	12
36.	.6 - 1.4	9	.04	16
136.	.65 - 2.2	20	0 AND .4	21
148.	.7 - 1.3	11.6	.38	8
306.	.8 - 9.9	10	.2	11
211.	1 - 25	SUMMARY OF ALL LORV VEHICLE FLIGHT TESTS		
30.	2	9	.05	15
70.	2 - 6	10 AND 15	0 AND .2	25
35.	2 - 10	9	.047	0
61.	2 - 10	9	NONSPHERICAL	16
71.	3 - 8	10	0 AND .3	0
305.	3 - 22	8	0	-
303.	4 - 20	8	0	20
302.	6 - 19	8	0	16
816.	6.1	10	0	30
202.	6.5 - 17	8 - 16	.03 - .15	16
128.	6.77	9	0 - .66	180
401.	8	9	0 - .36	15
203.	9 - 15	5.7 AND 8.3	VARIOUS SHAPES	20
54.	9.8	50	0	180
9.	10	8	0	12
81.	10	9	.04	25
304.	10 - 20	8	0	12
406.	10 - 20	OGIVE	0 - .12	15
523.	15 AND 18	10	.5 - .9	10
210.	16 - 25	9	0	7
209.	18 - 24	8	0	10
43.	19	9	.045	20

12.0 BOEING COMPUTER PROGRAMS

Computer programs referred to in this document are summarized here. A complete summary of major Boeing programs is available from Applied Mathematics Information Center. Reference 813, dated April 1964, also presents a summary of many aerothermodynamics computer programs.

With the initiation of BLITZ programming, many unrecorded programs probably exist.

Following is a summary of programs referred to in this document.

Unyawed Cone Flow Field Program (AS 0817, 1022)

This program, summarized in Reference 806, calculates the exact flow field of an unyawed supersonic circular cone. Either a perfect gas (AS 0817) or the equilibrium real air model of Hansen[116] (AS 1022) may be used. Results are obtained by solving the Taylor-Maccoll equations using an iterative technique. This program also calculates the laminar and turbulent skin friction on the cone using the reference methods discussed in Section 4.0. The drag coefficient for the cone in hypersonic low density flow is also calculated[824].

Inverse Method Blunt Body Program (AS 1583)

This program, summarized in References 814 and 812, calculates the inviscid subsonic flow field of a two-dimensional or axisymmetric blunt body traveling at supersonic or hypersonic speeds. This program based on the inverse method, can be used for a perfect gas, real equilibrium air, nonequilibrium air or real equilibrium air with radiation. For blunt cones, this program calcu-

lates the subsonic flow field around the blunt nose.

Method of Characteristics Body Program (AS 1096)

This program, summarized in References 804, 811 and 812, calculates the inviscid supersonic flow field around two dimensional or axisymmetric bodies at zero angle of attack. This program based on the method of characteristics, can be used for either a perfect gas, real equilibrium air or non-equilibrium air. The body may have any number of flares or have concave curvature. For blunt cones, this program calculates the supersonic portion of the flow field. When used with the Inverse Method Blunt Body Program (AS 1583) the complete flow field is calculated.

Highly Yawed Cone Flow Field Program (AS 2018)

This program, summarized in Reference 810, calculates the inviscid flow field on the windward side of highly yawed cones. This program which uses the inverse method of solution can be used for either a perfect gas or real equilibrium air.

The only restrictions to the program are that the bow shock wave must be attached, $M_\infty \geq 4.0$ and $\alpha \geq 5°$.

Laminar Boundary Layer Program #1 (AS 0438)

This program, summarized in Reference 820, calculates the locally similar boundary layer on a flat plate. The effects of dissociation, ionization and mass diffusion are included. Tabulated results from this program are presented in Reference 821.

Compressible Turbulent Boundary Layer Program (AS 1109)

This program, summarized in Reference 822, calculates the dissociated compressible turbulent boundary layer using the method developed by William Dorrance.

Three-Dimensional Newtonian Pressure Program (AS 2035)

This program, summarized in Reference 818, calculates the pressures, static forces and moments, and dynamic forces and moments on an arbitrary three dimensional shape using Newtonian theory. Any shape traveling at hypersonic speeds may be specified.

Axisymmetric Body Newtonian Program (AS 0828)

This program calculates the static forces and moments on an axisymmetric body using Newtonian theory.

Hypersonic Shock Expansion Dynamic Damping Programs (BLITZ)

Two BLITZ programs which solve the equations of Reference 517 for a sharp cone are available from D. W. Eastman. The first calculates the dynamic damping coefficients for zero angle of attack. The second calculates these coefficients for angles of attack other than zero.

13.0 APPENDIX - CORRECTED FIRST AND SECOND ORDER LINEARIZED THEORY CORRECTION

Reference 109 presents equations for calculating the supersonic static and dynamic aerodynamic coefficients for slender cones. Two misprints have been found in this reference. On page 20 the equation for Q should be

$$Q = \left(\frac{M}{\Delta+\beta^2}\right)^2\left[-2\beta^2\Delta + \frac{(N+1)\beta^4\tau^2}{(1-\beta^2\tau^2)} + \frac{(N-1)\beta^4\tau^2\Delta}{(1-\beta^2\tau^2)} + \frac{1}{4}\frac{\tau^2\beta^4(2+\beta^2\tau^2)}{(\beta^2+\Delta)(1-\beta^2\tau^2)}\right]$$

Omitted in Reference 109

On page 21 the equation for Γ_2 should be

$$\Gamma_2 = \left\{1. + .2M^2\left[1.-(1.+\tau^2)\left(\frac{M\beta^2}{\Delta+\beta^2}\right)^2\right]\right\}^{2.5}$$

Omitted in Reference 109

USE FOR TYPEWRITTEN MATERIAL ONLY

14.0 REFERENCES

These references, listed by originating company or publishing source, are the result of a comprehensive literature search.

The first item of each reference is the originator's or publisher's report number. When a second number appears on the right, the number is:

1) The Central Library report number, or,
2) The Defense Documentation Center AD- number, indicating the report was obtained directly from DDC by D. W. Eastman and may be borrowed from him.

If no second number appears, the report was obtained from a source which uses the first report number.

Reports can be obtained from one of the following sources

Central Library, Extension 5-6511

Many NACA Reports

(For classified reports call Ext. 5-1888)

All NASA Reports

Many AEDC Reports

Many Miscellaneous Reports

Flight Technology Files, Extension 6-6421

Some NACA Reports

Most NASA Reports

Some AEDC Reports

Some Miscellaneous Reports

USE FOR TYPEWRITTEN MATERIAL ONLY

Airplane Division Library, Extension 7-4431

Most NACA Reports

Most NASA Reports

Defense Documentation Center

All reports with AD- number can be ordered from DDC through the Central Library, if not available from D. W. Eastman.

USE FOR TYPEWRITTEN MATERIAL ONLY

ARNOLD ENGINEERING DEVELOPMENT CENTER

1. AEDC-TN-60-69 A16-TN-60-69
DETERMINATION OF OPTIMUM OPERATING PARAMETERS FOR THE 1-FOOT TRANSONIC TUNNEL UTILIZING CONE-CYLINDER BODIES OF REVOLUTION.
W. L. CHEW

2. AEDC-TR-60-15 A16-TR-60-15
AN INVESTIGATION OF THE INFLUENCE OF SEVERAL SHAPE PARAMETERS ON THE DYNAMIC STABILITY OF BALLISTIC RE-ENTRY CONFIGURATIONS.
J. A. BLACK, CONFIDENTIAL

3. AEDC-TDR-62-11 A16-TDR-62-11
DYNAMIC STABILITY TESTS OF THREE RE-ENTRY CONFIGURATIONS AT MACH 8.
L. K. WARD AND R. H. URBAN
DATA ALSO FOUND IN REFERENCE 537.

4. AEDC-TDR-62-87 AD-329241
DYNAMIC STABILITY INVESTIGATION OF A SMALL-SCALE MODEL OF THE SKYBOLT RE-ENTRY CONFIGURATION AT TRANSONIC SPEEDS.
C. D. RIDDLE AND W. E. CARLETON, CONFIDENTIAL

5. AEDC-TDR-62-92 A16-TDR-62-92
FORCE TESTS OF AVCO RE-ENTRY CONFIGURATIONS AT MACH NUMBERS 2, 5 AND 8.
R. E. BRILLHART, JR. AND J. C. DONALDSON

6. AEDC-TDR-62-205 A16-TDR-62-205
THE DRAG OF SPHERES IN RAREFIED HYPERVELOCITY FLOW.
M. KINSLOW AND J. L. POTTER

7. AEDC-TDR-63-19 A16-TDR-63-19
A CALORIMETRIC INVESTIGATION OF SOME PROBLEMS ASSOCIATED WITH A LOW-DENSITY HYPERVELOCITY WIND TUNNEL.
G. D. ARNEY, JR. AND D. E. BOYLAN

8. AEDC-TDR-63-35 A16-TDR-63-35
VISCOUS EFFECTS ON ZERO-LIFT DRAG OF SLENDER BLUNT CONES.
J. D. WHITFIELD AND B. J. GRIFFITH
DATA ALSO FOUND IN REFERENCE 537.

9. AEDC-TDR-63-98 AD-365790
DYNAMIC STABILITY TESTS ON A 0.217-SCALE MODEL OF THE CS-1FT RE-ENTRY VEHICLE AT MACH 10.
L. K. WARD, A. E. HODDAP, JR., AND B. L. USELTON, CONFIDENTIAL

10. AEDC-TDR-63-177 A16-TDR-63-177
HYPERSONIC FORCE, PRESSURE, AND HEAT TRANSFER INVESTIGATIONS OF SHARP AND BLUNT SLENDER CONES.
D. B. WILKINSON AND S. A. HARRINGTON

11. AEDC-TDR-63-208 AD-342869
PRESSURE DISTRIBUTION ON A MANEUVERABLE RE-ENTRY VEHICLE AT MACH 8 AND 10.
J. L. BURK AND G. H. MERZ, SECRET

12. AEDC-TDR-64-1 A16-TDR-64-1
COMPARISON OF HOTSHOT TUNNEL FORCE PRESSURE, HEAT TRANSFER AND SHOCK SHAPE DATA WITH SHOCK TUNNEL DATE.
E. E. EDENFIELD

13. AEDC-TDR-64-9 AD-347008
NOSE BLUNTNESS EFFECTS AND ROLL CONTROL ON A MANEUVERABLE RE-ENTRY VEHICLE AT MACH 2, 6 AND 10.
J. L. BURK AND G. H. MERZ, SECRET

14. AEDC-TDR-64-20 AD-346817
HYPERSONIC STABILITY AND PERFORMANCE CHARACTERISTICS OF A FAMILY OF MODIFIED CONOIDS.
E. L. CLARK, CONFIDENTIAL

15. AEDC-TDR-64-52 AD-348051
STATIC STABILITY TEST OF A MANEUVERING BALLISTICS RE-ENTRY VEHICLE AT MACH 19.
J. F. ROBERTS, SECRET

16. AEDC-TDR-64-59 AD-349247
FORCE AND PRESSURE MEASUREMENTS ON CONFIGURATIONS OF THE AVCO ECM AT MACH NUMBERS 2 TO 10.
J. D. GRAY AND A. ANDERSON, CONFIDENTIAL

17. AEDC-TDR-64-60 A16-TDR-64-60
EXPERIMENTAL DETERMINATION OF AERODYNAMIC DRAG ON A BLUNTED 10-DEG CONE AT ANGLES OF ATTACK IN HYPERSONIC, RAREFIED FLOW.
D. E. BOYLAN AND W. H. SIMS

18. AEDC-TDR-64-90 AD-349661
THE EFFECT OF CONTROL FLAPS ON STABILITY CHARACTERISTICS OF A MANEUVERABLE RE-ENTRY VEHICLE AT MACH 19.
J. F. ROBERTS AND A. H. BOUDREAU, SECRET

19. AEDC-TDR-64-98 A43-TDR-64-98
DYNAMIC STABILITY CHARACTERISTICS OF A 10-DEG CONE AT MACH NUMBER 10.
A. E. HODAPP, JR., B. L. USELTON, AND G. E. BURT

20. AEDC-TDR-64-125 AD-350810
STATIC STABILITY CHARACTERISTICS AND PRESSURE DISTRIBUTION ON SEVERAL MARK 12 DECOY CONFIGURATIONS AT MACH NUMBER 10.
J. R. MYERS AND B. W. ROBERTS, CONFIDENTIAL

21. AEDC-TDR-64-132 AD-351276
A COMPARISON OF TUNNEL AND FREE-FLIGHT HEAT TRANSFER TO SPHERICALLY BLUNTED CONES FROM MACH 8 TO 20.
R. H. EAVES, JR., AND O. J. GRIFFITH, CONFIDENTIAL

22. AEDC-TDR-64-136 AD-351593
DYNAMIC STABILITY TESTS OF A MANEUVERING BALLISTIC RE-ENTRY VEHCILE AT MACH 10.
A. E. HODAPP, JR., AND G. E. BURT, SECRET

23. AEDC-TDR-64-140 AD-352052
DYNAMIC STABILITY TESTS OF THE MARK 12 DECOY AT MACH 10.
A. E. HODAPP, JR. AND G. E. BURNT, CONFIDENTIAL

24. AEDC-TDR-64-141 AD-351580
AN INVESTIGATION OF THE STATIC STABILITY CHARACTERISTICS OF AN ABLATED MANEUVERABLE RE-ENTRY VEHICLE AT MACH 10.
J. L. BURK AND G. H. MERZ, SECRET

25. AEDC-TDR-64-179 AD-353160
HEAT TRANSFER TESTS OF A TRANSPIRATION-COOLED BOOST GLIDE RE-ENTRY VEHICLE NOSE CONE.
J. P. RHUDY AND J. D. MAGNAN, JR., SECRET

26. AEDC-TDR-64-188 AD-353324
PRESSURE DISTRIBUTION AT MACH 19 ON A MANEUVERABLE RE-ENTRY VEHICLE.
J. F. ROBERTS, A. H. BOUDREAU, AND R. A. WASSON, JR., SECRET

27. AEDC-TDR-64-204 AD-354244
PRESSURE DISTRIBUTION TESTS ON A BOOST-GLIDE RE-ENTRY VEHICLE AT MACH NUMBERS FROM 1.5 TO 10.
J. C. USELTON, SECRET

28. AEDC-TDR-64-205 AD-354562
EFFECTS ON MASS ADDITION ON THE STATIC STABILITY CHARACTERISTICS OF A MANEUVERABLE RE-ENTRY VEHICLE AT MACH 10.
J. L. BURK AND J. B. CARMAN, SECRET

29. AEDC-TDR-64-223 AD-354883
AEROTHERMODYNAMIC CHARACTERISTICS OF A MANEUVERABLE RE-ENTRY VEHICLE AT SUPERSONIC AND HYPERSONIC MACH NUMBERS.
J. L. BURK, S. D. MORRIS AND G. H. MERZ, SECRET

30. AEDC-TDR-64-224 AD-354815
STATIC STABILITY CHARACTERISTICS AND PRESSURE DISTRIBUTIONS FOR SEVERAL MARK 12 CONFIGURATIONS AT SUPERSONIC AND HYPERSONIC MACH NUMBERS.
J. R. MYERS AND C. J. SPURLIN, SECRET

31. AEDC-TDR-64-226 AD-450660
INVESTIGATION OF STING SUPPORT INTERFERENCE EFFECTS ON THE DYNAMIC AND STATIC STABILITY CHARACTERISTICS OF A 10-DEG CONE AT MACH NUMBERS 2.5, 3.0 AND 4.0.
B. L. USELTON

32. AEDC-TDR-64-238 AD-354847
EFFECTS OF MASS ADDITION ON THE AERODYNAMIC HEATING AND DRAG CHARACTERISTICS OF A SLENDER CONE WITH ZERO LIFT AT MACH 6 AND 10
O. L. DUNKIN AND J. B. CARMAN, SECRET

33. AEDC-TDR-64-272 ASTIC-009204
COMPARISONS OF FREE-FLIGHT AND WIND TUNNEL DATA ON SLENDER CONES.
B. J. GRIFFITH AND L. G. SILER

34. AEDC-TN-60-61 A16-TN-60-61
ON BASE PRESSURES AT HIGH REYNOLDS NUMBERS AND HYPERSONIC MACH NUMBERS.
J. D. WHITFIELD AND J. L. POTTER
DATA ALSO FOUND IN REFERENCE 537.

35. AEDC-TDR-64-267 AD-355721
DYNAMIC STABILITY TESTS OF THE MARK 12 RE-ENTRY VEHICLE AT SUPERSONIC AND HYPERSONIC SPEEDS.
A. E. HODAPP, JR., SECRET

36. AEDC-TDR-64-227 AD-355365
STATIC AND DYNAMIC STABILITY OF TWO SMALL SCALE MODELS OF THE MARK 12 RE-ENTRY VEHICLE AT TRANSONIC SPEEDS.
C. D. RIDDLE, SECRET

37. AEDC-TDR-62-166 A16-TDR-62-166
HYPERSONIC STATIC STABILITY OF BLUNT SLENDER CONES.
J. D. WHITFIELD AND W. WOLNY

38. AEDC-TR-65-3 AD-356599
AN INVESTIGATION OF STATIC STABILITY AND ROLL CONTROL CHARACTERISTICS OF A MANEUVERABLE FLIGHT TEST RE-ENTRY VEHICLE AT MACH 19.
J. F. ROBERTS AND A. H. BOUDREAU, SECRET

39. AEDC-TR-65-5 AD-356633
DYNAMIC STABILITY TESTS OF FOUR MARK 12 DECOY CONFIGURATIONS AT MACH 10.
A. E. HODAPP, JR., CONFIDENTIAL

40. AEDC-TR-65-8 AD-356632
STATIC STABILITY CHARACTERISTICS OF FOUR MARK 12 DECOY CONFIGURATIONS AT MACH NUMBER 10.
J. R. MYERS AND C. J. SPURLIN, CONFIDENTIAL

41. AEDC-TDR-64-214 AD-454078
ALTITUDE-VELOCITY TABLE AND CHARTS FOR IMPERFECT AIR.
C. H. LEWIS AND E. G. BURGESS III

42. AEDC-TR-65-39 AD-357032
LONGITUDINAL STATIC STABILITY AND DRAG CHARACTERISTICS OF VARIOUS MARK 12 DECOY CONFIGURATIONS AT MACH 19.
R. H. EAVES, JR., CONFIDENTIAL

43. AEDC-TR-65-28 AD-356789
LONGITUDINAL STATIC STABILITY AND DRAG CHARACTERISTICS OF THE G. E. MACH 12 RE-ENTRY VEHICLE AT MACH 19.
R. H. EAVES, JR., SECRET

44. AEDC-TN-60-93 A16-TN-60-93
INVESTIGATION OF HYPERSONIC FLOW OVER BLUNTED PLATES AND CONE.
J. P. RHUDY, R. S. HIERS, J. O. RIPPEY

45. AEDC-TDR-65-22 AD-457574
THE EFFECTS OF ACTIVE COOLING ON THE AEROTHERMODYNAMIC CHARACTERISTICS OF SLENDER BODIES OF REVOLUTION.
M.E.HILLSAMER AND S.R.MALLARD

46. AEDC-TN-61-164
FORCE AND PRESSURE TESTS ON A BLUNT CONE AT MACH NUMBERS FROM 2 TO 5.
J. H. JONES AND J. S. DEITERING
DATA ALSO FOUND IN REFERENCE 537.

47. AEDC-TN-62-33
FORCES AND PRESSURE TESTS ON A BLUNT CONE AT MACH NUMBER 8.
J. H. JONES AND J. S. DEITERING
DATA ALSO FOUND IN REFERENCE 537.

48. AEDC-TN-61-81
PRESSURE DISTRIBUTION AND SHOCK SHAPE OVER BLUNTED SLENDER CONES AT MACH NUMBERS FROM 16 TO 19.
C. H. LEWIS
DATA ALSO FOUND IN REFERENCE 537.

49. AEDC-TN-60-173
PRESSURE DISTRIBUTION TESTS OF SEVERAL SHARP LEADING EDGE WINGS, BODIES, AND BODY-WING COMBINATIONS AT MACH 5 AND 8.
R. E. RANDALL, D. R. BELL AND J. L. BURK
DATA ALSO FOUND IN REFERENCE 537.

50. AEDC-TDR-64-277 AD-609841
LAMINAR BOUNDARY-LAYER SEPARATION ON FLARED BODIES AT SUPERSONIC AND HYPERSONIC SPEEDS.
J. D. GRAY

51. AEDC-TR-65-67 AD-358285
HEAT-TRANSFER AND PRESSURE DISTRIBUTIONS ON A 6 DEG. CONE WITH SURFACE ROUGHNESS AND VARIABLE NOSE BLUNTNESS AT MACH. 10.
O. L. DUNKIN, CONFIDENTIAL

52. AEDC-TDR-65-80 A16-TDR-65-80
DYNAMIC STABILITY CHARACTERISTICS OF A 10-DEG CONE AT MACH NUMBER 20.
R. H. URBAN AND P. J. SHANAHAN

53. AEDC-TDR-64-7 AD-427313
PUBLICATIONS
A BIBIOGRAPHY OF WORK SPONSORED BY AEDC, WITH PUBLICATIONS LISTED IN CHRONOLOGICAL ORDER ACCORDING TO SUBJECT, ALSO CONTAINS AN AUTHOR INDEX.

54. AEDC-TR-65-62 AD-460154
LIFT, DRAG, AND STATIC STABILITY OF A BLUNT CONICAL MODEL IN HYPERSONIC RAREFIED FLOW.
D. E. BOYLAN

55. AEDC-TDR-63-209 AD-343682
AN INVESTIGATION OF THE CONTROL EFFECTIVENESS AND STATIC STABILITY CHARACTERISTICS OF THE SPRINT SECOND STAGE CONFIGURATION AT MACH NUMBERS OF 2, 4, 6, AND 8.
R. L. PALKO, A. D. RAY AND R. L. DAVIS, CONFIDENTIAL

56. AEDC-TR-65-99 AD-462716
BOUNDARY LAYER TRANSITION UNDER HYPERSONIC CONDITIONS.
J. L. POTTER AND J. D. WHITFIELD, CONFIDENTIAL

57. AEDC-TR-65-92 AD-359940
EFFECTS OF ABLATION ON THE DYNAMIC STABILITY CHARACTERISTICS OF AN 8 DEG CONE AT MACH 10.
G. E. BURT AND J. H. GREGSON, CONFIDENTIAL

58. AEDC-TR-65-100 AD-462717
THEORETICAL AND EXPERIMENTAL STUDIES OF HYPERSONIC VISCOUS EFFECTS.
C. H. LEWIS AND J. D. WHITFIELD

59. AEDC-TR-65-106 AD-360760
EVALUATION OF THE STATIC STABILITY AND CONTROL CHARACTERISTICS OF A 9 DEG CONE USING FLUID INJECTION AS A CONTROL DEVICE.
J. L. BURK AND J. E. BURDETTE, CONFIDENTIAL

60. AEDC-TR-65-129 AD-361609
PRESSURE DISTRIBUTION ON THE FINAL CONTROL SURFACE CONFIGURATION OF A MANEUVERABLE RE-ENTRY FLIGHT TEST VEHICLE AT MACH 10.
J. L. BURK AND J. F. BURDETTE, SECRET

61. AEDC-TR-65-135 AD-362022
STATIC STABILITY CHARACTERISTICS OF SLEIGH RIDE CONFIGURATION AT SUPERSONIC AND HYPERSONIC MACH NUMBERS.
J. R. MYERS AND C. J. SPURLIN, SECRET

62. AEDC-TR-65-155 AD-362994
STATIC STABILITY TEST ON AN 8 DEG CONE WITH ABLATION AT MACH 10.
F. K. HUBE, CONFIDENTIAL

63. AEDC-TR-65-156 AD-362983
DYNAMIC STABILITY CHARACTERISTICS OF A RE-ENTRY VEHICLE.
B. L. USELTON AND J. H. GREGSON, SECRET

ARNOLD ENGINEERING DEVELOPMENT CENTER

TRANSACTION OF THE SECOND TECHNICAL WORKSHOP ON DYNAMIC STABILITY TESTING, HELD AT AEDC APRIL 20-22, 1965

VOLUME I

64. MASS TRANSFER-DYNAMIC STABILITY TESTING IN THE WAVE SUPER-HEATER HYPERSONIC TUNNEL.
D. D. COLOSIMO, CORNELL AERONAUTICAL LABORATORY

65. STABILITY INVESTIGATIONS DURING SIMULATED ABLATION IN A HYPERVELOCITY WIND TUNNEL.
C. J. STALMACH, LTNG TEMCO VOUGHT

66. NOSE BLUNTNESS EFFECTS ON THE STABILITY DERIVATIVES OF SLENDER CONES.
O. WALCHNER AND J. T. CLAY, ARL, WRIGHT-PATTERSON AFB

VOLUME II

67. INSTRUMENTATION AND TECHNIQUES USED AT THE NAVAL ORDNANCE LABORATORY FOR THE DETERMINATION OF DYNAMIC DERIVATIVES IN THE WIND TUNNEL.
F. J. REGAN, U. S. NAVAL ORDNANCE LAB

68. INFLUENCE OF BOUNDARY-LAYER TRANSITION ON DYNAMIC STABILITY AT HYPERSONIC SPEEDS.
L. K. WARD, ARO, INC.

69. SANDIA CORPORATION REPRINT SC-R-65-907
DYNAMIC STABILITY DERIVATIVES FOR A 10 DEG BLUNT CONE AT MACH NUMBERS FROM 0.5 TO 21.
E. C. RIGHTLEY

70. FREE FLIGHT CONE DYNAMIC STABILITY TESTING AT HIGH AMPLITUDES OF OSCILLATION.
B. DAYMAN, JR., JET PROPULSION LAB

71. DYNAMIC STABILITY TESTING TECHNIQUES AT THE JET PROPULSION LABORATORY.
R. H. PRISLIN, JET PROPULSION LAB

VOLUME III IG-634-343

72. SIMULATION AND ANALYSIS OF THE EFFECT ON DYNAMIC STABILITY OF MASS ADDITION FROM A CHARRING ABLATION.
M. L. ROBERTS AND P. B. CLINE, GENERAL ELECTRIC CO., SECRET

73. AEDC-TR-65-166 AD-363989
FORCE TESTS ON A RE-ENTRY CONFIGURATION AT MACH 2 THROUGH 6.
J. H. JONES, SECRET

74. AEDC-TN-65-237 AD-367005
EFFECTS OF SYMMETRICALLY DISTRIBUTED MASS ADDITION ON THE SURFACE PRESSURES OF A 9 DEG CONE AT MACH NUMBERS 2, 4 AND 6
S. R. PATE AND L. M. JENKE, SECRET

75. AEDC-TR-65-230 AD-367264
SUPERSONIC AERODYNAMIC CHARACTERISTICS OF A BLUNT CONE CYLINDER FLARE CONFIGURATION WITH DISTRIBUTED MASS ADITION
S. R. PATE AND L. M. JENKE, SECRET

76. AEDC-TR-65-234 AD-627317
A COMPARISON OF EXPERIMENTAL AND THEORETICALLY PREDICTED PRESSURE DISTRIBUTIONS AND FORCE AND STABILITY COEFFICIENTS FOR A SPHERICALLY BLUNTED CONE AT M=10 AND ANGLES OF ATTACK
E. C. KNOX AND C. H. LEWIS

77. AEDC-TR-66-18 AD-369614
EFFECTS OF SYMMETRICALLY DISTRIBUTED MASS ADDITION ON THE AERODYNAMIC CHARACTERISTICS OF A 9 DEG CONE AT MACH NUMBER 7.97
S. R. PATE, SECRET

78. AEDC-TR-66-31 AD-369809
EFFECTS OF NOSE BLUNTNESS AND BASE SHAPE ON THE DYNAMIC STABILITY CHARACTERISTICS OF ABLATING AND NONABLATING 8 DEG CONES AT MACH 10
G. E. BURT AND J. H. GREGSON, CONFIDENTIAL

79. AEDC-TR-66-14 AD-370729
LATERAL JET INTERACTION EFFECTS ON A 9 DEG CONE AT MACH 10
W. T. STRIKE, JR.

80. AEDC-TR-66-45 AD-371288
AN EXPERIMENTAL STUDY OF AERODYNAMIC FORCES ON LIFTING BODIES UNDER THE INFLUENCE OF STRONG VISCOUS INTERACTION
D. E. BOYLAN, CONFIDENTIAL

81. AEDC-TR-66-50 AD-370876
LARGE AMPLITUDE DYNAMIC STABILITY TEST OF THE MARK 12 REENTRY VEHICLE AT MACH 10
B. L. USELTON AND J. H. GREGSON

82. AEDC-TR-66-16 AD-631149
EQUATIONS AND CHARTS FOR THE EVALUATION OF FORCES ON SPHERICALLY BLUNTED CONES BY THE NEWTONIAN THEORY
L. L. TRIMMER

NATIONAL ADVISORY COUNCIL FOR AERONAUTICS
NATIONAL AERONAUTICS AND SPACE ADMINISTRATION

101. NACA RM L51J09
AN INVESTIGATION OF THE AERODYNAMIC CHARACTERISTICS OF A SERIES OF CONE-CYLINDER CONFIGURATIONS AT A MACH NUMBER OF 6.86.
R. D. COOPER AND R. A. ROBINSON

102. NACA RM A52E22
FORCES AND MOMENTS ON POINTED AND BLUNT-NOSED BODIES OF REVOLUTION AT MACH NUMBERS FROM 2.75 TO 5.00.
D. H. DENNIS AND B. E. CUNNINGHAM
DATA ALSO FOUND IN REFERENCE 537.

103. NACA RM E52C10
AERODYNAMICS OF SLENDER BODIES AT MACH NUMBER OF 3.12 AND REYNOLDS NUMBERS FROM 2- TO 15,000,000. II - AERODYNAMIC LOAD DISTRIBUTIONS OF SERIES OF FIVE BODIES HAVING CONICAL NOSES AND CYLINDRICAL AFTERBODIES.
J. R. JACK AND L. I. GOULD

104. NACA TN 2423
THEORETICAL AERODYNAMIC CHARACTERISTICS OF BODIES IN A FREE-MOLECULE-FLOW FIELD.
J. R. STALDER AND V. J. ZURICK

105. NACA TN 3213
TRANSONIC FLOW PAST CONE CYLINDERS.
G. E. SOLOMON

106. NACA TN 3349
APPLICATION OF THE GENERALIZED SHOCK-EXPANSION METHOD TO INCLINED BODIES OF REVOLUTION TRAVELING AT HIGH SUPERSONIC AIRSPEEDS.
R. C. SAVIN

107. NACA TN 3393
AN EXPERIMENTAL INVESTIGATION OF THE BASE PRESSURE CHARACTERISTICS OF NON-LIFTING BODIES OF REVOLUTION AT MACH NUMBERS FROM 2.73 TO 4.98.
J. O. RELLER, JR. AND F. M. HAMAKER

108. NACA TN 3819
BASE PRESSURE AT SUPERSONIC SPEEDS ON TWO-DIMENSIONAL AIRFOILS AND ON BODIES OF REVOLUTION WITH AND WITHOUT FINS HAVING TURBULENT BOUNDARY LAYERS.
E. S. LOVE

109. NACA TN 3788
STABILITY DERIVATIVES OF CONES AT SUPERSONIC SPEEDS.
M. TOBAK AND W. R. WEHREND

110. NACA TN 4233
EXPERIMENTAL STUDY OF THE EQUIVALENCE OF TRANSONIC FLOW ABOUT SLENDER CONE-CYLINDERS OF CIRCULAR AND ELLIPTIC CROSS SECTION,
W. A. PAGE

111. NACA TN 4327
HYPERSONIC VISCOUS FLOW OVER SLENDER CONES.
L. TALBOT, T. KOGA, AND P. M. SHERMAN

112. NACA REPORT 1376
ELLIPTIC CONES ALONE AND WITH WINGS AT SUPERSONIC SPEEDS.
L. H. JORGENSEN

113. NACA REPORT 1386
INVESTIGATION OF THE DRAG OF VARIOUS AXIALLY SYMMETRIC NOSE SHAPES OF FINENESS RATIO 3 FOR MACH NUMBERS FROM 1.24 TO 7.4.
E. W. PERKINS, L. H. JORGENSEN, AND S. C. SOMMER

114. NASA MEMO 2-22-59L
SOME STATIC, OSCILLATORY, AND FREE-BODY TESTS OF BLUNT BODIES AT LOW SUBSONIC SPEEDS.
J. H. LICHTENSTEIN, L. R. FISHER, S. H. SCHER, AND G. F. LAWRENCE

115. NASA TR R-2
SLENDER-BODY THEORY BASED ON APPROXIMATE SOLUTION OF THE TRANSONIC FLOW EQUATION.
J. R. SPREITER AND A. Y. ALKSNE

116. NASA TR R-50
APPROXIMATIONS FOR THE THERMODYNAMIC AND TRANSPORT PROPERTIES OF HIGH TEMPERATURE AIR.
C. F. HANSEN

117. NASA TR R-127
TABLES OF AERODYNAMIC COEFFICIENTS OBTAINED FROM DEVELOPED NEWTONIAN EXPRESSIONS FOR COMPLETE AND PARTIAL CONIC AND SPHERIC BODIES AT COMBINED ANGLES OF ATTACK AND SIDESLIP WITH SOME COMPARISONS WITH HYPERSONIC EXPERIMENTAL DATA.
W. R. WELLS AND W. O. ARMSTRON

118. NASA TR R-209
A STUDY OF NONLINEAR LONGITUDINAL DYNAMIC STABILITY.
M. TOBAK AND W. E. PEARSON

119. NASA TN D-49
SOME ASPECTS OF AIR-HELIUM SIMULATION AND HYPERSONIC APPROXIMATIONS.
E. S. LOVE, A. HENDERSON, JR. AND M. H. BERTRAM

120. NASA TN D-176
WORKING CHARTS FOR RAPID PREDICTION OF FORCE AND PRESSURE COEFFICIENTS ON ARBITRARY BODIES OF REVOLUTION BY USE OF NEWTONIAN CONCEPTS.
R. W. RAINEY

121. NASA TN D-179
MEASUREMENTS OF PRESSURE AND LOCAL HEAT TRANSFER ON A 20 DEG CONE AT ANGLES OF ATTACK UP TO 20 DEG FOR A MACH NUMBER OF 4.95.
J. D. JULIUS

122. NASA TN D-634
EFFECTS OF CONE ANGLE, MACH NUMBER, AND NOSE BLUNTING ON TRANSITION AT SUPERSONIC SPEEDS.
K. R. CZARNECKI AND M. W. JACKSON

123. NASA TN D-753
PRESSURE MEASURMENTS ON SHARP AND BLUNT 5 DEG - AND 15 DEG - HALF-ANGLE CONES AT MACH NUMBER 3.86 AND ANGLES OF ATTACK TO 100 DEG.
J. L. AMICK

124. NASA TN D-840
AERODYNAMIC FORCE CHARACTERISTICS OF A SERIES OF LIFTING CONE AND CONE-CYLINDER CONFIGURATIONS AT A MACH NUMBER OF 6.83 AND ANGLES OF ATTACK UP TO 130 DEGREES.
J. A. PENLAND
DATA ALSO FOUND IN REFERENCE 537.

125. NASA TN D-859
UNSTEADY AERODYNAMIC FORCES ON A SLENDER BODY OF REVOLUTION IN SUPERSONIC FLOW.
R. BOND AND B. B. PACKARD

126. NASA TN D-1473
AIR-HELIUM SIMULATION OF THE AERODYNAMIC FORCE COEFFICIENTS OF CONES AT HYPERSONIC SPEEDS
C. L. LADSON AND T. A. BLACKSTOCK
APPENDIX-DESIGN AND CALIBRATION OF THREE HELIUM NOZZLES IN THE LANGLEY 11 INCH HYPERSONIC TUNNEL.
D. L. BARADEL AND T. A. BLACKSTOCK

127. NASA TN D-1506
STABILITY INVESTIGATION OF A BLUNTED CONE AND A BLUNTED OGIVE WITH A FLARED CYLINDER AFTERBODY AT MACH NUMBERS FROM 0.30 TO 2.85.
L. C. COLTRANE

NATIONAL ADVISORY COUNCIL FOR AERONAUTICS
NATIONAL AERONAUTICS AND SPACE ADMINISTRATION

128. NASA TN D-1606
AERODYNAMIC CHARACTERISTICS AT A MACH NUMBER OF 6.77 OF A 9 DEG CONE CONFIGURATION, WITH AND WITHOUT SPHERICAL AFTERBODIES, AT ANGLES OF ATTACK UP TO 180 DEG WITH VARIOUS DEGREES OF NOSE BLUNTING.
L. VEAL, JR.
DATA ALSO FOUND IN REFERENCE 537.

129. NASA TN D-1768
AN EXPERIMENTAL EVALUATION OF AERODYNAMIC DAMPING MOMENTS OF CONES WITH DIFFERENT CENTERS OF ROTATION.
W. R. WEHREND. JR.
DATA ALSO FOUND IN REFERENCE 537.

130. NASA TN D-2184
FORCE-COEFFICIENT AND MOMENT-COEFFICIENT CORRELATIONS AND AIR-HELIUM SIMULATION FOR SPHERICALLY BLUNTED CONES.
J. E. HARRIS

131. NASA TN D-2282
STATIC STABILITY CHARACTERISTICS OF BLUNT LOW-FINENESS-RATIO BODIES OF REVOLUTION AT A MACH NUMBER OF 24.5 IN HELIUM.
R. D. WITCOFSKI AND W. C. WOODS

132. NASA TN D-2283
A STUDY OF THE STABILITY AND LOCATION OF THE CENTER OF PRESSURE ON SHARP, RIGHT CIRCULAR CONES AT HYPERSONIC SPEEDS.
J. A. PENLAND

133. NASA TN D-2339
CORRELATION GRAPHS FOR SUPERSONIC FLOW AROUND RIGHT CIRCULAR CONES AT ZERO YAW IN AIR AS A PERFECT GAS.
M. H. BERTRAM

134. NASA TN D-2489
LONGITUDINAL CHARACTERISTICS OF SEVERAL CONFIGURATIONS AT HYPERSONIC MACH NUMBERS IN CONICAL AND CONTOURED NOZZLES.
J. P. ARRINGTON, R. C. JOINER, JR. AND A. HENDERSON, JR.

135. NASA TM X-194
DAMPING IN PITCH AND STATIC STABILITY OF A GROUP OF BLUNT BODIES AT MACH NUMBERS FROM 0.60 TO 0.95.
H. S. FLETCHER, CONFIDENTIAL

136. NASA TM X-369
WIND-TUNNEL TESTS OF THE STATIC AND DYNAMIC STABILITY CHARACTERISTICS OF FOUR BALLISTIC RE-ENTRY BODIES.
W. R. WEHREND, JR. AND D. E. REESE, JR., CONFIDENTIAL

137. NASA TM X-845
INVESTIGATION AT TRANSONIC MACH NUMBERS OF THE EFFECTS OF CONFIGURATION GEOMETRY ON SURFACE PRESSURE DISTRIBUTIONS FOR A SIMULATED LAUNCH VEHICLE.
T. C. KELLY, CONFIDENTIAL

138. NASA TM X-950
A STUDY OF THE STABILITY AND DRAG OF SEVERAL AERODYNAMIC SHAPES IN AIR, CARBON DIOXIDE, AND ARGON AT MACH NUMBERS FROM 3 TO 8.
G. P. MENEES AND W. G. SMITH, CONFIDENTIAL

139. NASA SP-3004
TABLES FOR SUPERSONIC FLOW AROUND RIGHT CIRCULAR CONES AT ZERO ANGLE OF ATTACK.
J. L. SIMS

140. NASA SP-3007 ASTIC-001742
TABLES FOR SUPERSONIC FLOW AROUND RIGHT CIRCULAR CONES AT SMALL ANGLES OF ATTACK.
J. L. SIMS

141. NACA RM A51K27
BODIES OF REVOLUTION FOR MINIMUM DRAG AT HIGH SUPERSONIC AIRSPEEDS.
A. J. EGGERS JR., D. H. DENNIS, AND M. M. RESNIKOFF

142. NASA TN D-1890
MEASUREMENT OF HEAT TRANSFER TO BODIES OF REVOLUTION IN FREE FLIGHT BY USE OF A CATCHER CALORIMETER.
G. T. CHAPMAN, C. T. JACKSON, JR.
DATA ALSO FOUND IN REFERENCE 537.

143. NACA REPORT 1081
A STUDY OF SECOND-ORDER SUPERSONIC FLOW THEORY.
M. D. VANDYKE

144. NACA TN-3391
FREE-FLIGHT MEASUREMENTS OF TURBULENT-BOUNDARY LAYER SKIN FRICTION IN THE PRESENCE OF SEVERE AERODYNAMIC HEATING AT MACH NUMBERS FROM 2.8 TO 7.0.
S. C. SOMMER AND B. J. SHORT

145. NACA TN-4063
EQUATIONS, TABLES AND FIGURES FOR USE IN THE ANALYSIS OF HELIUM FLOW AT SUPERSONIC AND HYPERSONIC SPEEDS.
J. N. MUELLER

146. NASA TR R-7
TURBULENT BOUNDARY LAYER ON A YAWED CONE IN A SUPERSONIC STREAM.
W. H. BRAUN

147. NASA TR R-82
TURBULENT SKIN FRICTION AT HIGH MACH NUMBERS AND REYNOLDS NUMBERS IN AIR AND HELUIM.
F. W. MATTING, D. R. CHAPMAN, J. R. NYHOLM, AND A. G. THOMAS

148. NASA MEMO 10-28-58L
AERMODYNAMIC CHARACTERISTICS OF SOME FAMILIES OF BLUNT BODIES AT TRANSONIC SPEEDS.
L. R. FISHER, A. L. KEITH JR., AND J. R. DICAMILLO
DATA ALSO FOUND IN REFERENCE 537.

149. NASA TN D-1781
EFFECTS OF NOSE BLUNTNESS, FINENESS RATIO, CONE ANGLE, AND MODEL BASE ON THE STATIC AERODYNAMIC CHARACTERISTICS OF BLUNT BODIES AT MACH NUMBERS OF 1.57, 1.80, AND 2.16 AND ANGLES OF ATTACK UP TO 180.
D. S. SHAW, D. E. FULLER AND C. D. BABB

150. NASA TN D-2201
LONGITUDINAL AERODYNAMIC CHARACTERISTICS OF BLUNTED CONES AT MACH NUMBER OF 3.5, 4.2, AND 5.0.
J. W. KEYES
DATA ALSO FOUND IN REFERENCE 537.

151. NASA TN D-962
LAMINAR HEAT-TRANSFER AND PRESSURE MEASUREMENTS AT A MACH NUMBER OF 6 ON SHARP AND BLUNT 15 DEG. HALF-ANGLE CONES AT ANGLES OF ATTACK UP 90.
R. J. CONTI
DATA ALSO FOUND IN REFERENCE 537.

152. NACA REPORT 1135
EQUATIONS, TABLES AND CHARTS FOR COMPRESSIBLE FLOW.
AMES RESEARCH STAFF

153. NACA RML53H21
INVESTIGATION OF REYNOLDS NUMBER EFFECTS FOR A SERIES OF CONE-CYLINDER BODIES AT MACH NUMBERS 1.62, 1.93 AND 2.41.
C. E. GRISBY AND E. L. OGBURN
DATA ALSO FOUND IN REFERENCE 537.

154. NASA TN D-1379
STATIC LONGITUDINAL STABILITY AND PERFORMANCE OF SEVERAL BALLISTIC SPACECRAFT CONFIGURATIONS IN HELIUM AT A MACH NUMBER OF 24.5.
P. J. JOHNSON AND C. D. SNYDER
DATA ALSO FOUND IN REFERENCE 537.

155. NACA RMA52613
THE EFFECT OF BLUNTNESS ON THE DRAG OF SPHERICAL-TIPPED TRUNCATED CONES OF FINENESS RATIO 3 AT MACH NUMBERS 1.2 TO 7.4.
S. C. SOMMER AND J. A. STARK
DATA ALSO FOUND IN REFERENCE 537.

156. NASA MEMO 3-2-59L
WIND-TUNNEL INVESTIGATION AT MACH NUMBERS FROM 1.60 TO 4.50 OF THE STATIC-STABILITY CHARACTERISTICS OF TWO NONLIFTING VEHICLES SUITABLE FOR RE-ENTRY.
K. L. TURNER AND D. S. SHAW
DATA ALSO FOUND IN REFERENCE 537.

157. NASA TN D-2062
A WIND-TUNNEL INVESTIGATION OF THE EFFECT OF CHANGES IN BASE CONTOUR ON THE DAMPING IN PITCH OF A BLUNTED CONE.
W. R. WEHREND, JR.
DATA ALSO FOUND IN REFERENCE 537.

158. NASA TR R-100
COLLECTION OF ZERO-LIFT DRAG DATA ON BODIES OF REVOLUTION FROM FREE-FLIGHT INVESTIGATIONS.
W. E. STONEY, JR.

159. NASA TN D-2182
INDUCED PRESSURES AND SHOCK SHAPES ON BLUNT CONES IN HYPERSONIC FLOW.
R. D. WAGNER, JR. AND R. WATSON

160. NASA TN D-342
EXPLORATORY STUDY OF THE REDUCTION IN FRICTION DRAG DUE TO STREAMWISE INJECTION OF HELIUM.
B. L. SWENSON.

161. NASA TN D-2786
AERODYNAMIC CHARACTERISTICS OF TWO TRAILBLAZER II BLUNTED 9 DEG. CONE REENTRY BODIES AT MACH 6.8 IN AIR AND 21.2 IN HELIUM.
H. R. SCHIPPELL, L. NEAL, JR., AND D. C. MARCUM, JR.

162. NASA TN D-2801
AERODYNAMIC FORCE AND MOMENT CHARACTERISTICS OF SPHERES AND CONES AT MACH 7.0 IN METHANE-AIR COMBUSTION PRODUCTS.
L. R. HUNT

163. NASA TM X-167
STATIC STABILITY CHARACTERISTICS OF A SERIES OF HYPERSONIC BOOST GLIDE CONFIGURATIONS AT MACH NUMBERS OF 1.41 AND 2.01.
G. V. FOSTER

164. NASA TM X-503
STEADY AND FLUCTUATING PRESSURES AT TRANSONIC SPEEDS ON TWO SPACE VEHICLE PAYLOAD SHAPES.
C. F. COE

165. NASA TM X-311
A WIND-TUNNEL INVESTIGATION OF THE AERODYNAMIC CHARACTERISTICS OF BODIES OF REVOLUTION AT MACH NUMBERS OF 2.37, 2.98, AND 3.90 AT ANGLES OF ATTACK TO 90 DEG.
F. M. SMITH

166. NASA TM X-244
INVESTIGATION OF THE PRESSURE DISTRIBUTIONS ON REENTRY NOSE SHAPES AT A MACH NUMBER OF 3.55.
W. A. LAWSON, R. W. MCDEARMON, AND R. W. RAINEY, CONFIDENTIAL

167. NASA TM X-543
INVESTIGATION AT A MACH NUMBER OF 1.99 OF TWO SERIES OF BLUNTED DELTA PLANFORM MODELS WITH SEVERAL CROSS-SECTIONAL SHAPES FOR ANGLES OF ATTACK FROM 0 TO 90 DEG.
C. M. JACKSON, JR., AND R. V. HARRIS, JR., CONFIDENTIAL

168. NASA TM X-568
SUPERSONIC AERODYNAMIC CHARACTERISTICS OF TRIANGULAR PLAN-FORM MODELS AT ANGLES OF ATTACK TO 90 DEG.
L. E. WIGGINS AND G. E. KAATTARI, CONFIDENTIAL

169. NASA TM X-588
SUMMARY OF AERODYNAMIC CHARACTERISTICS OF LOW-LIFT-DRAG-RATIO REENTRY VEHICLES FROM SUBSONIC TO HYPERSONIC SPEEDS.
R. W. RAINEY, CONFIDENTIAL

170. NASA TM X-536
HYPERSONIC AERODYNAMIC CHARACTERISTICS OF SEVERAL SERIES OF LIFTING BODIES APPLICABLE TO REENTRY.
W. D. ARMSTRONG, CONFIDENTIAL

171. NASA TM X-230
A WIND-TUNNEL INVESTIGATION OF EFFECTS OF NOSE BLUNTNESS, FACE SHAPE, AND AFTERBODY LENGTH ON THE AERODYNAMIC CHARACTERISTICS OF BODIES OF REVOLUTION AT MACH NUMBERS OF 2.37, 2.98, AND 3.90.
F. M. SMITH, CONFIDENTIAL

172. NASA TM X-337
DYNAMIC DIRECTIONAL STABILITY CHARACTERISTICS FOR A GROUP OF BLUNT REENTRY BODIES AT TRANSONIC SPEEDS.
H. G. WILEY, R. A. KILGORE, AND E. R. HILLJE, CONFIDENTIAL

NATIONAL ADVISORY COMMITTEE FOR AERONAUTICS
NATIONAL AERONAUTICS AND SPACE ADMINISTRATION

173. NASA TN D-807
FREE FLIGHT SKIN TEMPERATURE AND SURFACE PRESSURE MEASUREMENTS ON A HIGHLY POLISHED NOSE HAVING A 100 DEG TOTAL-ANGLE CONE AND A 10 DEG HALF-ANGLE CONICAL FLARE SECTION UP TO A MACH NUMBER OF 4.08.
B. RASHIS AND A. C. BOND

174. NACA RM L57J29 RIRM L57J29
SOME EFFECTS OF REYNOLDS NUMBER ON THE STABILITY OF A SERIES OF FLARED-BODY AND BLUNTED-CONE MODELS AT MACH NUMBERS FROM 1.62 TO 6.86.
A. B. KEHLET, CONFIDENTIAL

175. NASA TN D-2969
AN EXPERIMENTAL AND THEORETICAL INVESTIGATION OF THE PRESSURE DISTRIBUTION AND FLOW FIELDS OF BLUNTED CONES AT HYPERSONIC MACH NUMBERS.
J. W. CLEARY

176. NASA TN D-3058
AERODYNAMIC CHARACTERISTICS OF SPHERICALLY BLUNTED CONES AT MACH NUMBERS FROM 0.5 TO 5
R. V. OWENS

177. RM A54E03
FORCES AND MOMENTS ON INCLINED BODIES AT MACH NUMBERS FROM 3.0 TO 6.3
D. H. DENNIS AND B. L. CUNNINGHAM

178. NASA TN D-3193
EXPERIMENTAL STABILITY AND DRAG OF A POINTED AND A BLUNTED 30 DEG HALF ANGLE CONE AT MACH NUMBERS FROM 11.5 TO 34 IN AIR
P. F. INTRIERI

179. NASA TN D-3201
AERODYNAMIC CHARACTERISTICS OF THE SHARP RIGHT CIRCULAR CONE AT MACH 20.3 AND ANGLES OF ATTACK TO 110 DEG IN HELIUM
D. V. MADDALON

180. NASA TN D-3203
TRANSONIC AERODYNAMIC CHARACTERISTICS OF A SERIES OF RELATED BODIES WITH CROSS SECTIONAL ELLIPTICITY
B. SPENCER, JR.

181. NASA CR-413 (1966)
LINEAR AERODYNAMIC LOADS ON CONE-CYLINDRS AT MACH NUMBERS FROM 0.7 TO 2
R. L. HAMMER AND A. G. LOFF

NATIONAL ADVISORY COMMITTEE FOR AERONAUTICS
NATIONAL AERONAUTICS AND SPACE ADMINISTRATION

182. NASA TN D-3460
EFFECT OF BODY NOSE BLUNTING, CONTROL PLANFORM AREA, LEADING EDGE BLUNTNESS ON AERODYNAMIC CONTROL OF A 5 DEG SEMIVERTEX CONE AT A MACH NUMBER 6.9
J. A. PENLAND

183. NASA TN D-3462
NEWTONIAN AERODYNAMIC CHARACTERISTICS OF BLUNTED RIGHT ELLITICAL CONES FOR CONE THICKNESS RATIOS OF 0.25 TO 3
R. E. GRAHAM, R. H. LAMB AND PAUL D. ROMERE

184. NASA TN D-3525
STAGNATION AND STATIC PRESSURE ON A NOSE-MOUNTED 15 DEG CONICAL PROBE WITH VARIOUS FOREBODY CONFIGURATIONS
E. M. COATES, JR.

185. NASA TN D-2624
NEWTONIAN AERODYNAMICS FOR BLUNTED RAKED-OFF CIRCULAR CONES AND RAKED-OFF ELLIPTICAL CONES
E. E. MAYO, R. H. LAMB AND P. D. ROMERE

186. NASA TN D-3539
SUPERSONIC AERODYNAMIC CHARACTERISTICS OF A SERIES OF RELATED BODIES WITH CROSS SECTION ELLIPTICITY
R. H. FOURNIER, B. SPENCER, JR., AND W. A. CORLETT

187. NASA TN D-2550
APPLICATION OF GENERALIZED NEWTONIAN THEORY TO THREE DIMENSIONAL SHARP NOSE SHOCK DETACHED BODIES AT MACH 6 FOR ANGLES OF ATTACK UP TO 25 DEG
G. C. ASHBY AND T. J. GOLDBERG

AVCO CORPORATION, RESEARCH AND ADVANCED DEVELOPMENT DIVISION

201. RAD-SR-63-103 AD-337038
STATIC FORCE DATA OF PHASE II MARK 11 CONFIGURATIONS AT MACH NUMBERS FROM 0.4 TO 20
P. M. NOZZOLILLO, CONFIDENTIAL

202. RAD-TR-64-13 AD-350347
SUMMARY REPORT OF THE STATIC WIND TUNNEL AND DYNAMIC STABILITY TESTS FOR THE LORV PROGRAM
G. CHADWICK, M. DEGEN, J. GRECO, J. GRIMES, AND J. OTIS, SECRET

203. RAD-TR-64-21 AD-351697
SUMMARY REPORT OF THE STATIC WIND TUNNEL AND DYNAMIC STABILITY TESTS FOR THE MARK 11 DECOY PROGRAM
M. DEGEN AND A. W. NELSON, SECRET

204. RAD-TR-62-28 AD-351714
SUMMARY REPORT OF THE STATIC WIND TUNNEL AND BALLISTIC RANGE TESTS FOR THE MARK 11 PROGRAM
G. CHADWICK, M. DEGEN, P. NOZZOLILLO, AND T. SELLERS, CONFIDENTIAL

205. RAD-TM-62-110 AD-400497
AERODYNAMIC EFFECTS OF BLUNTING ON CONICAL BODIES
H. SCHMIDT AND W. VAN TASSELL

206. RAD-SR-62-8
STATIC FORCE AND PRESSURE DATA OF PHASE I MARK 11 CONFIGURATIONS AT MACH NUMBERS FROM 0.4 TO 20
P. M. OZZOLILLO, CONFIDENTIAL

207. RAD-TM-64-34 AD-443900
A LINEARIZED ANALYSIS CONCERNING BOUNDARY LAYER EFFECTS ON THE STATIC AND DYNAMIC BEHAVIOR OF SLENDER, ABLATING AND NONABLATING BODIES
N. THYSON

208. RAD-TM-65-1, VOL. 3, P. 113-121 AD-356697
RE-ENTRY ENVIRONMENT AND SYSTEMS TECHNOLOGY (REST) SEMI-ANNUAL PROGRESS REPORT, 1 JULY - 31 DEC 1964
SECRET

209. RAD-SR-64-307, ADDENDUM 1 AD-363097
LOW-OBSERVABLE REENTRY VEHICLE L-1 PRELIMINARY FLIGHT EVALUATION REPORT
SECRET

210. RAD-SR-65-259 AD-366903
LOW-OBSERVABLE REENTRY VEHICLE L-4 FLIGHT EVALUATION REPORT
SECRET

AVCO CORPORATION, RESEARCH AND ADVANCED DEVELOPMENT DIVISION

211. AERL 64-815 AD-353959
A PARAMETRIC STUDY OF THE STABILITY OF CONES
I. FRANK, W. HOUSE AND R. NORLING, SECRET

212. RAD-TM-65-35 AD-364642
DYNAMIC STABILITY WITH MASS ADDITION GROUND TESTING TECHNIQUES AND RESULTS
A. W. NELSON, CONFIDENTIAL

213. RAD-TM-65-36, VOL. II, P. 93 - 111 AD-364716
REENTRY ENVIRONMENT AND SYSTEMS TECHNOLOGY (REST) SEMIANNUAL PROGRESS REPORT, 1 JANUARY - 30 JUNE 1965
SECRET

214. SAME AS REFERENCE 213, P. 113-120

216. RAD-SR-66-31, VOL. I AD-370054
LOW OBSERVABLE REENTRY VEHICLE FLIGHT TEST PROGRAM SUMMARY REPORT
SECRET

301. BSD-TDR-63-110 AD-336938
INVESTIGATION OF BOUNDARY LAYER TRANSITION FOR REX-1 AND REX-3
E. POJDOWSKI, SECRET

302. BSD-TDR-63-171 AD-344050
WIND TUNNEL STATIC FORCE TESTS ON MODELS OF THE REX-1 RE-ENTRY VEHICLE
V. R. KULWICKI, CONFIDENTIAL

303. BSD-TDR-63-179 AD-341303
AERODYNAMIC CHARACTERISTICS OF THE REX VEHICLES
T. E. ERNST AND P. K. MEYER, SECRET

304. BSD-TDR-63-180 AD-342347
RESULTS OF DYNAMIC STABILITY WIND TUNNEL TESTS OF THE REX-1 CONFIGURATION
P. W. KULY, CONFIDENTIAL

305. BSD-TDR-63-254 AD-346499
REX-1 AND REX-2 REENTRY VEHICLES ADDITIONAL FLIGHT TEST DATA ANALYSIS
ADVANCED DEVELOPMENT BRANCH, SECRET

306. BSP-TDR-63-26 ADB-TN-7-63
BALLISTIC RANGE EVALUATION OF SPHERICAL AND ROUNDED BASE CONFIGURATIONS FOR THE LRCR RE-ENTRY VEHICLE
V. R. KULWICKI, CONFIDENTIAL

401. 63SD761 AD-341999
EXPERIMENTAL WIND TUNNEL RESULTS FOR THE STATIC STABILITY AND CONTROL EFFECTIVENESS OF A 9 DEG CONE WITH TRAILING FLAPS AT M=8
R. B. HOBBS, CONFIDENTIAL

402. 63SD762 AD-342003
EXPERIMENTAL WIND TUNNEL EVALUATION OF STABILITY AND CONTROL EFFECTIVENESS FOR A 9 DEG SPHERE CONE WITH TRAILING FLAPS AT M=10
R. B. HOBBS, CONFIDENTIAL

403. 64SD506 AD-347556
A CORRELATION OF HYPERSONIC DYNAMIC STABILITY WIND TUNNEL DATA FOR THE SKYBOLT AND IVX REENTRY VEHICLES
M. L. ROBERTS, SECRET

404. 64SD705 AD-349995
MANEUVERING BALLISTIC RE-ENTRY VEHICLE PROGRAM QUARTERLY PROGRESS REPORT NO. 3, REPORTING PERIOD 1 FEBRUARY THROUGH 30 APRIL 1964
SECRET

405. AERODYNAMICS DATA MEMO NO. 1.76 AD-343917
CORRELATION OF SPHERE CONE CENTER OF PRESSURE AND NORMAL FORCE COEFFICIENT SLOPE
J. L. BRIGGS, SECRET

406. 62SD917 C5-PR-53, VOL. 1
ADVANCED RE-ENTRY PROGRAMS,
SEMI-ANNUAL REPORT, VOL.1, DEC. 1962, P. 107.
STABILITY AND CONTROL EFFECTIVENESS OF TERMINALLY GUIDED RE-ENTRY VEHICLES
A. J. YUNGMAN, ET. AL., SECRET

407. 63SD672 AD-337406
ADVANCED RE-ENTRY PROGRAMS,
SEMI-ANNUAL REPORT, VOL.1, JUNE 1963, P. 70.
STABILITY AND CONTROL EFFECTIVENESS OF TERMINALLY GUIDED RE-ENTRY VEHICLES
A. J. YUNGMAN, ET. AL., CONFIDENTIAL

408. 64SD786 AD-351174
ADVANCED RE-ENTRY PROGRAMS, AEROPHYSICS AND OBSERVABLES,
SEMI-ANNUAL REPORT, VOL. 1, JUNE 1964, P. 46.
HYPERSONIC DYNAMIC STABILITY AND CONTROL OF RE-ENTRY VEHICLES
L. A. MARSHALL, ET. AL., SECRET

409. 64SD5305 AD-355932
ADVANCED RE-ENTRY PROGRAMS, AEROPHYSICS AND OBSERVABLES, SEMI-ANNUAL REPORT, VOL. 1, DEC. 1964, P. 62.
BOUNDARY LAYER TRANSITION
H. T. NAGAMATSU, SECRET

410. 62SD540 C5-62-SD-540
LOW DENSITY HYPERSONIC SIMILARITY OF CONES AND SLIGHTLY BLUNTED SPHERE CONES
W. D. MCCAULEY, CONFIDENTIAL

411. 64SD989 AD-353725
ROUGHNESS, BLUNTNESS, AND ANGLE OF ATTACK EFFECTS ON HYPERSONIC BOUNDARY LAYER TRANSITION
H. T. NAGAMATSU, B. C. GRABER, R. E. SHEER, JR., CONFIDENTIAL

412. 65SD663 AD-361726
ADVANCED RE-ENTRY PROGRAMS, AEROPHYSICS AND OBSERVABLES, SEMI-ANNUAL REPORT, VOL. 1, JUNE 1965, P. 53.
BOUNDARY LAYER TRANSITION
H. T. NAGAMATSU, ET. AL., SECRET

413. R62SD3 AD-362568
EXPERIMENTAL INVESTIGATION OF THE HYPERSONIC CHARACTERISTICS OF A SERIES OF BASIC LIFTING SHAPES
R. E. GEIGER AND C. J. HARRIS

414. 65SD52394 AD-369249
ADDENDUM A TO FLIGHT DATA REPORT FOR REENTRY MEASUREMENTS VEHICLE MISSION RX-25
SECRET

MISCELLANEOUS

501. ABMA REPORT DA-TN-42-58(1958)
FORCE TESTS OF A RELATED FAMILY OF TWENTY NOSE CONES FOR A RANGE OF MACH NUMBERS FROM 0.47 TO 1.93.
R.A. FELIX
DATA ALSO FOUND IN REFERENCE 537.

502. AERONATUICAL RESEARCH COUNCIL, TECH. REPORT C.P. NO. 271
71-E2-CP271

BASE PRESSURES IN SUPERSONIC FLOW.
G. E. GADD, D. W. HOLDER AND J. D. REGAN

503. AERONUTRONIC, C-943 AD-339536
A FORCE TEST OF THE DART WITH ARMS IN THE AEDC B-2 HYPERSONIC WIND TUNNEL AT MACH NUMBER 8.
W. T. DAVEY, CONFIDENTIAL

504. AIR FORCE BALLISTIC MISSILE DIVISION, TECHNICAL LIBRARY 60-2094
AD-605697

STABILITY CHARACTERISITCS OF CONES AND CYLINDERS AT LARGE ANGLES OF ATTACK AT MACH NUMBER 2.87.
W. T. DAVEY AND C. E. GRIGSBY

505. BALLISITC RESEARCH LAB., BRL-MR-1502 (1963) AD-345938
AERODYNAMIC PROPERTIES OF THE SKYBOLT NOSE CONE CONFIGURATION.
E. D. BOYER, CONFIDENTIAL

506. PROCEEDINGS OF THE 6TH U.S. NAVY SYMPOSIUM ON AEROBALLISTICS, NOV. 1963, BOOK NO. 623.4519063, SY68A AD-429753
AERODYNAMIC PHENOMENA ASSOCIATED WITH ADVANCED RE-ENTRY SYSTEMS.
I. SACKS AND E. SCHURMAN, AVCO CORP.

507. DOUGLAS AIRCRAFT CO., INC., ES-29700 C402-ES-29700
ANALYSIS OF PRESSURE TESTS ON SHARP AND BLUNT NOSED BODIES OF REVOLUTION FOR MACH NUMBERS FROM 0.2 TO 3.5.
D. N. MORRIS AND B. L. GROBLI

508. DOUGLAS AIRCRAFT CO., INC., SM-42125 AD-431541
AEDC 16 PWT STATIC AND DYNAMIC STABILITY OF THE SKYBOLT NOSE CONE. CONTAINS G. E. REPORT-62SD383 RESULTS OF SUPERSONIC WIND TUNNEL TESTS CONDUCTED IN THE AEDC 16 PWT TO EVALUATE THE STATIC AND DYNAMIC STABILITY CHARACTERISTICS OF THE SKYBOLT NOSE CONE.
R. B. HOBBS

509. DOUGLAS AIRCRAFT CO., INC., SM-42159 AD-437560
GAM-87A R/V HYPERSONIC STATIC STABILITY TEST.
CONTAINS G. E. REPORT-62SD480 TEST RESULTS STABILITY CHARACTERISITCS OF THE SKYBOLT NOSE CONE AT MACH 20 IN THE AEDC 50 HOT SHOT II.
R. B. HOBBS

MISCELLANEOUS

510. DOUGLAS AIRCRAFT CO., INC., SM-43059 AD-421440
BIBLIOGRAPHY ON BOUNDARY LAYER TRANSITION (1963).
A LIST BY AUTHOR OF 117 DOCUMENTS DIVIDED INTO 7 CATEGORIES.

511. CHANCE VOUGHT CORP., 2-59740/3R-479
PRELIMINARY INVESTIGATION OF THE EFFECTS OF MASS-INJECTION ON DYNAMIC STABILITY AT M 17.
T. C. POPE AND C. J. STALMACH, JR.

512. GENERAL APPLIED SCIENCE LAB., GASL-TR-444 AD-351427
EXPERIMENTAL STUDY OF CONTROL FORCES PRODUCED BY AIR INJECTION FROM AN AXISYMMERTRIC MODEL.
E. SANLORENZO AND L. SPADACCINI, CONFIDENTIAL

513. NAVAL ORDNANCE LAB., NAVORD REPORT 4334 (1956) AD-106329
AEROBALLISTIC RESEARCH REPORT 347, HYPERSONIC TUNNEL NO. 4 - THE DEVELOPMENT OF A WATER COOLED STRAIN GAGE BALANCE, (INCLUDING STING EFFECTS) AND ITS APPLICATION TO A STUDY OF NORMAL FORCE AND PITCHING MOMENTS OF A CONE AND CONE-CYLINDER AT MACH 5 TO 8.
L. L. LICCINI

514. NAVAL ORDNANCE LAB., NAVORD REPORT 1488, VOL. 5 (1959)
HANDBOOK OF SUPERSONIC AERODYNAMICS, SECTION 16, MECHANICS OF RAREFIED GASES.
S. A. SCHAAF AND L. TALBOT

515. PICATINNY ARSENAL TECH. MEMO 1493 (1964) AD-451469
SUPERSONIC FLOW ABOUT RIGHT CIRCULAR CONES AT ZERO YAW IN AIR AT THERMODYNAMIC EQUILIBRIUM, PART II - TABLES OF DATA.
H. E. HUDGINS, JR.
SEE REFERENCE 566, PART I - CORRELATION OF FLOW PROPERTIES

516. ROYAL AIRCRAFT ESTABLISHMENT, TN AERO 2863 AD-402730
EXPERIMENTS AT HYPERSONIC SPEEDS ON CIRCULAR CONES AT INCIDENCE.
D. H. PECKHAM

517. UNITED AIRCRAFT CORP., C910188-17 (1965) ASTIC-009971
HYPERSONIC STATIC AND DYNAMIC STABILITY OF WING-FUSELAGE CONFIGURATION.
M. R. FINK

518. WRIGHT AIR DEV. CENTER, WADC TECH. NOTE 57-28 AD-110742
METHODS OF ESTIMATING BASE PRESSURES ON AIRCRAFT CONFIGURATIONS.
C. B. HARGIS JR., P. H. DAVISON, AND S. B. SAVAGE, CONFIDENTIAL

519. ROYAL AIRCRAFT ESTABLISHMENT, TN AERO 2952
PRESSURE DISTRIBUTION MEASUREMENTS ON A SERIES OF SLENDER DELTA BODY SHAPES AT MACH NUMBERS OF 6.85 AND 8.60.
D. H. PECKHAM

520. UNIV. OF CALIF. TECH. REPORT HE-150-172 (1959) T43-HE-150-172
LOW DENSITY AERODYNAMIC CHARACTERISTICS OF A CONE AT ANGLES OF ATTACK.
G. J. MASLACH AND L. TALBOT
DATA ALSO FOUND IN REFERENCE 537.

521. UNIV. OF CALIF. TECH. REPORT HE-150-190 (1961) T43-20-135
EXPERIMENTAL DETERMINATION OF PITCHING MOMENT AND DAMPING COEFFICIENTS OF A CONE IN LOW DENSITY HYPERSONIC FLOW.
W. L. MAAS

522. M. I. T. DEPT. ELECT. ENGR. REPORT TR-5 (1949)
TABLES OF SUPERSONIC FLOW AROUND CONES OF LARGE YAW.
Z. KOPAL

523. ARMY MISSILE COMMAND, REDSTONE ARSENAL, ALABAMA
ARMY MSL CMD RF-TR-63-17 AD-340100
THE STATIC STABILITY AND DRAG OF THREE BLUNTED-CONE REENTRY BODIES AT MACH NUMBERS 15 AND 18.
D. J. SPRING

524. BALLISTIC RESEARCH LAB., BRL-MR-1522 (1963) ASTIC-002246
WIND TUNNEL TESTS OF THE REDSTONE B NOSE CONE AT MACH NUMBERS FROM 1.75 TO 5.00.
MAURICE A. SYLVESTER

525. BALLISTIC RESEARCH LAB., BRL-MR-1484 (1963) AD-343438
THE AERODYNAMIC CHARACTERISTICS OF TWO RVX CONFIGURATIONS.
CONFIDENTIAL

526. NAVAL ORDNANCE LAB., NAVORD REPORT 3584 (1953) AD-128203
CONE STATIC STABILITY INVESTIGATION AT MACH NUMBERS 1.56 THROUGH 4.24.
I. SHANTZ

527. AERONUTRONIC, U-1638 AD-275191
EXPERIMENTAL INVESTIGATION OF THE AERODYNAMIC CHARACTERISTICS OF 9 DEG. HALF-ANGLE CONES WITH VARYING DEGREES OF BLUNTNESS AT MACH NUMBER 9.
DATA ALSO FOUND IN REFERENCE 537.

528. MCDONNELL AIRCRAFT CORP., SERIAL NO. 14, REPORT 6670 ASTIC-008002
FORCES ON BODIES OF REVOLUTION IN FREE MOLECULAR FLOW BY THE NEWTONIAN-DIFFUSE METHOD.
E. F. BLICK

529. AIR FORCE SYSTEM COMMAND, ASD-TDR-63-663 AD-608303
DRAG COEFFICIENTS OF SEVERAL BODIES OF REVOLUTION AT TRANSONIC AND SUPERSONIC VELOCITY.
H. G. HEINRICH, S. R. HESS, AND G. STUMBIS

MISCELLANEOUS

530. BALLISITC RESEARCH LAB., BRL-MR-760 (1954)
THE EFFECTS OF FINENESS RATIO AND MACH NUMBER ON THE NORMAL FORCE AND CENTER OF PRESSURE OF CONICAL AND OGIVAL HEAD BODIES.
W. E. BUFORD AND S. SHATUNOFF
DATA ALSO FOUND IN REFERENCE 537.

531. BALLISTIC RESEARCH LAB., BRL-MR-759 (1954)
THE DYNAMIC PROPERTIES OF PURE CONES AND CONE CYLINDERS.
L. E. SCHMIDT
DATA ALSO FOUND IN REFERENCE 537.

532. SANDIA CORP., SC-RR-64-1796 AD-455?00
PRESSURE DISTRIBUTIONS ON SPHERE CONES.
D. M. ELLETT

533. U.S. ARMY MISSILE COMMAND, REDSTONE ARSENAL, ALA. RSIC-?25(1964)
AD-356?85
DRAG REDUCTION STUDIES OF MISSILES, A BIBLIOGRAPHY.
J. E. TERRY

534. NATIONAL PHYSICS LAB., LONDON, NPL AERO REPORT 1095(1964)
GSRL B-267
EXPERIMENTS WITH CONES IN LOW-DENSITY FLOWS AT MACH NUMBERS NEAR 2.
E. W. E. ROGERS, C. J. BERRY AND B. M. DAVIS

535. AIR RESEARCH COUNCIL, ENGLAND, A.R.C.R. AND M. NO. 3340 (1962)
PRESSURE DISTRIBUTIONS AND FLOW PATTERNS ON SOME CONICAL SHAPES WITH SHARP EDGES AND SYMMETRICAL CROSS-SECTIONS AT M=4.0.
I. C. SQUIRE

536. AMRAC PROCEEDINGS, VOL. XI, PART II, P. 129 ASTIC-009521
THE INFLUENCE OF SLENDER BODY TRANSITION ON A DOWNRANGE OPTICAL OBSERVABLES.
A. GUTTMAN, D. E. FLORENCE AND A. M. HECHT, GENERAL ELEC. CO., SECRET

537. SANDIA CORP., SC-R-64-1311 ASTIC-011776
A COMPILATION OF LONGITUDINAL AERODYNAMIC CHARACTERISTICS INCLUDING PRESSURE INFORMATION FOR SHARP- AND BLUNT-NOSE CONES HAVING FLAT AND MODIFIED BASES.
A. D. FOSTER

538. CONVAIR DIVISION, REPORT ZA-7-017 AD-311?84
SHARP AND BLUNTED CONE FORCE COEFFICIENTS AND CENTERS OF PRESSURE FROM WIND TUNNEL TESTS AT MACH NUMBERS FROM 0.50 TO 4.06.
W. J. GENDTNER
DATA ALSO FOUND IN REFERENCE 537.

539. TRANSACTIONS OF THE 8TH SYMPOSIUM ON BALLISTIC MISSILE AND SPACE TECHNOLOGY, OCT. 1963, VOL. III, P. 21. A64-14-1963 VOL. 3
EFFECTS OF MASS TRANSFER COOLING ON THE STATIC STABILITY AND DYNAMIC MOTIONS OF SLENDER ENTRY VEHICLES
C. A. SYVERTSON AND J. B. MCDEVITT, NASA, CONFIDENTIAL

540. SAME AS REF. 539, P. 41.
THE EFFECTS OF THE UNSTEADY BOUNDARY LAYER ON THE HYPERSONIC DYNAMIC STABILITY OF A SLIGHTLY BLUNTED CONES
M. L. ROBERTS, GENERAL ELECTRIC COMPANY, CONFIDENTIAL

541. UNIV. OF CALIF. ENG. PROJECTS HE-150-114 (1953)
CONE DRAG IN A RAREFIED GAS FLOW
D. C. IPSEN
DATA ALSO FOUND IN REFERENCE 537.

542. UNIV. OF CALIF. TECH. REPORT HE-150-205 (1962)
HYPERSONIC FLOW OVER A SLENDER CONE WITH GAS INJECTION.
H. H. KING
DATA ALSO FOUND IN REFERENCE 537.

543. NAVAL ORDNANCE LAB.,NAVORD REPORT 5635 (1957)
LOW-TO-HIGH SPEED DRAG COMPILATIONS FOR ROCKET TEST SLED COMPONENTS
J. LUBLINER, R. E. OLIVER AND A. J. A. MORGAN
DATA ALSO FOUND IN REFERENCE 537.

544. NAVAL ORDNANCE LAB., NAVORD REPORT 5668 (1953)
WAKE INVESTIGATION OF SHARP AND BLUNT NOSE CONES AT SUPERSONIC SPEEDS
R. LEHNERT AND V. L. SCHERMERHORN
DATA ALSO FOUND IN REFERENCE 537.

545. NAVAL ORDANCE LAB., NOLTR 62-35 (1962) U25-62-35
SUPERSONIC AERODYNAMIC HEAT TRANSFER AND PRESSURE DISTRIBUTION ON A SPHERE CONE MODEL AT HIGH ANGLES OF YAW
L. PASIUK
DATA ALSO FOUND IN REFERENCE 537.

546. GEORGE C. MARSHALL FLIGHT CENTER, REPORT MTP-AERO-61-38
AERODYNAMIC CHARACTERISTICS OF SPHERICALLY BLUNTED CONES AT MACH NUMBERS FROM 0.5 TO 5.0
DATA ALSO FOUND IN REFERENCE 537.

547. SANDIA CORP., SCTM 202-56-51
BASE AND SURFACE PRESSURE VARIATION WITH MACH NUMBER ON A RIGHT CIRCULAR CONE
J. D. IVERSON
DATA ALSO FOUND IN REFERENCE 537.

548. CALIF. INSTITUTE OF TECH., GALCIT MEMO NO. 69 (1963)
HYPERSONIC FLOW OVER A YAWED CIRCULAR CONE
R. R. TRACY

549. WRIGHT AIR DEV. CENTER, WADC TECH. REPORT 54-70. A2-TR-54-70
SURVEY ON HEAT TRANSFER AT HIGH SPEEDS.
E. R. G. ECKERT

550. WRIGHT AIR DEV. CENTER, WADC TECH. NOTE 58-182 A2-TN-58-182
PRESSURE AND LAMINAR HEAT TRANSFER RESULTS IN THREE-DIMENSIONAL HYPERSONIC FLOW.
V. ZAKKAY.

551. A F FLIGHT DYNAMICS LAB., TECH. REPORT FLD-TDR-64-129 ASTIC-008720
FLAT-PLATE BOUNDARY-LAYER TRANSITION AT HYPERSONIC SPEEDS.
R. E. DEEM, C. R. ERICKSON AND J. S. MURPHY

552. DAVID TAYLOR MODEL BASIN, WASH. D.C., REPORT 1903 (1964) AD-612269
ABLATION EXPERIMENTS WITH PLASTICS AT HYPERSONIC SPEEDS AND AT LOW HEAT-TRANSFER RATES.
V. VAN HISE AND M. J. MALIA

553. US AOMC-ARGMA-OML REPORT 6R8F (1958)
NORMAL FORCE, PITCHING MOMENT, AND CENTER OF PRESSURE OF SEVERAL SPHERICALLY BLUNTED CONES AT MACH NUMBERS OF 1.50, 2.18, AND 4.04.
A. S. MARKS
DATA ALSO FOUND IN REFERENCE 537.

554. LITTON SYSTEMS, INC., HADES-R-65-1, VOL. 1 AD-461744
VOL. 2 AD-461745
WIND TUNNEL CALIBRATION TESTS AND PRESSURE MEASUREMENTS ON A BLUNTED SLENDER CONE FROM MACH 0.3 TO 1.3.
G. K. GARDINER

555. UNIVERSITY OF MICHIGAN REPORT, AMRAC PROCEEDINGS, 4613-97-X
VOL. XII, PART II, P. 453
PRELIMINARY RESULTS OF A STUDY OF THE EFFECTS OF MASS TRANSFER ON AERODYNAMIC PITCH COEFFICIENTS.
J. S. HOLDHUSEN, J. J. CASEY AND D. G. DECOURSIN, FLUI DYNE CORP.

556. BRITISH AIRCRAFT CORP. LTD., BAC/GW/T.R.95 (1963) AD-350187
SURFACE PRESSURES ON POINTED AND BLUNTED CONES AT INCIDENCE UP TO MACH 8.
P. R. BIGNELL AND R. A. BREWER, CONFIDENTIAL
SECRET

557. GENERAL APPLIED SCIENCE LAB., GASL-TR-526 (1965)
STUDY OF HYPERSONIC INTERCEPTOR CONTROLS.
W. CHINITZ, CONFIDENTIAL

558. NAVAL ORDNANCE LAB., NAVORD REPORT 6110 (1958) U25-6110
A SUMMARY OF EXPERIMENTAL MAGNUS CHARACTERISTICS OF A 7 AND 5 CALIBER BODY OF REVOLUTION AT SUBSONIC THROUGH SUPERSONIC SPEEDS.
J. E. GREENE

559. LOCKHEED MISSILE AND SPACE CO., SRB-63-1 AD-422083
EXPERIMENTAL MEASUREMENTS OF VELOCITY AND TEMPERATURE PROFILES AND SKIN FRICTION COMPRESSIBLE FLOW. AN ANNOTATED BIBILOGRAPHY.
E. E. GRAZIANO

560. AEROSPACE RESEARCH LAB., ARL 64-214 ASTIC-016602
HYPERSONIC FLOW FIELD ABOUT A BLUNT NOSED CONE AT ANGLE OF ATTACK. PHASE II.
R. J. POLITCHKO AND B. O. HULTGREN

561. NAVWEPS REPORT 1488 (1961)
HANDBOOK OF SUPERSONIC AERODYNAMICS, SECTION B. BODIES OF REVOLUTION.

562. ARMY BALLISTIC MISSILE AGENCY, REDSTONE ARSENAL, ALA., DA-TN-42-58
FORCE TESTS OF A RELATED FAMILY OF 20 NOSE CONES FOR A RANGE OF MACH NUMBERS FROM 0.47 TO 1.93.
A. R. FELIX
DATA ALSO FOUND IN REFERENCE 537.

563. AERONUTRONIC, C-1103 AD-361755
AN INVESTIGATION OF THE ABLATION CHARACTERISTICS OF SLENDER CONES OF VARIOUS MATERIALS IN THE CHICAGO MIDWAY LABORATORIES ARC-JET FACILITY, PHASE III.
W. J. BISS, CONFIDENTIAL

564. AFFDL-TR-65-5 AD-465764
EFFECTS AND ANALYSIS OF MACH NUMBER AND REYNOLDS NUMBER ON LAMINAR SKIN FRICTION AT HYPERSONIC SPEEDS.
T. R. SIERON AND C. MARTINEZ, JR.

565. DOUGLAS AIRCRAFT CO., INC., SM-46429 AD-616236
FLOW SEPARATION IN HIGH SPEED FLIGHT, A REVIEW OF THE STATE OF THE ART.
J. E. WUERER AND F. I. CLAYTON

566. PICATINNY ARSENAL TECH. MEMO 1493 (1965) AD-468284
SUPERSONIC FLOW ABOUT RIGHT CIRCULAR CONES AT ZERO YAW IN AIR AT CHEMICAL EQUILIBRIUM, PART I - CORRELATION OF FLOW PROPERTIES.
H. E. HUDGINS, JR.
SEE REFERENCE 515, PART II - TABLES OF DATA

MISCELLANEOUS

567. NATIONAL RESEARCH COUNCIL OF CANADA AERONAUTICAL REPORT LR-418 (1964) AD-464622
A SURFACE FLOW SOLUTION AND STABILITY DERIVATIVES FOR BODIES OF REVOLUTION IN COMPLEX SUPERSONIC FLOW, PART I - THEORY AND REPRESENTATIVE RESULTS
L. H. OHMAN

568. NATIONAL RESEARCH COUNCIL OF CANADA AERONAUTICAL REPORT LR-419 (1964) ASTIC-019277
SAME AS REFERENCE 567.
PART II - RESULTS FOR TWO FAMILIES OF BODIES OF REVOLUTION FOR M = 1.1 TO 5
L. H. OHMAN

569. DOUGLAS AIRCRAFT CO., INC., WL TR-64-141 AD-359097
A STUDY OF THE AERODYNAMIC COEFFICIENTS OF A REENTRY VEHICLE UNDERGOING MASSIVE ABLATION
H. H. TANG, C. L. ARNE AND D. P. ENGH, SECRET

570. LOCKHEED MISSILE AND SPACE CO., LMSC/805162 (1965) AD-620217
ENGINEERING ANALYSIS OF BOUNDARY LAYERS AND SKIN FRICTION ON BODIES OF REVOLUTION AT ZERO ANGLE OF ATTACK
D. J. ECKSTROM

571. AERONUTRONIC, C-1393 AD-362520
WIND TUNNEL FORCE TESTS ON DARTS WITH SLIGHTLY-SWEPT LOW-ASPECT-RATIO ARMS AND DARTS WITH ANNULAR RINGS AT A MACH NUMBER OF 6.07
W. J. BLISS AND C. O. WHITE, CONFIDENTIAL

572. DOUGLAS AIRCRAFT CO., INC., CO2878 AD-362654
MANEUVERING RE-ENTRY CONTROL AND ABLATION STUDIES (MARCAS), FINAL REPORT, VOLUME I - JET INTERACTION CONTROLS
J. W. BARNES, F. W. SPAID AND J. G. DAVIES, SECRET

574. AIR FORCE INSTITUTE OF TECHNOLOGY, WRIGHT-PATTERSON AFB, OHIO
THESIS, GAM 65B/AE/65-6 AD-621443
A WIND-TUNNEL INVESTIGATION OF FORCES ON CONES AT LOW MACH NUMBERS
D. LITWACK, CAPT USAF

575. UNIV. OF CALIF. REPORT NO. AS-65-15 (1965) AD-473420
WALL TEMPERATURE EFFECTS ON THE ZERO LIFT VISCOUS DRAG OF BLUNTED CONES IN RAREFIED SUPERSONIC FLOW
D. R. CRAWFORD

576. JET PROPULSION LAB. TECHNICAL REPORT 32-677 (1964)
AERODYNAMIC CHARACTERISTICS OF BLUNT BODIES
J. O. NICHOLS AND E. A. NIERIENGARTEN

577. NOL BALLISTICS RANGE PROGRAM ON ABRES RESEARCH, FINAL TECHNICAL REPORT, OCT. 1964 - OCT. 1965 AD-475971

578. CORNELL AERONAUTICAL LAB, CAL REPORT NO. 141 (1965) ASTIC 032328
THE EFFECTS OF MASS TRANSFER ON THE DYNAMIC STABILITY ON SLENDER CONES
D. D. COLOSIMO

579. ELECTRO-OPTICAL SYSTEMS, INC., EOS RESEARCH NOTE NO. 29 (U965) AD-369990
A CORRELATION OF REENTRY AND LABORATORY BASE FLOW DATA
H. H. KING, SECRET

580. BALLISTIC RESEARCH LAB., BRL MR 1709 AD-630329
BASE PRESSURE MEASUREMENTS ON SHARP AND BLUNT 9 DEG CONES AT MACH NUMBERS FROM 3.50 TO 9.20
N. A. ZARIN

581. LOCKHEED MISSILE AND SPACE CO., SB-63-75 AD-440886
AERODYNAMIC CHARACTERISTICS OF BODIES OF REVOLUTION WITHOUT FINS, AN ANNOTATED BIBLIOGRAPHY
G. R. EVANS

582. AMRAC PROCEEDINGS, VOL. XIV, PART I, P. 117 AD-372900
HIGH ALTITUDE AERODYNAMIC DRAG ANALYSIS FOR WIND TUNNEL DATA
C. R. ORTLOFF AND R. A. HARTUNIAN, AEROSPACE CORP., SECRET

583. AMRAC PROCEEDINGS, VOL. XIV, PART I, P. 145 AD-372900
COMMENTS ON PAPER 5- HIGH ALTITUDE AERODYNAMIC DRAG ANALYSIS FROM WIND TUNNEL DATA
J. A. LAURMANN, DEFENSE RESEARCH CORP., SECRET

584. AMRAC PROCEEDINGS, VOL. XIV, PART I, P. 151 AD-372900
ANALYSIS OF THE EFFECTS OF PHASED CYCLIC BLOWING ON THE AERODYNAMIC PITCHING MOMENT DERIVATIVES OF SLENDER CONES IN HYPERSONIC FLOW
S. K. IBRAHIM AND J. S. HOLDHUSEN, FLUIDYNE CORP., UNCLASSIFIED REPORT IN SECRET PROCEEDINGS

585. BALLISTIC SYSTEMS DIVISION, BSD-TR-65-471 ASTIC-032447
HYPERSONIC LAMINAR BOUNDARY LAYER TRANSITION ON 8-FOOT LONG 10-DEG CONE
H. NAGAMATSU, B. C. GRABER AND R. E. SHEER, JR., G. E.

586. AERONAUTICAL RESEARCH COUNCIL, A.R.C. 27 582 (1965) AD-483081
GUN TUNNEL MEASUREMENTS OF LIFT, DRAG AND PITCHING MOMENT ON A 20 DEG CONE, A FLAT DELTA AND A CARET DELTA WING AT MACH 8.3
T. OPSTOWSKI

AMERICAN INSTITUTE OF AERONAUTICS AND ASTRONAUTICS
AIAA PAPERS

601. NO. 64-427
EFFECT OF BOUNDARY LAYER TRANSITION ON DYNAMIC STABILITY OVER LARGE AMPLITUDES OF OSCILLATION
P. JAFFE AND R. H. PRISLIN, CALIF. INSTITUTE OF TECH., PASADENA, CALIF.

602. NO. 65-127
FREE-FLIGHT BOUNDARY LAYER TRANSITION INVESTIGATIONS AT HYPERSONIC SPEEDS
N. W. SHEETZ, JR., U. S. NAVAL ORDNANCE LAB., SILVER SPRING, MD.

603. NO. 66-410
EFFECTS OF ABLATION ON HYPERSONIC AERODYNAMIC STABILITY CHARACTERISTICS
G. T. CHRUSCIEL AND S. S. CHANG, LOCKHEED MISSILES AND SPACE CO.

604. NO. 64-44
HYPERSONIC DRAG, STABILITY, AND WAKE DATA FOR CONES AND SPHERES
W. C. LYONS, JR., J. J. BRADY AND Z. J. LEVENSTEINS
U. S. NAVAL ORDNANCE LAB., SILVER SPRING, MD.
DATA ALSO FOUND IN REFERENCE 537.

605. NO. 66-457
EXPERIMENTAL RESULTS FOR MASSIVE BLOWING STUDIES
R. A. HARTUNIAN AND D. J. SPENCER, AEROSPACE CORP.

606. NO. 65-128
FLAT PLATE BOUNDARY LAYER TRANSITION AT HYPERSONIC SPEEDS
R. E. DEEM AND J. S. MURPHY, DOUGLAS AIRCRAFT CO.

607. NO. 66-495
A SHOCK TUNNEL INVESTIGATION OF THE EFFECTS OF NOSE BLUNTNESS, ANGLE OF ATTACK AND BOUNDARY LAYER COOLING ON BOUNDARY LAYER TRANSITION AT A MACH NUMBER OF 5.5
K. F. STETSON AND G. H. RUSHTON, AVCO CORP.

608. NO. 66-465
HIGH AMPLITUDE DYNAMIC STABILITY CHARACTERISTICS OF BLUNT 10-DEG CONES
R. H. PRISLIN, CAL. INSTITUTE OF TECHNOLOGY

609. NO. 66-467
AERODYNAMICS OF TYPICAL LIFTING BODIES UNDER CONDITIONS SIMULATING VERY HIGH ALTITUDES
D. E. BOYLAN AND J. L. POTTER, ARO, INC.

610. NO. 66-26
THE EFFECT OF CONTROLLED THREE DIMENSIONAL ROUGHNESS ON HYPERSONIC LAMINAR BOUNDARY LAYER TRANSITION
W. D. MC CAULEY, A. SAYDEH AND J. BUECHE, G. E.

AMERICAN INSTITUTE OF AERONAUTICS AND ASTRONAUTICS
AIAA PAPERS

611. NO. 66-27
BOUNDARY LAYER TRANSITION ON ABLATING CONES AT SPEEDS TO 7 KM/SEC
M. E. WILKINS AND M. E. TAUBER, NASA

612. NO. 66-414
EFFECTS OF ANGLE OF ATTACK AND NOSE BLUNTNESS ON THE HYPERSONIC FLOW OVER CONES
J. W. CLEARY, NASA

613. NO. 66-455
BOUNDARY LAYER SEPARATION IN HYPERSONIC FLOW
D. A. NEEDHAM AND J. L. STOLLERY, IMPERIAL COLLEGE, ENGLAND

AIAA CONFERENCES

651. AERODYNAMIC TESTING CONFERENCE, WASHINGTON, D. C. MARCH 1964,
P. 104-114. T62-35-1964
DYNAMIC STABILITY TESTING WITH ABLATION AT MACH 14 IN A LONG DURATION WIND TUNNEL
J. H. GRIMES, JR., ARO, CORP., AND J. J. CASEY, FLUI DYNE CORP.

652. ENTRY TECH. CONFERENCE, WILLIAMSBURG AND HAMPTON, VA., OCT. 1964,
P. 136-157.
BOUNDARY-LAYER TRANSITION ON A HIGHLY COOLED 10 DEGREE CONE IN HYPERSONIC FLOWS
H. T. NAGAMATSU AND R. E. SHEER, JR., G. E. RESEARCH LAB.,

AMERICAN INSTITUTE OF AERONAUTICS AND ASTRONAUTICS
AIAA JOURNALS

701. VOL. 1, NO. 2, FEB. 1963, P. 295-310.
RECENT ADVANCES IN HYPERSONIC FLOW RESEARCH.
H. K. CHENG, CORNELL AERONAUTICAL LAB. INC., BUFFALO, N. Y.

702. VOL. 1, NO. 2, FEB. 1963, P. 486-487.
CORRELATION OF HYPERSONIC STATIC-STABILITY DATA FROM BLUNT SLENDER CONES.
J. D. WHITFIELD AND W. WOLNY, ARO, INC.

703. VOL. 1 NO. 2, FEB. 1963, P. 490-491.
BOW SHOCK CORRELATION FOR SLIGHTLY BLUNTED CONES.
J. H. KLAIMON, THE BOEING COMPANY, SEATTLE, WASH.

704. VOL. 1, NO. 11, NOV. 1963, P. 2467-2473.
DRAG OF SPHERES IN RAREFIED HYPERVELOCITY FLOW.
M. KINSLOW AND J. L. POTTER, ARO, INC.

705. VOL. 1, NO. 11, NOV. 1963, P. 2656-2658.
AERODYNAMIC COEFFICIENTS IN THE SLIP AND TRANSITION REGIME.
E. F. BLICK, LOCKHEED MISSILE AND SPACE CO.

706. VOL. 2, NO. 2, FEB. 1964, P. 312-321.
MACH 8 TO 22 STUDIES OF FLOW SEPARATION DUE TO DEFLECTED CONTROL SURFACES.
D. S. MILLER AND R. HIJMAN, THE BOEING COMPANY, AND M. E. CHILDS, UNIV. OF WASH., SEATILE, WASH.

707. VOL. 2, NO. 4, APRIL 1964, P. 743-745.
PRESSURES IN THE STAGNATION REGIONS OF BLUNT BODIES IN RAREFIED FLOW.
J. L. POTTER AND A. B. BAILEY, ARO, INC.

708. VOL. 2, NO. 4, APRIL 1964, P. 755-756.
SKIN FRICTION OF SLENDER CONES IN HYPERSONIC FLOW.
J. RAAT, U. S. NAVAL ORDNANCE LAB., SILVER SPRING, MD.

709. VOL. 2, NO. 4, APRIL 1964, P. 771-772.
BOUNDARY-LAYER TRANSITION ON A SLENDER CONE IN HYPERSONIC FLOW.
A. MARTELLUCCI, GEN. APPLIED SCI. LAB., INC.

710. VOL. 2, NO. 5, MAY 1964, P. 836-844.
EFFECT OF MASS INJECTION ON THE DRAG OF A SLENDER CONE IN HYPERSONIC FLOW.
H. H. KING AND L. TALBOT, UNIV. OF CALIF., BERKELEY, CALIF.

711. VOL. 2, NO. 5, MAY 1964, P. 941-943.
DRAG MINIMIZATION USING EXACT METHODS.
S. A. POWERS, NORTHRUP CORP.

AMERICAN INSTITUTE OF AERONAUTICS AND ASTRONAUTICS
AIAA JOURNALS

712. VOL. 2, NO. 10, OCTOBER 1964, P. 1714-1722.
HYPERSONIC VISCOUS DRAG EFFECTS ON BLUNT SLENDER CONES.
J. D. WHITFIELD AND B. J. GRIFFITH, ARO, INC.

713. VOL. 2, NO. 10, OCTOBER 1964, P. 1846-1874.
WEAK INTERACTING HYPERSONIC FLOW OVER CONES.
W. HOELMER AND M. SAARLAS, UNIV. OF CINCINNATI, CINCINNATI, OHIO

714. VOL. 2, NO. 11, NOVEMBER 1964, P. 2054-2055.
CONE PRESSURE DISTRIBUTION AT LARGE AND SMALL ANGLES OF ATTACK.
M. D. HIGH AND E. F. BLICK, UNIV. OF OKLA., NORMAN, OKLA.

715. VOL. 3, NO. 2, FEB. 1965, P. 379-380.
COMPARISONS OF FREE-FLIGHT AND WIND-TUNNEL DATA ON SLENDER CONES.
J. D. WHITFIELD AND B. J. GRIFFITH, ARO, INC.

716. VOL. 3, NO. 3, MARCH 1965, P. 536-537.
EXTENSION OF REACTION CONTROL EFFECTIVENESS CRITERIA TO MACH 10 - EXPERIMENT AND THEORY.
P. W. VINSON, MARTIN COMPANY, ORLANDO, FLA.

717. VOL. 3, NO. 4, APRIL 1965, P. 577-590.
A SYNTHETIC VIEW OF THE MECHANICS OF RAREFIED GASES.
GORDON N. PATTERSON, INSTITUTE OF AEROSPACE STUDIES, UNIV. OF TORONTO, CANADA.

718. VOL. 3, NO. 4, APRIL 1965, P. 752-754.
HYPERSONIC STABILITY DERIVATIVES OF BLUNTED SLENDER CONES.
O. WALCHNER AND J. T. CLAY, AEROSPACE RESEARCH LAB., WRIGHT-PATTERSON AIR FORCE BASE, OHIO.

719. VOL. 3, NO. 4, APRIL 1965, P. 758-760.
HYPERSONIC BOUNDARY-LAYER TRANSITION DATA FOR A COLD-WALL SLENDER CONE.
R. J. SANATOR, J. P. DE CARLO, AND I. T. TORRILLO, REPUBLIC AVIATION CORP., FARMINGDALE, N. Y.

720. VOL. 3, NO. 4, APRIL 1965, P. 631-638.
EXPERIMENTAL INVESTIGATIONS OF THE COMPRESSIBLE TURBULENT BOUNDARY LAYER AT VERY HIGH REYNOLDS NUMBERS.
D. R. MOORE AND J. HARKNESS, LING-TEMCO-VOUGHT, INC., DALLAS, TEXAS.

721. VOL. 3, NO. 6, JUNE 1965, P. 1165-1166.
VISCOUS DRAG EFFECTS ON SLENDER CONES IN LOW-DENSITY HYPERSONIC FLOW.
J. D. WHITFIELD AND B. J. GRIFFITH, ARO, INC.

AMERICAN INSTITUTE OF AERONAUTICS AND ASTRONAUTICS
AIAA JOURNALS

722. VOL. 3, NO. 7, JULY 1965, P. 1363-1364
EXPLORATORY HYPERSONIC BOUNDARY LAYER TRANSITION STUDIES
A. HENDERSON, R. S. ROGALLO, W. C. WOODS AND C. R. SPITZER,
NASA LANGLEY

723. VOL. 3, NO.8, AUGUST 1965, P. 1391-1400
HYPERSONIC VISCOUS EFFECTS ON FREE-FLIGHT SLENDER CONES
B. DAYMAN, JR., JET PROPULSION LAB

724. VOL. 3, NO. 12, DECEMBER 1965, P. 2351-2352
EFFECT OF CONE ANGLE AND BLUNTNESS RATIO ON BASE PRESSURE
J. M. CASSANTO, G.E.

725. VOL. 4, NO. 4, APRIL 1966, P. 743-745
BASE PRESSURE MEASUREMENTS ON SHARP AND BLUNT 9 DEG CONES AT
MACH NUMBERS FROM 3.50 TO 9.20
N. A. ZARIN, BRL

726. VOL. 4, NO. 8, AUGUST 1966, P. 1469-1471
STABILITY DERIVATIVES OF SHARP CONES IN VISCOUS HYPERSONIC FLOW
R. J. KIND AND K. J. ORLIK-RUCKEMANN, NATL AERONAUTICAL EST., CAN.

AMERICAN INSTITUTE OF AERONAUTICS AND ASTRONAUTICS
JOURNALS OF SPACECRAFT AND ROCKETS

751. VOL. 1, NO. 4, JULY-AUGUST 1964, P. 437-439.
DYNAMIC STABILITY TESTING IN A MACH 14 BLOWDOWN WIND TUNNEL.
O. WALCHNER, F. M. SAWYER AND S. J. KOOB, AEROSPACE RESEARCH LAB., WRIGHT PATTERSON AIR FORCE BASE, OHIO.

752. VOL. 1, NO. 5, SEPTEMBER-OCTOBER 1964, P. 449-463.
RECENT DEVELOPMENTS IN WIND-TUNNEL TESTING TECHNIQUES AT TRANSONIC AND SUPERSONIC SPEEDS.
R. W. HENSEL, ARO, INC.

753. VOL. 2, NO. 1, JANUARY-FEBRUARY 1965, P. 106-108.
INFLUENCE OF ABLATION ON THE DYNAMICS OF SLENDER RE-ENTRY CONFIGURATIONS.
J. H. GRIMES JR., AVCO CORP., AND J. J. CASEY, FLUI DYNE CORP.

JOURNALS OF AEROSPACE SCIENCES

775. VOL. 23, NO. 10, OCT. 1956, P. 931-936.
EXPERIMENTS ON CIRCULAR CONES AT YAW IN SUPERSONIC FLOW.
M. HOLT AND J. BLACKIE.

776. VOL. 24, NO. 5, MAY 1957, P. 371-377.
CORRELATION OF CONE-CYLINDER NORMAL FORCE AND PITCHING MOMENT DATA BY THE HYPERSONIC SIMILARITY RULE.
W. H. DORRANCE AND R. G. NORELL.

777. VOL. 25, NO. 2, FEB. 1958, P. 103-108.
THE EFFECTS OF AFTERBODY LENGTH AND MACH NUMBER ON THE NORMAL FORCE AND CENTER OF PRESSURE OF CONICAL AND OGIVAL NOSE BODIES.
W. E. BUFORD.

778. VOL. 19, NO. 2,FEB. 1952, P. 111-119.
SUPERSONIC FLOW AROUND CONES AT LARGE YAW.
G. B. W. YOUNG AND C. P. SISKA

801. D2-81123
EXPERIMENTAL INVESTIGATION AND CORRELATION WITH THEORY OF THE SURFACE PRESSURE DISTRIBUTION ON SEVERAL SHARP AND BLUNTED CONES FOR INCOMPRESSIBLE FLOW.
W. E. JOHNSON

802. D2-9909
THE THERMODYNAMIC PROPERTIES OF AIR IN DISSOCIATION AND IONIZATION EQUILIBRIUM FROM 500 K TO 25,000 K.
R. J. ARAVE

803. D2-10596
PRESSURE DISTRIBUTION ON A SERIES OF BLUNTED CONE-CYLINDER-FLARE CONFIGURATIONS.
M. E. TAUBER

804. D2-10598
TWO DIMENSIONAL OR AXIALLY SYMMETRIC REAL GAS FLOWS BY THE METHOD CHARACTERISTICS, PART II - FLOW FIELDS AROUND BODIES.
D. W. EASTMAN

805. D2-11722
AN IMPROVED CALCULATION OF GAS PROPERTIES AT HIGH TEMPERATURES, AIR.
A. L. PINDROH AND T. C. PENG

806. D2-12066
SUMMARY OF THE IBM 7090 PROGRAM FOR CALCULATING THE EXACT SUPERSONIC FLOW FIELD ABOUT A SHARP NOSED CIRCULAR CONE AT ZERO ANGLE OF ATTACK.
D. W. EASTMAN

807. D2-12701
AN ANALYSIS OF PRESSURE DATA ON SEVERAL CIRCULAR AND ELLIPITIC CONES TESTED AT MACH NUMBER OF 6.08 AND AT ANGLES OF ATTACK FROM 40 TO 90 DEGREES.
D. W. EASTMAN AND M. E. TAUBER

808. D2-12765
DESIGN CHARTS AND ANALYSIS FOR HEAT TRANSFER AND OTHER PARAMETERS IN A TWO DIMENSIONAL SEPARATED FLOW.
R. J. DIXON AND R. H. PAGE

809. D2-20253-1
SLENDER RE-ENTRY VEHICLE BOUNDARY LAYER STUDY.
R. E. HEROLD

810. D2-20447-1
REAL GAS FLOW FIELDS ABOUT HIGHLY YAWED CONES BY THE INVERSE METHOD.
D. W. EASTMAN

811. D2-20874
TWO DIMENSIONAL OR AXIALLY SYMMETRIC REAL GAS FLOWS BY THE METHOD OF CHARACTERISTICS, PART IV - NONEQUILIBRIUM FLOW.
D. W. EASTMAN

812. D2-20978
NONEQUILIBRIUM FLOW FIELDS OF HYPERSONIC REENTRY VEHICLES.
D. W. EASTMAN AND C. A. OLSON

813. D2-22826
AEROTHERMODYNAMICS COMPUTER PROGRAM CATALOG.
M. B. DONOVAN

814. D2-35226
SUBSONIC FLOW FIELDS ABOUT BLUNT HYPERSONIC BODIES BY THE INVERSE METHOD.
D. W. EASTMAN

815. D2-36037-1
EXPERIMENTAL INVESTIGATION OF EXTERNAL BURNING ON AN 8 DEG. HALF-ANGLE CONE AT MACH 5. AND 6.1.
P. C. KRANZ AND D. A. PELKEY

816. D2-20414-1
CONTROL EFFECTIVENESS OF MANEUVERING RE-ENTRY VEHICLES.
R. A. PASCOE, DEFENSE LIMITED

817. D2-99531-1
HIBEX WIND TUNNEL TEST PROGRAM DATA ANALYSIS.
D. BERNSTEIN, D. S. KRASSER, J. BAKER, CONFIDENTIAL

818. D2-23872-1 ASTIC-013100
NEWTONIAN IMPACT ANALYSIS COMPUTER PROGRAM FOR ARBITRARY THREE DIMENSIONAL SHAPES, TECHNICAL AND MANAGEMENT PROPOSAL.
M. S. ROWIN

819. D2-22052
A SUMMARY OF PARAMETERS INFLUENCING BOUNDARY LAYER TRANSITION.
J. F. BRIDGE

820. D2-6444
IBM 704 COMPRESSIBLE LAMINAR BOUNDARY LAYER PROGRAM NUMBER 1.
C. C. CASSMEYER AND K. W. HALVORSON

821. D2-9058
SKIN FRICTION HANDBOOK.
M. DONOVAN AND D. W. EASTMAN.

822. D2-10849.
COMPRESSIBLE TURBULENT BOUNDARY LAYER SKIN FRICTION WITH DISSOCIATION.
M. DONOVAN AND F. R. HAMMOND.

823. D2-5887
AERODYNAMIC PRESSURE DISTRIBUTION HANDBOOK.
R. CHAPKIS AND M. TAUBER.

824. D2-36386-1
AERODYNAMIC COEFFICIENTS OF CONES IN HYPERSONIC, LOW DENSITY FLOW.
S. S. SVARC

Unclassified
Security Classification

DOCUMENT CONTROL DATA · R&D
(Security classification of title, body of abstract and indexing annotation must be entered when the overall report is classified)

1 ORIGINATING ACTIVITY (Corporate author)
The Boeing Company
P.O. Box 3707
Seattle, Washington 98124

2a REPORT SECURITY CLASSIFICATION
Confidential

2b GROUP 4

3 REPORT TITLE
AERODYNAMICS OF CONICAL BODIES

4 DESCRIPTIVE NOTES (type of report and inclusive dates)

5 AUTHOR(S) (Last name, first name, initial)
Eastman, Donald W.

6 REPORT DATE

7a TOTAL NO. OF PAGES

7b NO. OF REFS
823

8a CONTRACT OR GRANT NO.

b PROJECT NO.

c

d

9a ORIGINATOR'S REPORT NUMBER(S)
D2-36139-1

9b OTHER REPORT NO(S) (Any other numbers that may be assigned this report)

10 AVAILABILITY/LIMITATION NOTICES
U.S. Government agencies may obtain copies of this document directly from DDC. Other qualified DDC users shall request through The Boeing Company, Seattle, Wn.

11 SUPPLEMENTARY NOTES

12 SPONSORING MILITARY ACTIVITY

13 ABSTRACT

A compilation and evaluation of theoretical and experimental aerodynamic data are presented for conical shapes at Mach numbers from 0 to 25. Emphasis is placed on slender cones such as might be used for ballistic missile reentry. Plots for obtaining estimates of static and dynamic aerodynamic characteristics are included.

Several hundred references are listed by originating company or publishing source. Contents of the references are summarized by test condition and model geometry.

DD FORM 1 JAN 64 1473
U3 4802 1030 REV. 4/65
PART 1 OF 2

Unclassified
Security Classification

Unclassified
Security Classification

14 KEY WORDS	LINK A ROLE	LINK A WT	LINK B ROLE	LINK B WT	LINK C ROLE	LINK C WT
Ablation Effects						
Aerodynamic Characteristics						
Aerodynamic Controls						
Axial Force						
Base Drag						
Base Geometry						
Base Pressure						
Blowing Effects						
Boundary Layer Transition						
Center of Pressure						
Cones						
Drag						
Dynamic Damping						
Lift						
Low Density						
Normal Force						
Nose Bluntness						
Pitching Moment						
Pressure Coefficient						
Skin Friction						
Stability						
Viscous Effects						
Wave Drag						

INSTRUCTIONS

1. ORIGINATING ACTIVITY: Enter the name and address of the contractor, subcontractor, grantee, Department of Defense activity or other organization (corporate author) issuing the report.

2a. REPORT SECURITY CLASSIFICATION: Enter the overall security classification of the report. Indicate whether "Restricted Data" is included. Marking is to be in accordance with appropriate security regulations.

2b. GROUP: Automatic downgrading is specified in DoD Directive 5200.10 and Armed Forces Industrial Manual. Enter the group number. Also, when applicable, show that optional markings have been used for Group 3 and Group 4 as authorized.

3. REPORT TITLE: Enter the complete report title in all capital letters. Titles in all cases should be unclassified. If a meaningful title cannot be selected without classification, show title classification in all capitals in parenthesis immediately following the title.

4. DESCRIPTIVE NOTES: If appropriate, enter the type of report, e.g., interim, progress, summary, annual, or final. Give the inclusive dates when a specific reporting period is covered.

5. AUTHOR(S): Enter the name(s) of author(s) as shown on or in the report. Enter last name, first name, middle initial. If military, show rank and branch of service. The name of the principal author is an absolute minimum requirement.

6. REPORT DATE: Enter the date of the report as day, month, year, or month, year. If more than one date appears on the report, use date of publication.

7. TOTAL NUMBER OF PAGES: The total page count should follow normal pagination procedures, i.e., enter the number of pages containing information.

7b. NUMBER OF REFERENCES: Enter the total number of references cited in the report.

8a. CONTRACT OR GRANT NUMBER: If appropriate, enter the applicable number of the contract or grant under which the report was written.

8b, 8c, & 8d. PROJECT NUMBER: Enter the appropriate military department identification, such as project number, subproject number, system numbers, task number, etc.

9a. ORIGINATOR'S REPORT NUMBER(S): Enter the official report number by which the document will be identified and controlled by the originating activity. This number must be unique to this report.

9b. OTHER REPORT NUMBER(S): If the report has been assigned any other report numbers (either by the originator or by the sponsor), also enter this number(s).

10. AVAILABILITY/LIMITATION NOTICES: Enter any limitations on further dissemination of the report, other than those imposed by security classification, using standard statements such as:

(1) "Qualified requesters may obtain copies of this report from DDC."

(2) "Foreign announcement and dissemination of this report by DDC is not authorized."

(3) "U.S. Government agencies may obtain copies of this report directly from DDC. Other qualified DDC users shall request through _____."

(4) "U.S. military agencies may obtain copies of this report directly from DDC. Other qualified users shall request through _____."

(5) "All distribution of this report is controlled. Qualified DDC users shall request through _____."

If the report has been furnished to the Office of Technical Services, Department of Commerce, for sale to the public, indicate this fact and enter the price, if known.

11. SUPPLEMENTARY NOTES: Use for additional explanatory notes.

12. SPONSORING MILITARY ACTIVITY: Enter the name of the departmental project office or laboratory sponsoring (paying for) the research and development. Include address.

13. ABSTRACT: Enter an abstract giving a brief and factual summary of the document indicative of the report, even though it may also appear elsewhere in the body of the technical report. If additional space is required, a continuation sheet shall be attached.

It is highly desirable that the abstract of classified reports be unclassified. Each paragraph of the abstract shall end with an indication of the military security classification of the information in the paragraph, represented as (TS), (S), (C), or (U).

There is no limitation on the length of the abstract. However, the suggested length is from 150 to 225 words.

14. KEY WORDS: Key words are technically meaningful terms or short phrases that characterize a report and may be used as index entries for cataloging the report. Key words must be selected so that no security classification is required. Identifiers, such as equipment model designation, trade name, military project code name, geographic location, may be used as key words but will be followed by an indication of technical context. The assignment of links, roles, and weights is optional.

DD FORM 1 JAN 64 1473
U1 4802 1030 REV. 4/65
PART 2 OF 2

Unclassified
Security Classification